APPENDIX I

Meteorological Modeling (Appendix A) for the HGB Attainment Demonstration SIP Revision for the 1997 Eight-Hour Ozone Standard

Meteorological Modeling (Appendix A) for the HGB Attainment Demonstration SIP Revision for the 1997 Eight-Hour Ozone Standard

INDEX

Description		Page
Section	1.1 MM5 Modeling Overview	A-2
	1.2 MM5 Configuration	A-3
Section	2.1 MM5 Performance Evaluation Tools	A-5
	2.2 MM5 Modeling Performance	A-11
	2.3 2005ep0 Performance Evaluation	A-12
	2.4 2005ep1 Performance Evaluation	A-16
	2.5 2005ep2 Performance Evaluation	A-22
	2.6 2006ep0 Performance Evaluation	A-31
	2.7 2006ep1a Performance Evaluation	A-39
	2.8 2006ep1b Performance Evaluation	A-49
	2.9 2006ep1c Performance Evaluation	A-60
	2.10 2006ep1d Performance Evaluation	A-67
	2.11 References	A-79
ATTACHMENT 1	Sea Surface Temperature (SST) Characteristics	A-81
ATTACHMENT 2	Land Use and Land Cover (LULC) Characteristics	A-89
ATTACHMENT 3	Data Assimilation	A-98
ATTACHMENT 4	Application of Grell Cumulus Scheme	A-129

METEOROLOGICAL MODELING FOR THE HGB ATTAINMENT DEMONSTRATION SIP

1.1 MM5 Modeling Overview

The TCEQ is using the Fifth Generation Meteorological Model (MM5, version 3.7.3) developed jointly by the National Center for Atmospheric Research (NCAR) and Pennsylvania State University (Grell et al., 1994). This model, supported by a broad user community including the Air Force Weather Agency, national laboratories, and academia, is being used extensively for regulatory air quality modeling analyses throughout the United States. MM5 modeling was conducted for the time periods (episodes) listed in Table 1.1-1: *TexAQS II Meteorological Modeling Episodes*.

Table 1.1-1: Meteorological Modeling Episodes

Episode	All Grids Begin Date/Time (UTC)	Outer Grids End Date/Time (UTC)	Fine Grid End Date/Time (UTC)
2005ep0	May 18, 2005 06:00	June 4, 2005 06:00	June 4, 2005 06:00
2005ep1	June 15, 2005 06:00	July 1, 2005 06:00	July 1, 2005 06:00
2005ep2	July 25, 2005 06:00	August 9, 2005 09:00	August 9, 2005 07:00
2006ep0	May 29, 2006 06:00	June 17, 2006 06:00	June 17, 2006 06:00
2006ep1a	August 13, 2006 06:00	August 27, 2006 09:00	August 23, 2006 07:00
2006ep1b	August 27, 2006 06:00	September 16, 2006 09:00	September 16, 2006 07:00
2006ep1c	September 16, 2006 06:00	October 1, 2006 09:00	October 1, 2006 07:00
2006ep1d	October 1, 2006 06:00	October 13, 2006 09:00	October 13, 2006 07:00

A Lambert Conformal conic map projection (LCP), with geographical coordinates defined in Table 1.1-2: *Lambert Conformal Conic Map Projection* was used for the MM5 modeling.
MM5 was configured with three two-way nested outer domains (108 km, 36 km, and 12 km horizontal grid resolution) to cover the United States and regional areas of interest. A one-way 4 km fine grid domain covering the eastern half of Texas was established to focus on metropolitan areas with air quality degradation. Figure 1.1-1: *MM5 Domains and Vertical Layers for Meteorological Modeling Episodes* shows the MM5 nested domain configuration, which was established to accommodate the embedding of the CAMx nested domains with the same grid resolution, except for the MM5 36 km domain. That domain does not cover the far eastern part of the 36 km CAMx domain, so values from the MM5 108 km domain are used. Because of the distance from the Houston area, this replacement is expected to have a minimal effect on the simulation of meteorological parameters in the 4 km domain.

Vertically, MM5 is structured with 43 layers from the surface to approximately 20 km. Twenty layers are within the first 3000 meters in order to resolve boundary layer phenomena and to provide a one-to-one mapping with the first twenty layers for CAMx. Unlike CAMx, the same MM5 vertical layering structure is used for all of the domains.

Table 1.1-2: Lambert Conformal Conic Map Projection

First True Latitude (Alpha): 30°N
Second True Latitude (Beta): 60°N
Central Longitude (Gamma): 100°W
Projection Origin: (100°W, 40°N)
Spheroid: Perfect Sphere, Radius = 6370 km

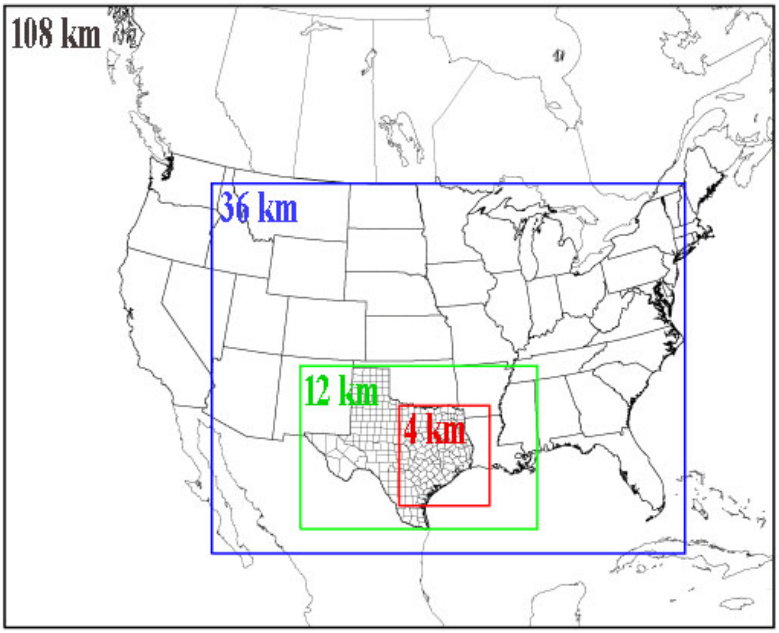

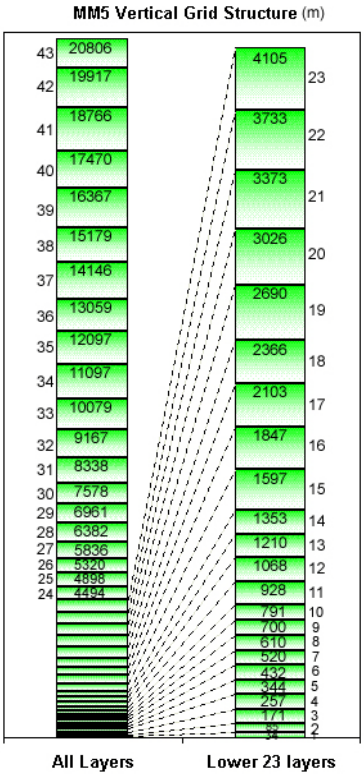

Domain	Range Easting (km)	Range Northing (km)	Grid Points Easting	Grid Points Northing
108 km	(-2808, 2808)	(-2268, 2268)	53	43
36 km	(-1296, 2160)	(-1728, 972)	97	76
12 km	(-648, 1080)	(-1548, -360)	145	100
4 km	(72, 372)	(-1380, -648)	166	184

Figure 1.1-1: MM5 Domains and Vertical Layers for Meteorological Modeling Episodes

1.2 MM5 Configuration

The final meteorological modeling configuration for the TexAQS II episodes was the result of numerous sensitivity tests, model performance evaluation, model input development, previous modeling experience, and contracted modeling review. The pre-processing of the MM5 input data followed the standard program progression of TERRAIN, REGRID, and INTERPF (NCAR, 2005b). The NESTDOWN program was used to interpolate the 12 km domain output to the 4 km domain input. The following bullets feature the essential parameters that were specified for the pre-processing programs:

TERRAIN

- Central Latitude and Longitude: 40.00 ° North and -100.00 ° West
- LSMDATA=1 to create data for the land-surface model
- Updated land use and land cover (LULC), land/water mask, vegetation fraction, and soil types using satellite based data
- Further details can be found in Attachment 2: Land Use and Land Cover (LULC) Characteristics.

REGRID

- National Center for Environmental Prediction (NCEP) North American Model (NAM) gridded output (formerly Eta model) used for model initialization (NCEP, 2009)
- Soil data added for NCEP - Oregon State Univ. - Air Force - Hydrological Research Laboratory (NOAH) land-surface model (NCAR, 2005a; Chen and Dudhia, 2001)

INTERPF

- Base state variables were set to Houston summer values: 1013 hPa sea-level pressure, a reference temperature lapse rate of 45 (K/ln p) , and a 304 °K sea-level temperature

MM5 was configured with parameterizations and improved input data to optimize the performance of the wind field. Wind speed and direction are important parameters predicted by the meteorological model for air quality modeling purposes because the wind field determines the proper transport and dispersion of pollutants. To improve the representation of the wind field and other parameters by MM5, the land use characteristics and sea surface temperatures on all domains were updated with high resolution satellite measurements. In the coastal Houston area the temperature gradient between the land and water is a defining feature of the local meteorological processes (Banta et al., 2005) and these data improvements were designed to help MM5 resolve them. The meteorological modeling appendices for the satellite-based LULC and SST data provide additional details regarding their development and use in MM5.

Based on previous modeling exercises by the TCEQ, and guidance from the EPA (EPA, 2007), and NCAR (Grell et. al,. 1994), the TexAQS II meteorological modeling employed data assimilation to improve model performance. This modeling tool allows the MM5 model to "relax" towards observed wind data during the model run through a process called Four-Dimensional Data Assimilation (FDDA), or nudging (Stauffer and Seaman, 1990; Stauffer et al., 1991; Stauffer and Seaman, 1994). The outer domains (108 km, 36 km, and 12 km) were nudged towards the gridded analysis of the North American Model (NAM) run by the National Centers for Environmental Prediction NCEP NAM (NCEP, 2009) for winds, temperature, and water vapor using the MM5 default nudging parameters. The fine scale 4km domain was nudged to quality assured observational data obtained during the TexAQS II from upper air wind profilers. Details of the data and nudging methodology can be found in Attachment 3: Data Assimilation.

Other MM5 schemes and options typically modified for air quality applications are shown in Table 1.2-1 below. A description of using the Grell cumulus scheme (Grell et al., 1994) on the 4 km domain can be found in Attachment 4: Application of Grell Cumulus Scheme. The choices for the other parameters were based on the MM5 configurations investigated as part of the Dec. 2004 HGB SIP revision and the Proposed HGB 2007 eight-hour ozone RFP SIP revision.

Table 1.2-1: TexAQS II MM5 modeling scheme choices

Domain	Nudging Type	PBL	Cumulus	Radiation	Land-Surface Model	Microphysics
108, 36, 12 km	Analysis 3-D	Eta	Grell	RRTM	NOAH	Simple Ice
4 km	Observational	Eta	Grell	RRTM	NOAH	Simple Ice

Notes: PBL = Planetary Boundary Layer
RRTM = Rapid Radiative Transfer Model
NOAH = NCEP Oregon State Air Force Hydrological Research Laboratory

MM5 output was post-processed using the Environ program MM5CAMx to convert the meteorological fields to the CAMx grid and input format (Environ, 2008). The TexAQS II MM5 output was processed with MM5CAMx options consistent with the choice of the Eta PBL scheme used in MM5. Since the Eta PBL scheme determines vertical mixing from a predicted turbulent kinetic energy (TKE), the MM5CAMx program was run with a switch to use this TKE

information in its calculation of the vertical diffusivity coefficients required for input into CAMx. The minimum threshold for vertical diffusivity (K_V) was set to 1.0.

2.1 MM5 Performance Evaluation Tools

2.1.1 Observations

To evaluate the performance of MM5, comparisons to observed data are made. For surface data, the TCEQ Continuous Air Monitoring Stations (CAMS) are used for comparison. There were over 100 CAMS in the MM5 4 km domain and more than 40 in the Houston Region 12 area (Figure 2.1.1-1: *All MM5 4km TCEQ CAMS (left) and Region 12 CAMS (right)*) during the 2005 and 2006 modeling periods. Because of the large number of CAMS monitors in the Houston region, an area wide average may smooth out smaller scale features. Zones of CAMS monitors were chosen to represent smaller geographic areas as defined in Figure 2.1.1-2: *CAMS in Model Performance Zones*. Evaluating model runs using the Houston Region and Zone averages instead of individual CAMS monitors proved to be efficient, allowing for the evaluation of more modeling sensitivities for the eight TexAQS II meteorological modeling episodes.

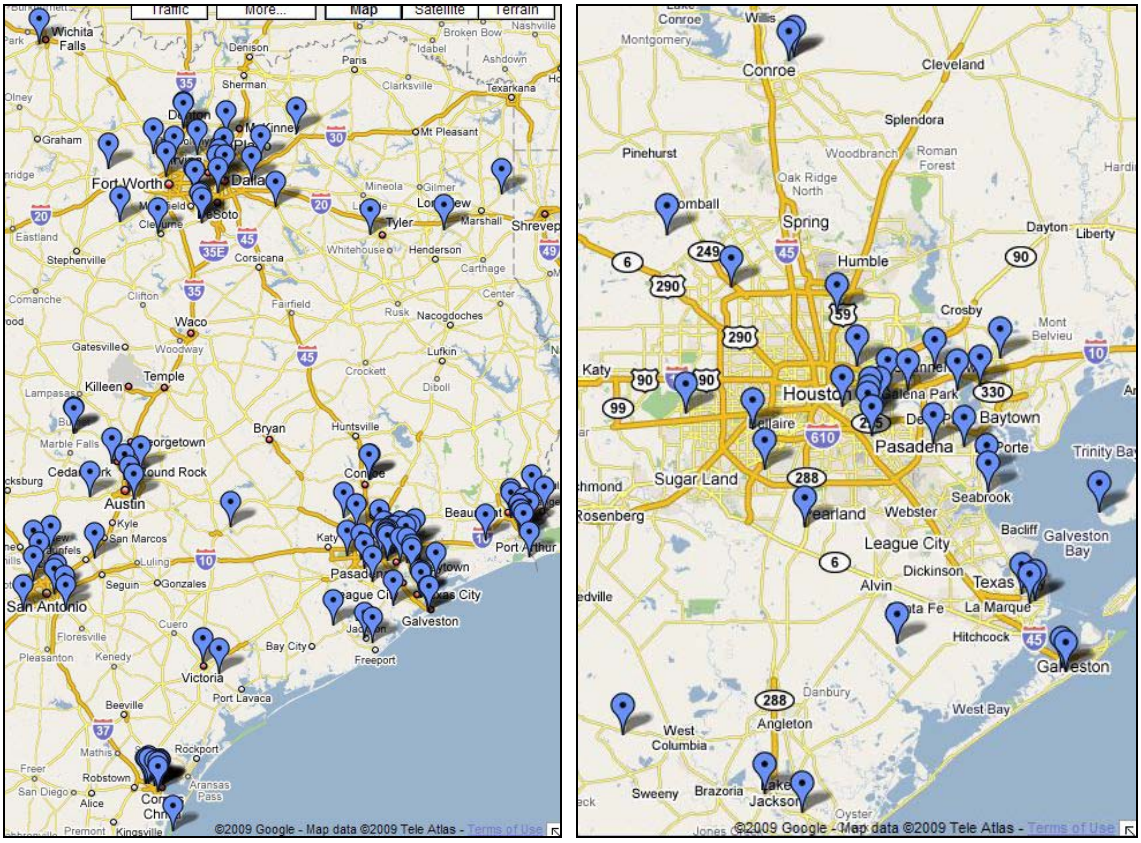

Figure 2.1.1-1: All MM5 4km TCEQ CAMS (left) and Region 12 CAMS (right)

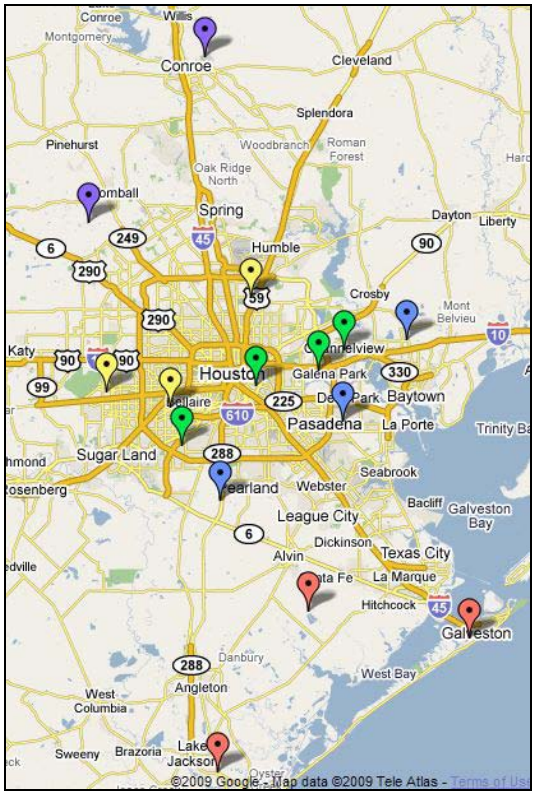

Downwind

Northwest Harris Co. C26
Conroe Relocated C78

Northwest Core

Westhollow C410
Bayland Park C53
Aldine C8

Southeast Core

Croquet C409
Regional Office C81
HRM-3 C603
Channelview C15

Ship Channel

Manvel Croix Park C84
Deer Park C35
Wallisville Road C617

Coastal Zone

Clute C11
Mustang Bayou C619
Galveston Airport C34

Figure 2.1.1-2: CAMS in Model Performance Zones

The TexAQS II profiler network was used to evaluate the performance of MM5's winds above the surface layer (Figure 2.1.1-3: *TexAQS II profilers in 4km MM5 domain*). Up to 15 profilers collected data during the 2005 and 2006 modeling episodes, including estimates of planetary boundary layer (PBL) depth.

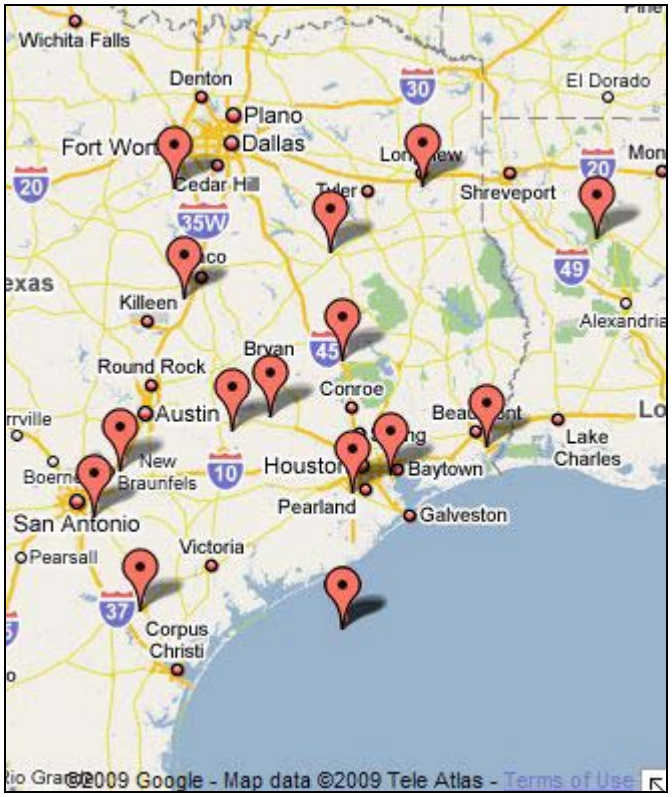

Figure 2.1.1-3: TexAQS II profilers in 4km MM5 domain

2.1.2 Time Series Panel

Time series panels comparing modeled and observed CAMS surface wind direction, wind speed, and temperature were created to evaluate the model's performance over an entire episode. The observations are hourly averages of individual and grouped monitors (e.g., Zones, TCEQ Region-wide, or domain-wide). As an example of a time series panel, Figure 2.1.2-1: *Region 12 average wind speed time series for 2006ep1a episode*, shows the time series of wind speed averaged over all Region 12 monitors from the 2006ep1a episode. The X axis of the time series panels is the date and time in Central Standard Time (CST) of the modeling episode. The Y axis represents the range of values of the parameter (e.g. wind speed). The title of the panel indicates the geographic region, parameter (wind speed, temperature, etc), model and run name.

The compared model hourly values are from the monitor's corresponding model grid cell. MM5's first model layer cell value (red line – MM5) and the probe height interpolated cell value (blue line – MM5probe) are both plotted. For wind direction, the probe height and first model layer values are usually the same. For wind speed the probe height is slightly slower and for temperature the probe height is warmer than the middle of the first model layer. The first model layer values are passed to the photochemical model so they are important to evaluate. Also shown are time series of bias and mean absolute error using the model's first layer values.

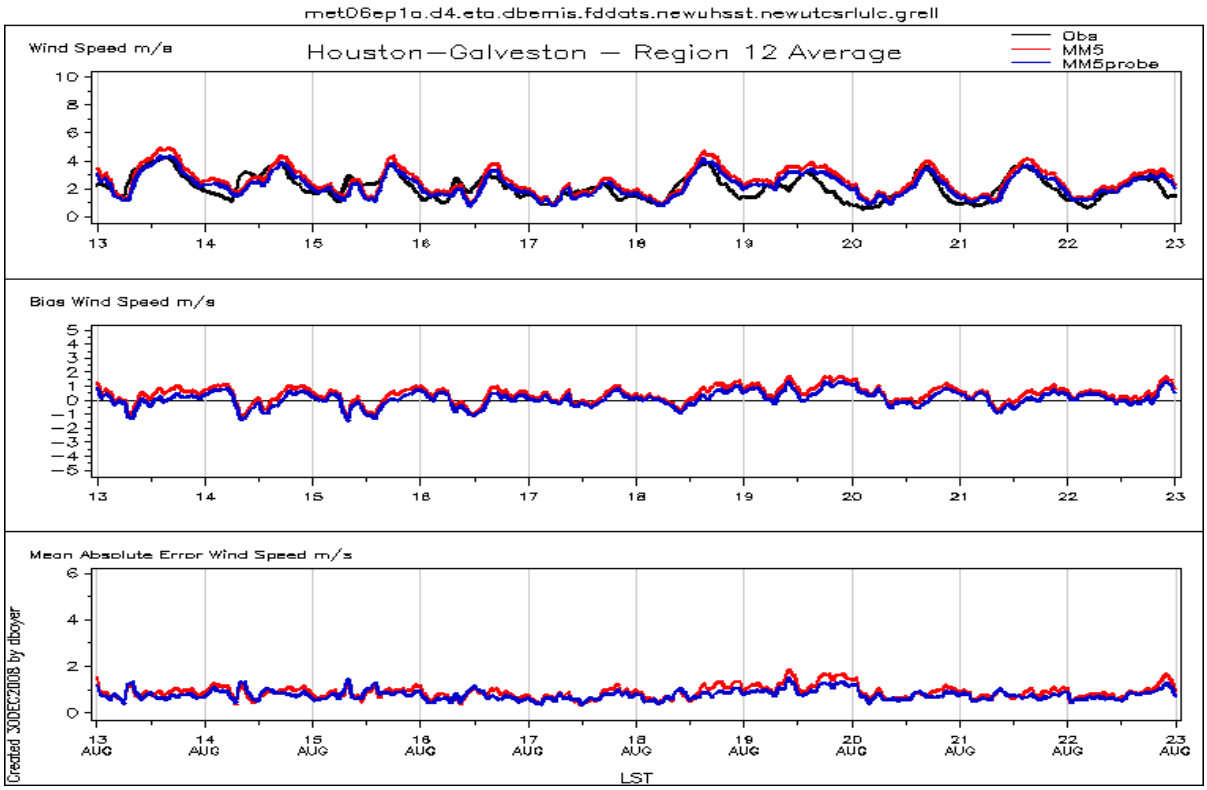

Figure 2.1.2-1: Region 12 average wind speed time series for 2006ep1a episode

2.1.3 Scatter Plots

Scatter plots of model versus observations were created to correlate how well the model statistically performs at monitors (groups of monitors), episode days, and model layers. As with the time series, the model is compared to individual, zones, region-wide, and domain-wide groups of monitors for every hour (per day or episode). For surface data, the observations are compared to the model's first layer values. The percent of hours (all, day, or night) where the model is within the accuracy benchmarks (e.g. wind direction less than or equal to 30 degrees or wind speed less than or equal to 2 meters per second) is depicted in the upper right of the plot. Tables of these accuracy percentages are also presented to summarize the scatter plots.

A linear regression line is fitted to the data and is shown in green. The correlation equation and coefficient of determination R^2 for the regression line is above the plot in green. For the model to perfectly fit the data the regression line would fall on the one-to-one line and the R^2 would be 1.0. The R^2 indicates how well MM5 predicts the observations, with higher values indicating better model performance. As the model is an imperfect representation of the real world and the observations have biases, errors, and limitations, a perfect fit is not expected. In fact a perfect fit (or very close to it) may be reason to suspect that MM5 is being nudged too hard (see Attachment 3: Data Assimilation). For wind direction, the regression line and R^2 may not be meaningful since both 0° and 360° symbolize north winds.

The plot titles are the same as the time series. For surface data scatter plots, the X axis is the modeled data and the Y axis is the observations. For the upper air wind data scatter plots, the X axis is the observations and the Y axis is the modeled data. The total number of date-time points (hours) and observations (hour-monitor pairs) that comprise the plot are listed next to the parameter name. Figure 2.1.3-1: *Southwest Core Zone average wind speed scatter plot for 2006ep1c episode* shows an example or the Southeast Core Zone's wind speed over the 2006ep1c episode.

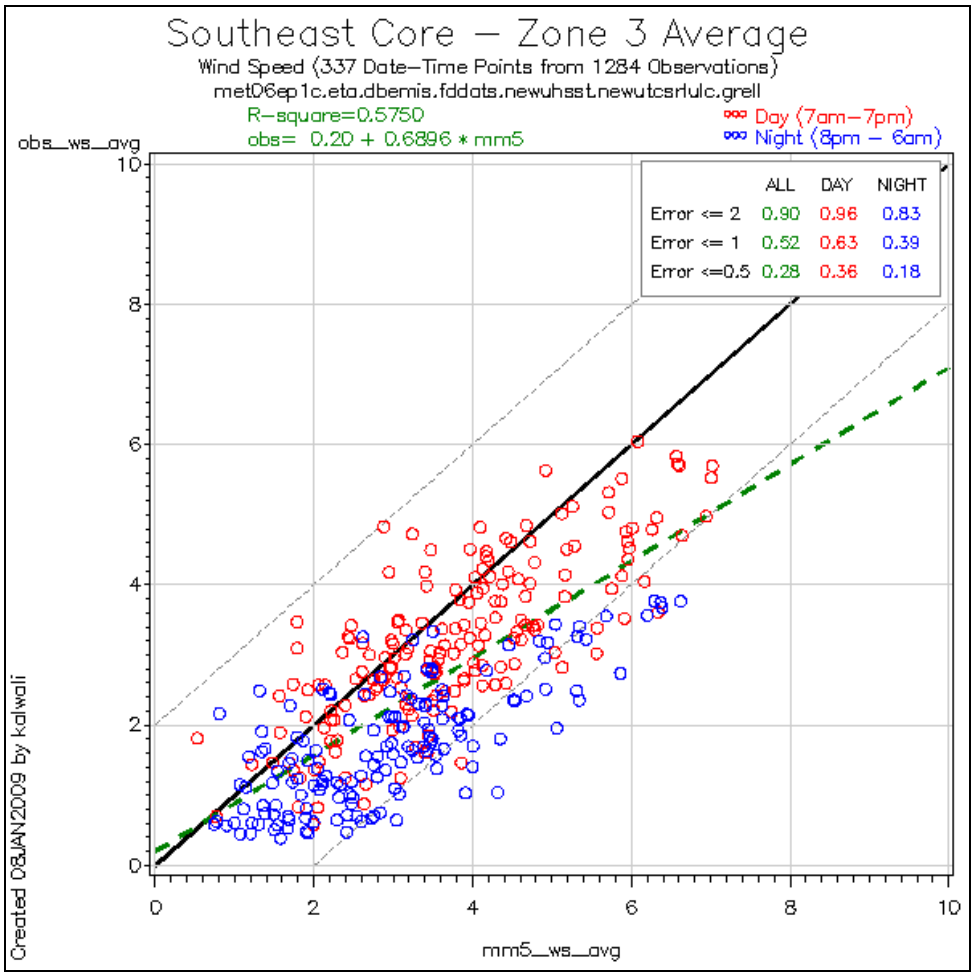

Figure 2.1.3-1: Southwest Core Zone average wind speed scatter plot for 2006ep1c episode

2.1.4 Time-height plots

Time-height plots represent the upper air horizontal wind conditions at profiler locations over one episode day. Vertical winds (rising or descending air) are not shown. The model winds (CAMx input) are shown as blue vectors and the observed winds (profiler) are shown as red vectors. Each hour of the episode day is depicted on the x-axis. Winds from just above the surface to 3 km are illustrated by vectors pointing in the compass direction from where the wind is blowing. A

longer vector indicates faster wind speeds. In figure 2.1.4-1 below, at midnight CST on 5/19/2005 a southwest wind greater than 10 m/s blows at 2.5 km above the surface at the La Porte profiler (red vector). The model predicts winds from the south and much lighter (blue vector). Observed winds were not available above 2.5 km on this day.

Also on these plots are the model (blue) and profiler (red) estimated planetary boundary layer (PBL) depths shown by horizontal lines between hours. The observed data is generally only available during daylight hours. At 10:00 AM CST in Figure 2.1.4-1 below, the model and observed PBL depth agree well but differ by 500 meters at noon.

Based on Knoderer et al. (2008), the morning rise of the PBL may be more important to ozone production than the peak mixing depth. The morning rise was focused on for model performance evaluation as well as gross differences. More information regarding the derivation of mixing heights from the radar wind profiler data can be found in Knoderer and MacDonald (2007).

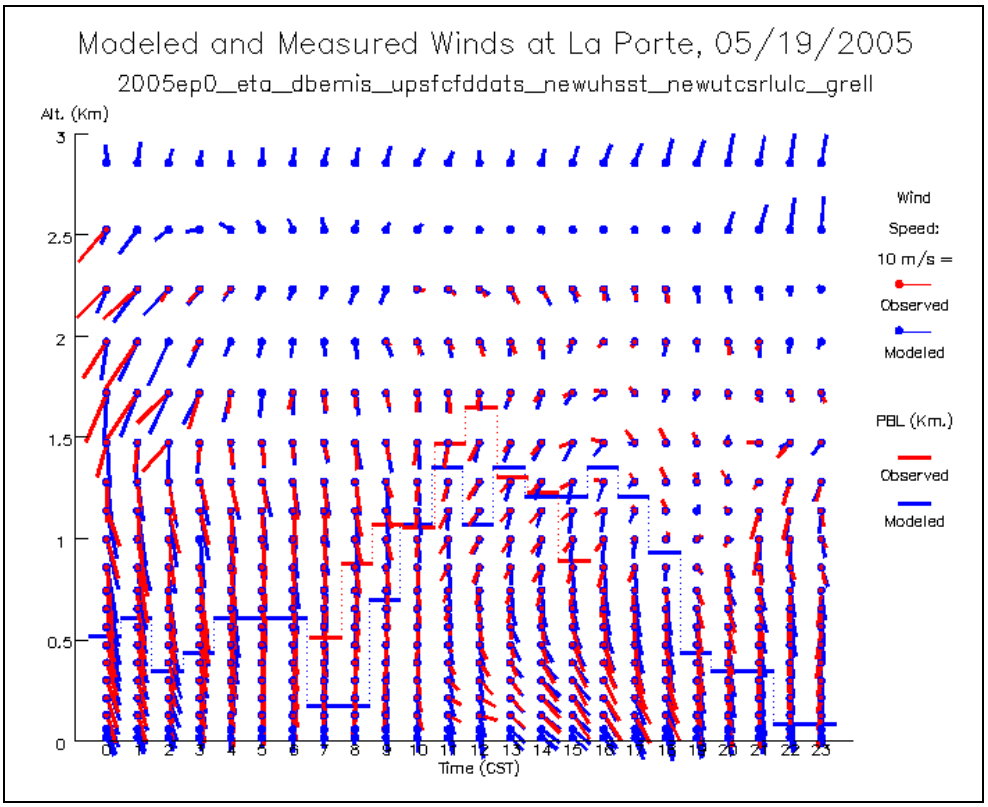

Figure 2.1.4-1: Time-height plot example (5/19/2005 at La Porte profiler)

2.1.5 Surface Wind Field Plots

Surface wind field plots show the surface layer of CAMx input winds (mm5camx converted) compared to observations for one hour. The tail of each vector points in the compass direction from which the wind is blowing. Modeled winds are shown in blue; observed winds are shown in red. This plot type yields a visual depiction of the observed wind flow, and how well the model represents that flow. Galveston Bay breezes, sea breezes from the Gulf of Mexico, thunderstorm outflow, and other wind phenomena can be identified using these plots. Figure 2.1.5: *Surface wind field plots for June 5, 2006 at 12:00 CST showing Galveston Bay breeze (left) and August 28, 2006 at 16:00 CST* shows an example of a Galveston Bay breeze (left) and spurious surface divergence patterns (right) that appear inconsistent with observations in eastern Harris County.

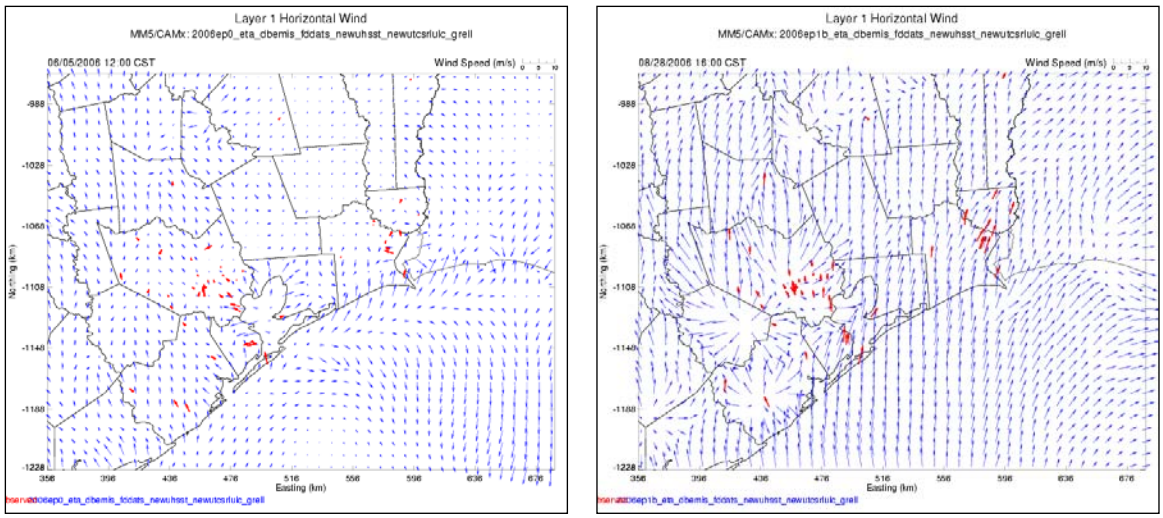

Figure 2.1.5-1: Surface wind field plots for June 5, 2006 at 12:00 CST showing Galveston Bay breeze (left) and August 28, 2006 at 16:00 CST showing spurious surface divergence patterns that were not observed (right)

2.1.6 Trajectories

One of the most useful and intuitive methods for evaluating modeled wind fields is by using wind trajectories. A forward trajectory shows the path an air parcel from some location (say, a major emission source), takes as it moves with the wind. A back trajectory shows the path that an air parcel followed before arriving at a specific location (say, a monitor). Because the trajectories inherently describe source-receptor relationships, they are especially appropriate for air-quality applications.

TCEQ calculated forward and back trajectories with endpoints at several locations in the HGB area (plus two in the Beaumont/Port Arthur area) for every hour of every episode day modeled using a FORTRAN program obtained from Carl Berkowitz at Pacific Northwest National Laboratories. This program is based on a simple kinematic model that used an inverse distance-squared weighting scheme to evaluate the u- and v-wind components of each trajectory (Berkowitz et al, 2005) Input for this program is five-minute average wind speed and direction observations from a total of 72 surface meteorological sites in and around the HGB area. This program was also used to calculate back-trajectories used in the PSCF-based emissions reconciliation work described elsewhere in this SIP revision.

The trajectory program was used to develop sets of comparable trajectories based on observational data and meteorological fields as follows: First, hourly mean modeled wind components were extracted from the meteorological data files at the location of each of the 72 surface meteorological sites. Five-minute observations were generated by simply replicating the hourly mean wind speed and direction 12 times. Observed hourly observations were similarly used to generate five-minute averages by replicating the hourly observations 12 times each (this was done to make the comparisons between the model-based and observation-based trajectories fair). Both the modeled and measured data were formatted for input to the FORTRAN program, and trajectories were generated using each set of inputs. Trajectories were generated both from the raw MM5 output files, and also from the CAMx input files which have been processed by the MM5CAMx data formatting and conversion program. Both forward and backward trajectories were generated for each hour of each episode day, but only forward trajectories generated from the CAMx inputs are used in the model performance evaluation discussed in this appendix.

An example comparing model-based and observation trajectories is shown in Figure 2.1.6-1. In this plot, it is easy to see the path an air parcel takes as it leaves each starting location at 6 AM. The first dot along the trajectory represents the air parcel's position after one hour, the next dot two hours, etc. The larger circles represent monitoring locations, colored according to the

observed peak 8-hour ozone concentration observed at that site on that day. Both sets of trajectories show light wind speeds starting from the northwest, then veering clockwise through the day to become southeasterly by early afternoon. In this case, the modeled winds replicate the observations reasonably well, and at the end of the day the trajectory points from each set of trajectories usually agree to within 20-30 km.

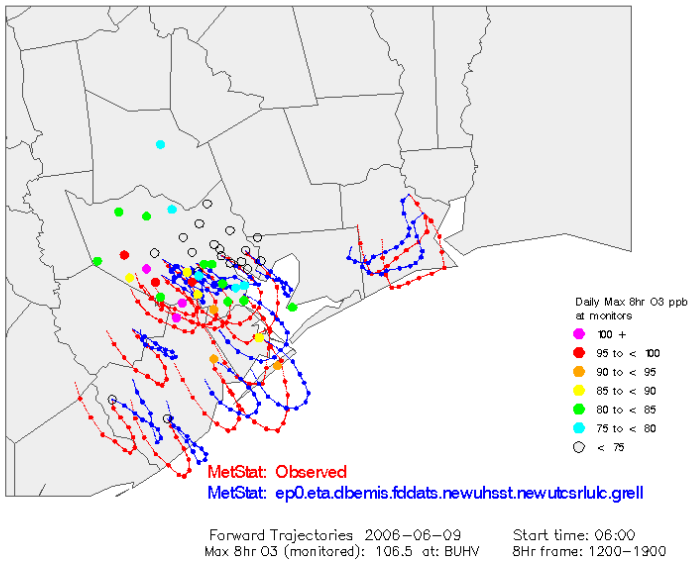

Figure 2.1.6-1: 6 AM forward wind trajectories based on modeled and observed one-hour average wind components for June 9, 2006

2.2 MM5 Modeling Performance

The following section describes the performance of the final MM5 modeling configuration for each of the TexAQS II episodes, as listed in Table 1.1-1. Due to the large number of episode days, the performance evaluation will focus on the days when high ozone and notable meteorological phenomena occurred (Knoderer et al., 2008; Nielsen-Gammon, 2007a; Nielsen-Gammon, 2007b; TCEQ, 2005; TCEQ, 2006). Wind field performance was deemed to be the most important for photochemical modeling input followed by temperature, planetary boundary layer height, and other important features.

The MM5 modeling was evaluated by comparing the hourly modeled and measured wind speed, wind direction, and temperature for all monitors in the HGB area. Figure 2.2-1: *Meteorological Modeling Performance Accuracy Statistics* exhibits the percent of hours for which the average absolute difference between the modeled and measured wind speed, wind direction, and temperature, for all monitors in the HGB area, was within the specified accuracy benchmarks (Emery et. al., 2001)(e.g., wind speed less than or equal two meters per second: i.e. WSPD $\leq$ 2 m/s). All performance evaluation products are available on TCEQ's ftp site (ftp://ftp.tceq.state.tx.us/pub/OEPAA/TAD/Modeling/HGB8H2/mm5).

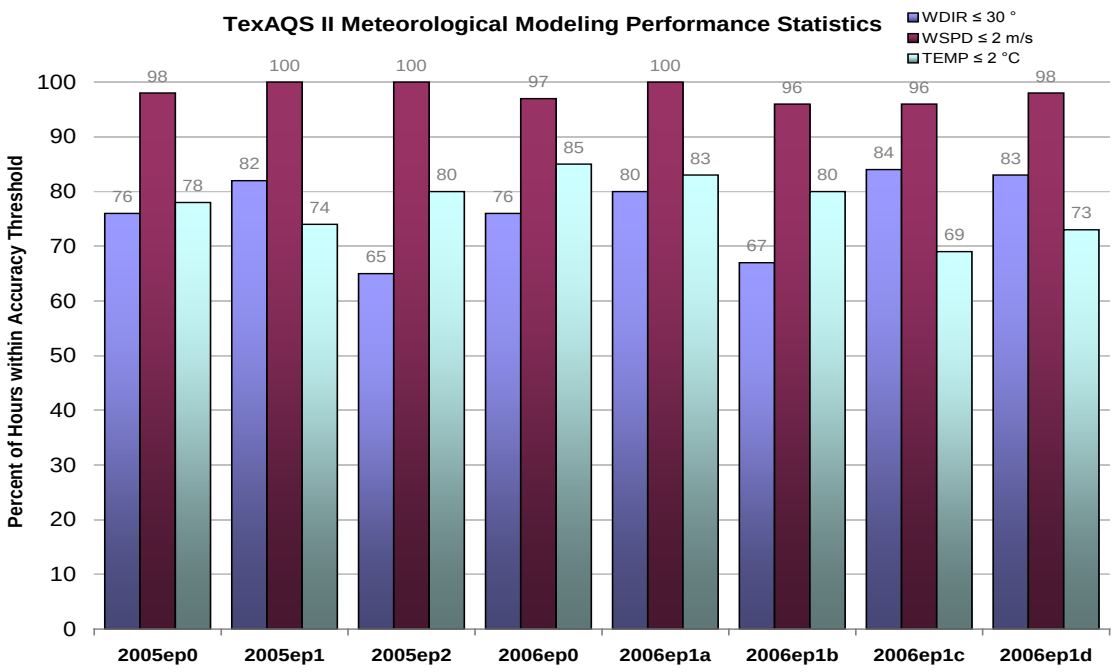

Figure 2.2-1: Meteorological Modeling Performance Accuracy Statistics
Notes: WDIR = Wind Direction
WSPD = Wind Speed
TEMP = Temperature

Table 2-2-1: Average Houston Region 12 Percent Accuracy for all Meteorological Modeling Episodes

Episode	Wind Direction (°) Error ≤ 30 / 20 / 10	Wind Speed (m/s) Error ≤ 2 / 1 / 0.5	Temperature (°C) Error ≤ 2 / 1 / 0.5
2005ep0	76 / 67 / 49	98 / 73 / 40	78 / 49 / 30
2005ep1	82 / 71 / 40	100 / 93 / 60	74 / 50 / 28
2005ep2	65 / 54 / 33	100 / 75 / 43	80 / 57 / 31
2006ep0	76 / 63 / 45	97 / 72 / 38	85 / 57 / 33
2006ep1a	80 / 67 / 43	100 / 83 / 43	83 / 61 / 39
2006ep1b	67 / 54 / 33	96 / 63 / 26	80 / 52 / 25
2006ep1c	84 / 76 / 57	96 / 57 / 29	69 / 33 / 16
2006ep1d	83 / 66 / 33	98 / 75 / 42	73 / 51 / 32

2.3 2005ep0 Performance Evaluation

May-June 2005 episode (2005ep0) Summary

High ozone days occurred on May 27 and June 2. On May 27, two monitors had 8-hour averages above 90 ppb, and three had values over 100 ppb, with the domain high 0f 116 ppb. June 2 had the episode highest values for the episode. There were three monitors reporting 8-hour ozone averages in the 90's and 10 monitors over 100 ppb. Of those ten, three were over 120 ppb. The domain and episode peak value for 8-hour ozone was 125 ppb on June 2.

This episode began with several days having generally tropical (e.g. southerly) flow. One these days, and similar days on other episodes, the background air quality is generally good. However, light winds still contributed to a number of exceedances. The most important meteorological features include a frontal passage on May 26 and the passage of a high pressure center on June 1st. High ozone periods followed each of these events.

General Model Performance

Table 2.3-1: *Average Houston Region 12 Percent Accuracy by Episode, Zone, and Peak Days* summarizes wind direction, wind speed, and temperature according to three threshold metrics. For the entire episode, region-wide performance is generally good, especially for wind speed. Previous modeling efforts used a threshold of 2 m/s to establish good performance. The present MM5 modeling is within that bound 98% of the time. A tighter standard can therefore be considered: almost three-fourths of the wind speed data is within 1 m/s of observed data. For wind direction accuracy, a threshold of 20 degrees is consistent with goals set in previous modeling. For this episode, modeled wind directions were within 20 degrees of reported data two-thirds of the time.

Table 2.3-1: **Average Houston Region 12 Percent Accuracy by Episode, Zone, and Peak Days**

Number of days	**Geographic Area**	**Wind direction (°) % Accuracy < 30 / 20 / 10**	**Wind Speed (m/s) % Accuracy < 2.0 / 1.0 / 0.5**	**Temperature (°C) % Accuracy < 2.0 / 1.0 / 0.5**
Entire Episode	Region 12	76 / 67 / 49	98 / 73 / 40	**78 / 49 / 30**
Entire Episode	Zone 1	72 / 61 / 40	94 / 68 / 39	**74 / 46 / 27**
Entire Episode	Zone 2	66 / 56 / 34	93 / 56 / 33	**70 / 44 / 24**
Entire Episode	Zone 3	69 / 56 / 34	95 / 60 / 33	**75 / 46 / 26**
Entire Episode	Zone 4	64 / 54 / 29	92 / 57 / 31	**60 / 30 / 15**
Entire Episode	Zone 5	55 / 45 / 24	90 / 53 / 29	**74 / 44 / 20**
May 27	Region 12	75 / 58 / 17	100 / 83 / 63	**92 / 83 / 67**
June 2	**Region 12**	**67 / 58 / 50**	**100 / 96 / 58**	**92 / 58 / 25**

Ideally, modeled temperature would be within one degree of data. However, known temperature biases in MM5 often lead to using a more relaxed threshold of 2 degrees.

One noticeable feature of this episode is that performance is best near the coast and becomes somewhat less as one moves towards interior zones further inland. On the other hand, it is encouraging to note that on May 27 and June 2, the modeled wind speed was better than the episode average and wind direction.

May 27, 2005 Features

On May 25, a frontal system approached from the northeast. From Figure 2.3-1: *Region 12 average wind direction time series for 2005ep0 episode* the domain winds shift to the north and the front passes on the 26. On May 27, the winds veer around to the east. Thus, ozone precursors from two days prior – transported north by southerly winds - plus continental air from the east likely re-circulated into the Houston area and contributed to local ozone production. Morning winds were generally light and by afternoon continued to veer to the south so that the urban air mass crossed back over the ship channel.

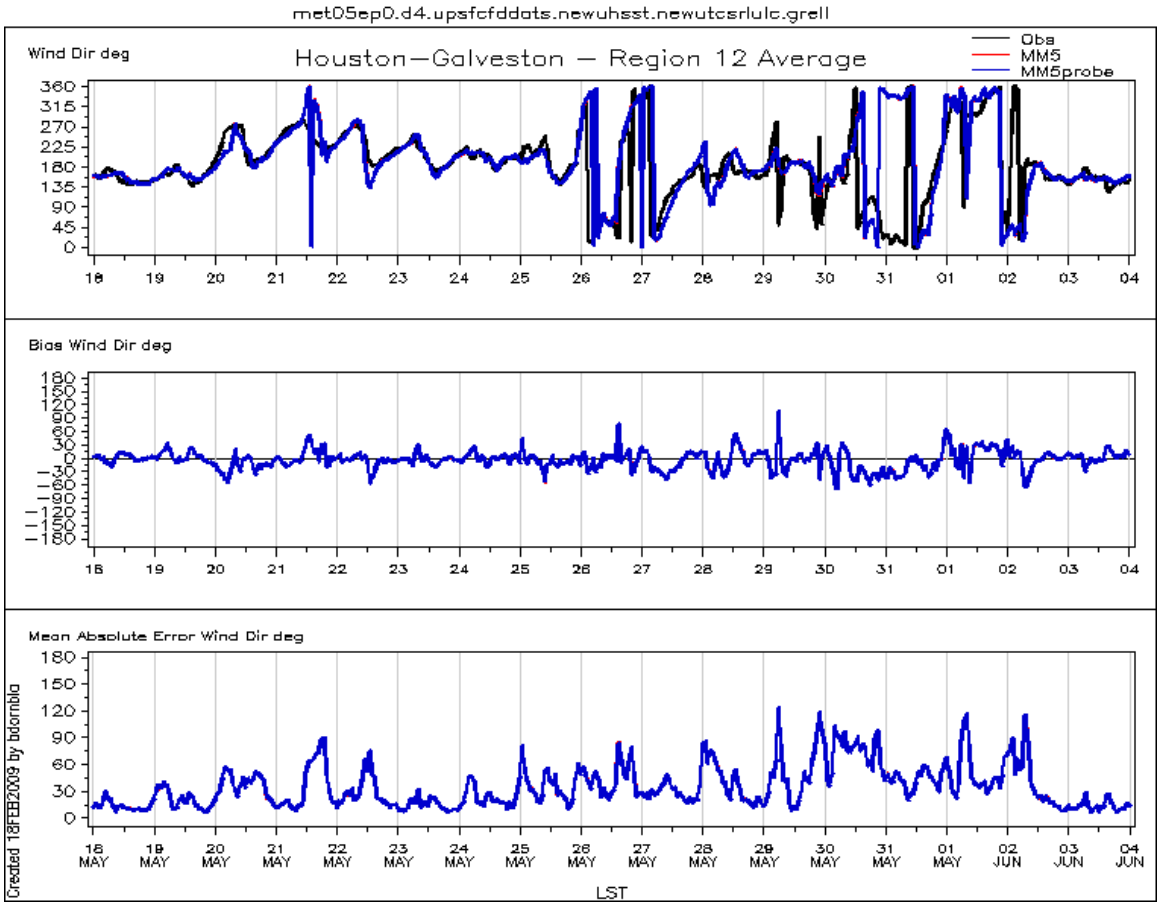

Figure 2.3-1: Region 12 average wind direction time series for 2005ep0 episode

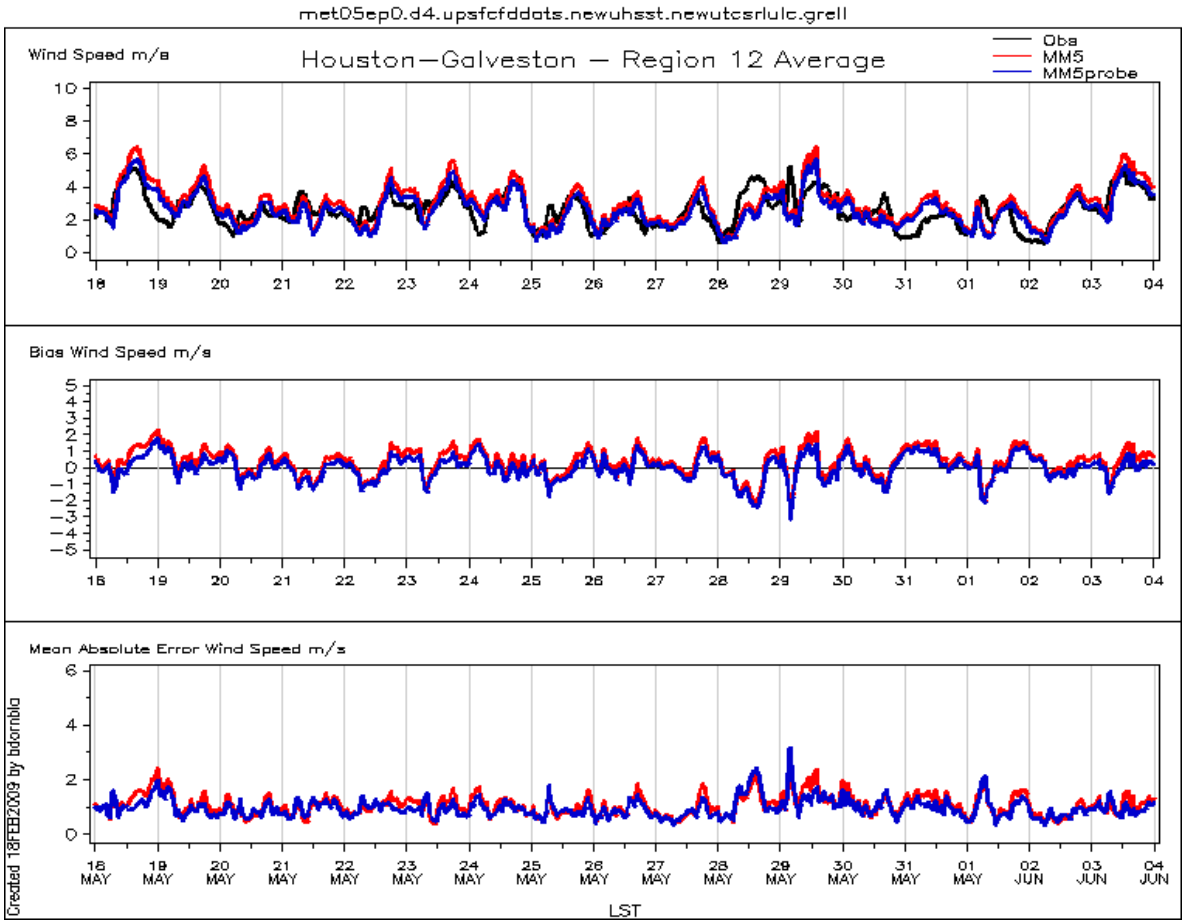

Figure 2.3-2: **Region 12 average wind speed time series for 2005ep0 episode**

June 2, 2005 Features

Winds were generally from the northwest during the day of June 1 followed by a flow-reversal in the late afternoon and early evening. This rather abrupt change can be seen in wind direction time series. The morning of June 2 had light winds from the south generally between 1 and 2 m/s. Thus, the peak was seen north of the ship channel later in the day, but the local emissions were added to those of the previous day.

The trajectory plots in Figure 2.3-3a: *12-hour forward trajectory at 6:00 CST on June 1, 2005* and Figure 2.3-3b: 12-hour forward trajectory at 18:00 CST on June 1, 2005 show different performance for daytime and evening winds. As seen in the second figure, MM5 wind speeds are too strong as stagnation begins (although the next day statistics look good). The model will capture the veering to the south although is likely to shift the peak ozone a bit to the west of the actual location.

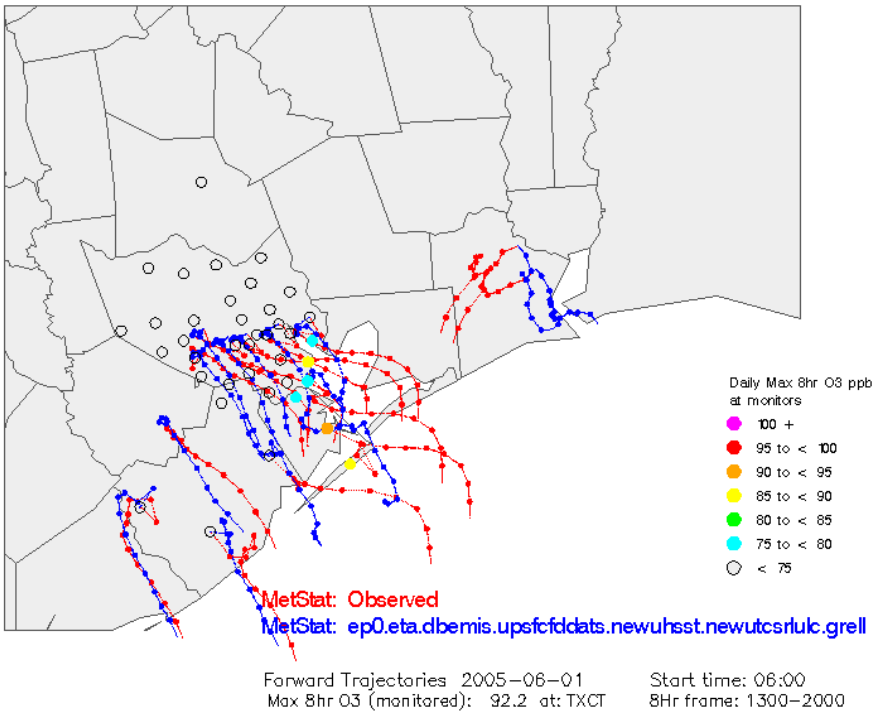

Figure 2.3-3a: 12-hour forward trajectory at 6:00 CST on June 1, 2005

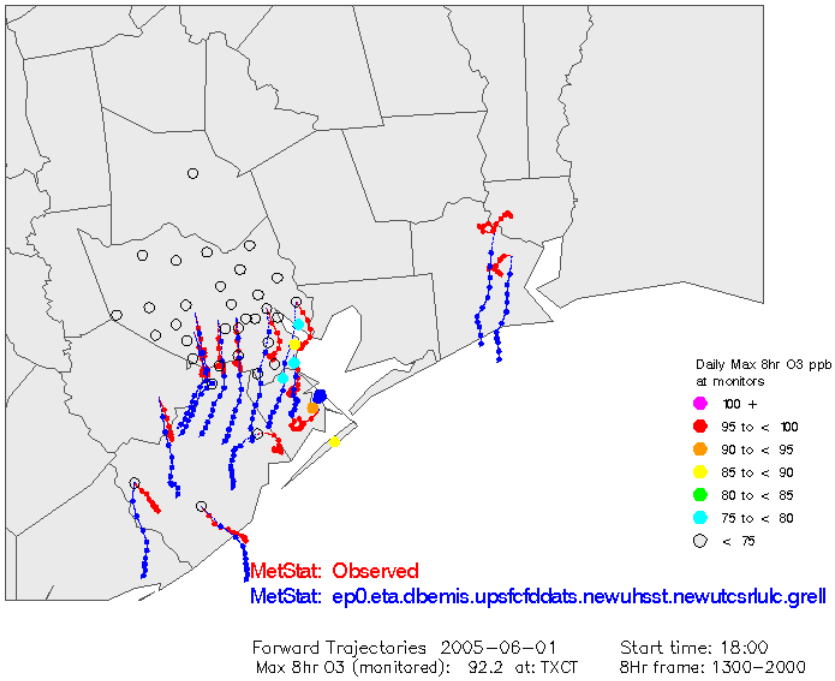

Figure 2.3-3b: 12-hour forward trajectory at 18:00 CST on June 1, 2005

2.4 2005ep1 Performance Evaluation

June 2005 episode (2005ep1) Summary

During this period there were days with a typical coastal oscillation, but the generally easterly component to veering winds suggest that background ozone added to the local contribution. The 21st had eleven sites in exceedance, and three monitors recording eight-hour ozone over 100 ppb. On June 22, 15 sites had eight-hour ozone exceedances, with an episode high ozone of 103 ppb.

General model performance

The performance metrics described above for wind speed, wind direction, and temperatures look very good across the entire episode. Also, there does not seem to be a discernable trend of decreasing accuracy as one moves inland from the coast. Both the peak days of June 21 and June 22 have very good wind speed accuracy. On the other hand, while June 22 has wind direction performance which matches the episode average, June 21 is somewhat less accurate.

Table 2.4-1: **Average Houston Region 12 Percent Accuracy by Episode, Zone, and Peak Days**

Number of days	**Geographic Area**	**Wind direction (°) % Accuracy < 30 / 20 / 10**	**Wind Speed (m/s) % Accuracy < 2.0 / 1.0 / 0.5**	**Temperature (°C) % Accuracy < 2.0 / 1.0 / 0.5**
Entire Episode	Region 12	82 / 71 / 40	100 / 93 / 60	**74 / 50 / 28**
Entire Episode	Zone 1	75 / 61 / 37	98 / 75 / 40	**71 / 45 / 19**
Entire Episode	Zone 2	67 / 54 / 31	98 / 81 / 43	**73 / 48 / 27**
Entire Episode	Zone 3	75 / 61 / 36	100 / 83 / 48	**73 / 51 / 22**
Entire Episode	Zone 4	66 / 52 / 30	97 / 73 / 40	**61 / 33 / 16**
Entire Episode	Zone 5	56 / 45 / 25	93 / 63 / 33	**64 / 41 / 21**
June 21	Region 12	67 / 58 / 17	100 / 83 / 46	**100 / 25 / 17**
June 22	**Region 12**	**75 / 71 / 17**	**96 / 88 / 54**	**83 / 46 / 13**

The time series in Figure 2,4-1: *Region 12 average wind direction time series for 2005ep1 episode* shows several key features of the episode. Following generally southerly flow, the approach of a front on the 18th caused winds to back from southwest back to the northeast. The high ozone day of the 21st is preceded by generally easterly flow which may contribute high background ozone. The days of June 21-22 showed classic flow reversal on top of regionally veering of winds carrying emissions around from the ship channel to the southeast and back over southwest Harris County. June 23 through June 28 had daily winds shifting from northeast to southeast leading to consistent and repeated exceedances to the west and northwest of the Houston downtown.

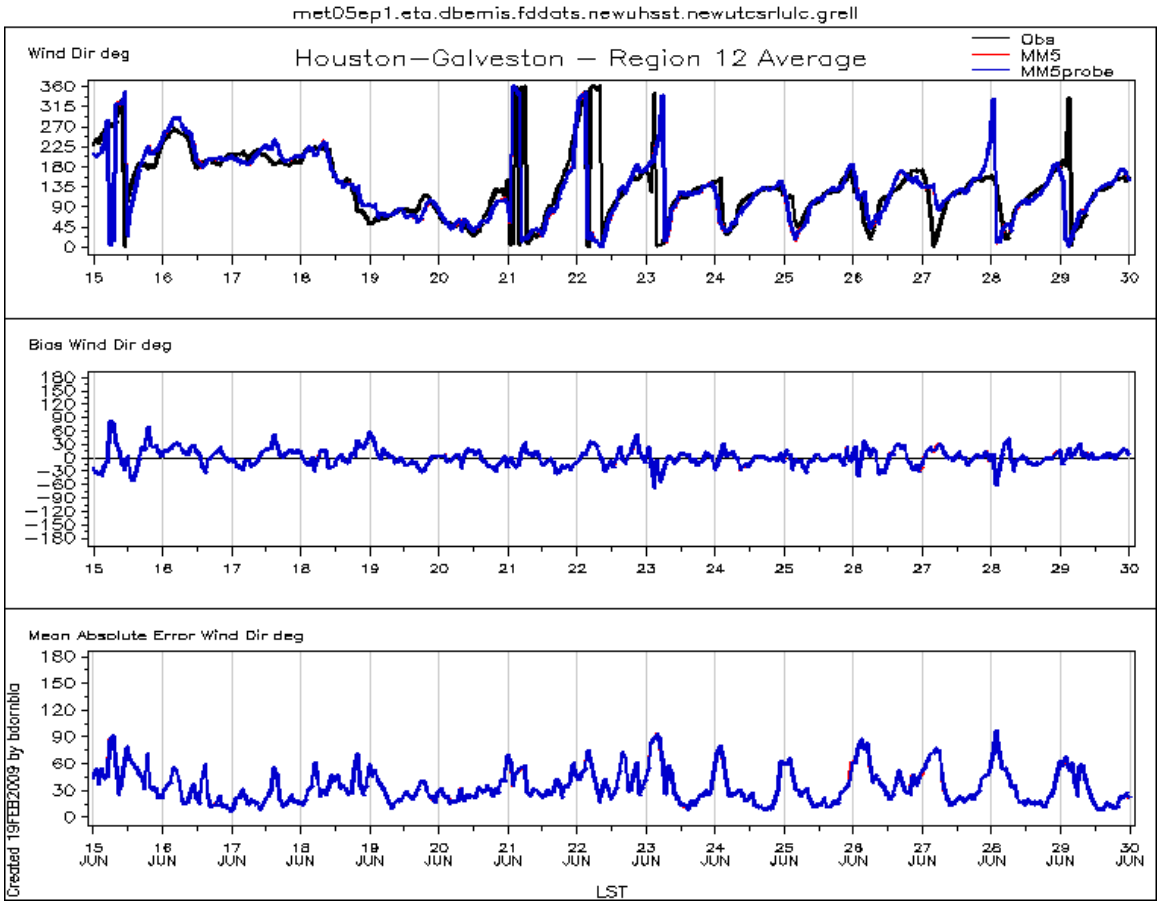

Figure 2.4-1: Region 12 average wind direction time series for 2005ep1 episode

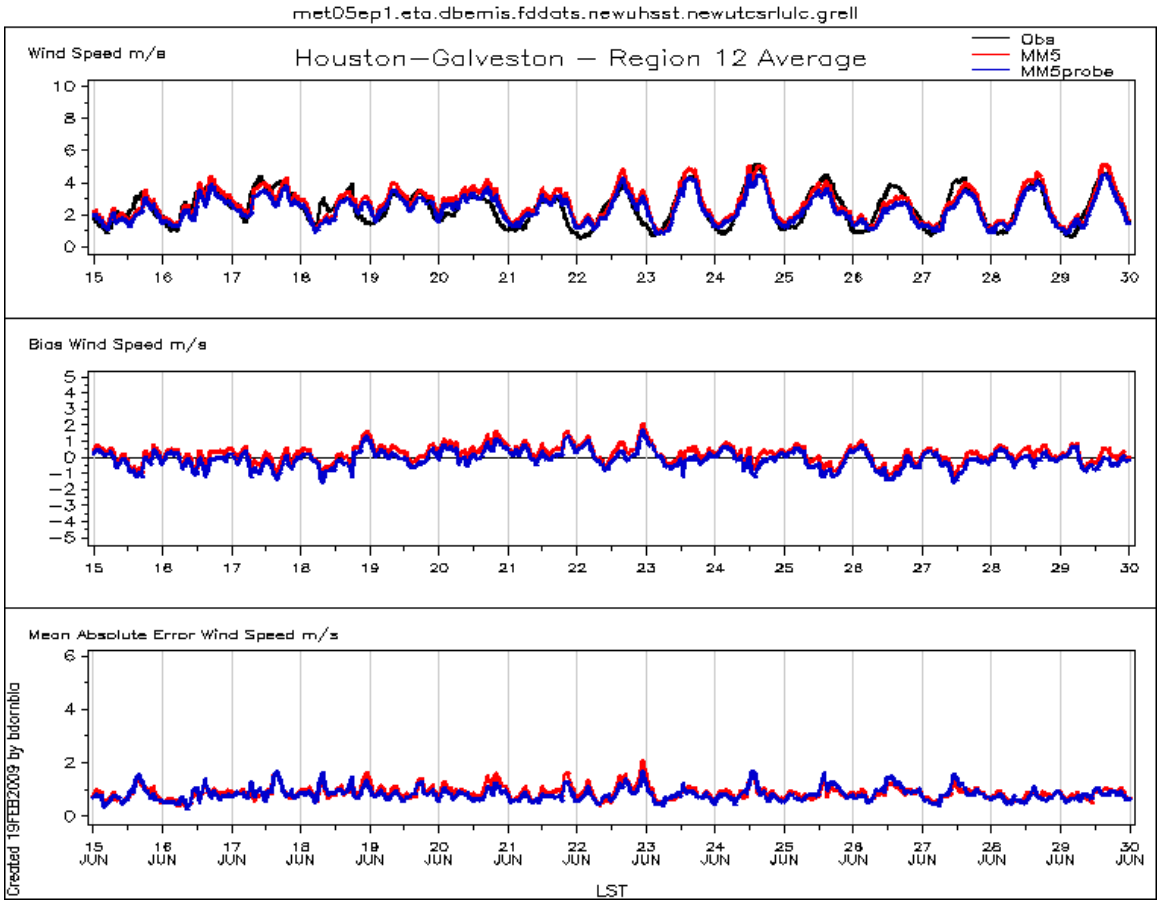

Figure 2.4-2: Region 12 average wind speed time series for 2005ep1 episode

June 21 Features

The MM5 wind direction and wind speed time series in Figures 2.4-1: *Region 12 average wind direction time series for 2005ep1 episode* and 2.4-2: *Region 12 average wind speed time series for 2005ep1 episode* indicate generally good performance on our two key days. Figure 2.4-3: *Region 12 average wind direction and speed scatter plots for June 21, 2005* show performance for stations reporting on June 21. These plots have additional information which distinguishes the averages calculated for each of the day time hours from the night time hours. During two night time hours, MM5 slightly over-predicts wind speeds. During four night time hours, the average of predicted wind directions differs from the observed hourly averages by more than thirty degrees. These differences are likely not significant for CAMx modeling since the directional errors are more likely at very light wind speeds.

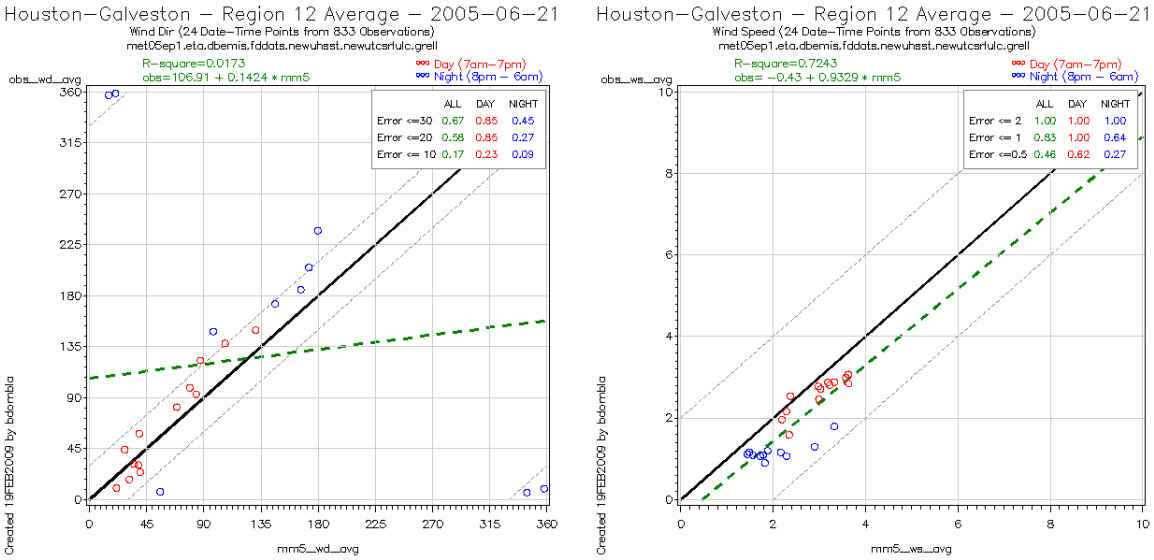

Figure 2.4-3: Region 12 average wind direction and speed scatter plots for June 21, 2005

The good performance statistics suggest that CAMx modeling on June 21 and 22 should have reliable meteorological inputs. On the other hand, previous modeling experience has shown that when there is a strong flow reversal or a nearly complete rotation of winds through the day – based upon the hourly averages of HGB sites – that very localized features near Galveston Bay can complicate the "big picture." One example of a subtle effect on the veering of the wind due to local features of Galveston Bay is shown in Figure 2.4-4: *Surface wind field plots for June 21, 2005, at 12:00 CST* in which surface winds are plotted for noon on June 21st. Near Texas City, to the south of the ship channel, observed winds have pushed perpendicularly to the shoreline of the Bay. These localized winds are from the southeast while MM5 winds are still from the northeast. The trajectories in Figure 2.4-5: *12-hour forward trajectory at 8:00 CST on June 21, 2005*, indicate that small differences in the MM5 winds near Galveston Bay may produce a veering which is more gradual than actually occurred that day.

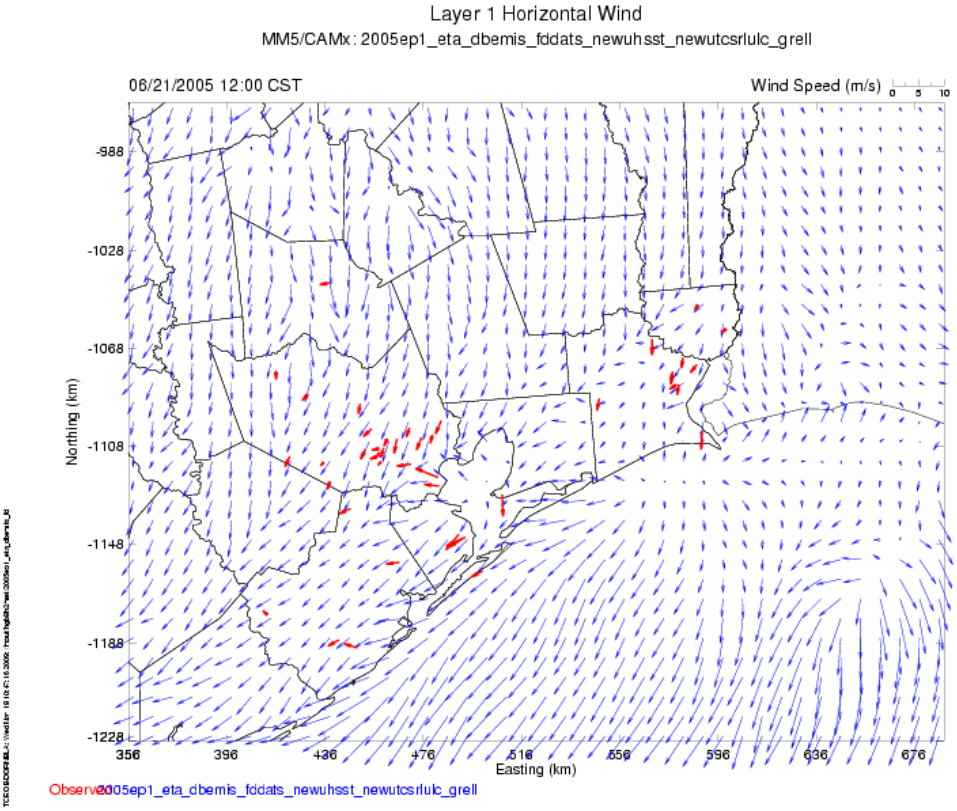

Figure 2.4-4: Surface wind field plots for June 21, 2005 at 12:00 CST

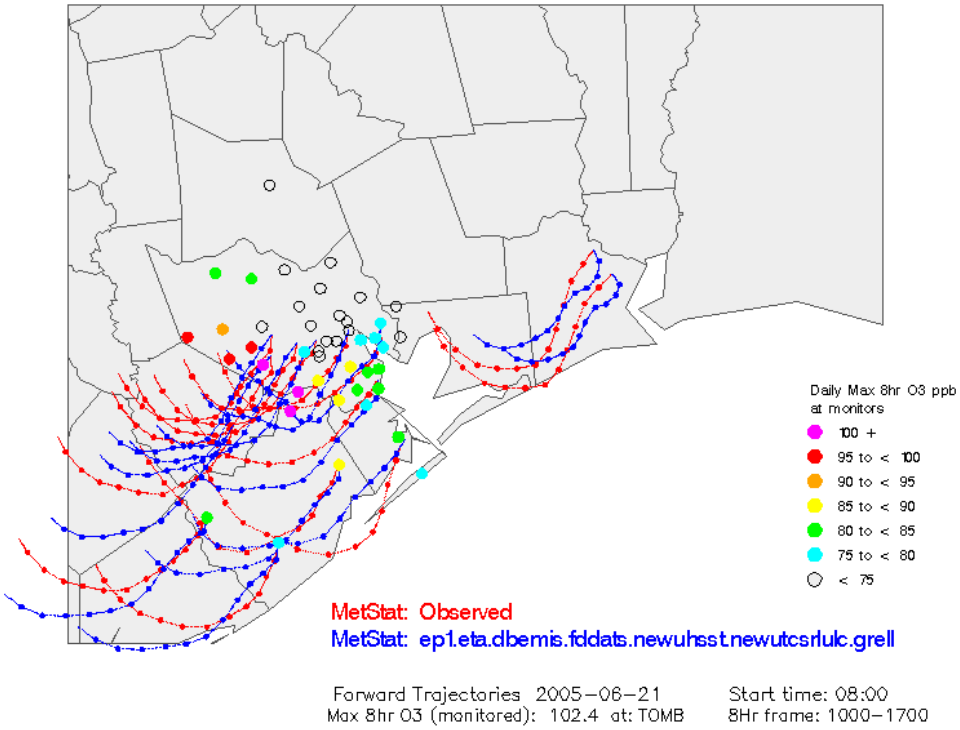

Figure 2.4-5: 12-hour forward trajectory at 8:00 CST on June 21, 2006

June 22 Features

The scatter plot in Figure 2,4-6: *Region 12 average wind direction and speed scatter plots for June 22, 2005* indicates that on June 22 MM5 modeled wind direction was excellent throughout the day. As on many episode days, there is a slightly high bias in wind speeds during the night

time hours, as is seen in right side of the figure, but only one of those hours strays close to our preferred threshold. Many graphics have subtle features. The day time wind speeds in the scatter plot look very good, albeit with a very small negative bias. However, the consequence of even a tiny bias, if it is persistent can show up on a trajectory plot. In Figure 2.4-7: *12-hour forward trajectory at 8:00 CST on June 22, 2005* the accumulated biases across several hours show MM5-based trajectory patterns which are "tighter" than those based on CAMS observations. This is the reverse of what was seen on June 21.

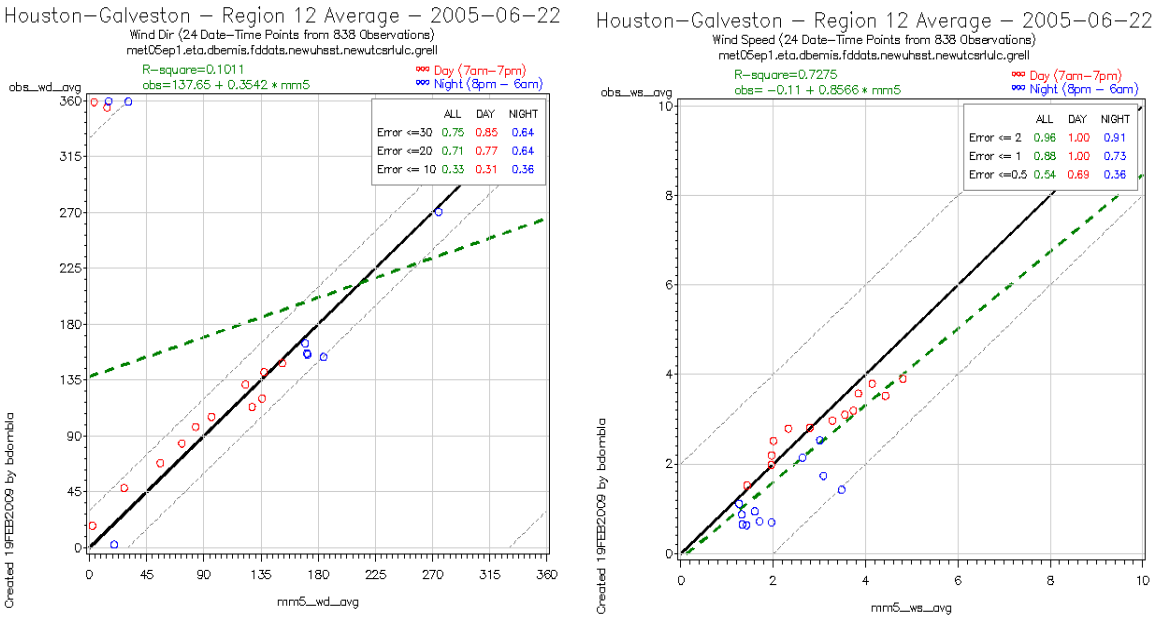

Figure 2.4-6: Region 12 average wind direction and speed scatter plots for June 22, 2005

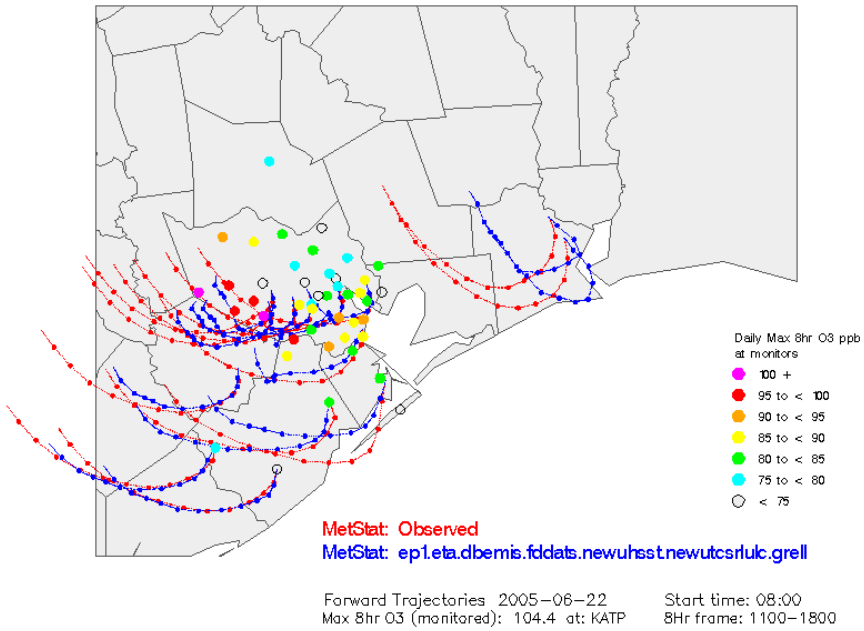

Figure 2.4-7: 12-hour forward trajectory at 8:00 CST on June 22, 2005

2.5 2005ep2 Performance Evaluation

The 2005ep2 episode features three periods of high ozone: July 28-30, August 1-3, and August 6-7. The first period was dominated by a slow-moving and weak cold front while the two other periods resulted from high pressure-induced coastal oscillation. Afternoon thunderstorms occurred on many days during this episode, and the model only had limited success in reproducing these storms and the resultant wind patterns.

MM5 reproduced the observed wind speeds relatively well, with wind speed within two m/s almost 100 percent of the time for most areas (Table 2.5-1: *Error percentages for 2005ep2 episode*.). Wind direction errors were higher, especially at night, when wind speeds were low (Figure 2.5-1). Note that observed wind direction is less accurate when wind speeds are low. Figures 2.5-2 and 2.5-3 exhibit the wind direction and wind speed time series of the average of all Houston monitors. MM5 follows the observations closely for almost all time periods. The overnight wind patterns appear to have the highest bias and error, due to the model's overestimate of the calmer winds. Temperature performance was degraded by the presence of locally-triggered thunderstorms, and by the poor placement of clouds and storms associated with a slow-moving cold front. On most days, though, MM5 replicated the diurnal pattern of temperature well (Figure 2.5-4: *Region 12 average temperature time series for 2005ep2 episode*).

Table 2.5-1: Error percentages for 2005ep2 episode

Geographic Area/Zone	Wind Direction (°) Error ≤ 30 / 20 / 10	Wind Speed (m/s) Error ≤ 2 / 1 / 0.5	Temperature (°C) Error ≤ 2 / 1 / 0.5
Region 12	65 / 54 / 33	100 / 75 / 43	80 / 57 / 31
Coastal	56 / 42 / 22	99 / 76 / 42	77 / 44 / 21
Ship Channel	54 / 40 / 24	97 / 54 / 27	80 / 53 / 31
Southeast Core	57 / 44 / 22	98 / 66 / 36	78 / 52 / 30
Northwest Core	48 / 37 / 22	94 / 60 / 29	67 / 35 / 16
Downwind	40 / 27 / 15	84 / 42 / 23	78 / 49 / 29

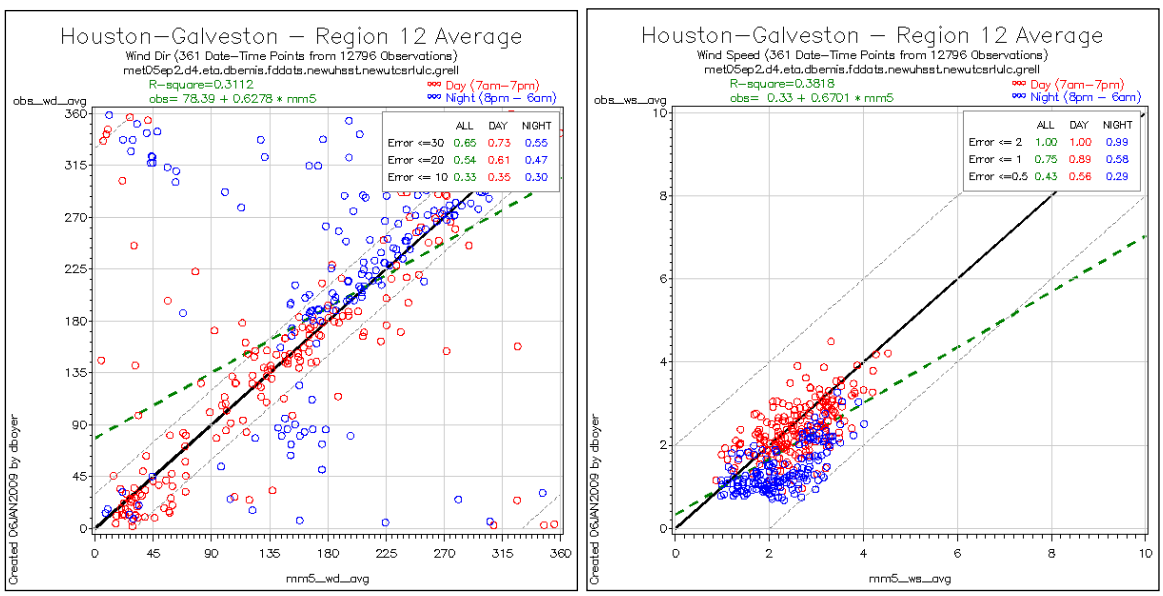

Figure 2.5-1: Region 12 average wind speed and direction scatter plot

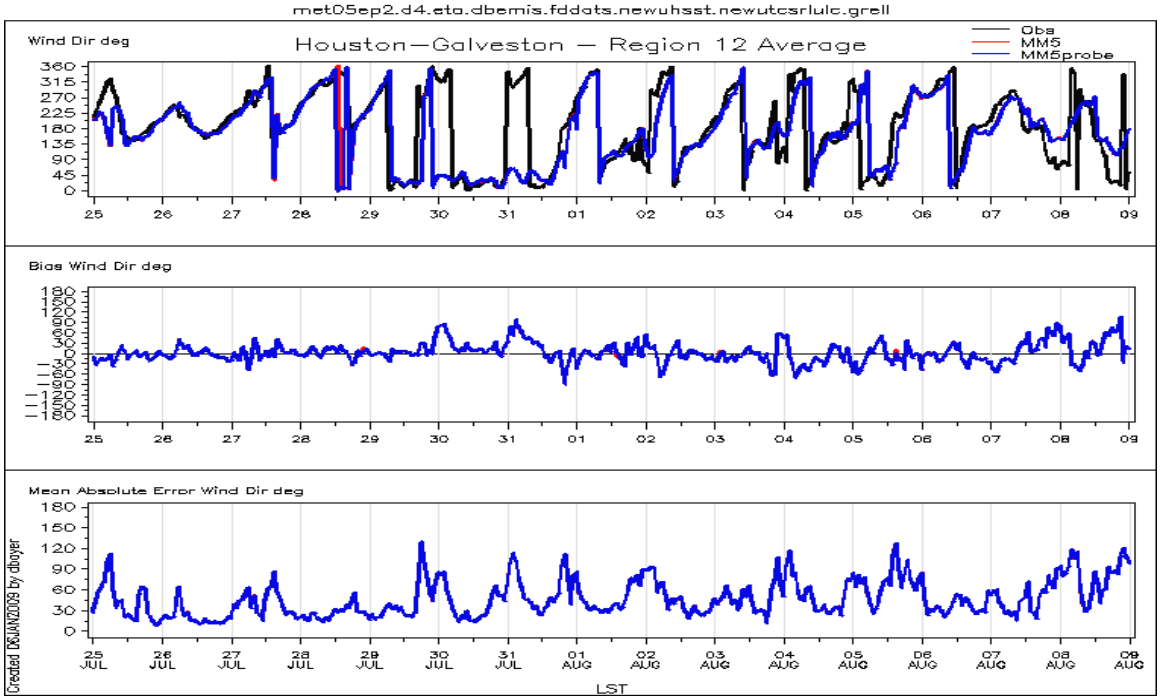

Figure 2.5-2: Region 12 average wind direction time series for 2005ep2 episode

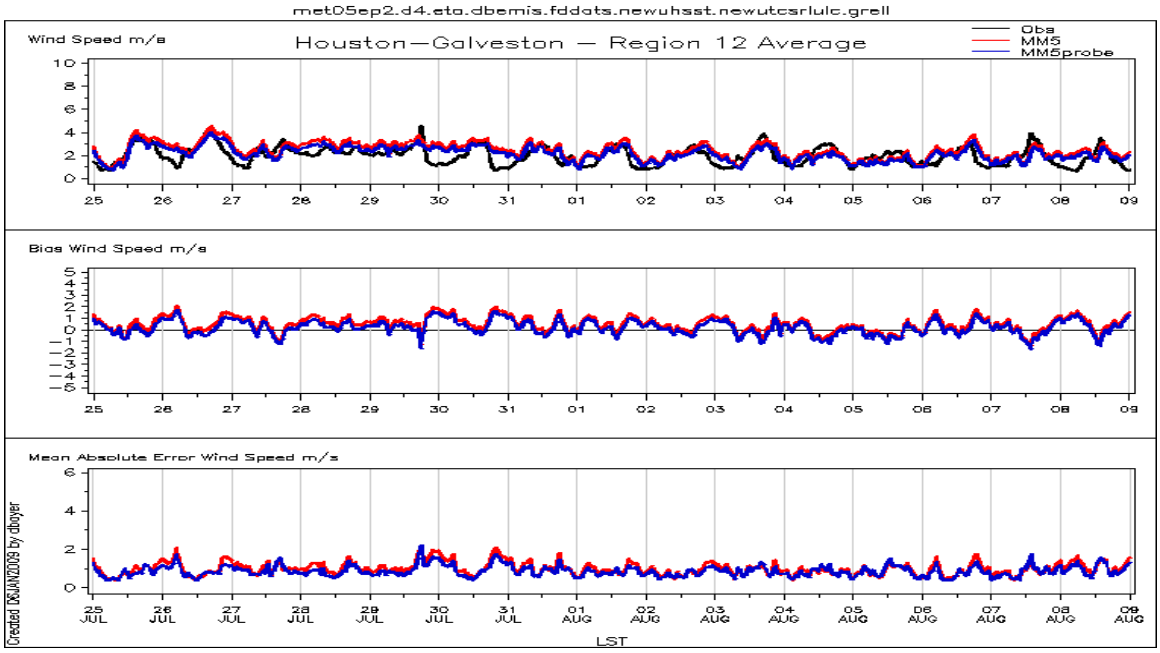

Figure 2.5-3: Region 12 average wind speed time series for 2005ep2 episode

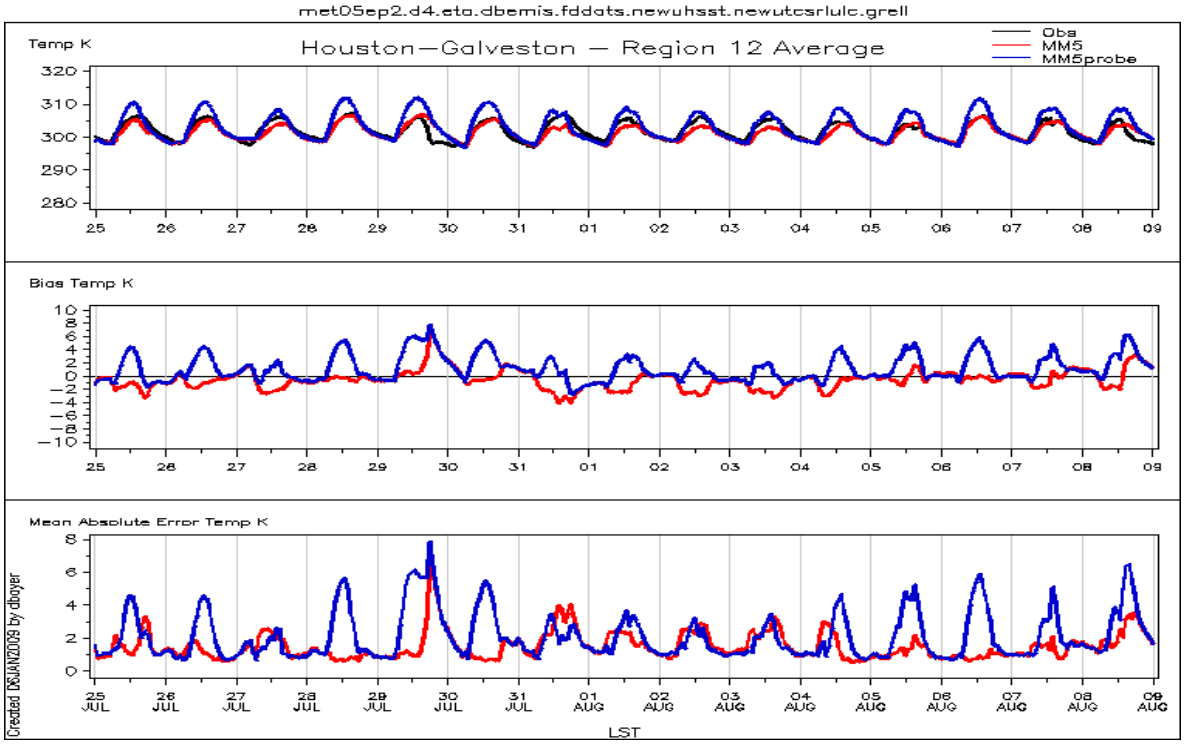

Figure 2.5-4: Region 12 average temperature time series for 2005ep2 episode

July 28, 2005

This day was the first of the 2005ep2 episode for which more than one monitor recorded an exceedance of the eight-hour ozone standard. Three monitors were equal or greater than 85 ppb, with the Seabrook Friendship Park C45 monitor observing the highest concentration of 95 ppb of ozone. Meteorological conditions were dominated by a stalled cold front in the Houston area, which didn't push out of the area until July 30. Winds were generally from the northwest during the morning. A Galveston Bay breeze developed at mid-day, which was overcome by a stronger south-easterly sea breeze from the Gulf of Mexico.

MM5's wind performance on this day was quite good, especially for wind speed. Figure 2-5-5 shows the scatter plot for wind direction and speed for all hours on 7/28/05. MM5 predicted an average wind speed within 2 m/s of the observations 100% of the time for the Houston area. Wind direction performance on July 28 was better than the episode average (Table 2.5-1: *Error percentages for 2005ep2 episode*), with outlier hours occurring mostly during the daytime wind shifts. Table 2.5-2*: Error percentages for July 28, 2005* shows that the wind speed performance in all of the monitoring zones was similar, except for the Downwind zone, where MM5 over-predicted the wind speeds. This error could be due to the difficulty of replicating the slow-moving front in the northern part of the 4km domain. Temperature performance on this day was very good, with very high percentages of Region 12 and Zone averages within 1 degree Celsius of the observations.

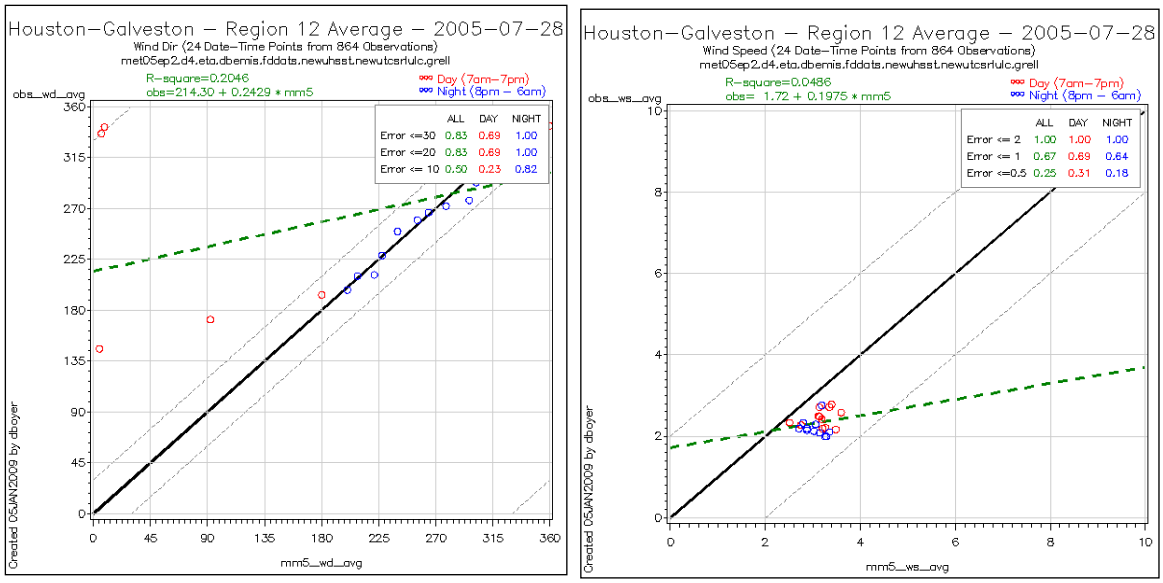

Figure 2.5-5: Region 12 Average wind direction and speed scatter plots for July 28, 2005

Table 2.5-2: Error percentages for July 28, 2005

Geographic Area/Zone	Wind Direction (°) Error ≤ 30 / 20 / 10	Wind Speed (m/s) Error ≤ 2 / 1 / 0.5	Temperature (°C) Error ≤ 2 / 1 / 0.5
Region 12	83 / 83 / 50	100 / 67 / 25	100 / 100 / 46
Coastal	67 / 58 / 38	100 / 75 / 46	96 / 42 / 17
Ship Channel	67 / 42 / 13	92 / 46 / 21	100 / 92 / 63
Southeast Core	83 / 67 / 46	100 / 83 / 33	100 / 92 / 67
Northwest Core	71 / 54 / 29	100 / 67 / 29	100 / 71 / 46
Downwind	67 / 50 / 38	67 / 08 / 04	83 / 67 / 50

Aloft, MM5 resolved much of the flow and planetary boundary layer (PBL) structure according to the profiler locations. As Figure 2.5-6*: Time-height plot for La Porte profiler on July 28, 2005* exhibits, winds were generally from the northwest and less than 10 m/s above the surface. MM5 captures these winds well and simulates the growth of the PBL closely.

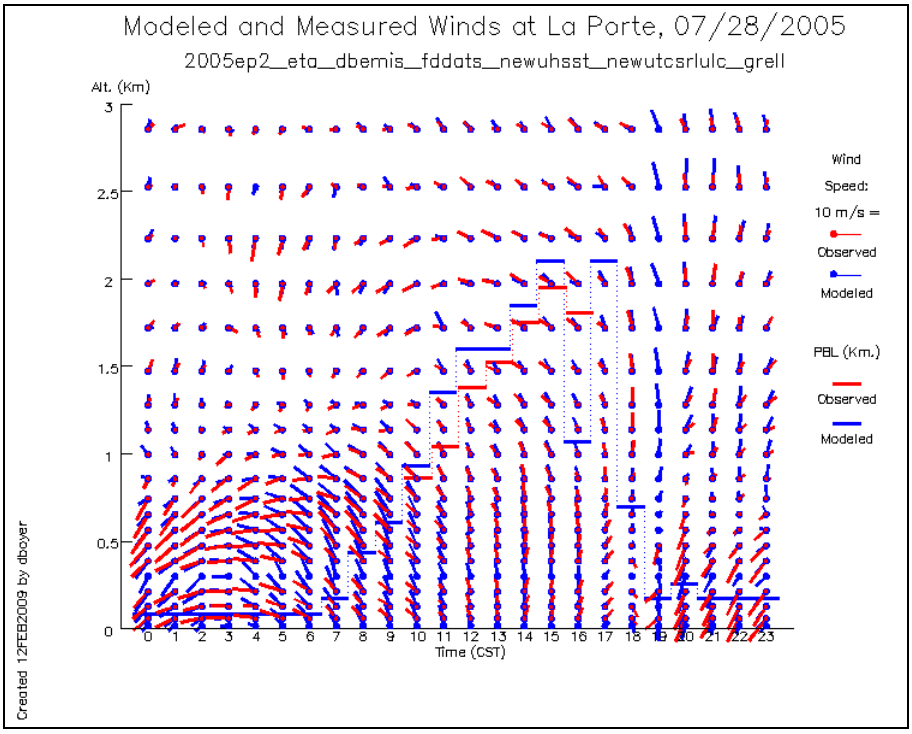

Figure 2.5-6: Time-height plot for La Porte profiler on July 28, 2005

Forward trajectories (Figure 2.5-7: *12-hour forward trajectory at 08:00 CST on July 28, 2005*) indicated that MM5 has difficulty depicting the wind shift that occurs with the sea breeze. The MM5 trajectories are too long, indicating the wind speeds are slightly over–predicted, and they curve in the wrong direction. Because of the inaccurate transport on this day, the photochemical model places the high ozone plume to the south and west of the observed peak at the Seabrook Friendship Park C45 monitor.

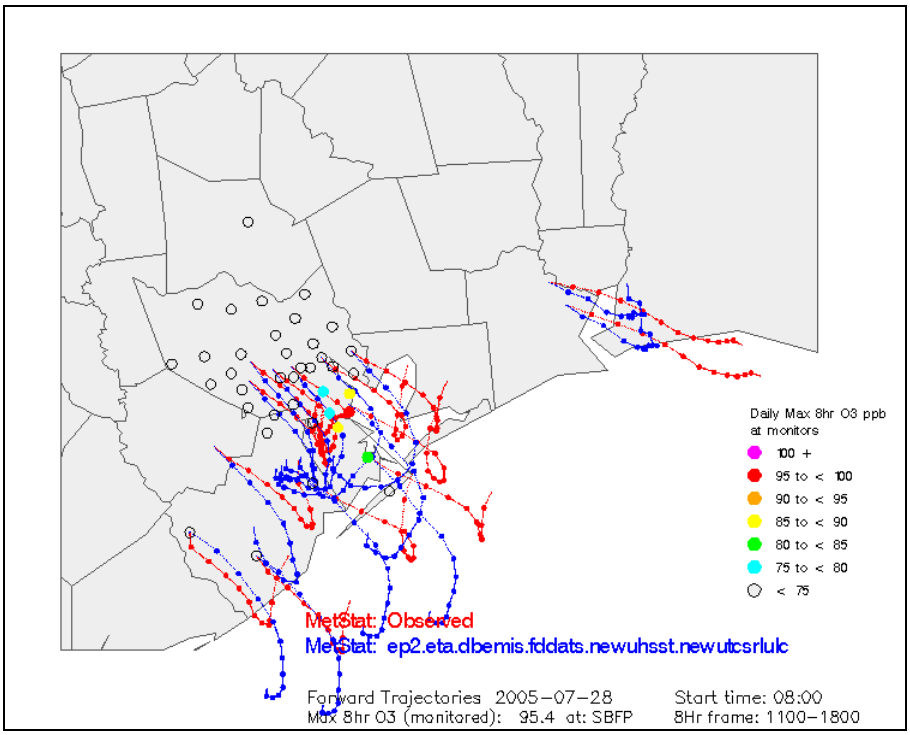

Figure 2.5-7: 12-hour forward trajectory at 08:00 CST on July 28, 2005

August 2, 2005

Eleven stations recorded an exceedance of the eight-hour ozone standard on this day, mostly on the west side of the city. The highest eight-hour ozone reading of the episode occurred at the West Houston monitor, with a peak of 104.6 ppb. Light winds rotated from the north in the morning to the south in the afternoon, following the high pressure coastal oscillation pattern. Scattered clouds were numerous and convective activity developed to the northeast of Houston as a result of the bay and sea breeze throughout the late afternoon.

MM5 reproduced the surface wind speed and wind direction patterns acceptably on this day. The Houston area average time series for wind speed and direction shown above show good agreement between the model and the observations. Figure 2.5-8: *Region 12 average wind direction and speed scatter plots for August 2, 2005* below displays the Houston area scatter plots for wind direction and speed on August 2, 2009. The scatter plot shows wind speeds fall within one m/s of the observations for almost all hours. However, a few nighttime wind directions do not show good agreement. Most of the nighttime hours experienced calm conditions, so the wind direction measurements may not be as accurate as the daytime measurements. The impact of these wind direction errors show up in Table 2.5-3: *Error percentages for August 2, 2005*. The accuracy of modeled wind directions along the coast are below the Region 12 average, and the downwind (to the west and northwest of downtown Houston) monitors furthest from the coast have very poor wind direction performance.

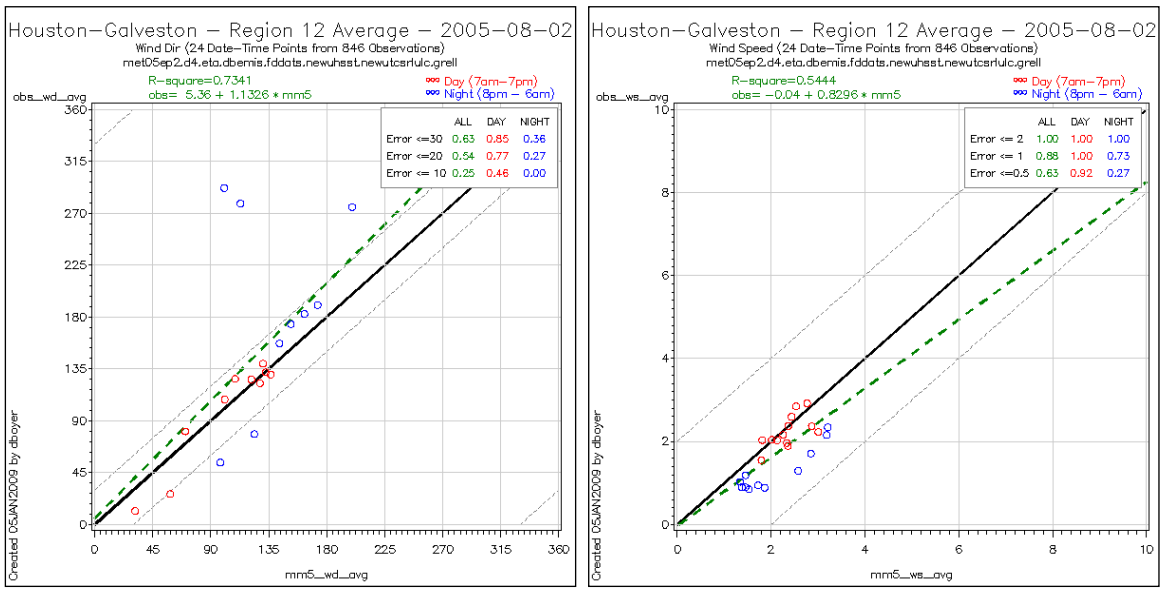

Figure 2.5-8: Region 12 average wind direction and speed scatter plots for August 2, 2005

Table 2.5-3: Error percentages for August 2, 2005

Geographic Area/Zone	Wind Direction (°) Error ≤ 30 / 20 / 10	Wind Speed (m/s) Error ≤ 2 / 1 / 0.5	Temperature (°C) Error ≤ 2 / 1 / 0.5
Region 12	63 / 54 / 25	100 / 88 / 63	63 / 54 / 29
Coastal	54 / 25 / 04	100 / 79 / 58	58 / 29 / 17
Ship Channel	75 / 50 / 38	100 / 67 / 33	67 / 38 / 33
Southeast Core	58 / 46 / 06	100 / 67 / 42	71 / 46 / 21
Northwest Core	54 / 42 / 21	88 / 67 / 42	58 / 29 / 13
Downwind	08 / 08 / 04	83 / 63 / 42	71 / 29 / 17

According to the upper air winds at the La Porte profiler (Figure 2.5-9: *Time-height plots for the La Porte (left) and Jefferson County (right) profilers on August 2, 2005*), MM5 replicated the observed winds quite well. The model had difficulty resolving the very calm winds (dots with no or small lines) but the flow patterns were well represented. PBL height estimates from La Porte

were not available on this day. At the Jefferson County profiler, however the winds were well simulated but the PBL height was underestimated due to clouds along the coast near Beaumont in MM5.

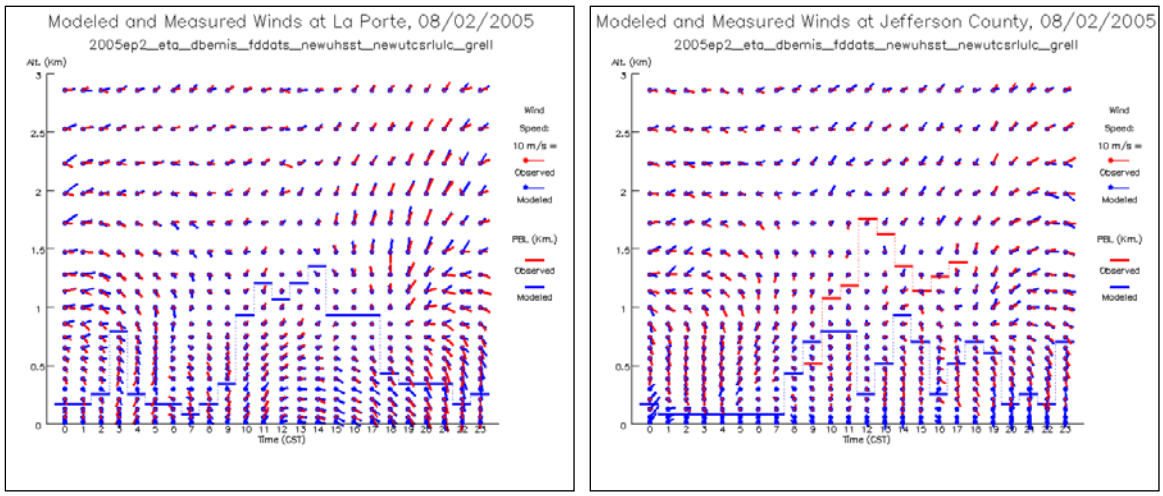

Figure 2.5-9: Time-height plots for the La Porte (left) and Jefferson County (right) profilers on August 2, 2005

As shown by Figure 2.5-10: *12-hour forward trajectory at 08:00 CST on August 2, 2005* the modeled trajectories produce similar trajectories as the observed data. However, the model appears to veer the winds too fast to the southeast. The higher ozone in the photochemical model may be pushed too far east and north of the observed peaks.

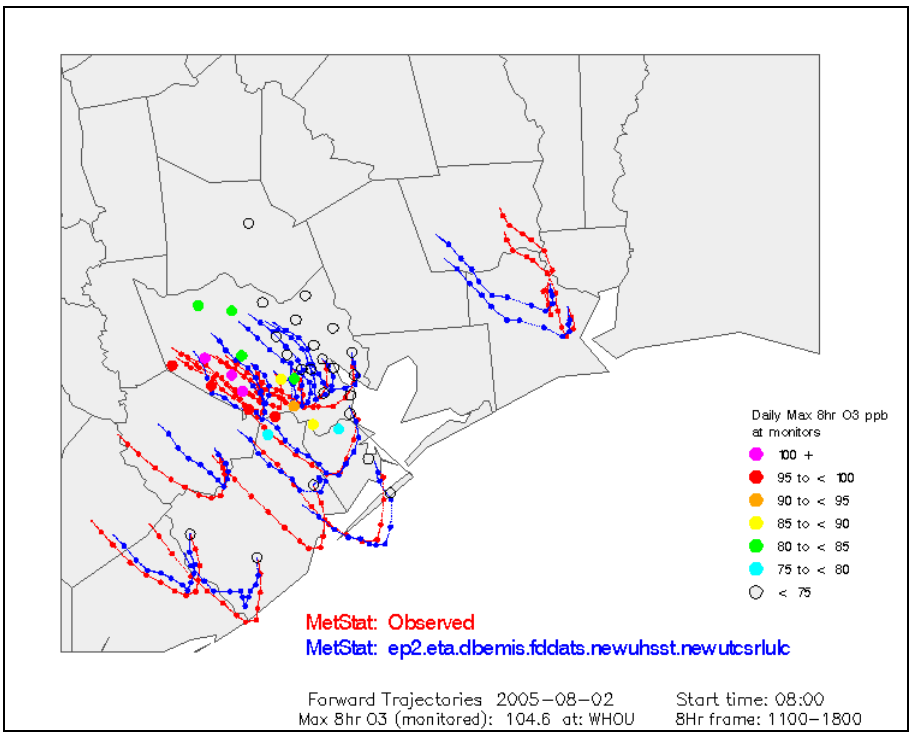

Figure 2.5-10: 12-hour forward trajectory at 08:00 CST on August 2, 2005

August 6, 2005

Four monitors exceeded the eight-hour ozone standard of 85 ppb on August 6, 2005, all occurring on the southeast side of Houston. Winds were light on this day, starting from the northwest and rotating to the southeast with the onset of the sea breeze just after midday. Scattered clouds were

observed all day with thunderstorms occurring in the afternoon to the northwest and southwest of Houston.

MM5 produced a surface wind field that followed the observed patterns well on this day. The model appeared to be slightly behind the timing of the land/sea breeze pattern as is shown in the wind direction time series (Figure 2.5-2: *Region 12 average wind direction time series for 2005ep2 episode*). The regional average wind speeds produced by MM5 during the morning and late afternoon are slightly higher than the observed speeds, which were less than 3 m/s on average. Also, the mid-day period is well represented during the few calm hours. The wind field accuracy statistics exhibit good performance by MM5 with no large deviations from the observations (Figure 2.5-11: *Region 12 average wind direction and speed scatter plots for August 6, 2005* and Table 2.5-4: *Percent accuracy statistics for August 6, 2005*).

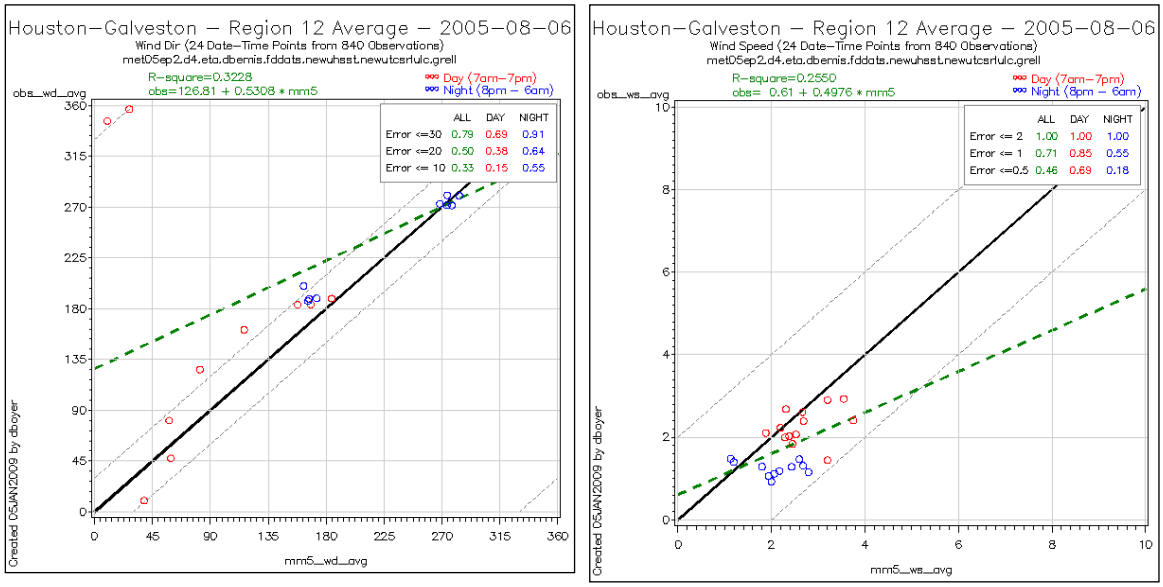

Figure 2.5-11: Region 12 average wind direction and speed scatter plots for August 6, 2005

Table 2.5-4: Percent accuracy statistics for August 6, 2005

Geographic Area/Zone	Wind Direction (°) Error ≤ 30 / 20 / 10	Wind Speed (m/s) Error ≤ 2 / 1 / 0.5	Temperature (°C) Error ≤ 2 / 1 / 0.5
Region 12	79 / 50 / 33	100 / 71 / 46	100 / 100 / 75
Coastal	83 / 75 / 38	100 / 71 / 25	96 / 79 / 46
Ship Channel	58 / 54 / 29	96 / 63 / 33	96 / 88 / 54
Southeast Core	67 / 29 / 04	100 / 67 / 25	96 / 75 / 50
Northwest Core	63 / 54 / 38	88 / 54 / 38	92 / 63 / 46
Downwind	50 / 29 / 08	88 / 42 / 25	100 / 83 / 42

At the La Porte profiler (Figure 2.5-12: *Time-height plots for the La Porte (left) and Huntsville profilers (right) on August 6, 2005*), MM5 replicated the observed wind shift from the northwest to the south well. The MM5 PBL estimates through 10:00 AM CST accurately followed the morning PBL rise but comparisons of afternoon hours were not available as the profiler estimates stopped at 13:00 CST. Results at the Jefferson County and Huntsville profilers also showed well-represented morning PBL rises. Afternoon PBL estimates were mixed, with both over- and under-predictions, as shown by the Huntsville profiler time-height plots. The morning PBL rise may be a more important metric for ozone production than peak mixing height, as reported by Knoderer et al. (2008).

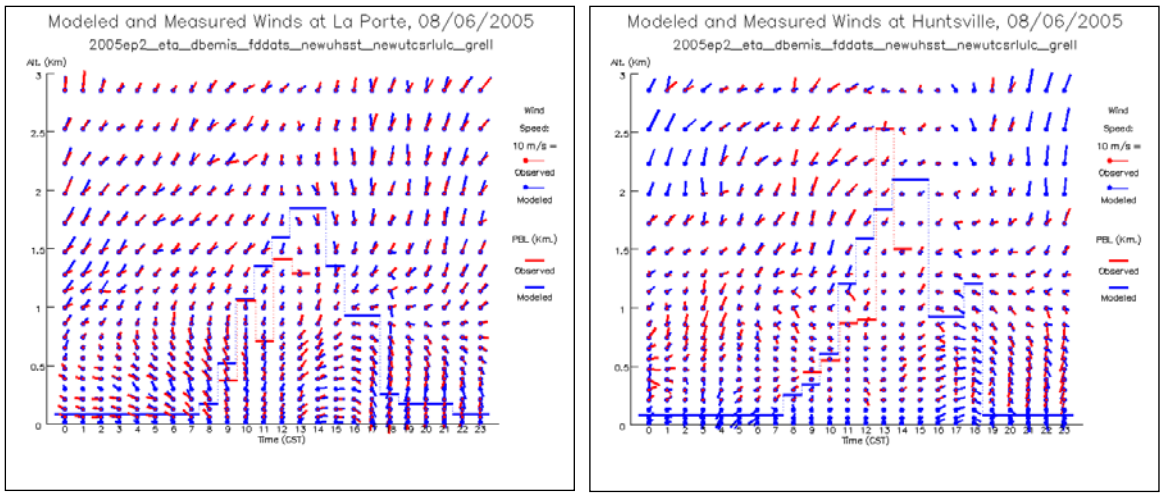

Figure 2.5-12: Time-height plots for the La Porte (left) and Huntsville profilers (right) on August 6, 2005

As shown by Figure 2.5-13: *12-hour forward trajectory at 08:00 CST on August 6, 2005* the modeled trajectories produce similar looping trajectories as the observed data. However, the model appears to produce winds that are too fast, especially from the east and northeast. The higher ozone in the photochemical model may be pushed farther west than the observed peaks.

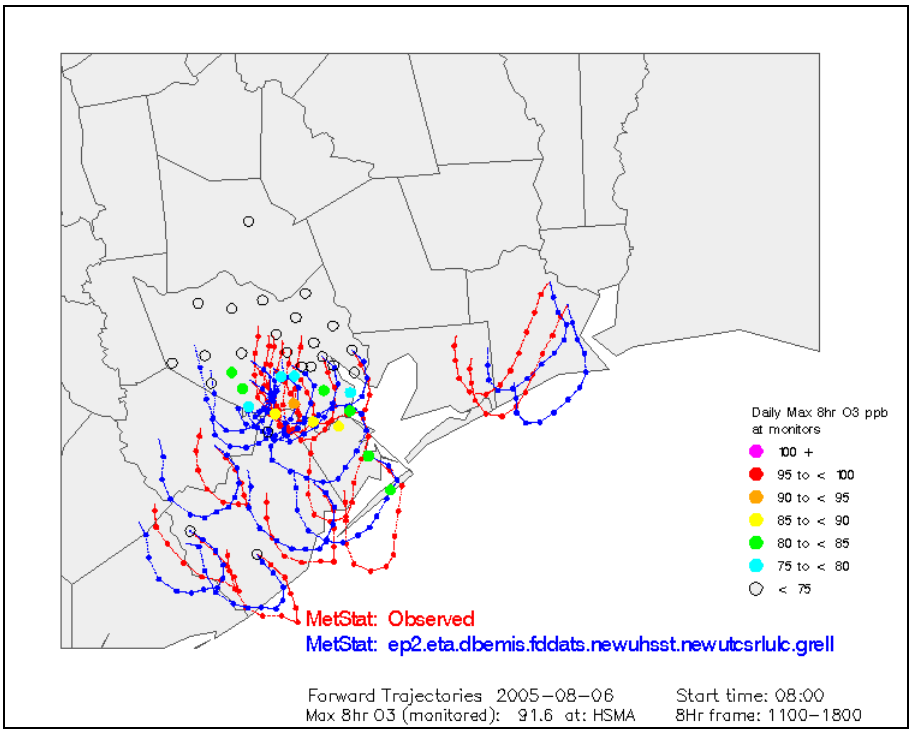

Figure 2.5-13: 12-hour forward trajectory at 08:00 CST on August 6, 2005

2.6 2006ep0 Performance Evaluation

The June 2006 episode had two days with very high 8 hour average ozone values. On June 8, the HGB area recorded a peak 8 hour average of 122 ppb. On June 14, there was a domain-wide peak of 118 ppb. Perhaps the most striking aspect of this episode, though, is that there were many high values across many sites and many days.

The episode had notable tropical circulations and thunderstorms early in the modeling period. Throughout the majority of the period veering and backing winds were influenced by different frontal passages. The persistent feature leading to high ozone can be perhaps be deduced by

comparing Figure 2.6-1**:** *Region 12 average wind direction time series for 2006ep0 episode*, with Figure 2.4-1: *Region 12 average wind direction time series for 2005ep1 episode*. The veering and backing behavior during this episode are "biased" into the southwest quadrant rather than the southeasterly quadrant seen during the June 2005 episode. Thus, exeedances seem to have been more widely distributed.

General Model Performance

Our summary of model performance across the HGB domain and through our modeling zones is provided in Table 2.6-1: *Average Houston Region 12 Percent Accuracy by Episode, Zone, and Peak Days*. It is encouraging to note that domain-wide performance is above average on our two peak days of June 8 and June 14. It is striking that more than 75 percent of the time our wind direction and wind speed meet thresholds of 20 degrees and 1 m/s respectively.

Table 2.6-1: **Average Houston Region 12 Percent Accuracy by Episode, Zone, and Peak Days**

Number of days	**Geographic Area**	**Wind direction (°) % Error < 30/20/10**	**Wind Speed (m/s) % Error < 2/1/0.5**	**Temperature (°C) % Error < 2/1/0.5**
Entire Episode	Region 12	76 / 63 / 45	97 / 72 / 38	**85 / 57 / 33**
June 8	Region 12	79 / 75 / 46	96 / 75 / 63	**96 / 58 / 54**
June 24	Region 12	92 / 79 / 50	100 / 83 / 42	**100 / 58 / 29**
Entire Episode	Zone 1	69 / 57 / 35	96 / 76 / 48	**81 / 55 / 29**
Entire Episode	Zone 2	67 / 57 / 35	94 / 57 / 30	**80 / 55 / 35**
Entire Episode	Zone 3	69 / 55 / 36	93 / 56 / 25	**83 / 54 / 29**
Entire Episode	Zone 4	68 / 52 / 34	94 / 58 / 30	**76 / 38 / 19**
Entire Episode	**Zone 5**	**52 / 39 / 21**	**82 / 48 / 25**	**85 / 53 / 31**

The time series displayed in Figures 2.6-1: *Region 12 average wind direction time series for 2006ep0 episode* and 2.6-2: *Region 12 average wind direction time series for 2006ep0 episode* generally support the tabulated performance above. A couple of features are worth noting. An approaching cold front on June 7 impacted wind direction performance on June 8. Also Tropical Storm Alberto disrupted predicted winds on June 12. Since a large-scale recirculation of winds was a key feature of June 14, the performance on the preceding couple of days may be important in CAMx performance

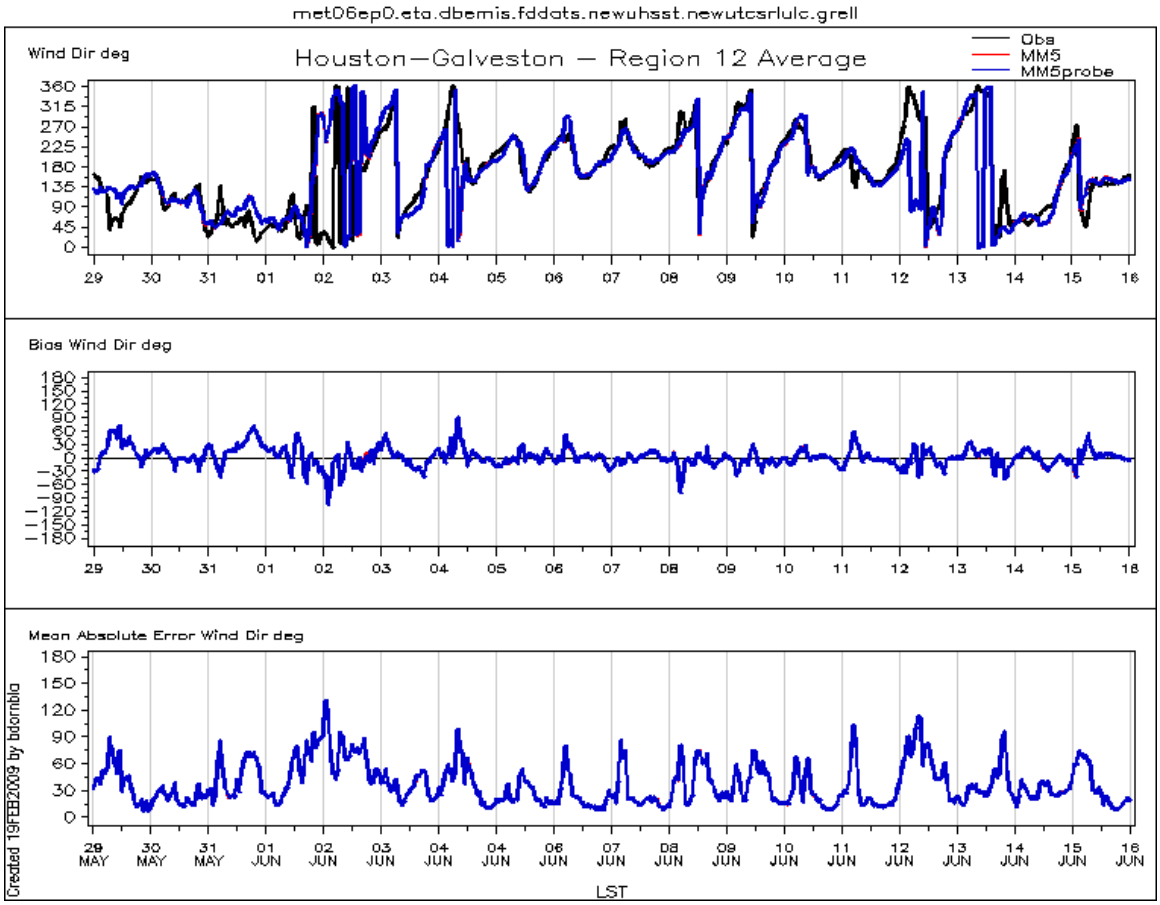

Figure 2.6-1: **Region 12 average wind direction time series for 2006ep0 episode**

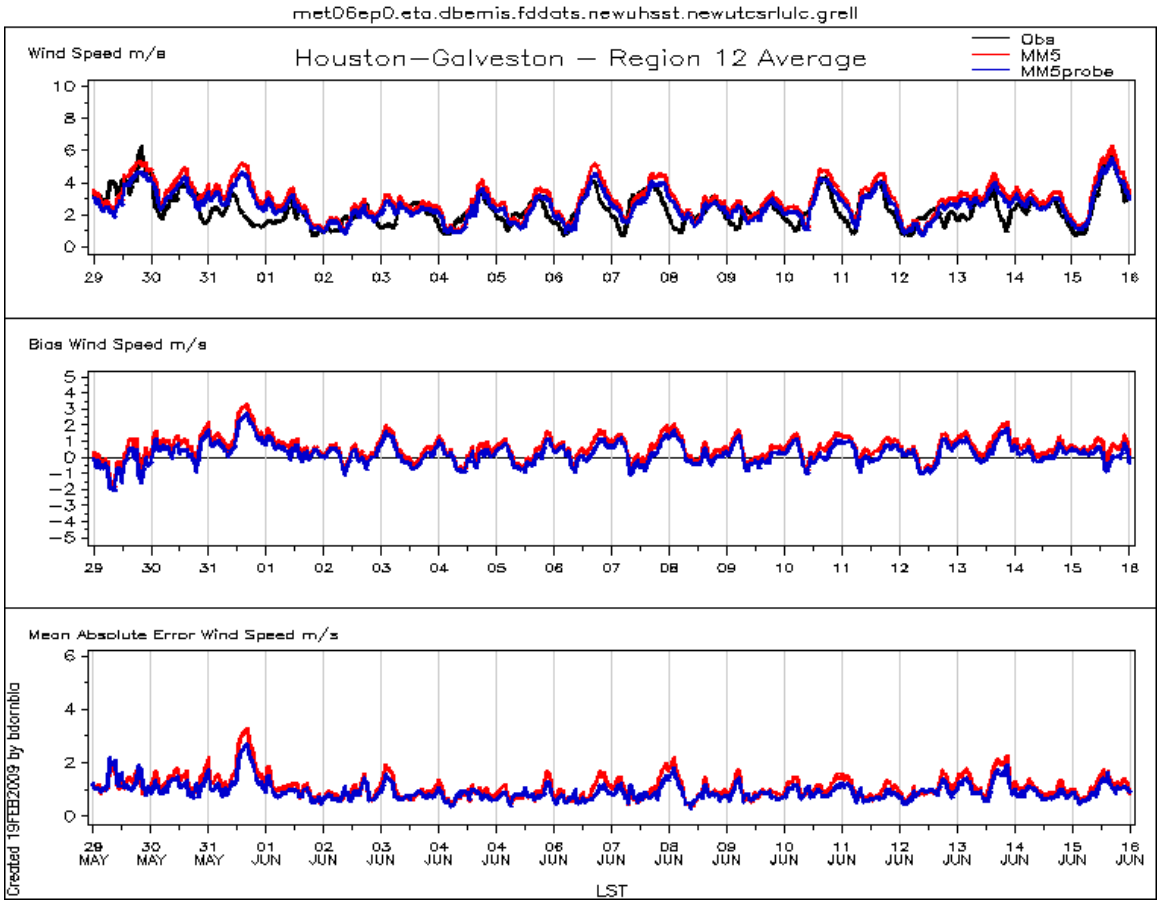

Figure 2.6-2: Region 12 average wind direction time series for 2006ep0 episode

June 8, 2006 Features

The wind speed bias during the early morning hours seen in the regional time series presented earlier is clearly evident in the Figure 2.6-3: *Region 12 average wind direction and speed scatter plots for June 8, 2006*. The impact on forward trajectories started at midnight can be seen in Figure 2.6-4: *12-hour forward trajectory at midnight on June 8, 2006.* On the other hand, starting the trajectories at 11 am shows wind speeds are much more consistent with observations. Looking next at wind direction, the regional time series for wind direction indicated a sharp southerly bias occurred in the early morning of June 8 . Yet, our scatter plot for wind direction shows apparently good over-all bias. Despite the two hours with obvious directional errors, there is also the difficulty discussed previously for interpreting scatter plots in which small persistent biases accumulate because we don't distinguish the ordering of hour comparisons. The impact of this is seen in the trajectory plot in Figure 2.6-4*: 12-hour forward trajectory at midnight on June 8, 2006*. For a start time of 11 CST, the good wind speed performance is reflected in trajectory lengths which look similar for both observational data and MM5 data. However, a subtle bias has appeared so that trajectories seem to be biased clockwise to the east of where they should be. Thus, our daily ozone peaks and requisite mixing of precursors may have been misplaced despite the quite good statistics and low bias.

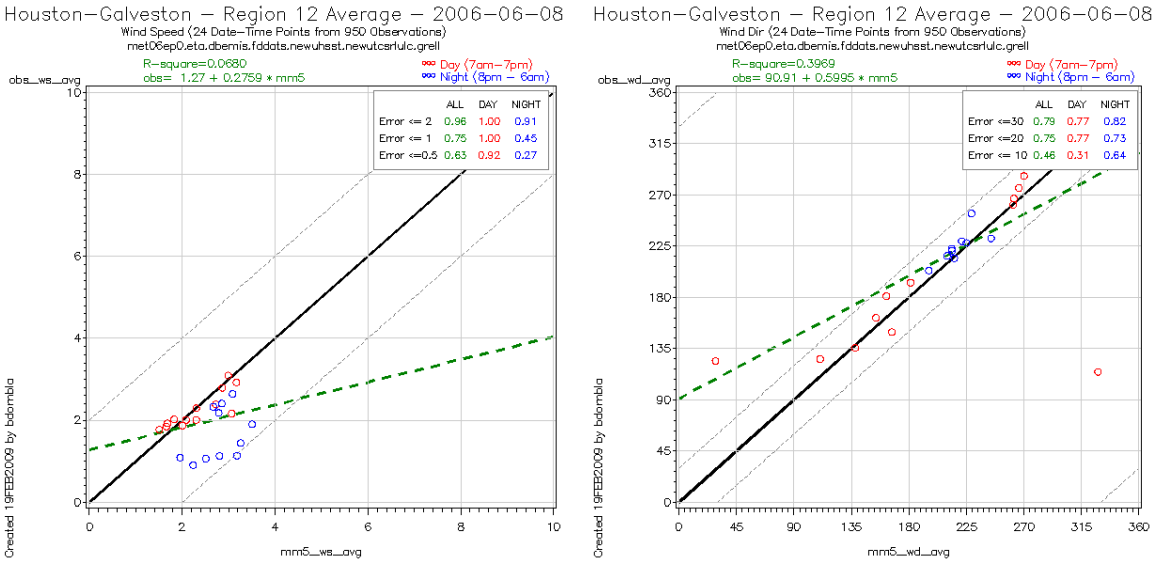

Figure 2.6-3: Region 12 average wind direction and speed scatter plots for June 8, 2006

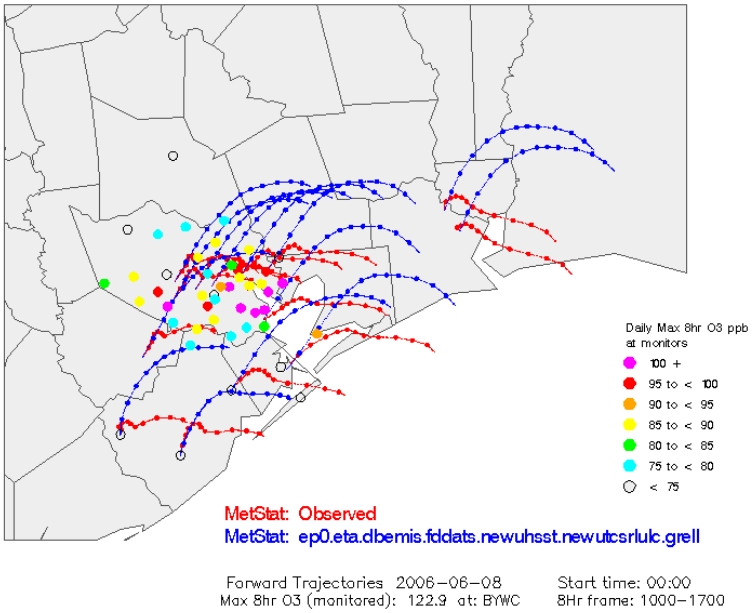

Figure 2.6-4: 12-hour forward trajectory at midnight on June 8, 2006

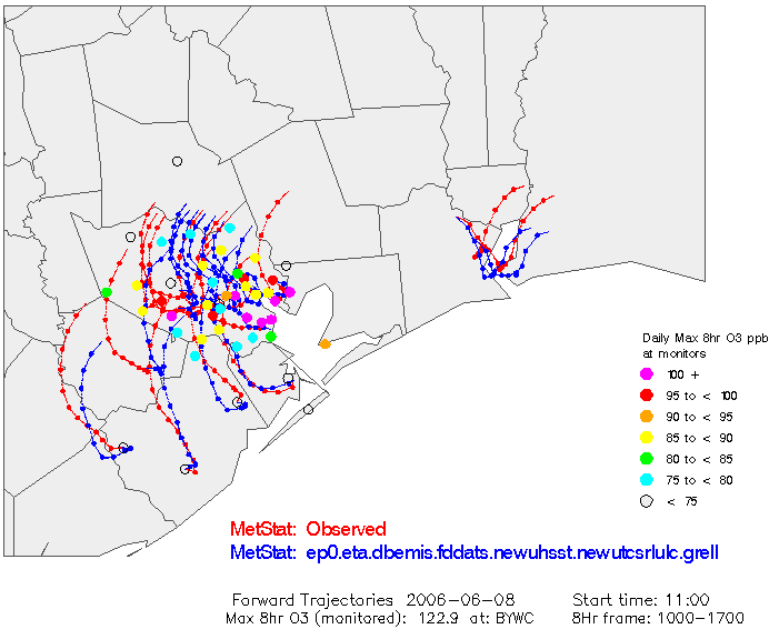

Figure 2.6-5: 12-hour forward trajectory at 11:00 CST on June 8, 2006

June 14, 2006 Features

A close examination of the scatter plots for wind direction and wind speed in Figures 2.6-6: *Region 12 average wind direction and speed scatter plots for June 14, 2006*, respectively show some interesting features. As seen in Table 2.6-1: *Average Houston Region 12 Percent Accuracy by Episode, Zone, and Peak Days*, performance across Region 12 was very good on June 14. Wind direction were predicted to within 20 degrees of observations across all sites and hours 79 percent of the time that day while wind speeds were within 1 m/s 83 percent of the time. From our Region 12 time series, one can see that our error is within our desired threshold of about 30 degrees, and yet there seems to be a slight counterclockwise bias at night, and a more clockwise bias during the day. The small positive biases shown in our Region 12 time series for wind speed are well with our desired thresholds but persistent.

The cumulative effects of a counterclockwise bias and slightly faster wind speeds impacts the trajectories in Figure 2.6-7: *12-hour forward trajectory at 8:00 CST on June 14, 2006.* Predicted wind directions matched observations during most early morning hours but had a more northerly component near dawn.

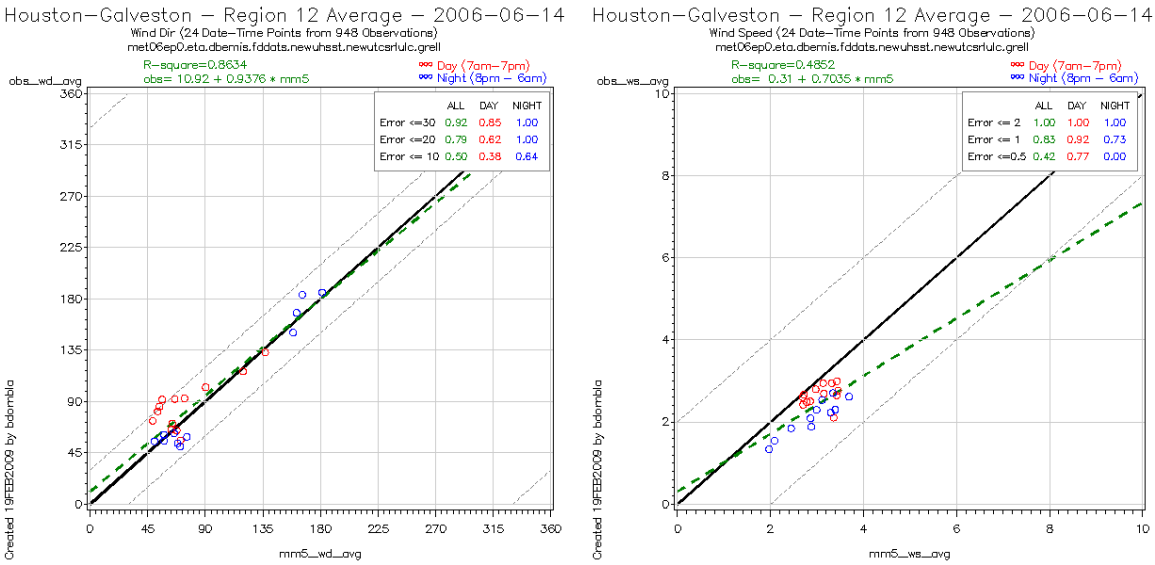

Figure 2.6-6: Region 12 average wind direction and speed scatter plots for June 14, 2006

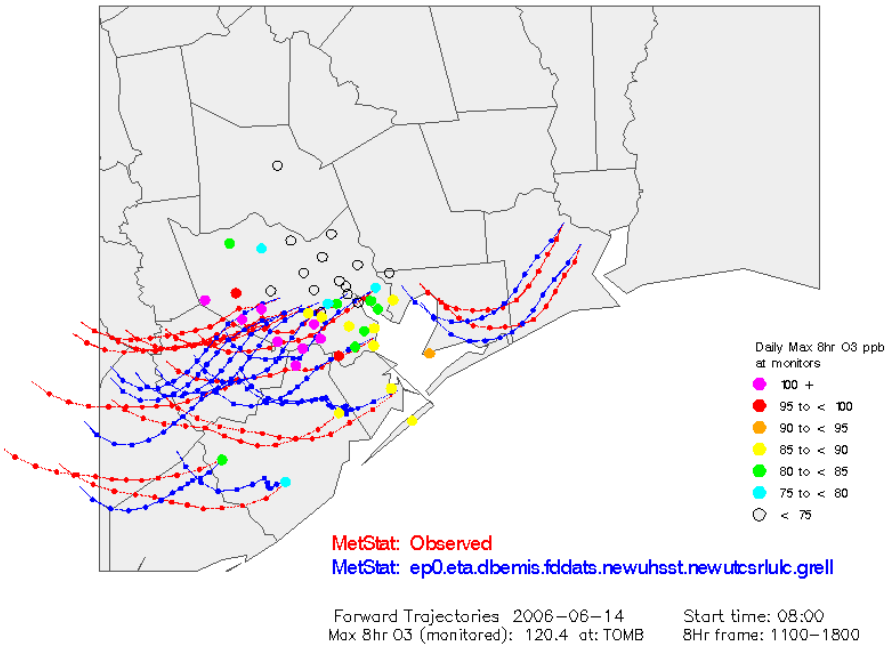

Figure 2.6-7: 12-hour forward trajectory at 8:00 CST on June 14, 2006

In the trajectory plot below, the clockwise bias in wind direction seen Figure 2.6-7 has become evident as the modeled trajectories are consistently rotated clockwise with respect to trajectories constructed from observational data. The similar length of the two sets of trajectories confirms that daytime wind speeds were very close to observed values.

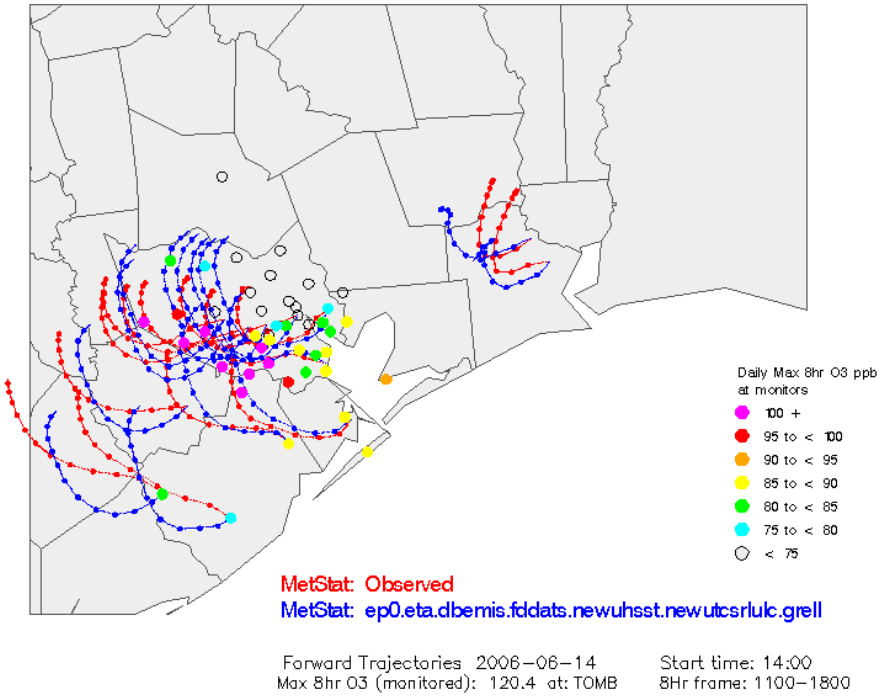

Figure 2.6-8: 12-hour forward trajectory at 14:00 CST on June 14, 2006

One additional feature that is likely to impact air quality on June 14 can be inferred from the height-time cross section at the site of the La Porte profiler. Generally high background ozone values were observed at CAMS sites north of Houston early on this day. Inspection of Figure 2.6-9: *Time-height plots for the La Porte profiler on June 14, 2006* below, one sees that surface winds at La Porte were generally easterly during the early morning hours. The easterly components were persistent through about one kilometer above ground level (AGL). Above that level, the winds are generally from the northwest which is from the ship channel and portions of the urban core. During the middle of the day, low level winds become very light but the mixing height grows and any precursors that have been transported from the northwest can mix down to near the surface.

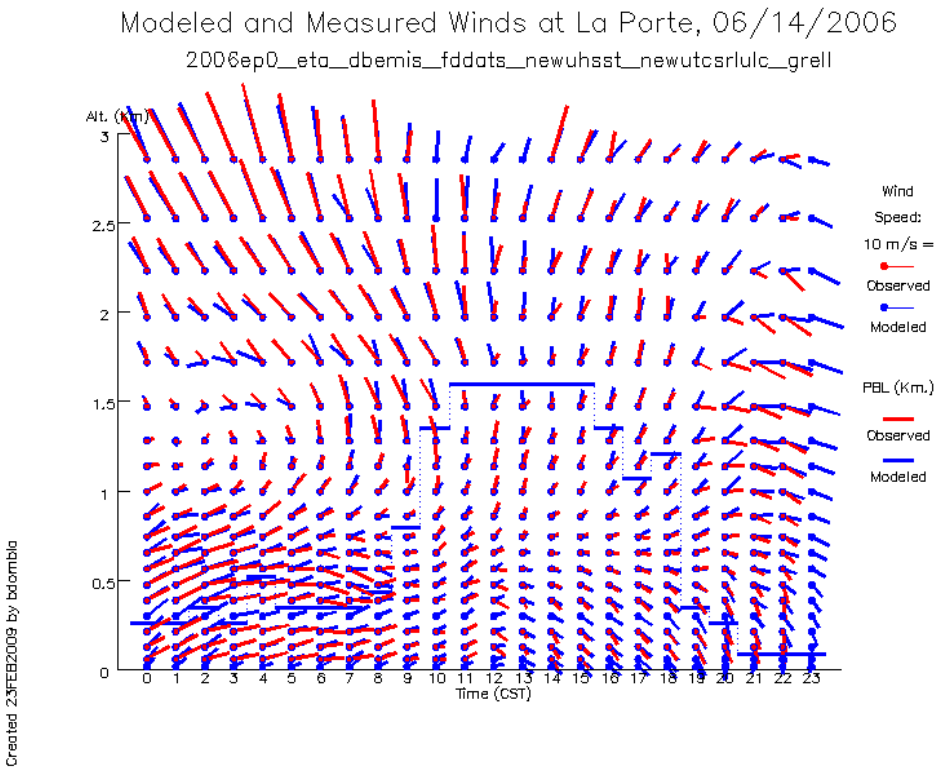

Figure 2.6-9: Time-height plots for the La Porte profiler on June 14, 2006

2.7 2006ep1a Performance Evaluation

The 2006ep1a episode (August 13 – 27, 2006) was the first part of the TexAQS II intensive monitoring effort (August 15 – October 15, 2006). As a weak cold front approached and moved through southeast Texas, the Houston area experienced ozone exceedances from August 16-18. Winds were generally light during this period, with the sea breeze dominating flow in the afternoons.

MM5 reproduced the wind and temperature conditions during this episode well (Table 2.7-1: *Percent accuracy statistics for 2006ep1a episode* and Figure 2.7-1: *Region 12 average wind direction and speed scatter plots for 2006ep1a episode*

Table 2.7-1: Percent accuracy statistics for 2006ep1a episode

Geographic Area/Zone	Wind Direction (°) Error ≤ 30 / 20 / 10	Wind Speed (m/s) Error ≤ 2 / 1 / 0.5	Temperature (°C) Error ≤ 2 / 1 / 0.5
Region 12	80 / 67 / 43	100 / 83 / 43	83 / 61 / 39
Coastal	66 / 54 / 30	98 / 74 / 42	80 / 51 / 28
Ship Channel	69 / 55 / 35	100 / 74 / 39	90 / 55 / 32
Southeast Core	77 / 62 / 38	98 / 61 / 30	90 / 63 / 39
Northwest Core	68 / 59 / 36	99 / 64 / 31	76 / 46 / 22
Downwind	56 / 41 / 29	90 / 51 / 28	77 / 46 / 20

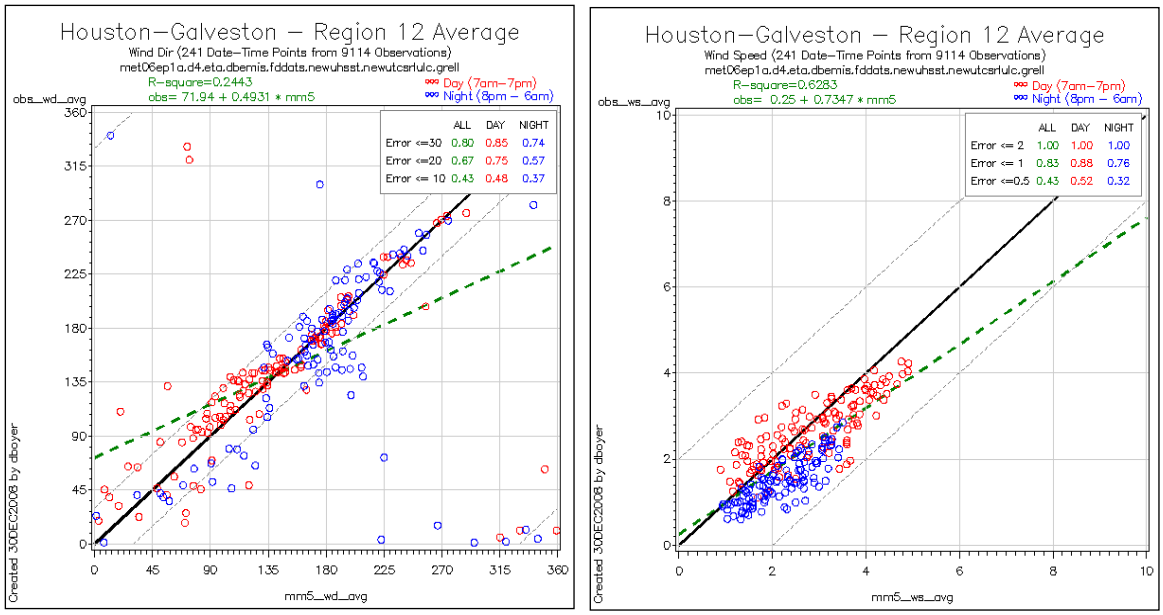

Figure 2.7-1: Region 12 average wind direction and speed scatter plots for 2006ep1a episode

The Houston Region 12 average percent accuracy statistics are the best overall compared to other episodes (compare to Figure 3.3.1-2 of Chapter 3.3.1). This is further represented by the time series of winds and temperature where the model follows the observations closely over the entire episode (Figures 2.7-2: *Region 12 average wind direction time series for 2006ep1a episode* through 2.7-4: *Region 12 average temperature time series for 2005ep2 episode*).

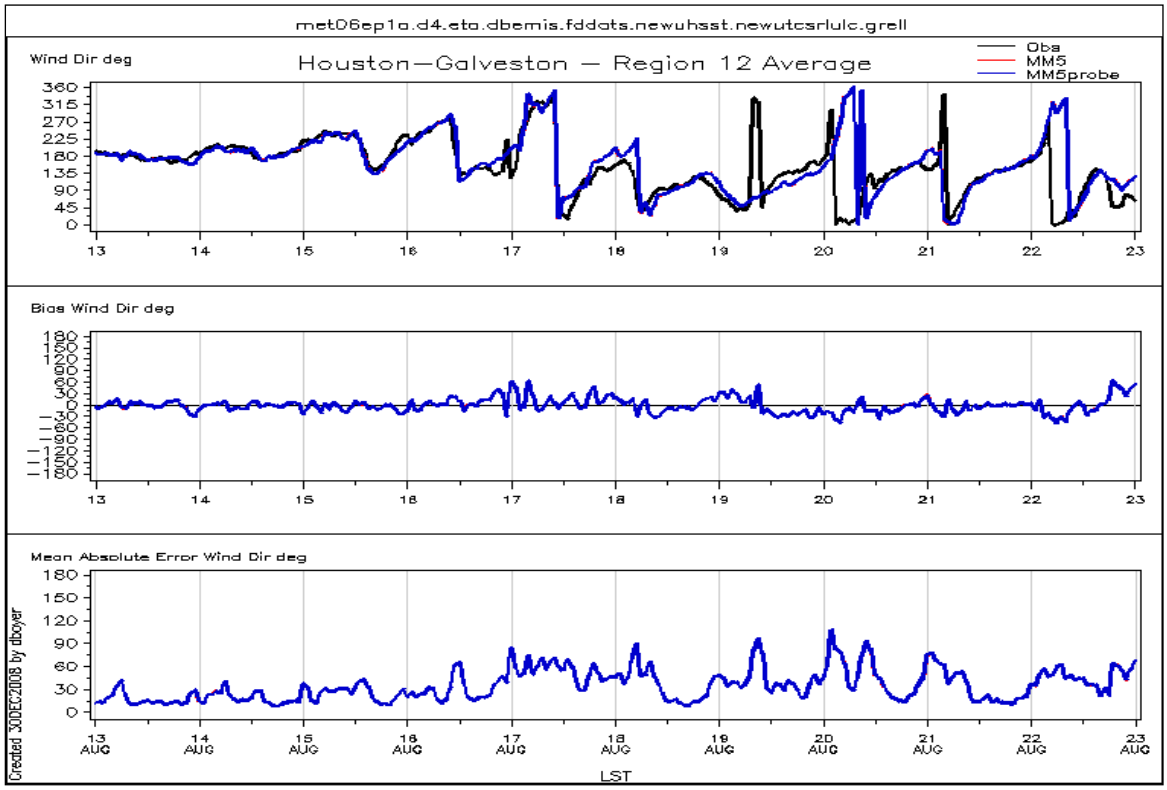

Figure 2.7-2: Region 12 average wind direction time series for 2006ep1a episode

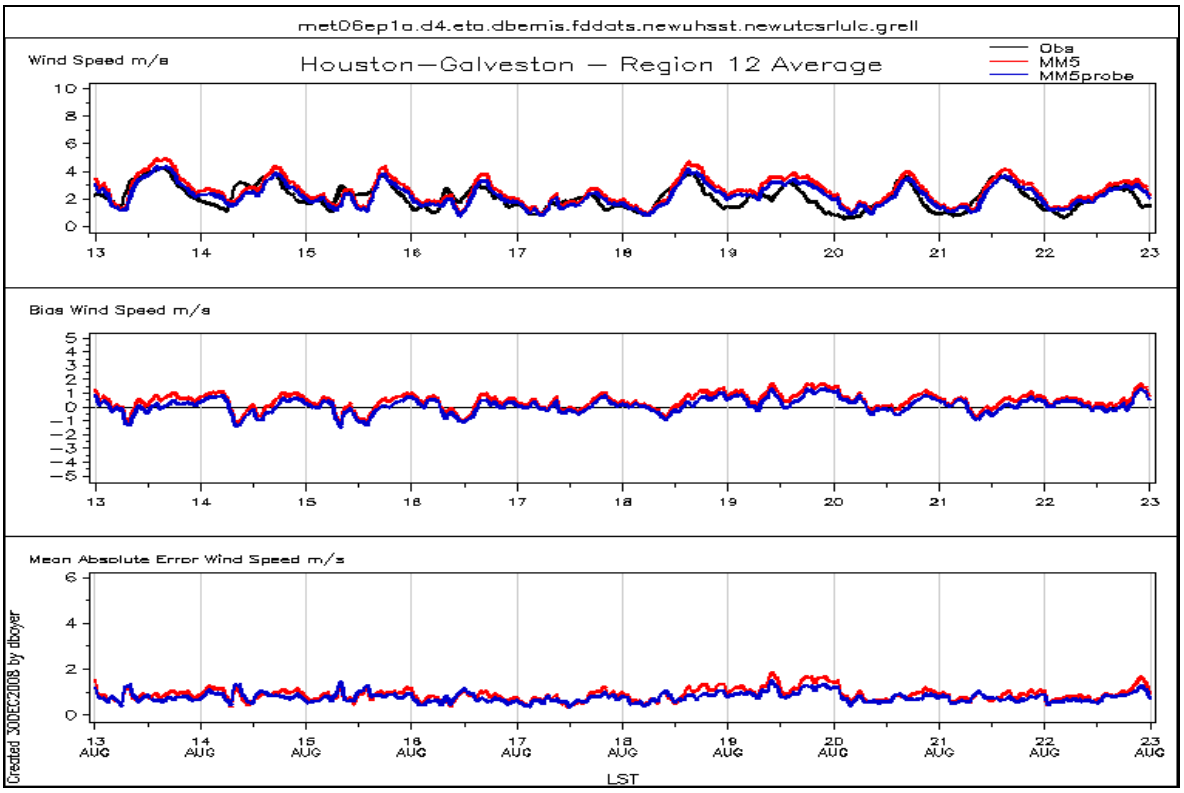

Figure 2.7-3: Region 12 average wind speed time series for 2006ep1a episode

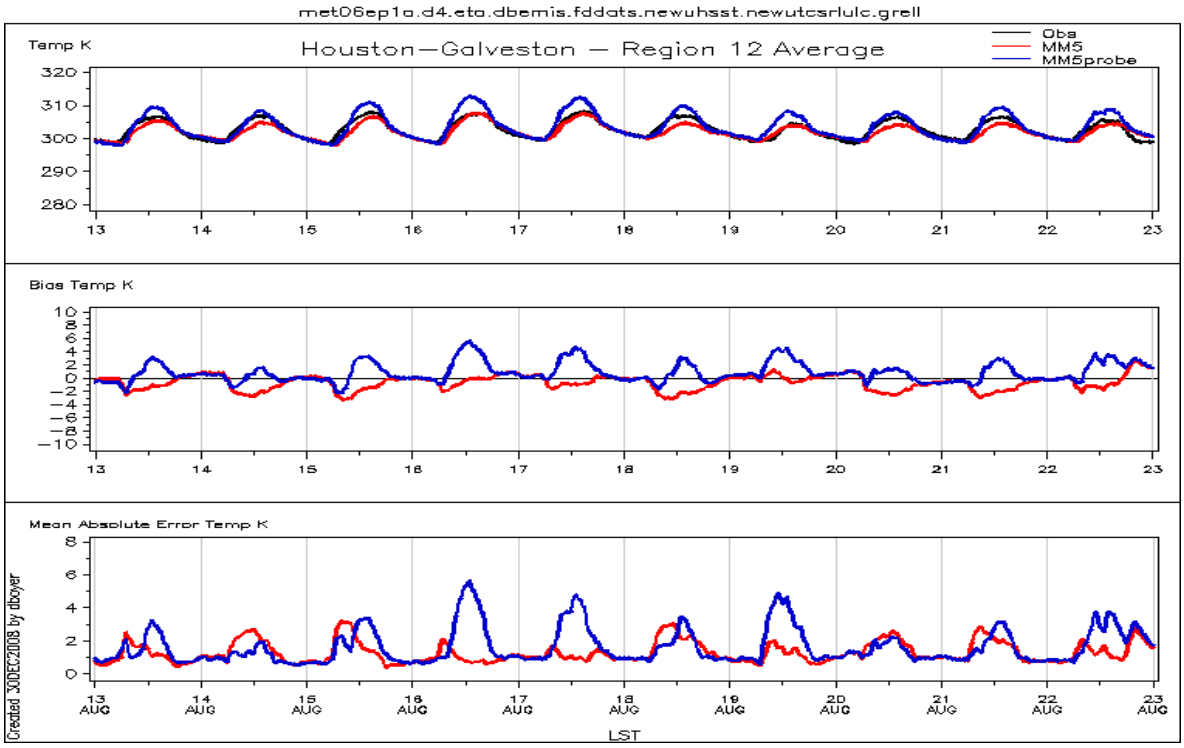

Figure 2.7-4: Region 12 average temperature time series for 2006ep1a episode

August 16, 2006

Six monitors exceeded 85 ppb of ozone on August 16, 2006, all on the north to northeast side of Houston. The peak eight hour value of 95 ppb occurred at Mercer Arboretum C557. Winds were light from the west in the morning before stalling out around noon. A bay and sea breeze from

the south-southeast dominated the afternoon flow. Thunderstorms developed over Louisiana in the late afternoon but did not impact Houston. Temperatures were in the upper 90s.

As with most days in this episode, MM5 acceptably reproduced the wind patterns on August 16, 2006. As Figure 2.7-5: *Region 12 average wind direction and speed scatter plots for August 16, 2006* exhibits, MM5 produced wind direction and wind speeds within the benchmarks for most hours. These statistics show that MM5 followed the veering winds well. For the daytime hours, MM5 slightly under-predicted the wind speed, and slightly over-predicted the nighttime wind speed. Table 2.7-2: *Percent accuracy statistics for August 16, 2006* shows that same overall performance occurred throughout the Houston area, according to the Zone accuracy statistics.

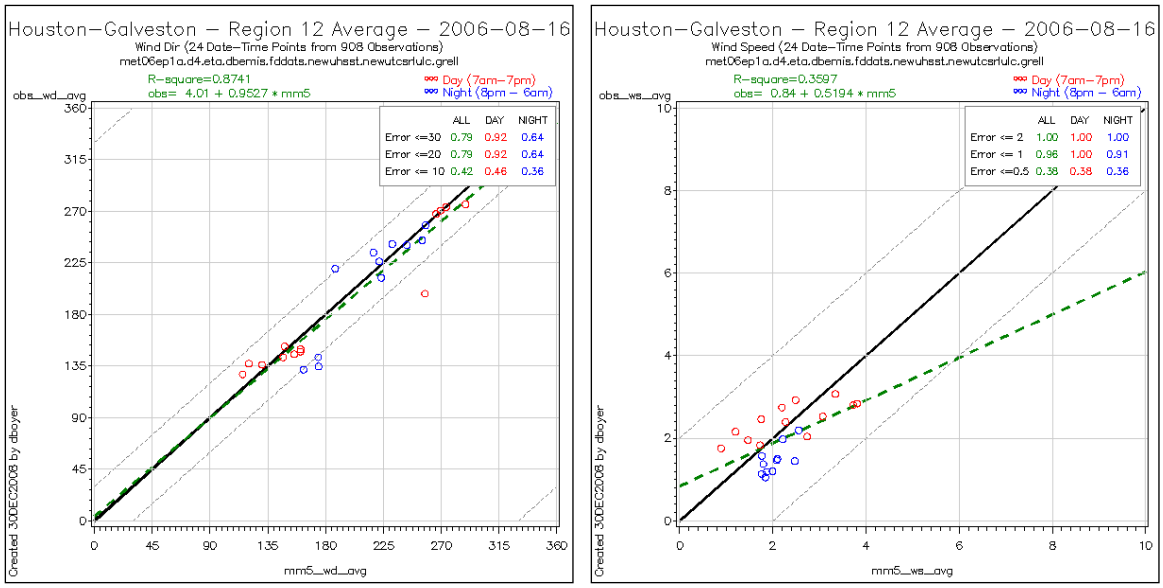

Figure 2.7-5: Region 12 average wind direction and speed scatter plots for August 16, 2006

Table 2-7-2: Percent accuracy statistics for August 16, 2006

Geographic Area/Zone	Wind Direction (°) Error ≤ 30 / 20 / 10	Wind Speed (m/s) Error ≤ 2 / 1 / 0.5	Temperature (°C) Error ≤ 2 / 1 / 0.5
Region 12	79 / 79 / 42	100 / 96 / 38	96 / 83 / 58
Coastal	63 / 54 / 25	100 / 71 / 38	88 / 71 / 46
Ship Channel	71 / 63 / 33	100 / 88 / 38	100 / 83 / 63
Southeast Core	92 / 75 / 42	100 / 79 / 29	100 / 71 / 38
Northwest Core	88 / 75 / 42	100 / 79 / 33	92 / 63 / 38
Downwind	67 / 50 / 33	100 / 67 / 50	92 / 58 / 42

Figure 2.7-6: *Wind field plots for the 12:00 CST (left) and 17:00 CST (right) on August 16, 2006* shows the entire wind field of the CAMx input for August 16, 2006 at 12:00 CST; red arrows show observed winds, pointing in the direction that the wind blows to, and blue arrows show the modeled winds. For most of the observation network, winds are calm, which are indicated by small arrows or dots. However, along Galveston Bay, a bay breeze has developed, and the model winds match the observations closely. This is an important feature to capture, because the morning westerly winds can carry pollutants over Galveston Bay, and the bay breeze can then return the aged pollutants onshore, where they can encounter fresh emissions. At 17:00 CST, the southerly sea breeze has overtaken the bay breeze flow; the model replicates this feature properly as well.

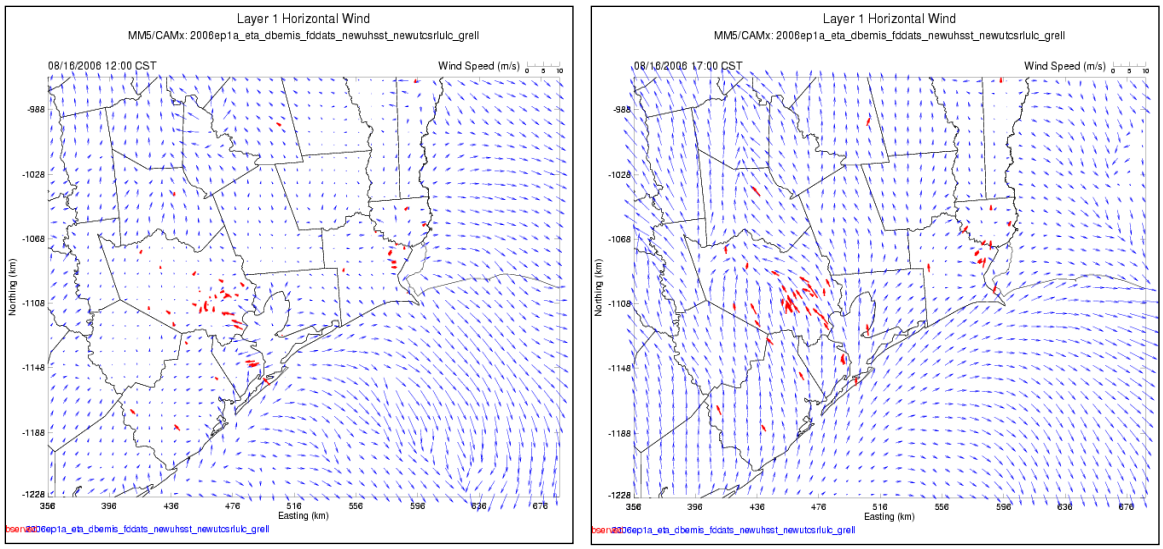

Figure 2.7-6: Wind field plots for the 12:00 CST (left) and 17:00 CST (right) on August 16, 2006

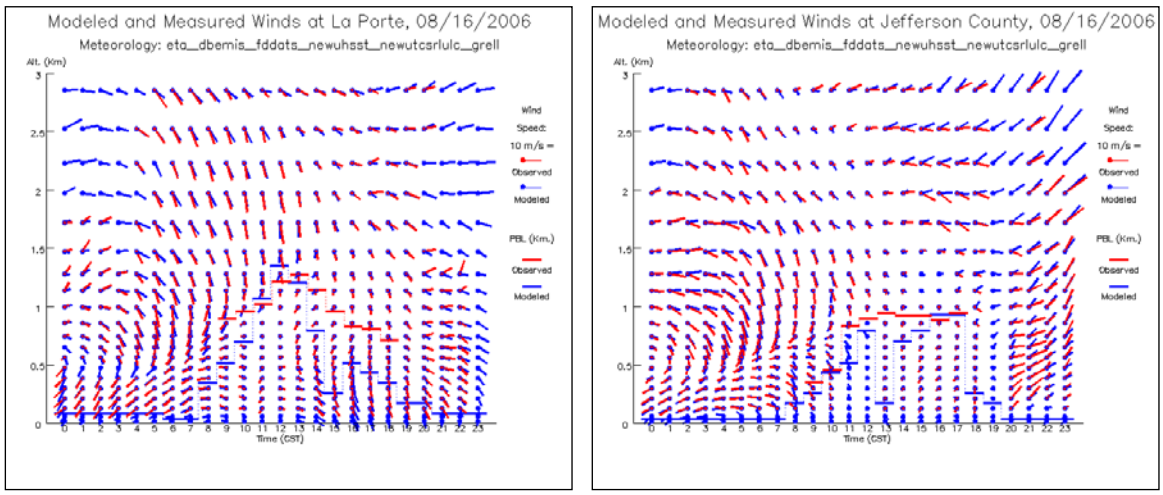

Figure 2.7-7: Time-height plots for the La Porte (left) and Jefferson County (right) profilers on August 16, 2006

At the La Porte profiler (Figure 2.7-7: *Time-height plots for the La Porte (left) and Jefferson County (right) profilers on August 16, 2006*), MM5 accurately followed the change in wind direction and speed throughout the lower levels of the atmosphere for the entire day. The mid-day hours were especially well predicted through the first kilometer, when the wind was calm. On other days, MM5 has difficulty accurately replicating calm conditions. The morning rise and afternoon decay of the PBL may be slightly under-predicted. At the Jefferson County profiler, MM5 successfully predicted the upper air wind flow. The calm conditions last much longer above the surface near Beaumont, and MM5 again simulates this well. The PBL height estimates were very comparable, except at 13:00 CST, when clouds may have affected this site in the model.

As shown by Figure 2.7-8: *12-hour forward trajectory at 08:00 CST on August 16, 2006*, the modeled and observed trajectories exhibit morning westerly winds, shifting to southeasterly in the afternoon. The model appears to produce winds along the ship channel with too much of an easterly component. The lengths of the observed and modeled trajectories are very similar, indicating that the wind speed was well modeled. Based on this figure, the higher ozone in the photochemical model may be just west of the observed peaks, due to the small wind direction error.

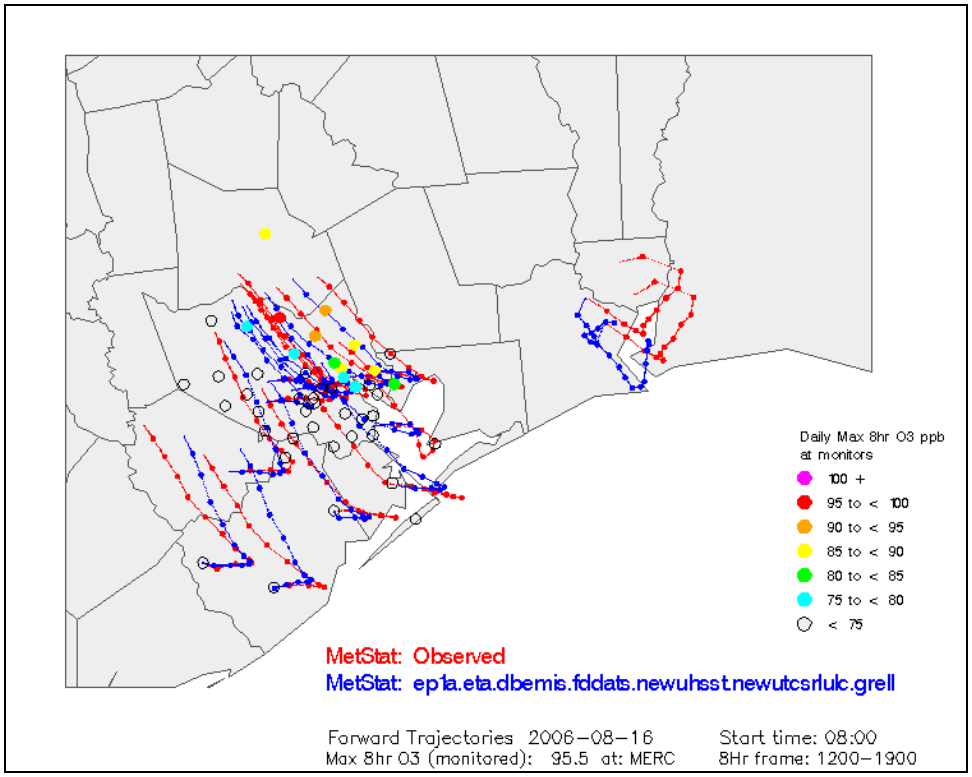

Figure 2.7-8: 12-hour forward trajectory at 08:00 CST on August 16, 2006

August 17, 2006

On this hot day (98 degrees Fahrenheit) winds were light from the north in the morning, calm at mid-day, and light east-southeast in the afternoon as the cold front slowly dissipated near Houston. A weak bay breeze developed along Galveston Bay at 12:00 CST and lasted through 19:00 CST before the sea breeze from the Gulf of Mexico dominated the flow. The sea breeze started at 14:00 CST but had difficulty overcoming the north wind following the cold front. This resulted in further stagnation in the Houston area. Nielsen-Gammon (2007a) noted that the previous day's ozone could have been recirculated due to the light winds of both August 16 and 17. The partly cloudy skies, high temperatures, and light recirculating winds brought good conditions for ozone formation. Fourteen monitors exceeded the eight hour ozone standard, including the peak of 113 ppb at Tom Bass C558. Most of the exceedances occurred south of the Ship Channel and in western Houston.

MM5 predicted the light wind speeds within 0.5 m/s for almost all hours of the day (Figure 2.7-9: *Region 12 average wind direction and speed scatter plots for August 17, 2006*). The wind direction statistics show MM5 had some difficulty with the variable winds, but this should not impact the photochemical modeling significantly, because the speeds were so low (Table 2.7-3: *Percent accuracy statistics for August 17, 2006*). Modeled temperatures were generally within one degree Fahrenheit of the observed throughout Houston.

Table 2.7-3: Percent accuracy statistics for August 17, 2006

Geographic Area/Zone	Wind Direction (°) Error ≤ 30 / 20 / 10	Wind Speed (m/s) Error ≤ 2 / 1 / 0.5	Temperature (°C) Error ≤ 2 / 1 / 0.5
Region 12	63 / 46 / 17	100 / 96 / 75	100 / 88 / 46
Coastal	50 / 33 / 17	100 / 88 / 63	83 / 42 / 08
Ship Channel	46 / 33 / 21	100 / 79 / 67	100 / 75 / 46
Southeast Core	54 / 33 / 17	100 / 83 / 46	100 / 96 / 67
Northwest Core	46 / 33 / 21	100 / 92 / 54	96 / 58 / 17
Downwind	13 / 08 / 04	96 / 71 / 42	88 / 54 / 29

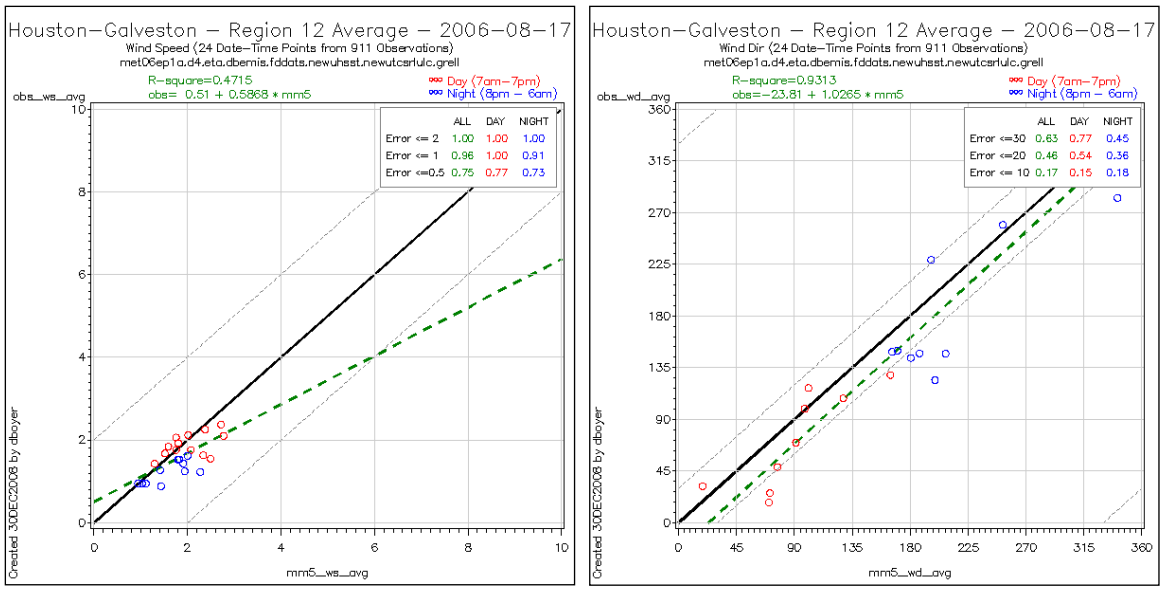

Figure 2.7-9: Region 12 average wind direction and speed scatter plots for August 17, 2006

The time height plots from the La Porte and Jefferson County (Figure 2-7-10: *Time-height plots for the La Porte (left) and Jefferson County (right) profilers on August 17, 2006*) show the north winds on August 17, 2006. Near the surface, the winds are calm, and rotate from the north to the southeast. MM5 follows these patterns well, except during early morning hours about one kilometer above the surface. The PBL estimates follow the observations very well, including the morning rise, though the afternoon modeled PBL at Jefferson County was too low. Modeled clouds moving from the east may have impacted the predicted mixing depth around Beaumont.

Based on the observed and modeled 12 hour trajectories, MM5 simulated the wind conditions well along the ship channel and central Houston (Figure 2.7-11: *Surface wind field plots for the 14:00 CST (left) and 19:00 CST (right) on August 17, 2006*). However, along Galveston Bay and the Gulf of Mexico, MM5 rotated the winds too early. This is most likely due to the modeled sea breeze penetrating inland too early, as shown by Figure 2.7-12: *12-hour forward trajectory at 08:00 CST on August 17, 2006*. As a result of this error, a stronger recirculation may occur in the photochemical model to produce more ozone than observed.

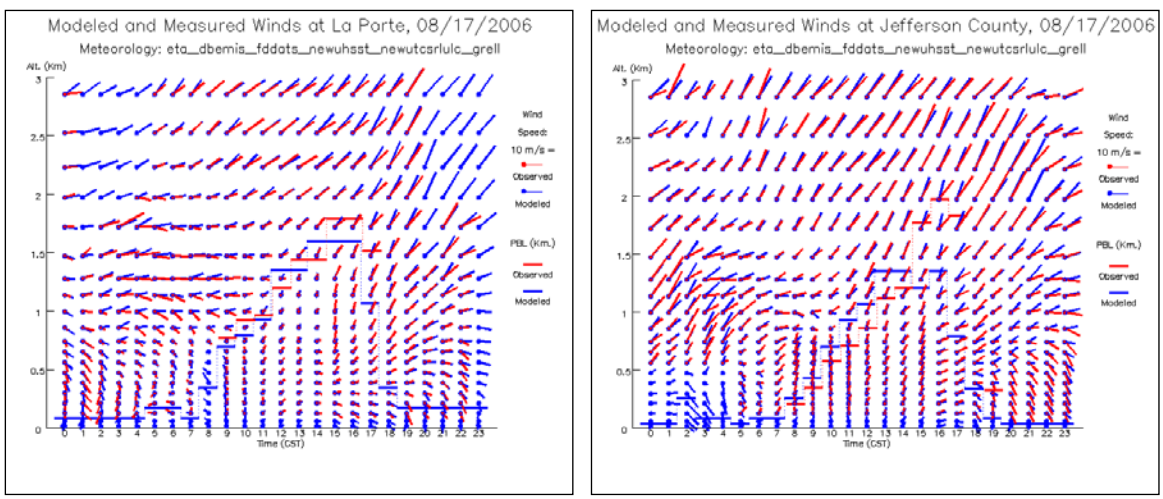

Figure 2.7-10: Time-height plots for the La Porte (left) and Jefferson County (right) profilers on August 17, 2006

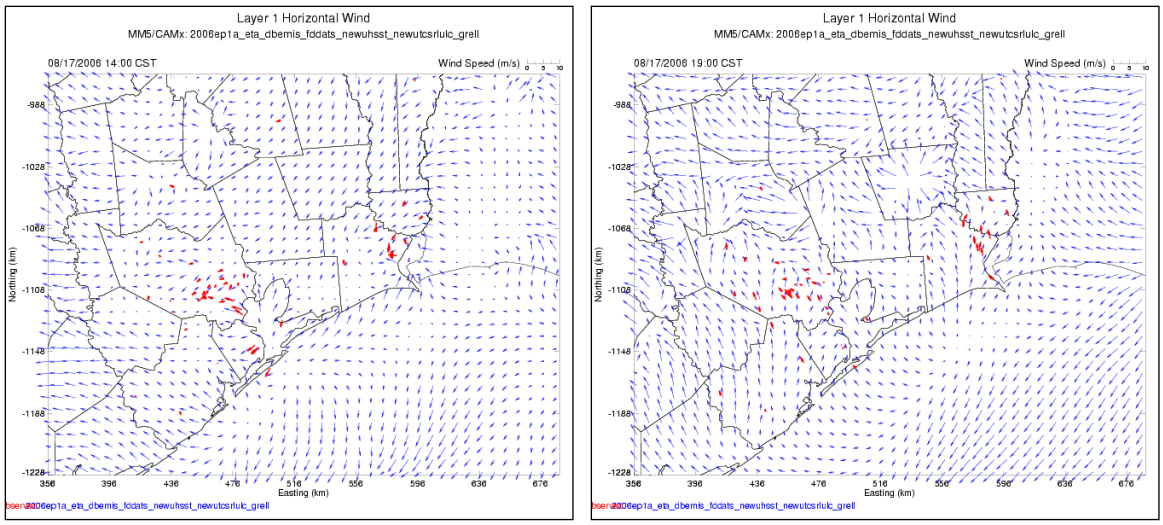

Figure 2.7-11: Surface wind field plots for the 14:00 CST (left) and 19:00 CST (right) on August 17, 2006

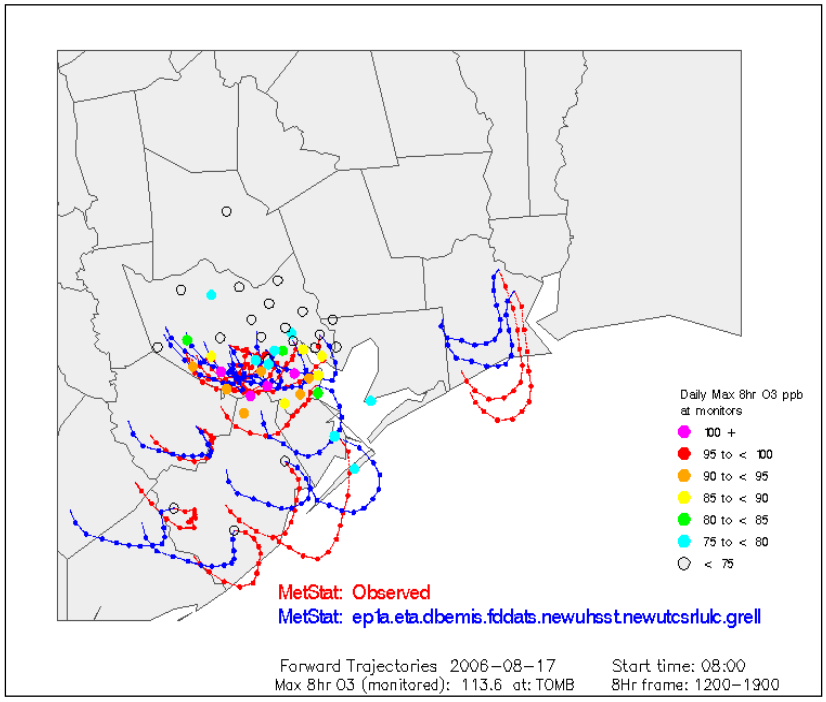

Figure 2.7-12: 12-hour forward trajectory at 08:00 CST on August 17, 2006

August 18, 2006

August 18, 2006 was the last high ozone day of this episode, with only the Katy Park C559 monitor exceeding at 89 ppb. Winds were calm in the early morning hours and then light from the northeast starting at 07:00 CST. By 10:00 CST the winds were steady from the east at 2 meters/second. Wind speed peaked around 15:00 CST at 4 meters/second and slowly weakened as the wind turned more southeasterly. Temperatures were above 90 °F for most of the Houston area under scattered cumulus skies. The calm winds from the previous day and into the morning of August 18 may have increased the background ozone, allowing for an exceedance.

Wind speeds were accurately represented by MM5 for this day, with almost 80% of the hours within one meter/second of the observations. Wind direction was well simulated except for a few early morning hours when MM5 predicted south-southwest winds. In reality south-southeast winds existed. Temperatures were under-predicted throughout the Houston area, as morning convection and precipitation in MM5 (not shown) may have limited afternoon temperatures and mixing.

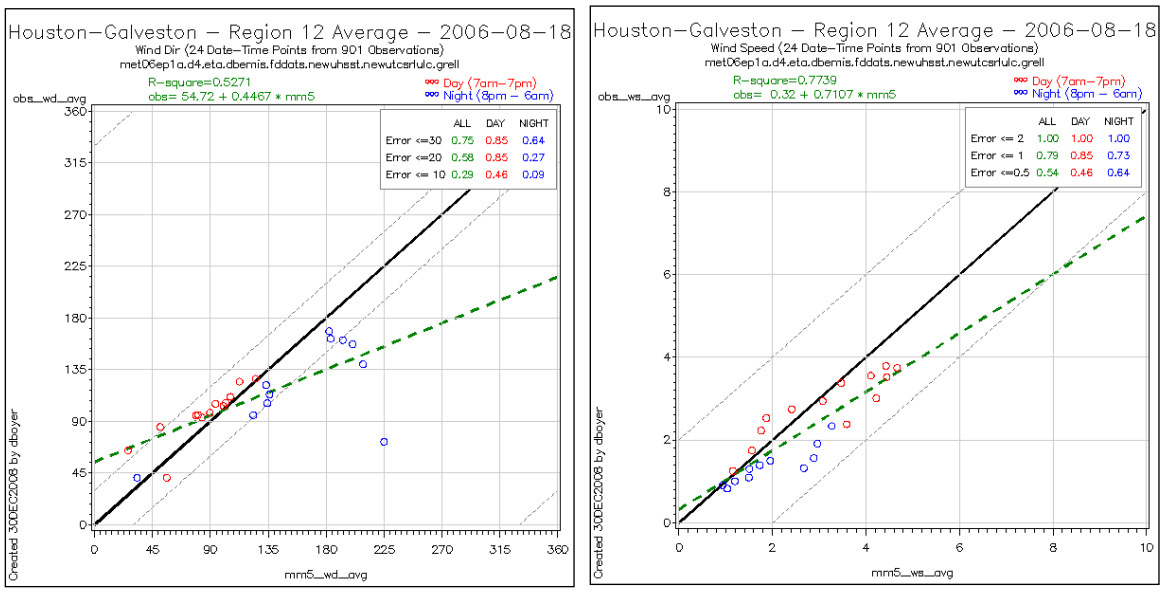

Figure 2.7-13: Region 12 average wind direction and speed scatter plots for August 18, 2006

Table 2.7-4: Percent accuracy statistics for August 18, 2006

Geographic Area/Zone	Wind Direction (°) Error ≤ 30 / 20 / 10	Wind Speed (m/s) Error ≤ 2 / 1 / 0.5	Temperature (°C) Error ≤ 2 / 1 / 0.5
Region 12	75 / 58 / 29	100 / 79 / 54	63 / 42 / 38
Coastal	75 / 63 / 33	100 / 79 / 38	56 / 33 / 25
Ship Channel	71 / 50 / 38	100 / 83 / 54	71 / 38 / 21
Southeast Core	83 / 75 / 50	96 / 54 / 38	79 / 38 / 29
Northwest Core	75 / 67 / 42	100 / 71 / 29	63 / 21 / 00
Downwind	54 / 46 / 38	92 / 54 / 29	83 / 42 / 17

Unlike August 16 and August 17, 2006, stagnant conditions did not occur around mid-day on August 18 (Figure 2.7-14: *Surface wind field plots for the 12:00 CST (left) and 18:00 CST (right) on August 18, 2006*). Instead, an easterly breeze continued until approximately 18:00 CST, as shown by the observations' red arrows in the right hand of the figure. As shown by the blue arrows, the model tracks these conditions well. At 18:00 CST the model has too much of an easterly component, which may cause the modeled high ozone to be placed west and south of the observed peak at Katy Park.

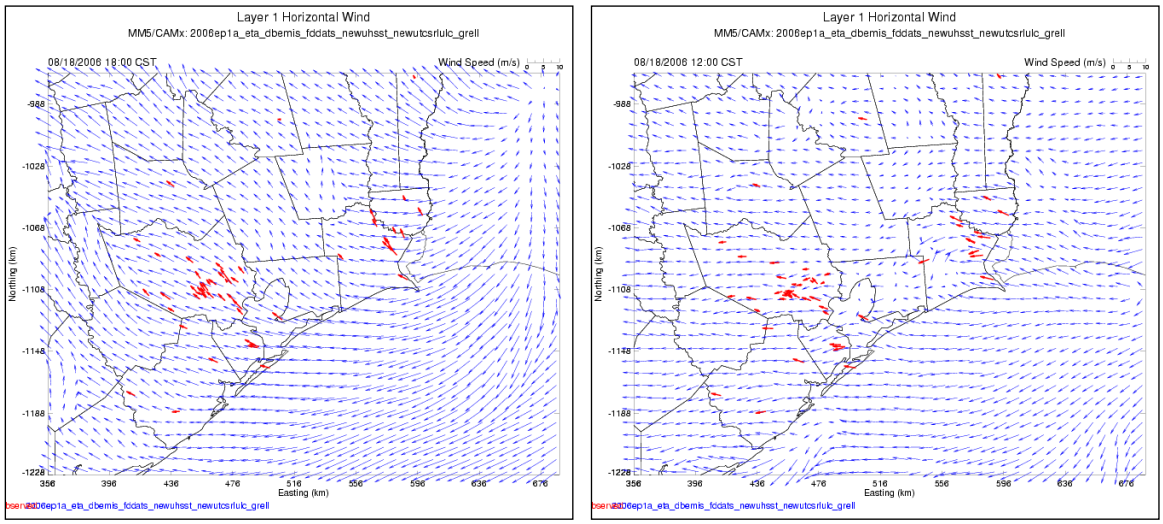

Figure 2.7-14: Surface wind field plots for the 12:00 CST (left) and 18:00 CST (right) on August 18, 2006

The upper air wind flow from the La Porte profiler (Figure 2.7-15: *Time-height plots for the La Porte (left) and Huntsville (right) profilers on August 18, 2006*) shows that the upper air winds had similar patterns to the surface flow. East winds exist from 07:00 – 13:00 CST before winds from the southeast take over for the rest of the day. MM5 represents these conditions well except for a few early morning hours above 1 kilometer, and near-surface winds after 14:00 CST, when the wind direction is slightly off. At Huntsville, northerly winds occur in the morning through the lowest three kilometers, before the wind speed dies at 09:00 CST. At 12:00 CST, easterly winds develop. MM5 generally replicates these wind conditions well. At both profilers, the peak mixing depth is under-predicted. The morning rise is well represented at Huntsville while PBL performance at La Porte is disappointing, except for a few late morning hours.

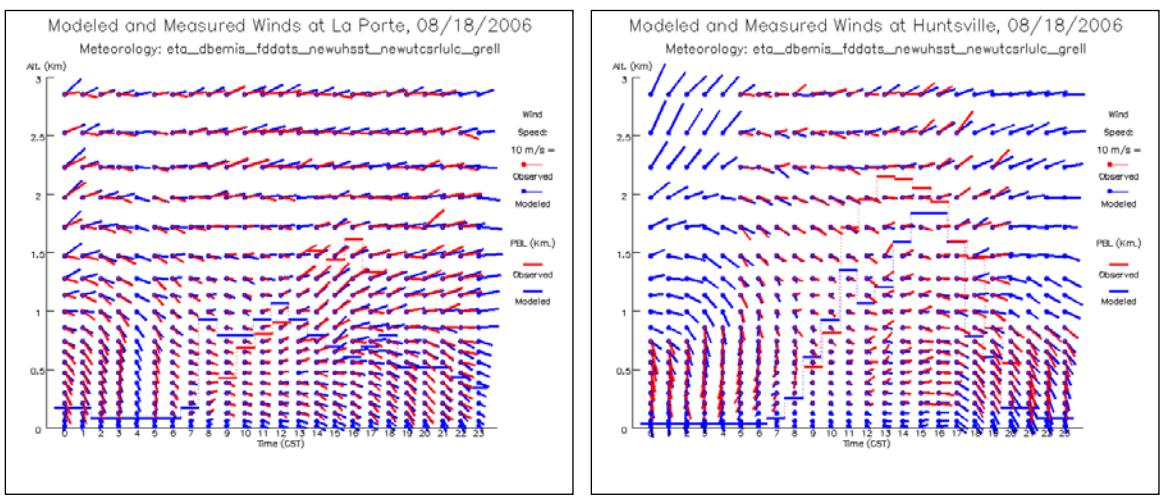

Figure 2.7-15: Time-height plots for the La Porte (left) and Huntsville (right) profilers on August 18, 2006

The modeled and observed trajectories on August 18, 2006 are very similar in length and orientation (Figure 2.7-16: *12-hour forward trajectory at 08:00 CST on August 18, 2006*). The only difference appears to be a slight displacement to the south, due to the late turning of the winds to the southeast. The wind error may place the modeled ozone plumes to the south and west of the observed peaks.

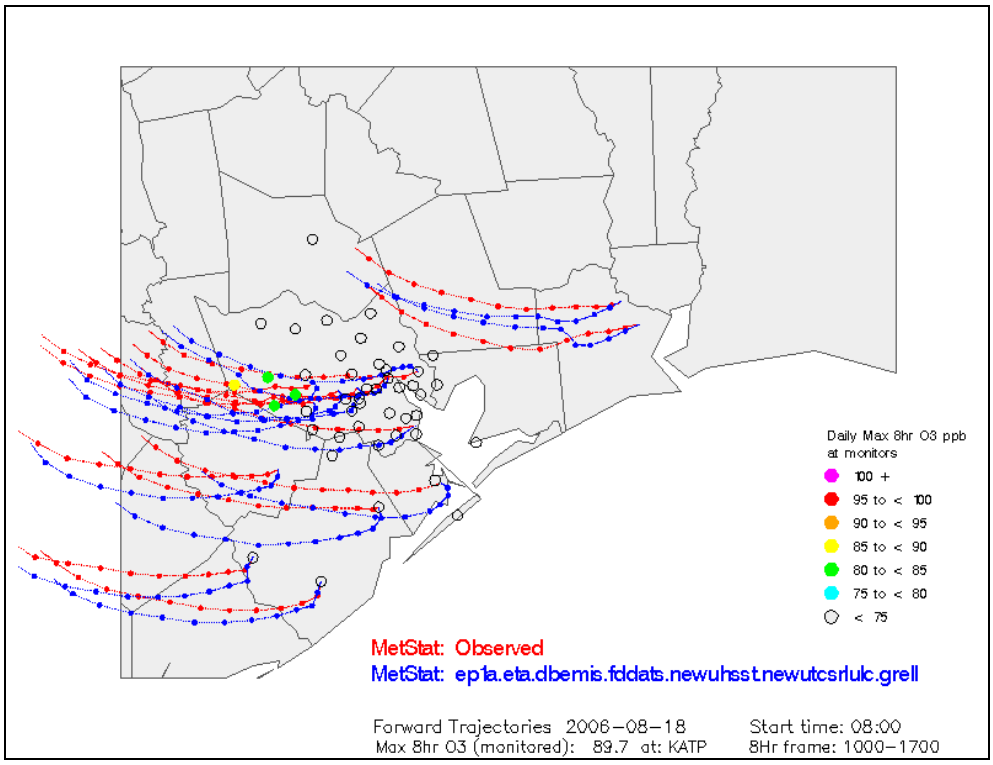

Figure 2.7-16: 12-hour forward trajectory at 08:00 CST on August 18, 2006

2.8 2006ep1b Performance Evaluation

The 2006ep1b episode has four periods of high ozone: August 31- September 1, September 3, September 6-7, and September 13-14, 2006

During August 27 to September 16, 2006, there were several cold fronts that passed over Houston. Three of the high ozone days occurred a day after the passage of a cold front.

The MM5 model simulated the episode well and reproduced the main meteorological features accurately. The error associated with the wind direction, wind speed and temperature for the entire episode for all sites was 80, 100, and 89 percent respectively. The error associated with the wind direction, wind speed and temperature for the entire episode for region 12 (Houston-Galveston) was 67, 96, and 80 percent respectively as show in Table 2.8-1: *Error percentages for 2006ep1b episode* and Figure 2.8-1: *Region 12 average wind speed and direction scatter plots for 2006ep1b episode*.

Table 2.8-1: Error percentages for 2006ep1b episode

Duration	Geographic Area/Zone	Wind Direction (°) Error % 30 / 20 / 10	Wind Speed (m/s) Error % 2 / 1 / 0.5	Temperature (°C) Error % 2 / 1 / 0.5
Episode Average	All Sites	80 / 65 / 39	100 / 70 / 30	89 / 57 / 27
Episode Average	Region 12	67 / 54 / 33	96 / 63 / 26	80 / 52 / 25
Episode Average	Coastal	62 / 49 / 27	90 / 56 / 32	81/ 52 / 28
Episode Average	Ship Channel	62 / 50 / 28	93 / 51 / 23	80 / 49 / 26
Episode Average	Southeast Core	59 / 48 / 26	90 / 55 / 27	81 / 51 / 29
Episode Average	Northwest Core	56 / 40 / 21	91 / 55/ 30	73 / 44 / 20
Episode Average	Downwind	52 / 39 / 20	82 / 37 / 20	76/ 44 / 23

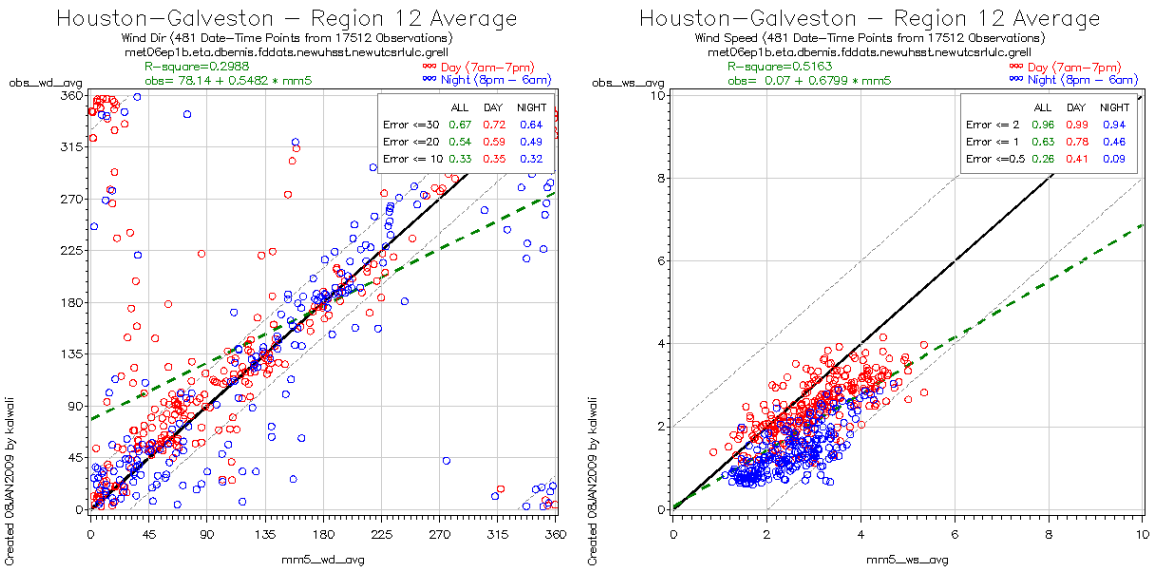

Figure 2.8-1: Region 12 average wind speed and direction scatter plots for 2006ep1b episode

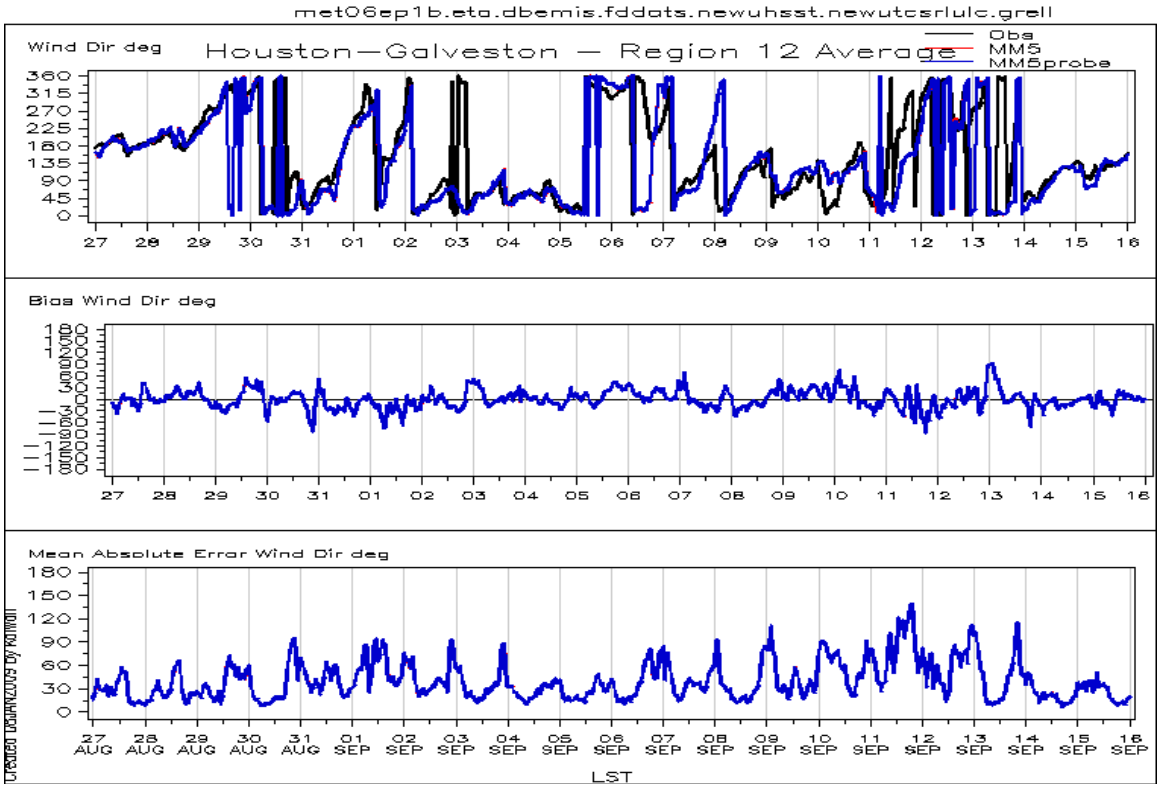

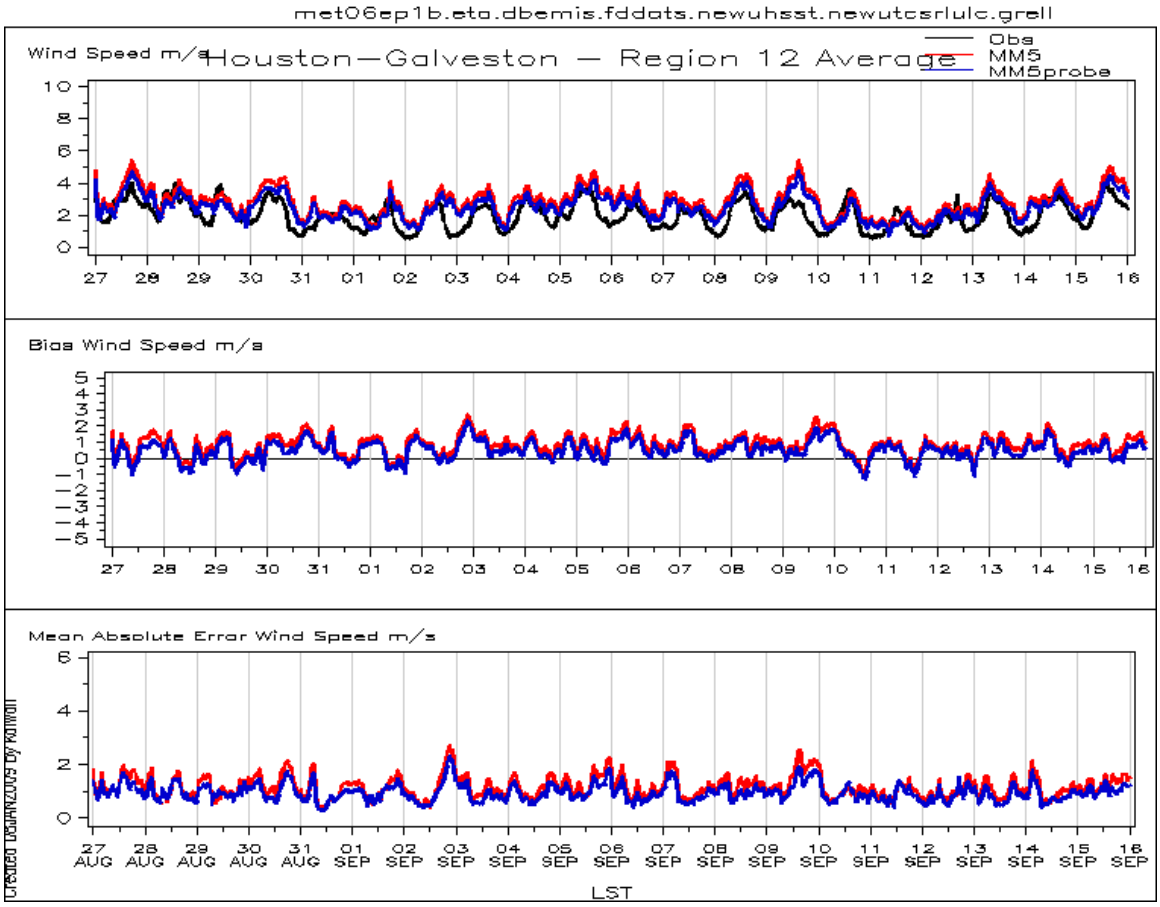

Figure 2.8-2: Region 12 average wind direction and wind speed time series for 2006ep1b episode

August 31, 2006

On that day, 14 monitors recorded an exceedance of the eight-hour ozone standard greater than 85 ppb. The Houston Westhollow C410 monitor recorded the maximum eight-hour ozone of 127.1 ppb at 1100 CST. Regional background levels of ozone, in the air coming into the Houston area, ranged from about 55 to 68 ppb as indicated by the peak eight-hour averages at Kingwood CAMS 555, Crosby CAMS 553, and Smith Point CAMS 96.

The sky was mostly clear during the day. Regional winds were generally light and from the northeast. Local winds were light northeasterly changing to light easterly in the middle of the day and then becoming moderate southeasterly during the late afternoon and evening hours. The high temperature was 94 degrees Fahrenheit (°F) at George Bush Houston Intercontinental Airport, 92°F at Hobby Airport, and 88°F at Galveston Airport.

The error associated with the wind direction, wind speed and temperature for the entire episode for region 12 (Houston-Galveston) was 71, 100, and 79 respectively as show in Table 2.8-2; *Error percentages for August 31, 2006,* and Figure 2.8-5: *Region 12 Average wind direction and speed scatter plots for August 31, 2006*. Figure 2.8-6: *Time-height plot for La Porte profiler on August 31, 2006,* shows a good agreement between the profiler winds and the MM5 output for most of the day and the vertical level.

The 12-hour forward trajectories starting at 6 am on August 31, 2006 as depicted in figure 2.8-7: *12-hour forward trajectory at 06:00 CST on August 31, 2006* show the trajectories generated using the MM5 data are longer and to the south of the trajectories generated using the CAMS data. This would results the location of the maximum ozone to be to the south of the location of the maximum ozone for that day.

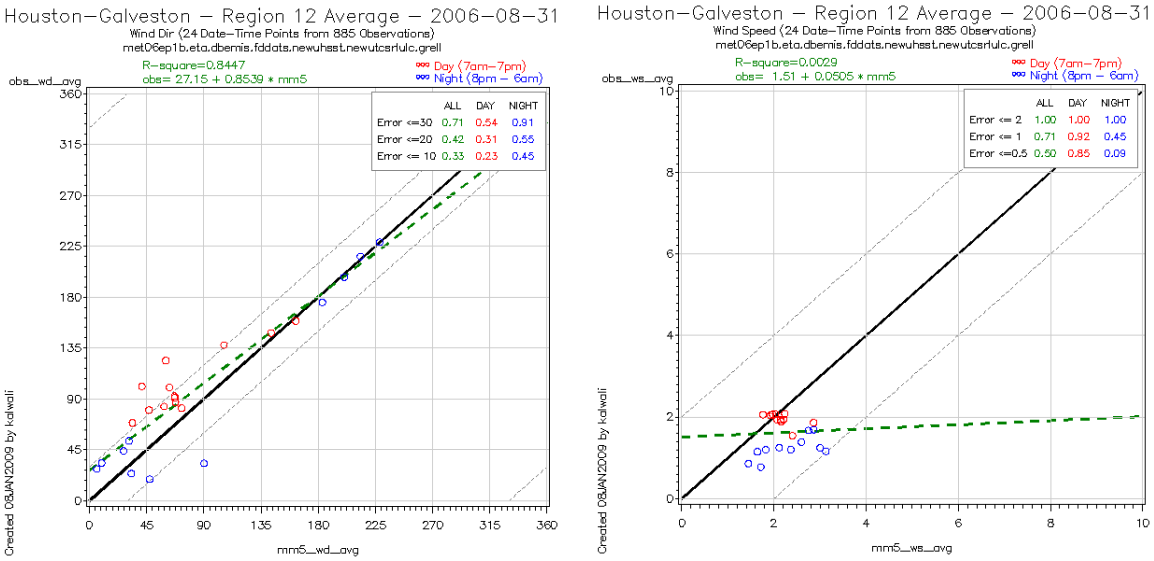

Figure 2.8-5: Region 12 Average wind direction and speed scatter plots for August 31, 2006

Table 2.8-2: Error percentages for August 31, 2006

Duration	Geographic Area/Zone	Wind Direction (°) Error % 30 / 20 / 10	Wind Speed (m/s) Error % 2 / 1 / 0.5	Temperature (°C) Error % 2 / 1 / 0.5
8/31/2006	Region 12	71 / 42 / 33	100 / 71 / 50	79 / 46 / 29
8/31/2006	Coastal	71/50/38	88/46/33	75/42/25
8/31/2006	Ship Channel	54 / 33 / 21	96 / 63 / 58	96 / 58 / 21
8/31/2006	Southeast Core	46 / 42 / 25	100 / 67 / 50	100 / 54 / 21
8/31/2006	Northwest Core	42 / 25 / 08	92 / 63 / 42	67 / 38 / 21
8/31/2006	Downwind	29 / 21 / 13	96 / 54 / 33	79 / 42 / 13

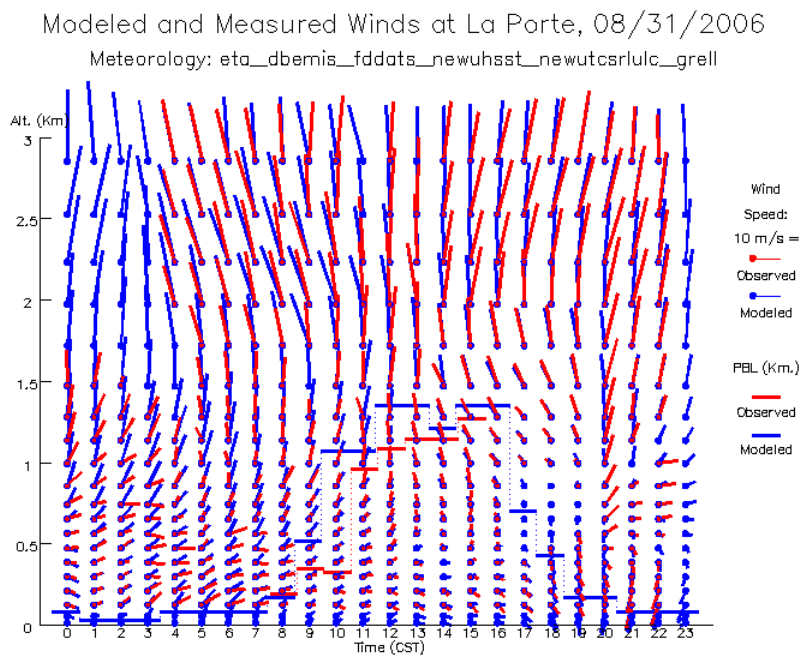

Figure 2.8-6: Time-height plot for La Porte profiler on August 31, 2006

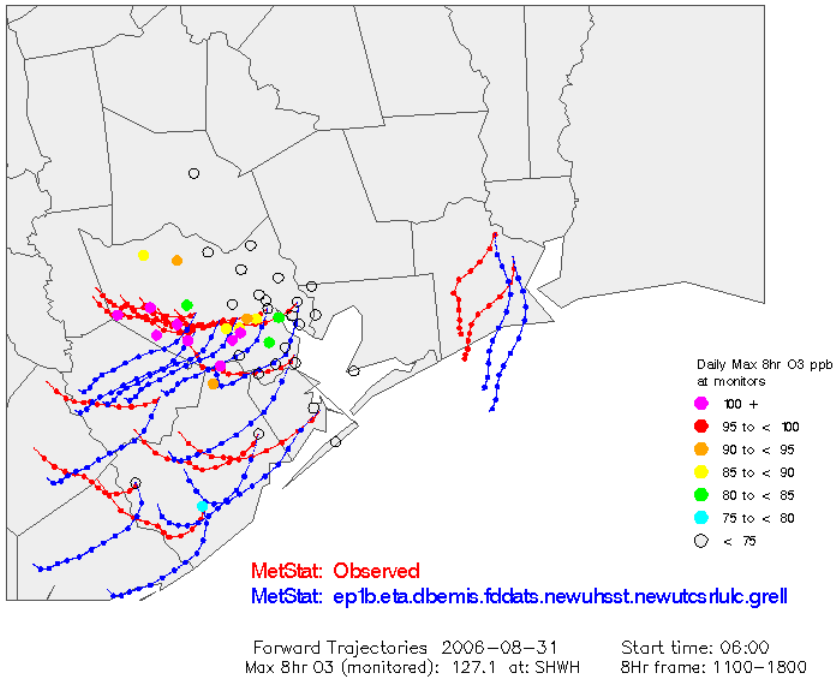

Figure 2.8-7: 12-hour forward trajectory at 06:00 CST on August 31, 2006

September 1, 2006

On this day, 27 monitors recorded an exceedance of the eight-hour ozone standard greater than 85 ppb. The Houston Deer Park 2 monitor recorded the maximum eight-hour ozone of 121.8 ppb at 1100 CST. Regional background levels of ozone, in the air coming into the Houston area, were at least about 63 to 66 ppb as indicated by the peak eight-hour averages at Danciger CAMS 618, Lake Jackson CAMS 1016, and Mustang Bayou CAMS 619.

In the early morning, the skies were clear, becoming partly cloudy in the late morning and afternoon. Light west-northwesterly winds in the early morning, becoming light easterly mid-day with the bay breeze and then moderate southeasterly in the late afternoon and evening with the sea breeze. The high temperature was 96 degrees Fahrenheit (F) at George Bush Houston Intercontinental Airport, 92 degrees F at Hobby Airport, and 91 degrees F at Galveston Airport.

The error associated with the wind direction, wind speed and temperature for the entire episode for region 12 (Houston-Galveston) was 50, 100, and 92 respectively as show in Table 2.8-3: *Error percentages for September 1, 2006* and Figure 2.8-8: *Region 12 Average wind direction and speed scatter plots for September 1, 2006*.

Table 2.8-3: Error percentages for September 1, 2006

Duration	Geographic Area/Zone	Wind Direction (°) Error % 30 / 20 / 10	Wind Speed (m/s) Error % 2 / 1 / 0.5	Temperature (°C) Error % 2 / 1 / 0.5
9/1/2006	Region 12	50 / 42 / 25	100 / 50 / 33	92 / 63 / 21
9/1/2006	Coastal	29 / 13 / 04	79 / 63 / 42	96 / 79 / 42
9/1/2006	Ship Channel	67 / 63 / 21	96 / 42 / 17	75 / 42 / 38
9/1/2006	Southeast Core	54 / 38 / 29	92 / 42 / 21	79 / 63 / 25
9/1/2006	Northwest Core	42 / 25 / 13	92 / 46 / 25	83 / 29 / 04
9/1/2006	Downwind	21 / 13 / 08	83 / 38 / 21	88 / 63 / 29

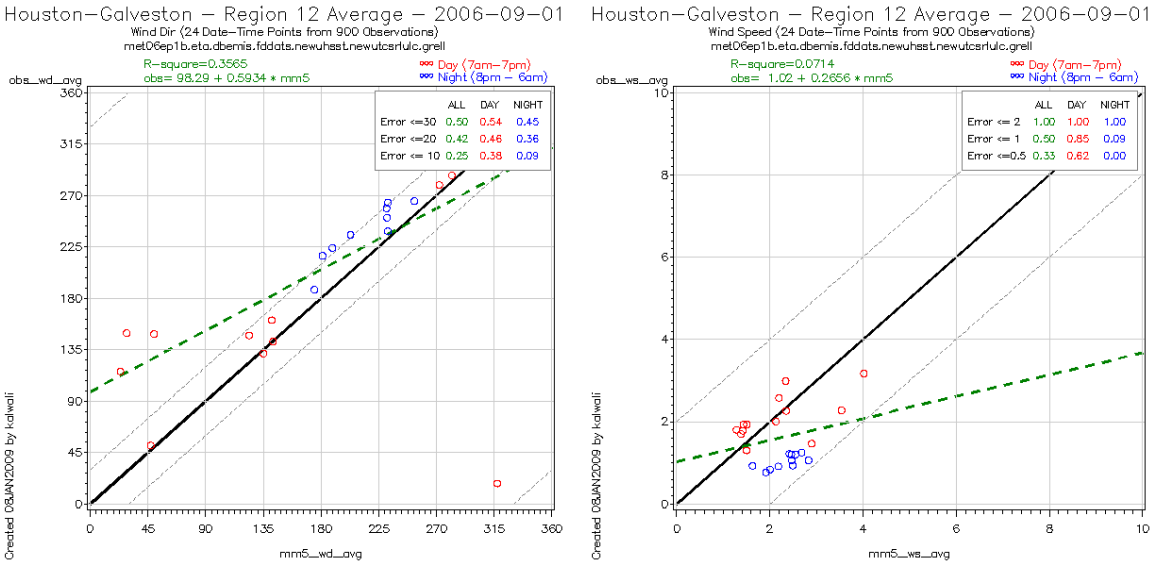

Figure 2.8-8: Region 12 Average wind direction and speed scatter plots for September 1, 2006

Figure 2.8-9: *Time-height plot for La Porte profiler on September 1, 2006* shows a good agreement between the profiler winds and the MM5 output for most of the day and the vertical level

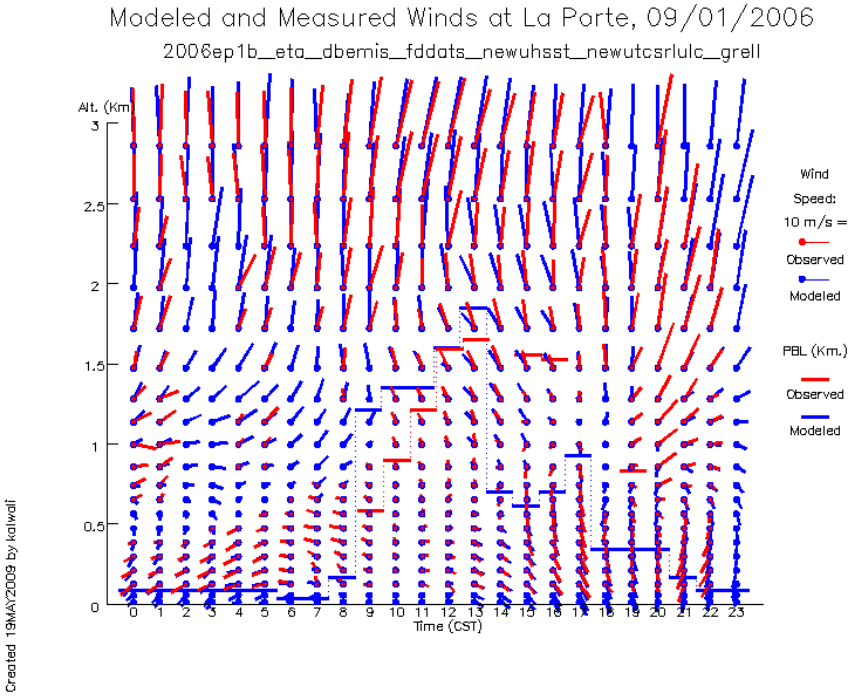

Figure 2.8-9: Time-height plot for La Porte profiler on September 1, 2006

The 12-hour forward trajectories starting at 6 am on September 1, 2006 as depicted in figure 2.8-10: *12-hour forward trajectory at 06:00 CST on September 01, 2006* show that in the Jefferson County, the MM5 trajectories or similar to the observed trajectories, but slightly to the west. In Brazoria County, for the first four hours, the MM5 trajectories are similar to the observed trajectories. However, after that they are different as the MM5 trajectories travel to the west then north while the observed trajectories travel to the east then north. In Harris County, the MM5 and observed trajectories curl around and travel a very limited distance representing a stagnant circulation.

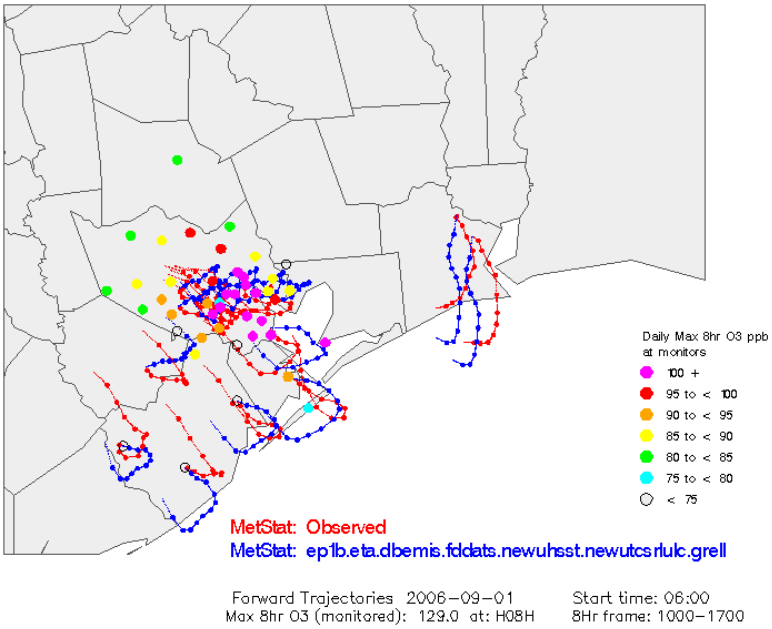

Figure 2.8-10: 12-hour forward trajectory at 06:00 CST on September 01, 2006

September 7, 2006

On September 7, 12 monitors recorded an exceedance of the eight-hour ozone standard greater than 85 ppb. The Houston Bayland Park C53 monitor recorded the maximum eight-hour ozone of 110.5 ppb at 1000 CST. Regional background levels of ozone, in the air coming into the Houston area, were at least about 61 to 72 ppb as indicated by the peak eight-hour averages at Conroe CAMS 78, Kingwood CAMS 555, Crosby CAMS 553, and Galveston CAMS 34.

As for the weather, there were occasionally some cirrus clouds with scattered cumulus clouds in the afternoon. Regional winds were light and from the northeast. Winds from the east-northeast (3-6 mph) occurred during the morning, veering to southeasterly (3-6 mph) in the late afternoon. The high temperature was 93 degrees F at George Bush Houston Intercontinental Airport, 91degrees F at Hobby Airport, and 88 degrees F at Galveston Airport.

The error associated with the wind direction, wind speed and temperature for the entire episode for region 12 (Houston-Galveston) was 63, 88, and 100 respectively as show in Table 2.8-4: *Error percentages for September 7, 2006* and Figure 2.8-11: *Region 12 Average wind direction and speed scatter plots for September 7, 2006.*

Table 2.8-4: Error percentages for September 7, 2006

Duration	Geographic Area/Zone	Wind Direction (°) Error % 30 / 20 / 10	Wind Speed (m/s) Error % 2 / 1 / 0.5	Temperature (°C) Error % 2 / 1 / 0.5
9/7/2006	Region 12	63 / 46 / 17	88 / 71 / 29	100 / 46 / 25
9/7/2006	Coastal	42 /29 /13	83 /67 /50	100 /67/ 46
9/7/2006	Ship Channel	54 / 38 / 17	92 / 63 / 33	96 / 79 / 21
9/7/2006	Southeast Core	63 / 42 / 21	83 / 58 / 25	88 / 58 / 17
9/7/2006	Northwest Core	46 / 25 / 13	83 / 50 / 33	54 / 33 / 25
9/7/2006	Downwind	63 / 42 / 21	83 / 38 / 21	96 / 33 / 21

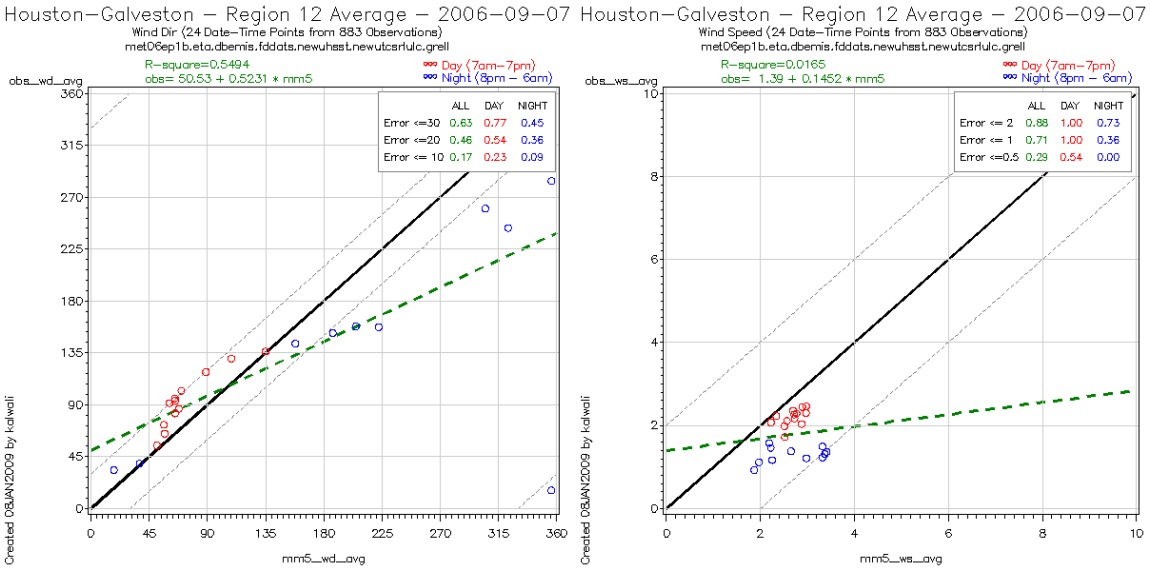

Figure 2.8-11: Region 12 Average wind direction and speed scatter plots for September 7, 2006.

Figure 2.8-12: *Time-height plot for La Porte profiler on September 1, 2006* shows a good agreement between the profiler winds and the MM5 output for most of the day and the vertical level.

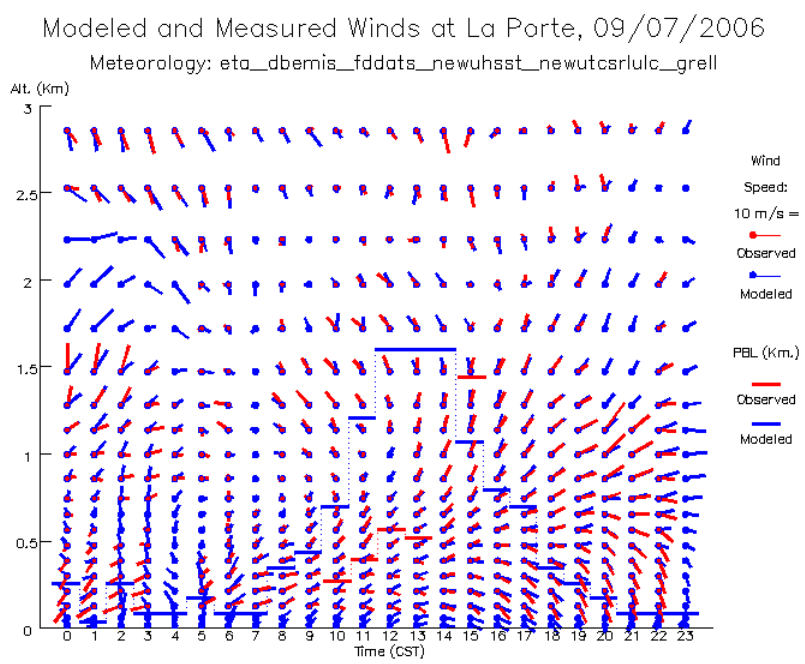

Figure 2.8-12: Time-height plot for La Porte profiler on September 1, 2006

The 12-hour forward trajectories starting at 6 am on September 7, 2006 as depicted in figure 2.8-13: *12-hour forward trajectory at 06:00 CST on September 7, 2006* show that most of the trajectories generated using the MM5 data are parallel and to the south of the trajectories generated using the CAMS data.

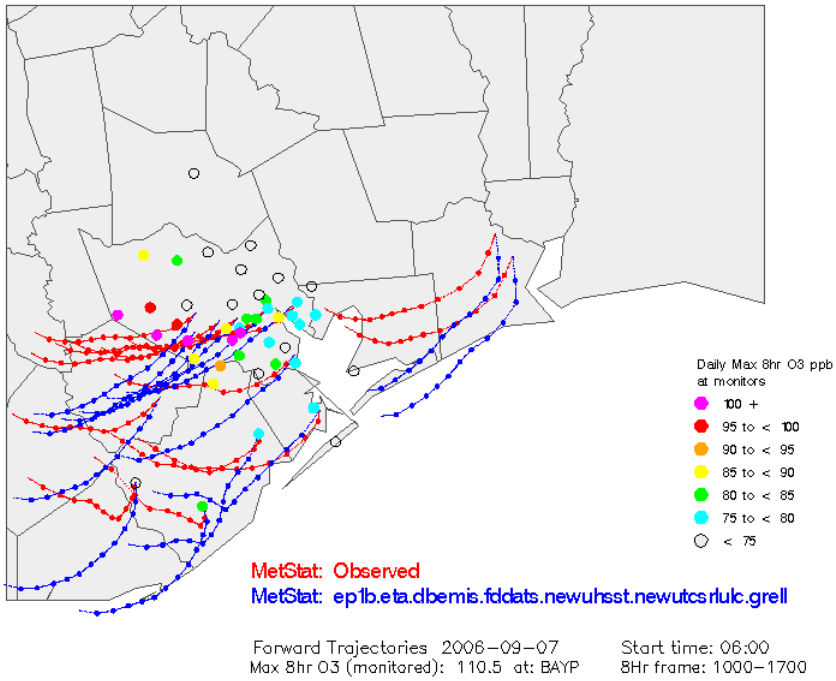

Figure 2.8-13: 12-hour forward trajectory at 06:00 CST on September 7, 2006

September 14, 2006

On that day, 8 monitors recorded an exceedance of the eight-hour ozone standard greater than 85 ppb. The West Houston C554 monitor recorded the maximum eight-hour ozone of 118.9 ppb at 1100 CST. Regional background levels of ozone, in the air coming into the Houston area, were at least about 56 to 74 ppb as indicated by the peak eight-hour averages at Kingwood CAMS 555, Crosby CAMS 553, Smith Point C96, and Galveston CAMS 34.

The weather was clear in the morning with scattered boundary-layer cumulus from late morning onward. Scattered thundershowers occurred in the afternoon south and southwest of Houston. East-northeasterly winds at 6-8 mph during the early morning, veering to easterly later in the morning and finally southeasterly at 6-10 mph during the afternoon. The high temperature was 92 degrees Fahrenheit at George Bush Houston Intercontinental Airport, 91degrees at Hobby Airport, and 88 degrees at Galveston Airport.

The error associated with the wind direction, wind speed and temperature for the entire episode for region 12 (Houston-Galveston) was 92, 96, and 79 respectively as show in Table 2.8-5: *Error percentages for September 14, 2006* and Figure 2.8-14: *Region 12 Average wind direction and speed scatter plots for September 14, 2006*.

Table 2.8-5: Error percentages for September 14, 2006

Duration	Geographic Area/Zone	Wind Direction (°) Error % 30 / 20 / 10	Wind Speed (m/s) Error % 2 / 1 / 0.5	Temperature (°C) Error % 2 / 1 / 0.5
9/14/2006	Region 12	92 / 88 / 50	96 / 71 / 25	79 / 67 / 38
9/14/2006	Coastal	92 / 67 / 50	96 / 58 / 33	83 / 67 / 29
9/14/2006	Ship Channel	88 / 71 / 58	96 / 71 / 33	79 / 42 / 13
9/14/2006	Southeast Core	92 / 79 / 54	96 / 58 / 25	100 / 63 / 42
9/14/2006	Northwest Core	75 / 54 / 33	100 / 63 / 38	71 / 54 / 17
9/14/2006	Downwind	79 / 67 / 38	79 / 42 / 17	63 / 21 / 08

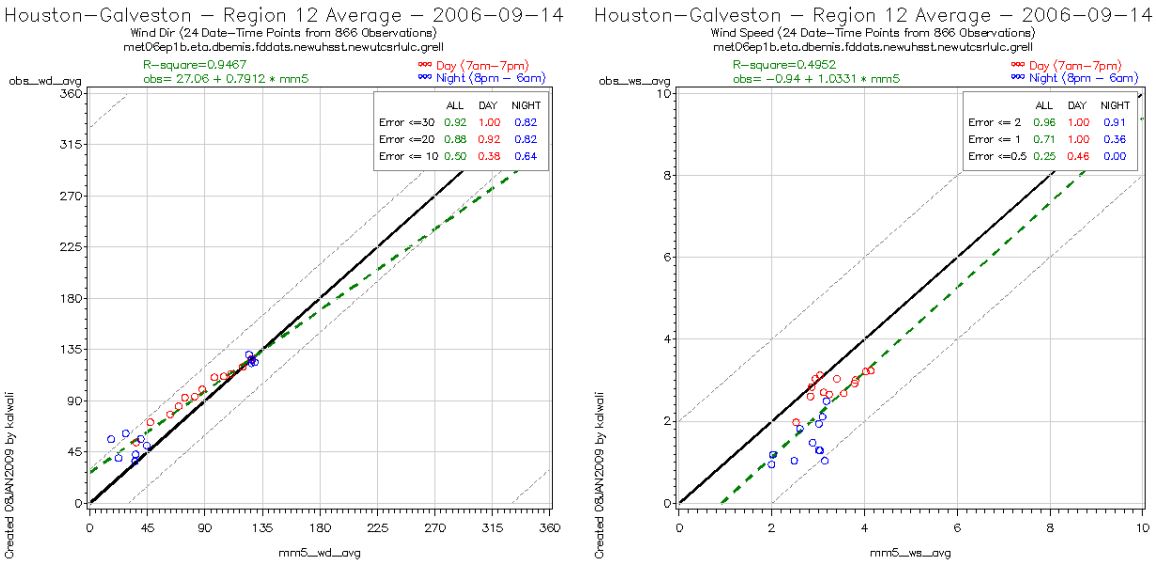

Figure 2.8-14: Region 12 Average wind direction and speed scatter plots for September 14, 2006

Figure 2.8-15: *Time-height plot for La Porte profiler on September 14, 2006* shows a good agreement between the profiler winds and the MM5 output for most the day and the vertical levels, except for the lower levels from 1-6 and 10-11 CST and the upper levels at 20 CST where the observed winds were stronger and from the north.

The 12-hour forward trajectories starting at 6 am on September 14, 2006 as depicted in figure 2.8-16*: 12-hour forward trajectory at 06:00 CST on September 14, 2006* show that most of the trajectories generated using the MM5 data are parallel and to the south of the trajectories generated using the CAMS data.

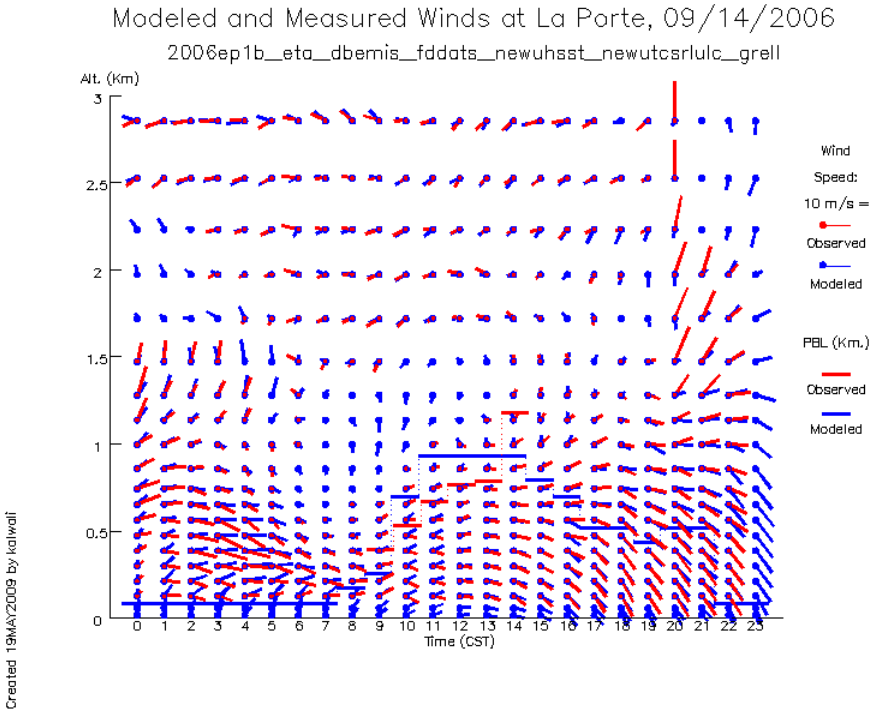

Figure 2.8-15: Time-height plot for La Porte profiler on September 14, 2006

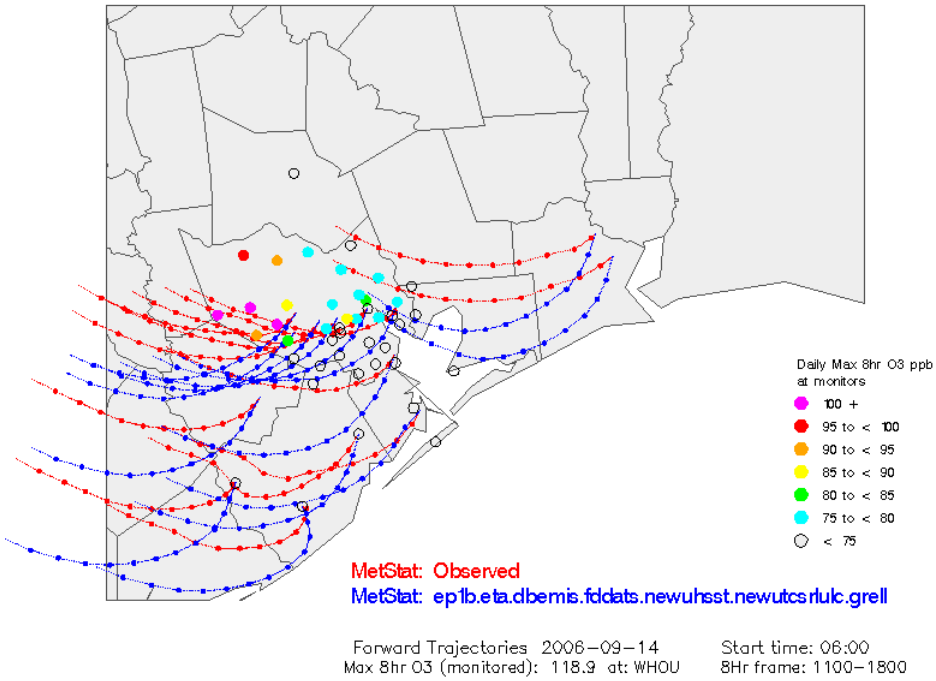

Figure 2.8-16: 12-hour forward trajectory at 06:00 CST on September 14, 2006

2.9 2006ep1c Performance Evaluation

The 2006ep1c episode has two periods of high ozone: September 20, 2006, and September 26-27.

During September 16 -29, 2006, there were three cold fronts that passed over Houston on September 18, 24, and 28, 2006. Two of the high ozone days occurred two days after the passage of the first two cold fronts and the third high ozone day occurred a day after the passage of the third cold front.

The MM5 model simulated the episode well and reproduced the main meteorological features close to the actual observations. The error associated with the wind direction, wind speed and temperature for the entire episode for all sites was 94, 100, and 75 respectively. The error associated with the wind direction, wind speed and temperature for the entire episode for region 12 (Houston-Galveston) was 84, 96, and 69 respectively as show in Table 2.9-1: *Error percentages for 2006ep1c episode* and Figure 2.9-1: *Region 12 average wind speed and direction scatter plots for 2006ep1c episode*.

Table 2.9-1: Error percentages for 2006ep1c episode

Duration	Geographic Area/Zone	Wind Direction (°) Error % 30 / 20 / 10	Wind Speed (m/s) Error % 2 / 1 / 0.5	Temperature (°C) Error % 2 / 1 / 0.5
Episode Average	All Sites	94 / 83 / 57	100 / 69 / 37	75 / 43 / 28
Episode Average	Region 12	84 / 76 / 57	96 / 57 / 29	69 / 33 / 16
Episode Average	Coastal	85 / 74 / 39	86 / 54 /28	73 / 39 / 17
Episode Average	Ship Channel	81 / 69 / 47	86 / 49 / 28	62 / 28 / 12
Episode Average	Southeast Core	77 / 67 / 45	90 / 52 / 28	74 / 41 / 18
Episode Average	Northwest Core	77 / 66 / 34	85 / 45 / 23	59 / 27 / 13
Episode Average	Downwind	74 / 65 / 45	79 / 39 / 22	53 / 20 / 08

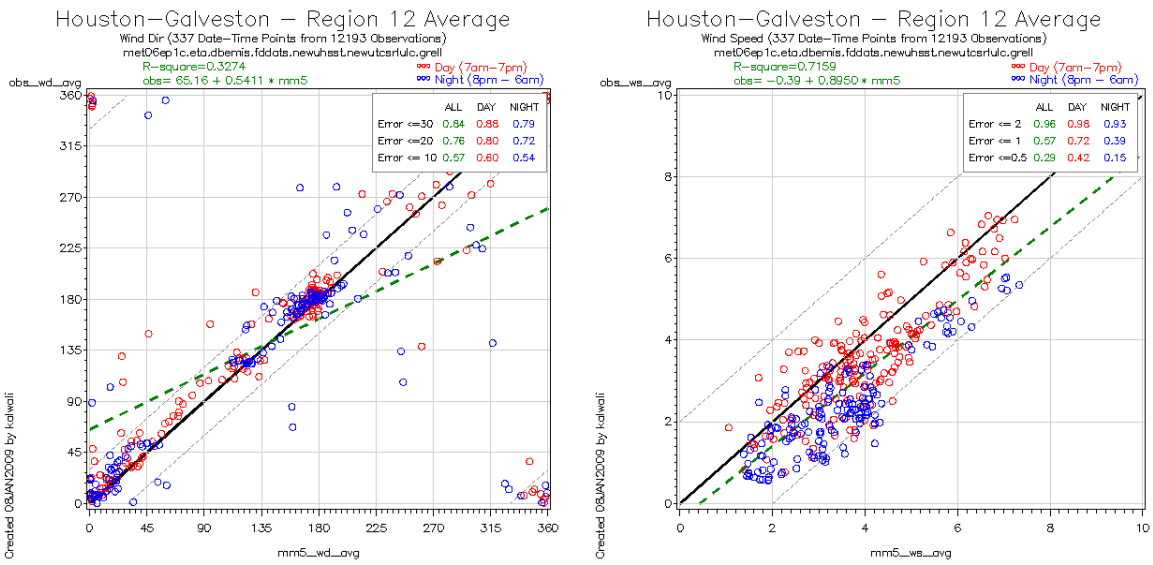

Figure 2.9-1: Region 12 average wind direction and wind speed scatter plots for 2006ep1c episode

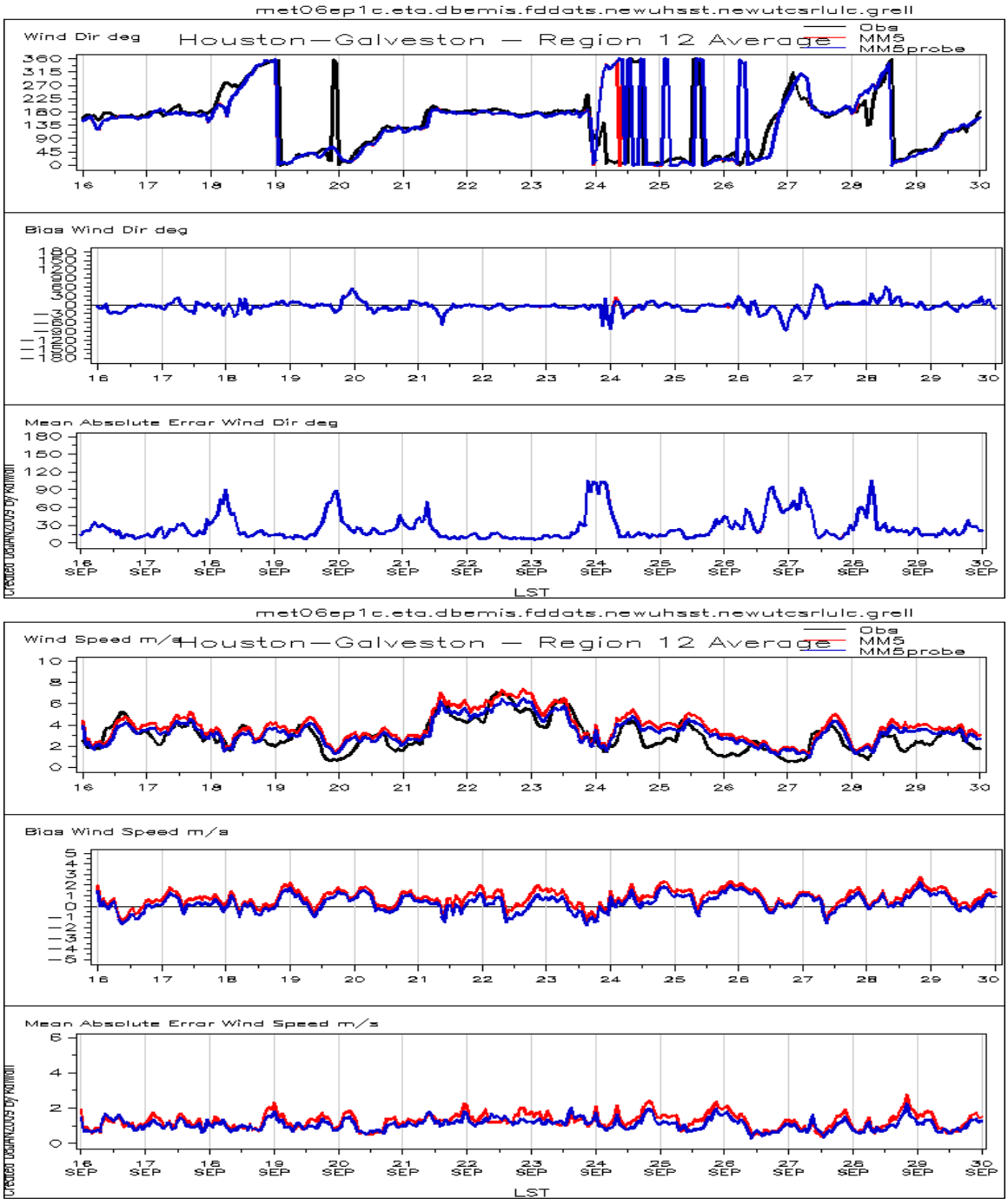

Figure 2.9-2: Region 12 average wind direction and wind speed time series for 2006ep1c episode.

The good statistical performance described in the above can be graphically tracked in the Figure 2.9-2: *Region 12 average wind direction time series for 2006ep1c episode.* On one key day of this episode, September 20, wind speed and wind direction errors are low during most of the daylight hours. The other key day of September 27 has noticeable wind direction errors during the early to midmorning hours, and then looks good for the rest of the day.

.

September 20, 2006
On that day, 1 monitor recorded an exceedance of the eight-hour ozone standard greater than 85 ppb. The Bayland Park C53/A146 monitor recorded the maximum eight-hour ozone of 86.7 ppb at 1000 CST. Regional background levels of ozone, in the air coming into the Houston area, were at least about 62 to 65 ppb as indicated by the peak eight-hour averages at Crosby CAMS 553, Smith Point CAMS 96, and Galveston CAMS 34

Skies were clear all day. Light easterly winds in the morning, becoming light to occasionally moderate from the east to southeast in the afternoon. The high temperature was 88 degrees Fahrenheit at George Bush Houston Intercontinental Airport, 86 degrees at Hobby Airport, and 85 degrees at Galveston Airport.

The error associated with the wind direction, wind speed and temperature for the entire episode for region 12 (Houston-Galveston) was 96, 100, and 71 respectively as show in Table 2.9-2: *Error percentages for September 20, 2006* and Figure 2.9-5: *Region 12 Average wind direction and speed scatter plots for September 20, 2006*.

Figure 2.9-6: *Time-height plot for La Porte profiler on September 20, 2006* shows that the profiler winds at La Porte agreed well with the MM5 winds for all vertical levels for the entire day except for the period from 1-4 CST for all vertical levels where the profiler winds were from the east- southeast and the MM5 winds from the east-northeast.

The 12-hour forward trajectories starting at 6 am on September 20, 2006 as depicted in figure 2.9-7: *12-hour forward trajectory at 06:00 CST on September 20, 2006* show the trajectories generated the MM5 data are parallel to the trajectories generated using the CAMS data, but slightly to the south. This would push the plumes from the industrial sources to the south of the location of the maximum ozone for that day.

Table 2.9-2: Error percentages for September 20, 2006

Duration	Geographic Area/Zone	Wind Direction (°) Error % 30 / 20 / 10	Wind Speed (m/s) Error % 2 / 1 / 0.5	Temperature (°C) Error % 2 / 1 / 0.5
9/20/2006	Region 12	96 / 83 / 42	100 / 54 / 38	71 / 21 / 8
9/20/2006	Coastal	100 / 88 / 50	79 / 54 / 33	71 / 29 / 08
9/20/2006	Ship Channel	83 / 63 / 29	83 / 54 / 46	58 / 21 / 13
9/20/2006	Southeast Core	92 / 79 / 46	92 / 54 / 29	58 / 25 / 13
9/20/2006	Northwest Core	88 / 79 / 38	96 / 58 / 29	58 / 21 / 13
9/20/2006	Downwind	70 / 75 / 50	83 / 50 / 29	42 / 25 / 13

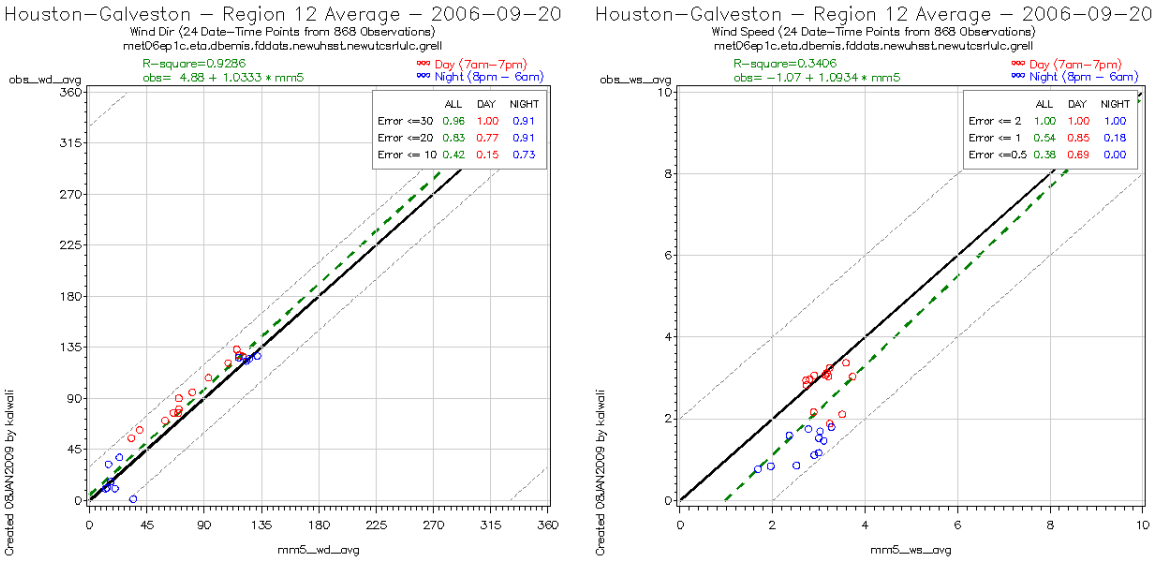

Figure 2.9-5: Region 12 Average wind direction and speed scatter plots for September 20, 2006

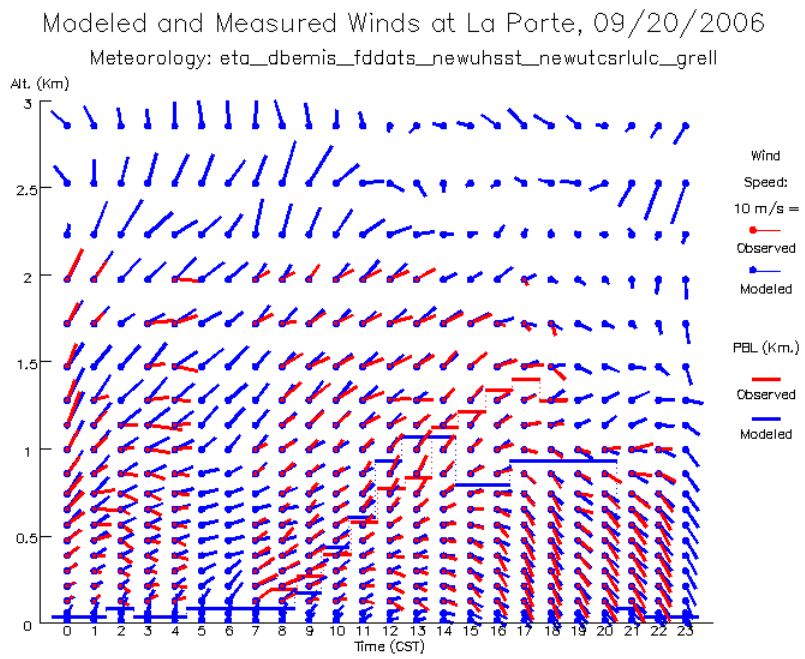

Figure 2.9-6: Time-height plot for La Porte profiler on September 20, 2006

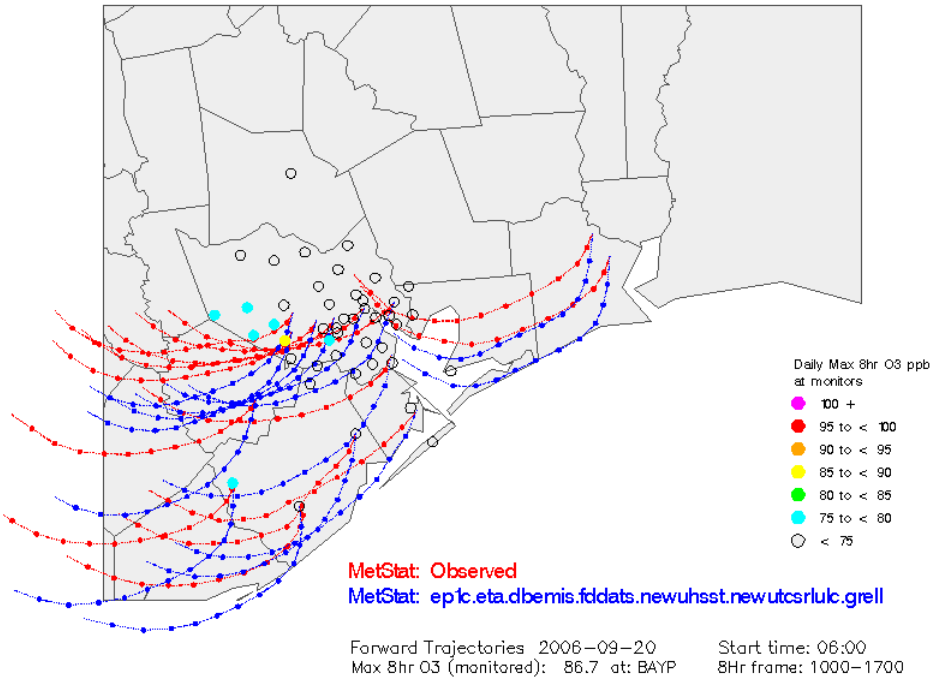

Figure 2.9-7: 12-hour forward trajectory at 06:00 CST on September 20, 2006

September 27, 2006

On that day, 2 monitors recorded an exceedance of the eight-hour ozone standard greater than 85 ppb. The Meyer Park C561/A146 monitor recorded the maximum eight-hour ozone of 90.5 ppb at 1000 CST. Regional background levels of ozone, in the air coming into the Houston area, ranged from about 57 to 81 ppb as indicated by the peak eight-hour averages at Galveston CAMS 34, Lake Jackson CAMS 1016, Danciger CAMS 618, and Katy Park CAMS 559.

Skies were clear with some scattered cirrus clouds. Light west to southwest winds occurred in the early morning, becoming light to moderate from the southwest to south mid-day and southerly in the late afternoon and early evening. The high temperature was 88 degrees Fahrenheit at George Bush Houston Intercontinental Airport, 86 degrees at Hobby Airport, and 83 degrees at Galveston Airport.

The error associated with the wind direction, wind speed and temperature for the entire episode for region 12 (Houston-Galveston) was 75, 100, and 67 respectively as show in Table 2.9-3: *Error percentages for September 27, 2006* and Figure 2.9-8 *Region 12 Average wind direction and speed scatter plots for September 27, 2006*.

Table 2.9-3: Error percentages for September 27, 2006

Duration	Geographic Area/Zone	Wind Direction (°) Error % 30 / 20 / 10	Wind Speed (m/s) Error % 2 / 1 / 0.5	Temperature (°C) Error % 2 / 1 / 0.5
9/27/2006	Region 12	75 / 67 / 63	100 / 54 / 17	67 / 33 / 17
9/27/2006	Coastal	71 / 77 / 67	96 / 71 / 46	83 / 46 / 33
9/27/2006	Ship Channel	75 / 58 / 38	92 / 46 / 13	79 / 29 / 17
9/27/2006	Southeast Core	75 / 58 / 38	92 / 54 / 25	67 / 29 / 04
9/27/2006	Northwest Core	71 / 58 / 46	88 / 46 / 17	58 / 33 / 29
9/27/2006	Downwind	79 / 75 / 42	88 / 38 / 25	63 / 33 / 17

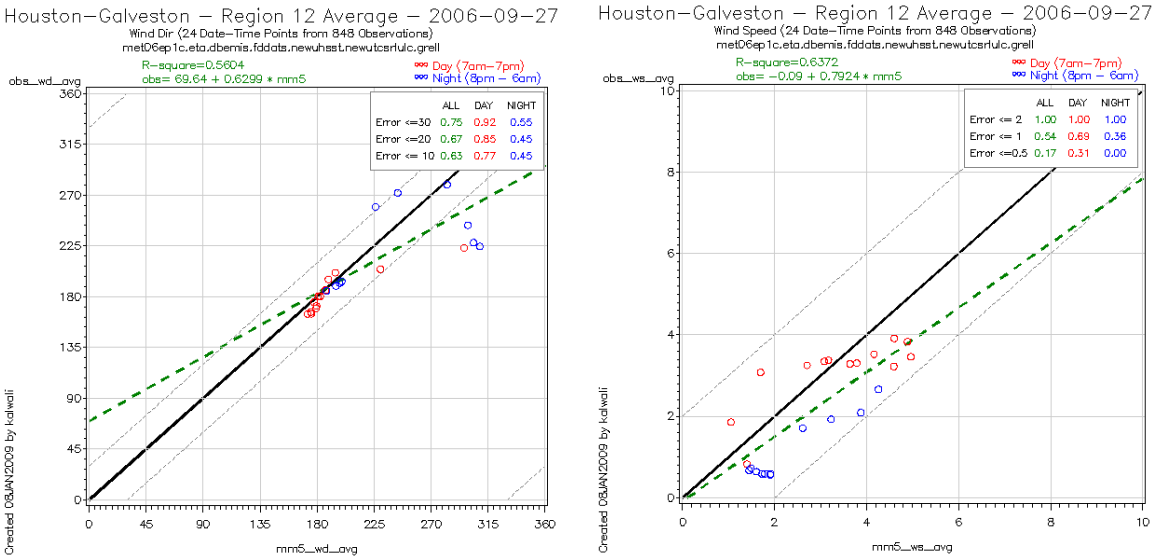

Figure 2.9-8: Region 12 Average wind direction and speed scatter plots for September 27, 2006

Figure 2.9-9: *Time-height plot for La Porte profiler on September 27, 2006* shows that the profiler winds at La Porte agreed well with the MM5 winds for all vertical levels for the entire day. The observed PBL, when available, agreed with the modeled PBL during most of the day.

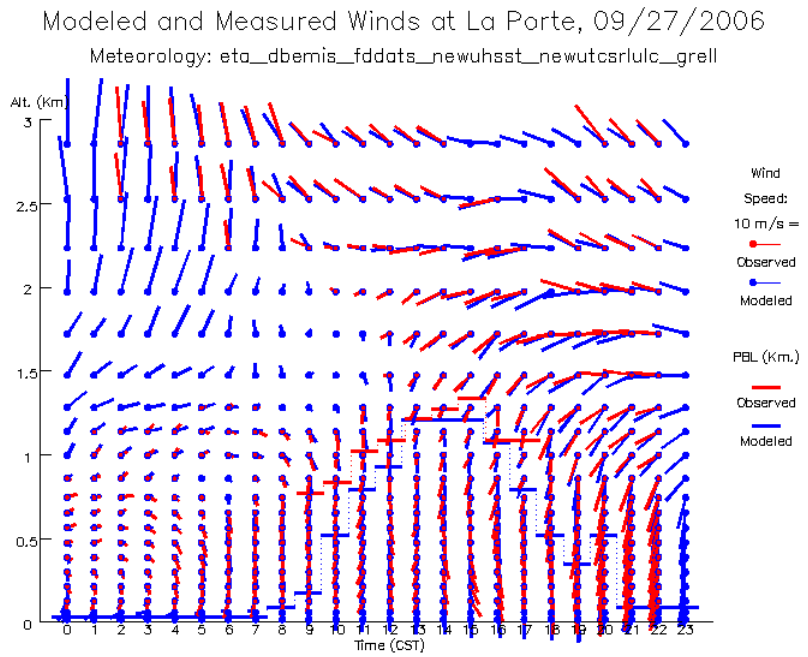

Figure 2.9-9: Time-height plot for La Porte profiler on September 27, 2006

The 12-hour forward trajectories starting at 6 am on September 27, 2006 as depicted in figure 2.9-10 show the trajectories generated the MM5 data agree with the trajectories generated using the CAMS data except for the first 4 hours were the former traveled to the south.

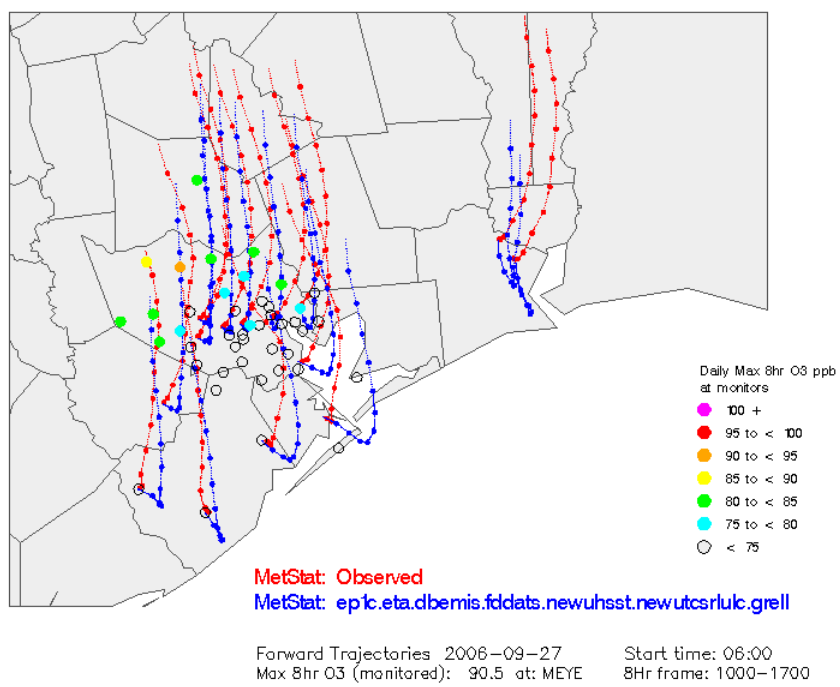

Figure 2.9-10: 12-hour forward trajectory at 06:00 CST on September 27, 2006

2.10 2006ep1d Performance Evaluation

The 2006ep1d episode has two periods of high ozone: October 6-7, and October 11, 2006.

During October 1-11, 2006, there were two cold fronts that passed over Houston on October 6 and 10, 2006. On October 1, 2006 the winds were 10 knots blowing from the southeast and on October 5, 2006 the winds were variable with a cold front still in the northern part of Texas. The remaining days were under the influence of a high pressure.

The first high ozone day occurred on the same day of the passage of the first cold front, and the remaining two high ozone days occurred a day after the passage of the cold fronts.

The MM5 model simulated the episode well and reproduced the main meteorological features close to the actual observations. The error associated with the wind direction, wind speed and temperature for the entire episode for all sites was 91, 100, and 74 respectively. The error associated with the wind direction, wind speed and temperature for the entire episode for region 12 (Houston-Galveston) was 83, 98, and 73 respectively as show in Table 2.10-1: *Error percentages for 2006ep1c episode* and Figure 2.10-1: *Region 12 average wind speed and direction scatter plots for 2006ep1d episode*.

Table 2.10-1: Error percentages for 2006ep1c episode

Duration	Geographic Area/Zone	Wind Direction (°) Error % 30 / 20 / 10	Wind Speed (m/s) Error % 2 / 1 / 0.5	Temperature (°C) Error % 2 / 1 / 0.5
Episode Average	All Sites	91 / 83 / 55	100 / 74 / 42	74 / 48 / 27
Episode Average	Region 12	83 / 66/ 33	98 / 75 / 42	73 / 51 / 32
Episode Average	Coastal	75 / 59 / 35	96 / 68 / 39	76 / 42 / 19
Episode Average	Ship Channel	66 / 50 / 29	94 / 62 / 32	68 / 45 / 23
Episode Average	Southeast Core	72 / 60 / 36	98 / 72 / 39	83 / 52 / 27
Episode Average	Northwest Core	65 / 48 / 25	95 / 73 / 41	65 / 40 / 25
Episode Average	Downwind	50 / 36 / 17	85 / 46 / 25	51 / 28 / 14

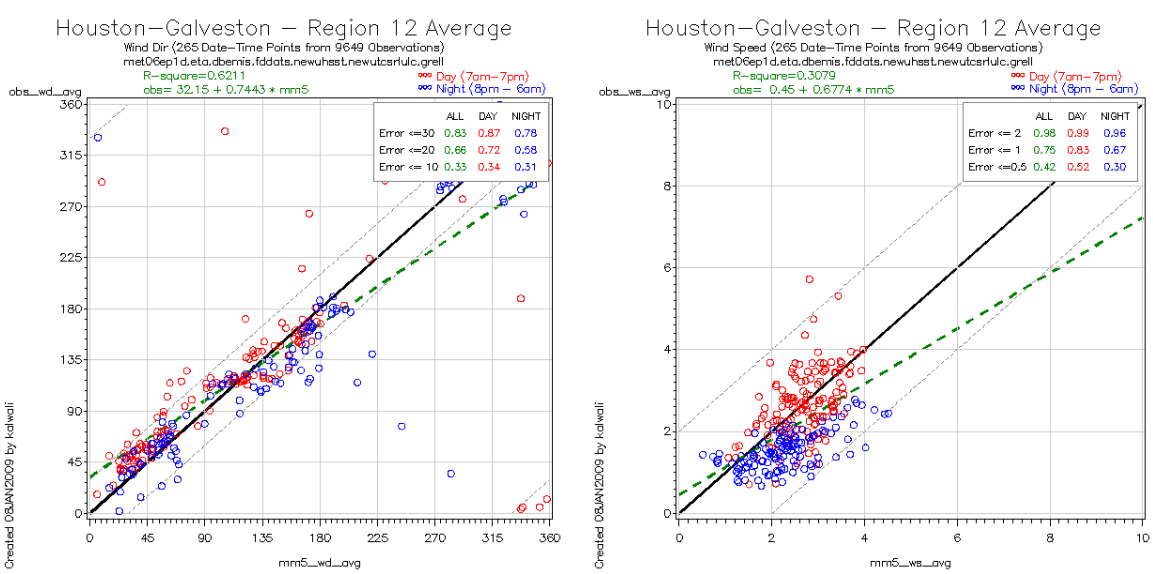

Figure 2.10-1: Region 12 average wind speed and direction scatter plots for 2006ep1d episode

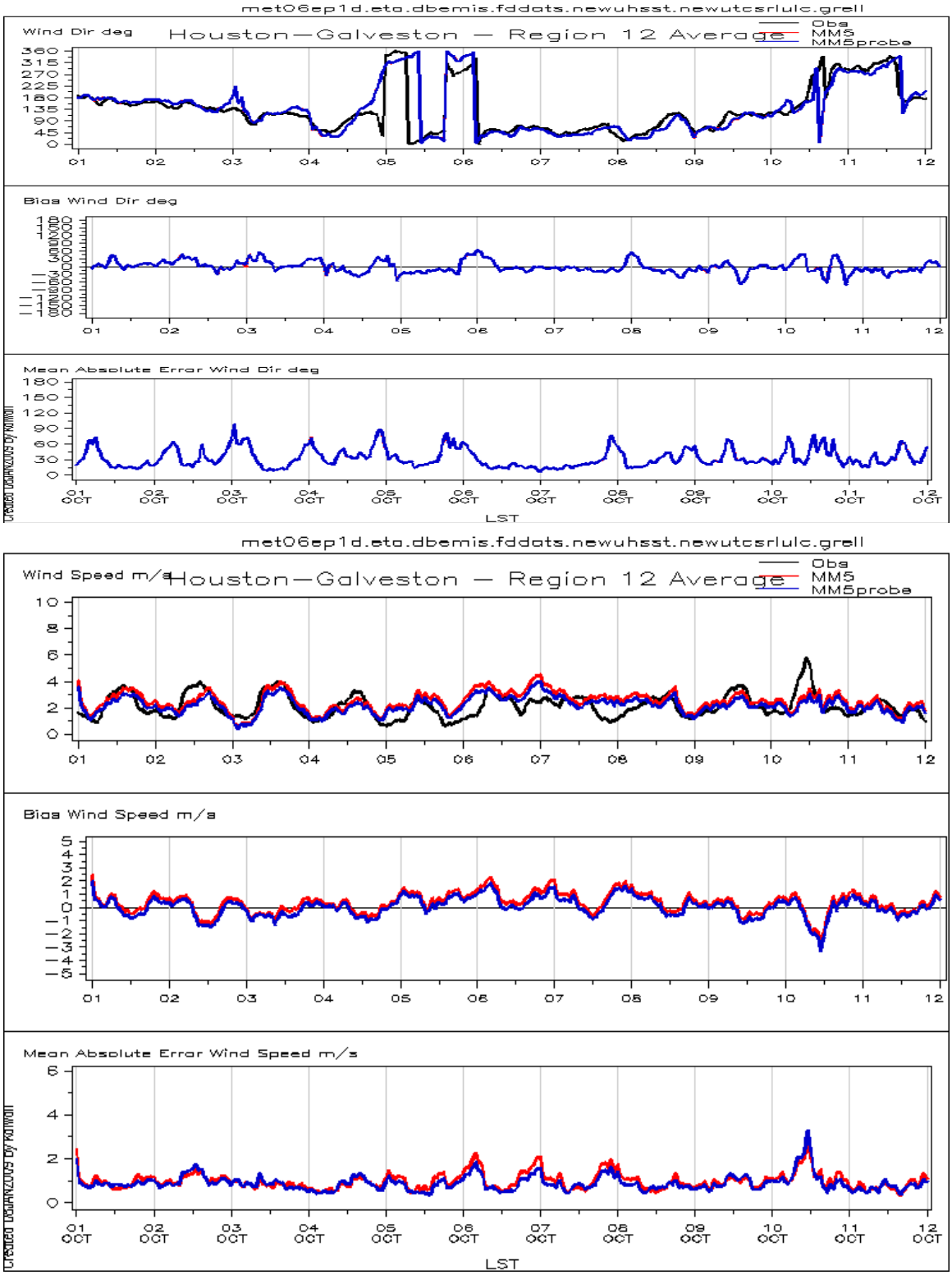

Figure 2.10-2: Region 12 average wind direction time series for 2006ep1d episode

October 6, 2006

Three monitors recorded an exceedance of the eight-hour ozone standard greater than 85 ppb. The Tom Bass C558 monitor recorded the maximum eight-hour ozone of 95.3 ppb at 1000 CST. Regional background levels of ozone, in the air coming into the Houston area, ranged from about 52 to 61 ppb as indicated by the peak eight-hour averages at Conroe CAMS 78, Kingwood CAMS 555, and Crosby CAMS 553.

Mostly clear skies with a high pressure centered to the northeast. Regional winds were generally from the northeast. Local winds were from the east-northeast at 5-10 mph during the morning, becoming variable during the afternoon partly due to onset of Bay and Gulf breezes. The high temperature was 93 degrees Fahrenheit at George Bush Houston Intercontinental Airport, 91 degrees at Hobby Airport, and 88 degrees at Galveston Airport.

The MM5 model performed well for that day as can be seen in Table 2.10-2: *Error percentages for October 6, 2006* and figure 2.10-5: *Region 12 Average wind direction and speed scatter plots for October 6, 2006*. The performance of the wind direction using the 30 degree threshold, wind speed using the 2 m/s threshold and temperature using the 2 degrees threshold in the Houston-Galveston region were 79, 88, and 83 respectively.

Table 2.10-2: Error percentages for October 6, 2006

Duration	Geographic Area/Zone	Wind Direction (°) Error % 30 / 20 / 10	Wind Speed (m/s) Error % 2 / 1 / 0.5	Temperature (°C) Error % 2 / 1 / 0.5
10/6/2006	Region 12	79 / 75 / 50	88 / 42 / 25	83 / 50 / 21
10/6/2006	Coastal	79 / 54 / 29	100 / 67 / 29	96 / 63 / 21
10/6/2006	Ship Channel	67 / 58 / 38	83 / 46 / 17	67 / 38 / 17
10/6/2006	Southeast Core	79 / 67 / 54	88 / 50 / 29	100 / 58 / 25
10/6/2006	Northwest Core	75 / 71 / 29	83 / 46 / 21	63 / 21 / 04
10/6/2006	Downwind	92 / 75 / 42	50 / 21 / 0	50 / 21 / 13

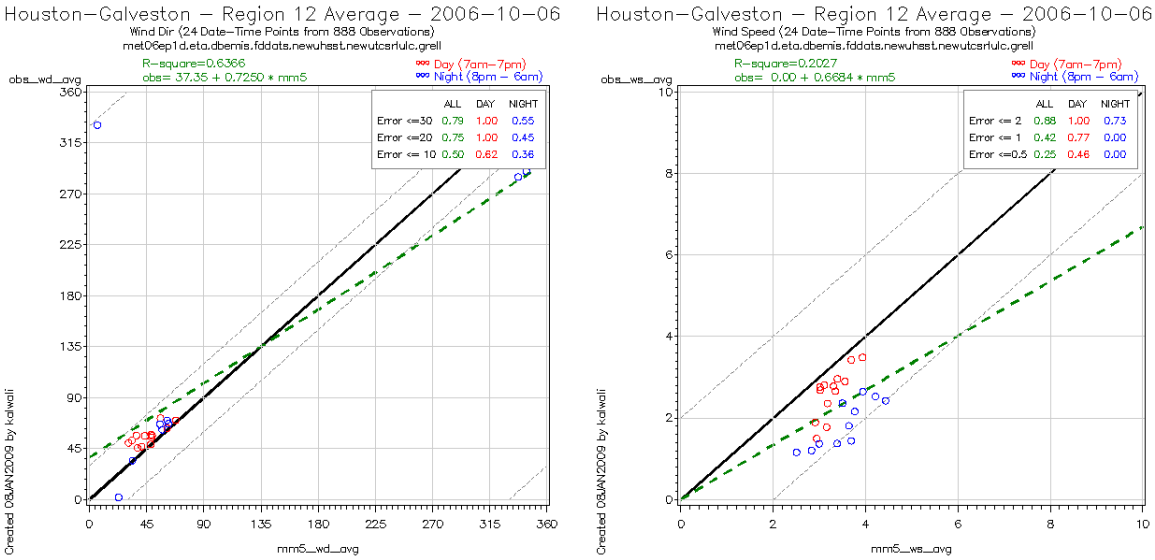

Figure 2.10-5: Region 12 Average wind direction and speed scatter plots for October 6, 2006

Profiler winds for La Porte profiler was missing before 6pm on that day as shown in figure 2.10-6: *Time-height plot for La Porte profiler on October 6, 2006*. On the hours where there was data (18-23 CST), the MM5 modeled winds agreed well with the profiler data.

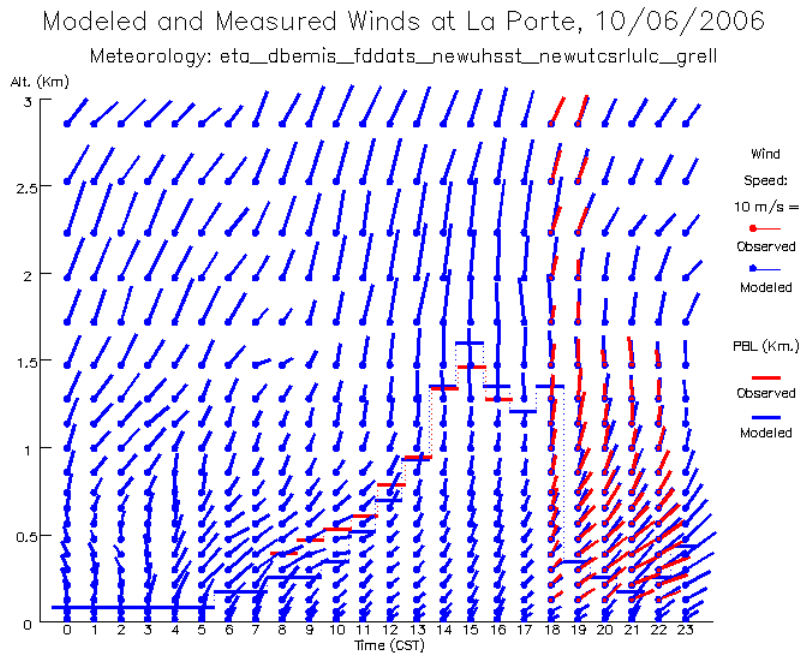

Figure 2.10-6: Time-height plot for La Porte profiler on October 6, 2006

The 12-hour forward trajectories starting at 6 am on October 11, 2006 as depicted in figure 2.10-7: *12-hour forward trajectory at 06:00 CST on October 6, 2006* show the trajectories heading towards the location of maximum 8-hr ozone in southeast Houston.

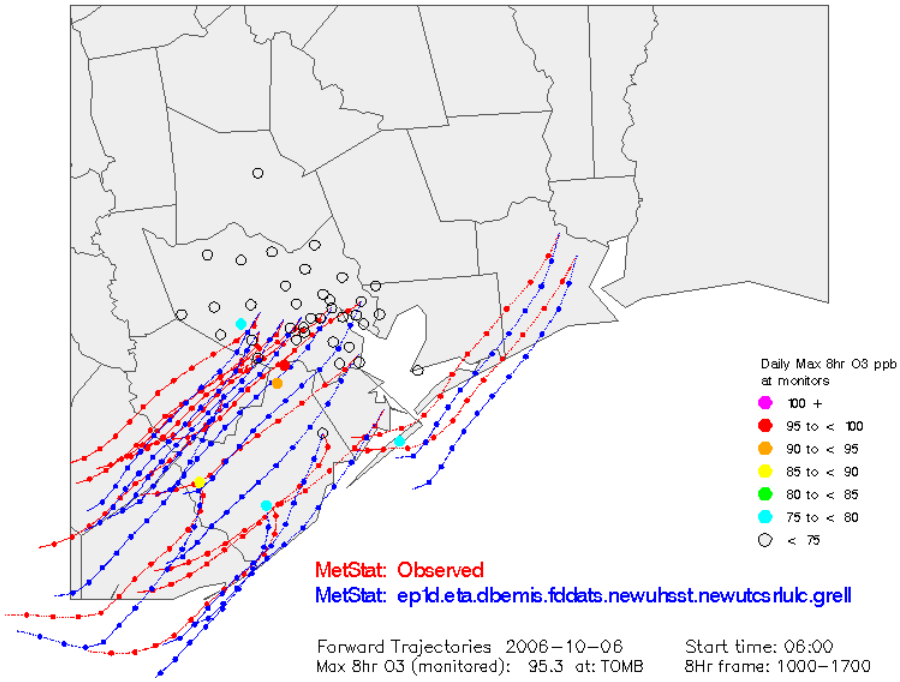

Figure 2.10-7: 12-hour forward trajectory at 06:00 CST on October 6, 2006.

October 7, 2006

On that day, only one monitor recorded an exceedance of the eight-hour ozone standard greater than 85 ppb. The Manvel Croix Park C84 monitor recorded the maximum eight-hour ozone of 87 ppb at 1000 CST. Regional background levels of ozone, in the air coming into the Houston area,

ranged from about 45 to 53 ppb as indicated by the peak eight-hour averages at Conroe CAMS 78, Kingwood CAMS 555, and Crosby CAMS 553. The high temperature was 83 degrees Fahrenheit at George Bush Houston Intercontinental Airport, 84 degrees at Hobby Airport, and 81 degrees at Galveston Airport.

Mostly clear skies in the morning with cirrus clouds in the afternoon. Winds were light to moderate from the northeast in the morning and early afternoon. Bay and Gulf breezes developed along the coast during the afternoon and with winds becoming more easterly in the late afternoon.

The MM5 model performed very well on that day, as displayed in table 2.10-3: *Error percentages for October 7, 2006* and figure 2.10-7: *Region 12 Average wind direction and speed scatter plots for October 7, 2006*. The performance of the wind direction using the 30 degree threshold, wind speed using the 2 m/s threshold and temperature using the 2 degrees threshold in the Houston-Galveston region were 100, 96, and 75 respectively. The daytime wind speed performance was better than the nighttime. The MM5 upper winds compared with the La Porte profiler data shown in Figure 2-10.8: *Time-height plot for La Porte profiler on October 7, 2006* also compared well except for the lower winds between 13-18 and 21-22 CST, where the profiler winds were east-southeasterly and the MM5 winds were northwesterly.

Table 2.10-3: Error percentages for October 7, 2006

Duration	Geographic Area/Zone	Wind Direction (°) Error % 30 / 20 / 10	Wind Speed (m/s) Error % 2 / 1 / 0.5	Temperature (°C) Error % 2 / 1 / 0.5
10/7/2006	Region 12	100 / 88 / 33	96 / 54 / 29	75 / 50 / 33
10/7/2006	Coastal	75 / 63 / 38	96 / 50 / 25	100 / 75 / 54
10/7/2006	Ship Channel	71 / 50 / 29	83 / 42 / 25	67 / 33 / 17
10/7/2006	Southeast Core	88 / 67 / 42	96 / 50 / 33	96 / 54 / 29
10/7/2006	Northwest Core	92 / 71 / 21	83 / 71 / 38	58 / 21 / 13
10/7/2006	Downwind	67 / 50 / 33	79 / 38 / 33	42 / 17 / 13

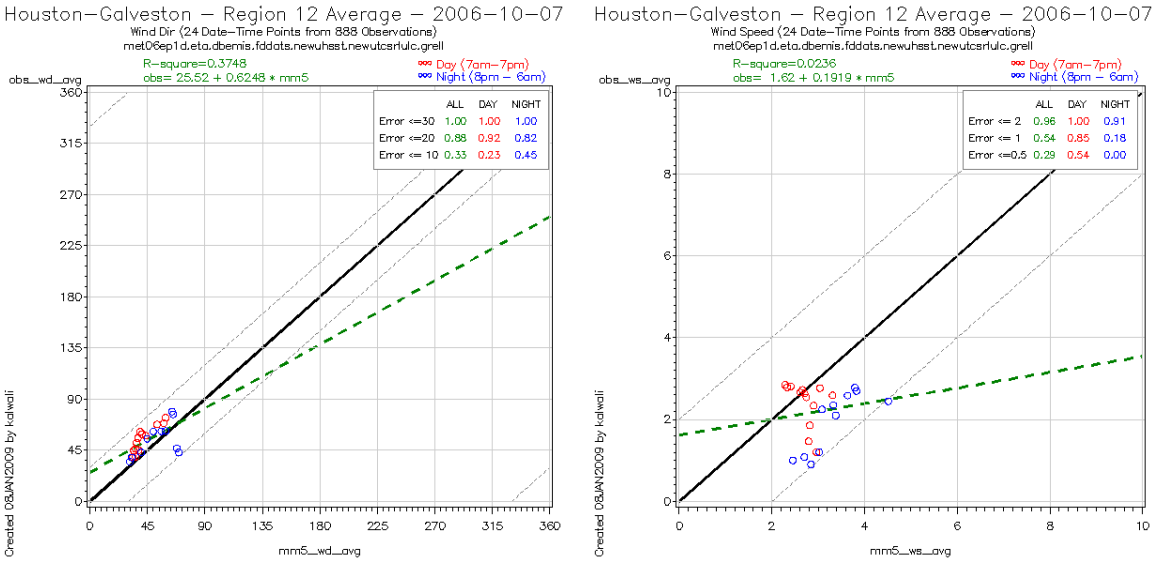

Figure 2.10-7: Region 12 Average wind direction and speed scatter plots for October 7, 2006

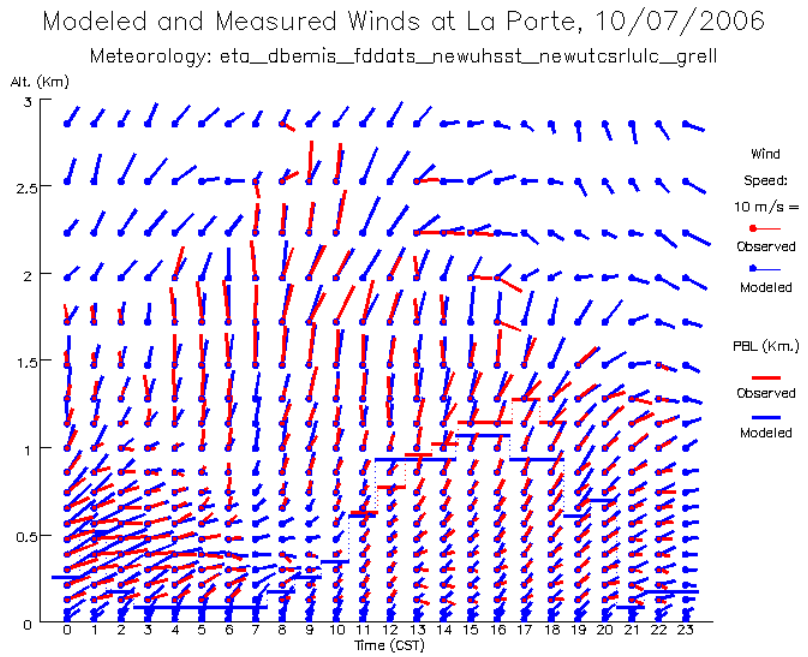

Figure 2.10-8: Time-height plot for La Porte profiler on October 7, 2006

The 12-hour forward trajectories starting at 6am CST using the MM5 data (blue) compared well with the ones using the observed data (red), as shown in Figure 2.10-9: *12-hour forward trajectory at 06:00 CST on October 7, 2006.* The trajectories travel to the southwest of Houston where the maximum 8-hour ozone values were observed.

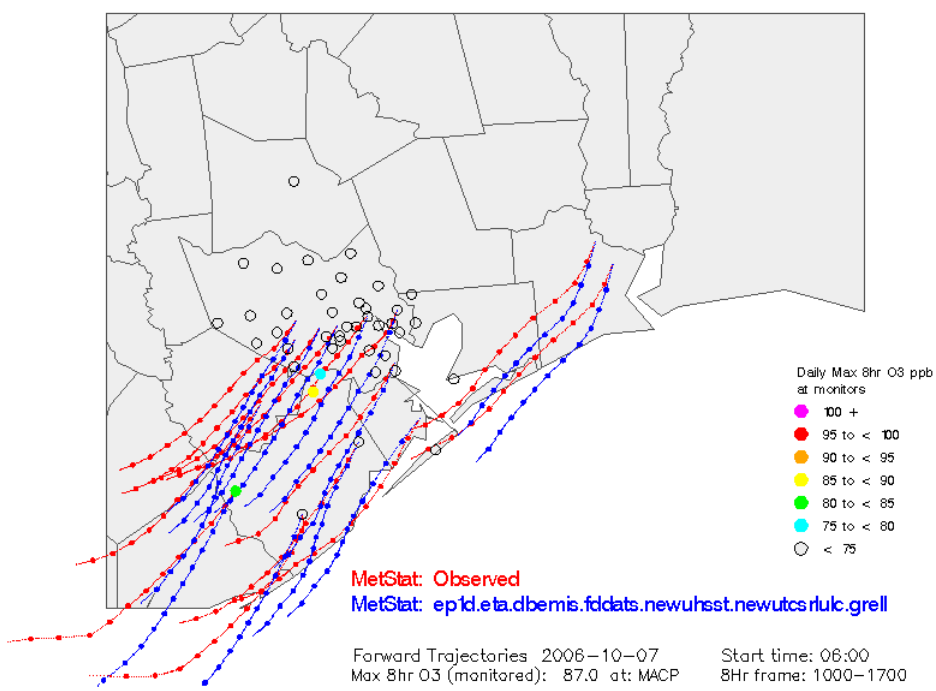

Figure 2.10-9: 12-hour forward trajectory at 06:00 CST on October 7, 2006
October 11, 2006

On that day, 3 monitors recorded an exceedance of the eight-hour ozone standard greater than 85 ppb. The 1850 Hawkins Camp Road C96/C638 monitor recorded the maximum eight-hour ozone of 90.4 ppb at 1400 CST. Regional background levels of ozone, in the air coming into the

Houston area, ranged from about 42 to 53 ppb as indicated by the peak eight-hour averages at Katy Park CAMS 559, Northwest Harris County CAMS 26, and Conroe Airport CAMS 78.

During that day, the weather was foggy with overcast low-level clouds until mid morning, then skies becoming mostly clear by the afternoon. Scattered medium and high cirrus clouds moved over the area late in the day. Light northwesterly winds in the morning, becoming light and variable by the early afternoon**.** The high temperature was 85 degrees Fahrenheit at George Bush Houston Intercontinental Airport, 86 degrees at Hobby Airport, and 81 degrees at Galveston Airport.

The MM5 model performed well for that day as can be seen in table 2.10-4: *Error percentages for October 11, 2006* and figure 2.10-10: *Region 12 Average wind direction and speed scatter plots for October 11, 2006*. The performance of the wind direction using the 30 degree threshold, wind speed using the 2 m/s threshold and temperature using the 2 degrees threshold in the Houston-Galveston region were 83, 100, and 79 respectively.

Table 2.10-4: Error percentages for October 11, 2006

Duration	Geographic Area/Zone	Wind Direction (°) Error % 30 / 20 / 10	Wind Speed (m/s) Error % 2 / 1 / 0.5	Temperature (°C) Error % 2 / 1 / 0.5
10/11/2006	Region 12	83 / 58/ 17	100 / 96 / 75	79 / 63 / 25
10/11/2006	Coastal	54 / 33 / 17	100 / 88 / 54	75 / 33 / 08
10/11/2006	Ship Channel	79 / 46 / 25	100 / 83 / 46	75 / 46 / 29
10/11/2006	Southeast Core	83 / 79 / 42	100 / 83 / 38	88 / 58 / 25
10/11/2006	Northwest Core	63 / 38 / 13	100/ 79 / 63	75 / 46 / 25
10/11/2006	Downwind	58 / 46 / 21	100 / 83 / 50	42 / 21 / 08

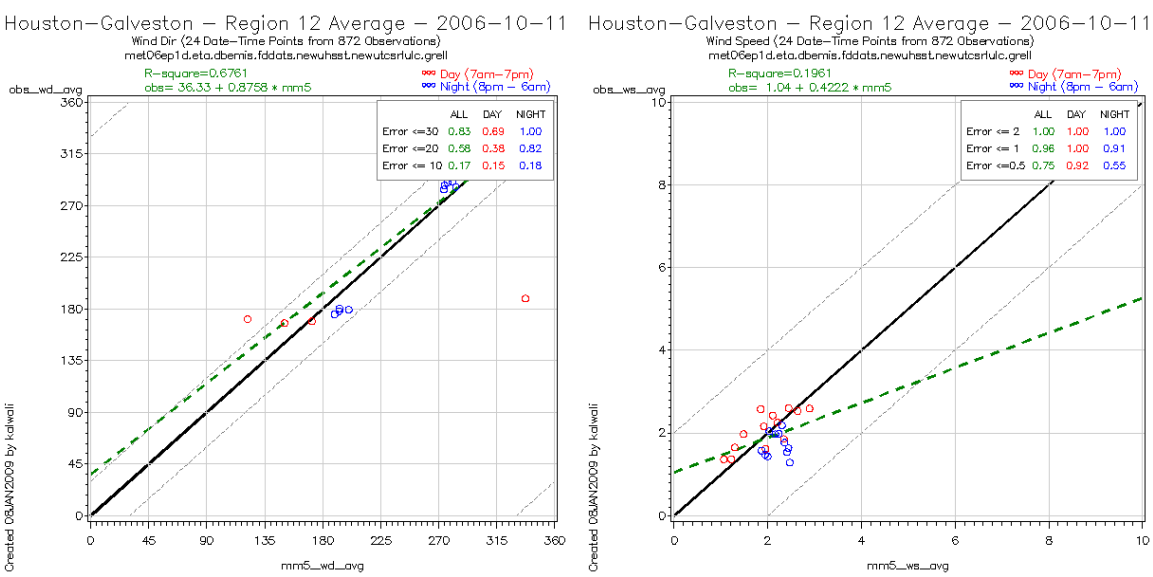

Figure 2.10-10: Region 12 Average wind direction and speed scatter plots for October 11, 2006

The 12-hour forward trajectories starting at 6 am on October 11, 2006 as depicted in figure 2.10-11: *12-hour forward trajectory at 06:00 CST on October 11, 2006*, show the trajectories using the MM5 data traveling to near the location of maximum 8-hr ozone in the southwestern part of Houston close to the Bay, but somewhat to the east of the same trajectories generated using the CAMS observations (in red).

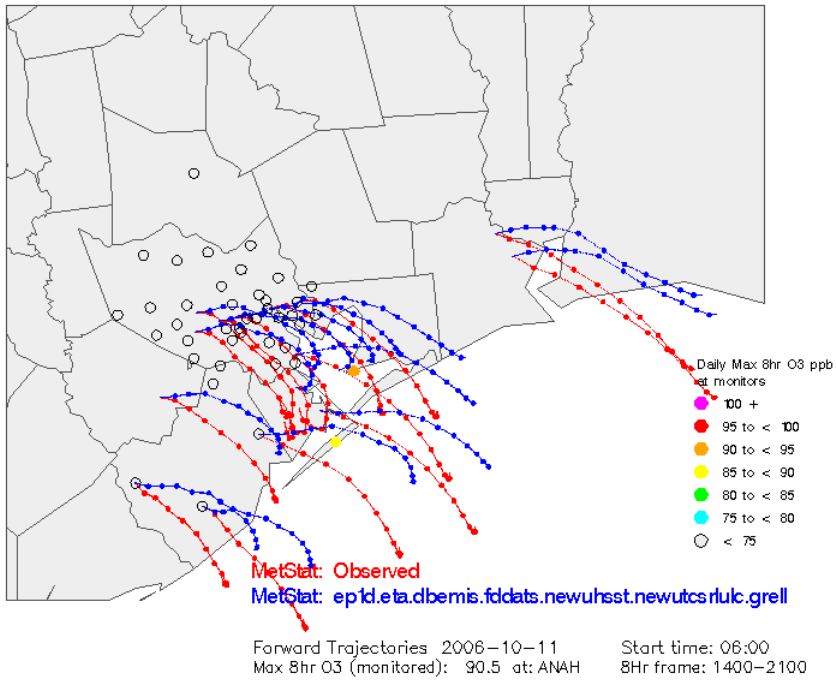

Figure 2.10-11: 12-hour forward trajectory at 06:00 CST on October 11, 2006

On the previous day (October 10, 2006), a cold front passed over Houston in the middle of the day bringing numerous showers and strong northwesterly winds. From Figure 2.10-12: *Region 12 average wind direction time series for October 10, 2006*, and Figure 2.10-13: *Region 12 average wind speed time series for October 10, 2006*, one sees a shift in wind direction from southwest to northwest and an increase in wind speed around 12 p.m.

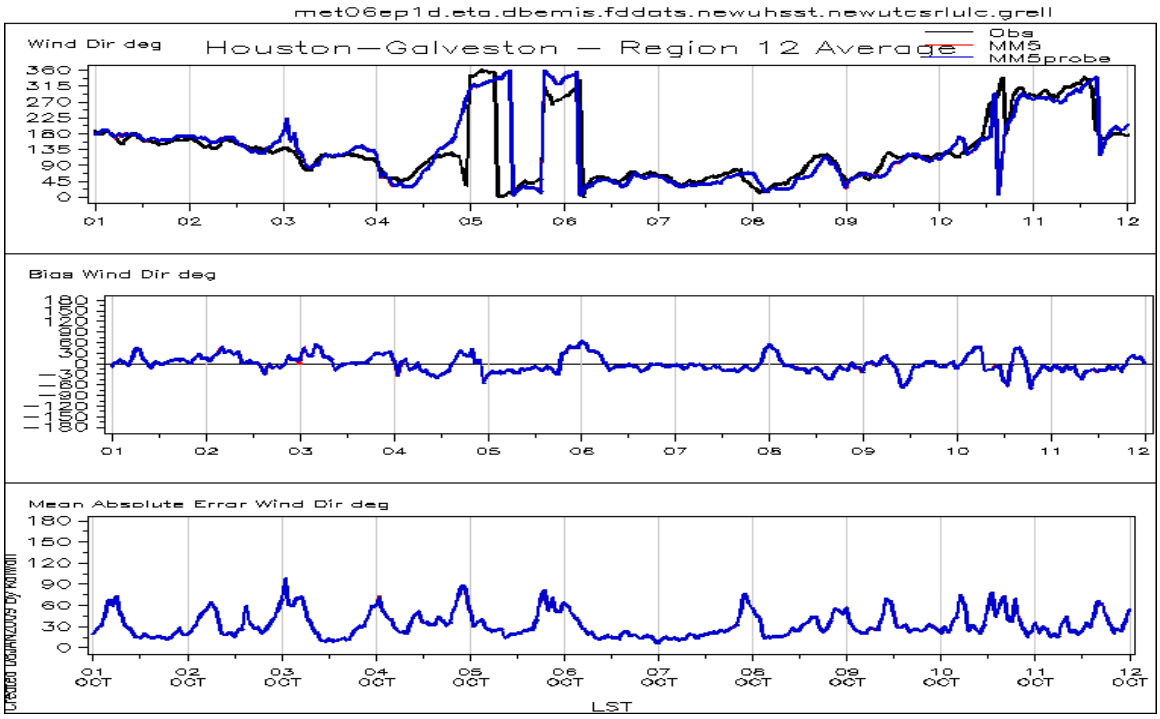

Figure 2.10-12: Region 12 average wind direction time series for October 10, 2006

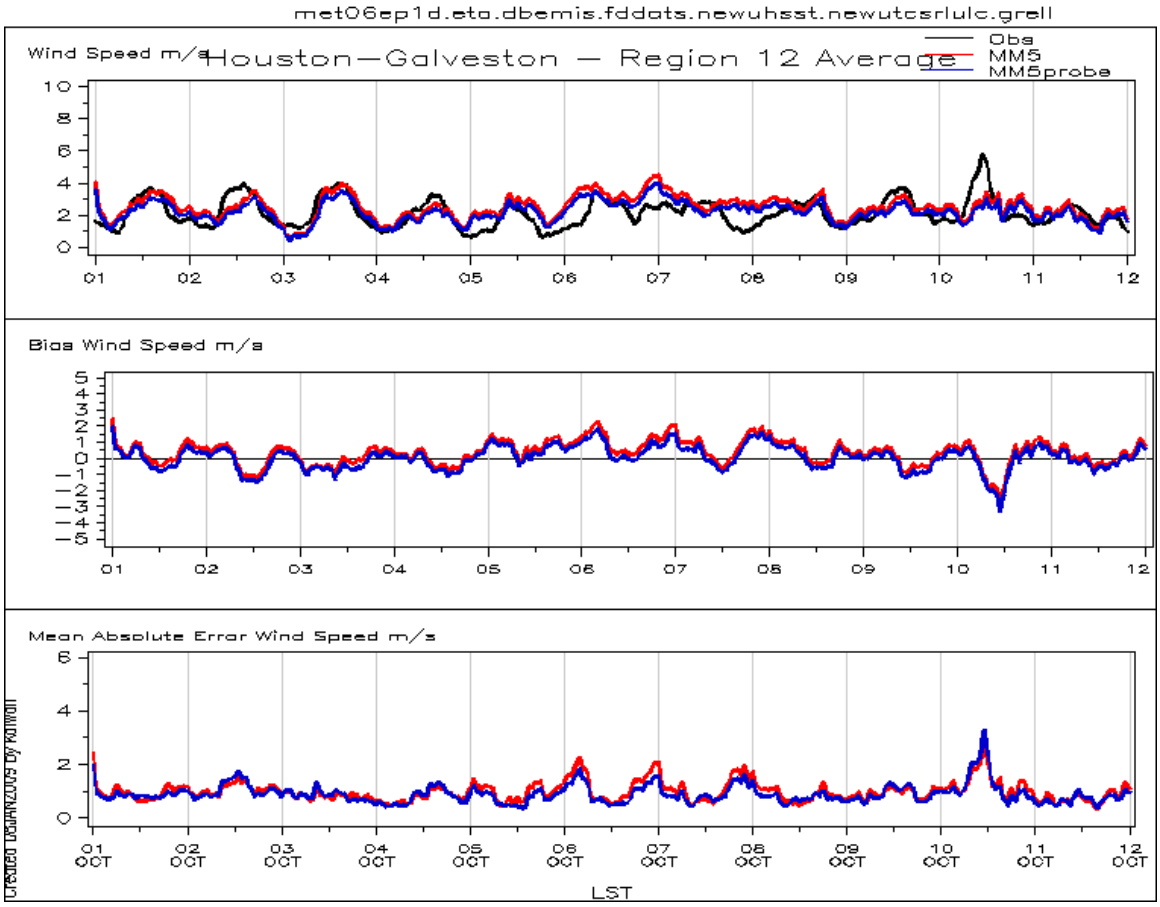

Figure 2.10-13: Region 12 average wind speed time series for October 10, 2006

Figure 2.10-14: *Region 12 average humidity and temperature for October 10, 2006,* shows a sharp drop in humidity and temperature around 12 CST when the cold front passed. The La Porte profiler shows that on that day, between 12 and 14 CST there was a shift in the wind direction from southwesterly to northwesterly from the surface to at least 3km above the ground, as shown in Figure 2.10-15: *Time-height plot for La Porte profiler on October 10, 2006.* Note that the maximum 8-hour ozone on that day was only 49 ppb.

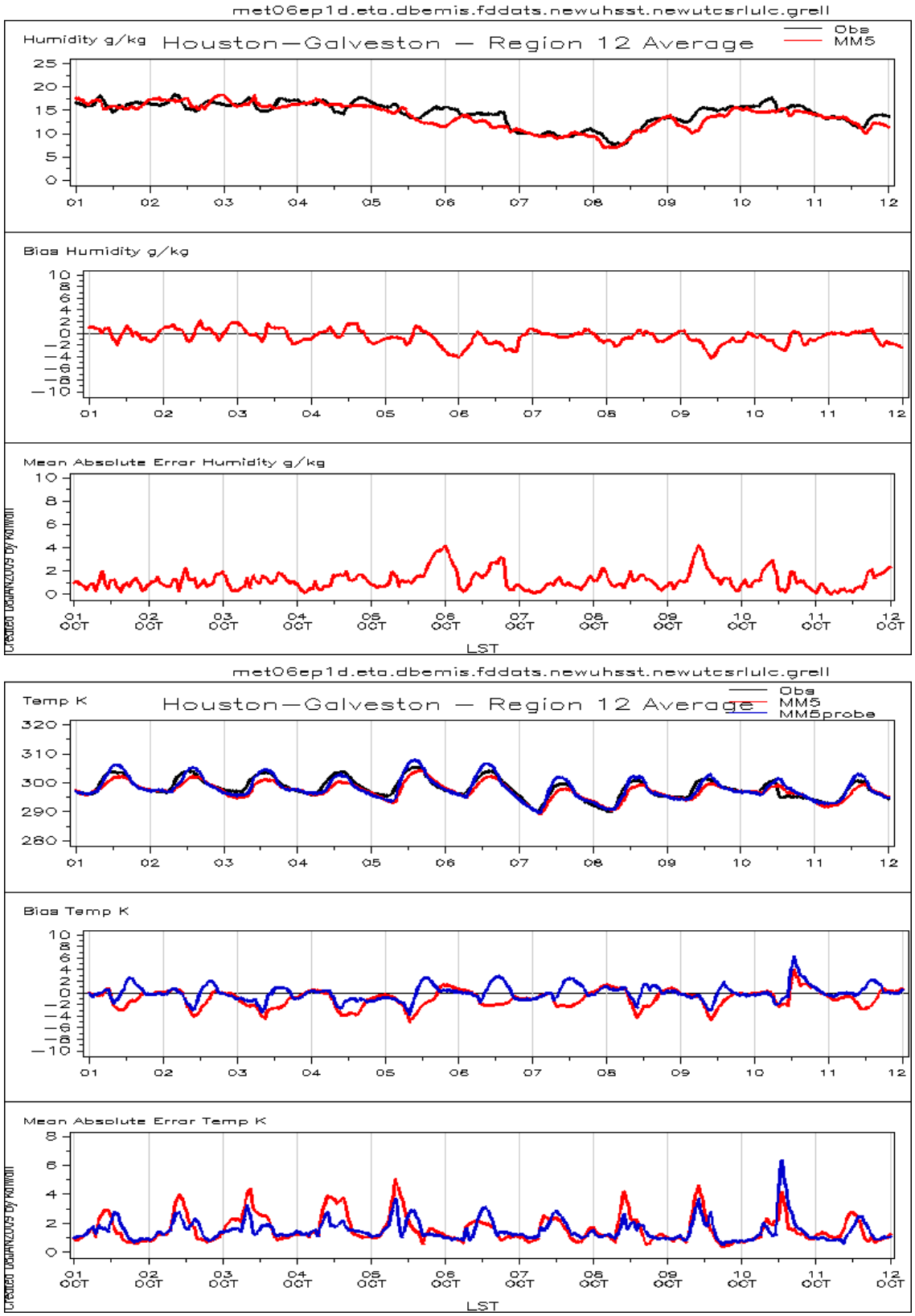

Figure 2.10-14: Region 12 average humidity and temperature for October 10, 2006

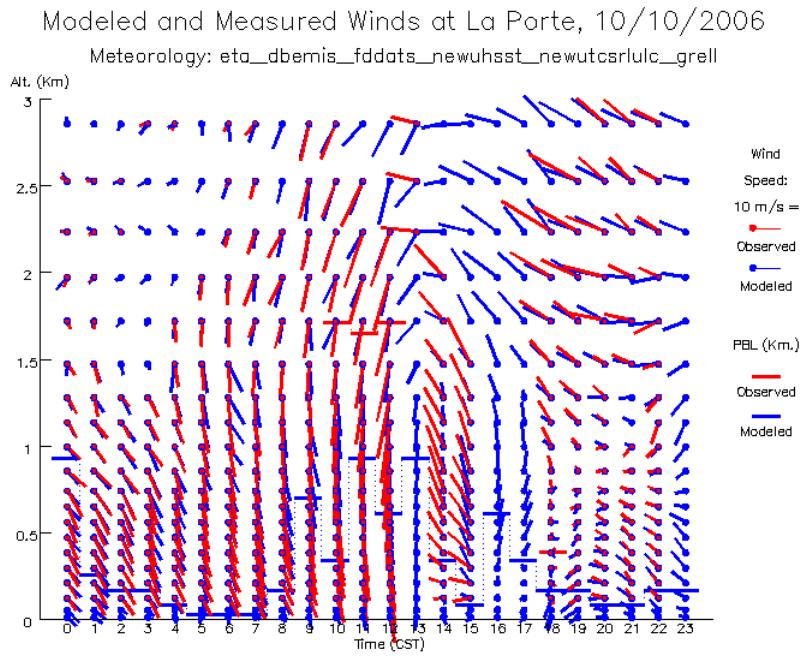

Figure 2.10-15: Time-height plot for La Porte profiler on October 10, 2006

2.11 References

Banta, R. M., C. J. Senff, J Nielsen-Gammon, L. S. Darby, T. B. Ryerson, R. J. Alvarez, S. P. Sandberg, E. J. Williams and M. Trainer (2005), A bad air day in Houston, *Bulletin of the American Meteorological Society*, *86*(5), 657+, 10.1175/BAMS-86-5-657

Berkowitz, C.M., Spicer, C.W., Doskey, P.V., 2005. Hydrocarbon observations and ozone production rates in western Houston during the Texas 2000 air quality study. Atmospheric Environment 39 (19), 3383–3396.

Chen, F., and J. Dudhia (2001), Coupling an advanced land-surface hydrology model with the Penn State - NCAR MM5 modeling system. Part I: Model implementation and sensitivity, Mon. Wea. Rev., 129, 569–585.

Emery, C., E. Tai, and G. Yarwood (2001), Enhanced Meteorological Modeling and Performance Evaluation for Two Texas Ozone Episodes, Final Report to the Texas Natural Resource Conservation Commission under TNRCC Umbrella Contract No. 582-0-31984, Environ International Corporation, Novato, CA.

Environ (2008), Description from MM5CAMx README file contained in mm5camx.21feb08.tar.gz archive, http://www.camx.com/files/mm5camx.21feb08.tar.gz, Environ Holdings, Inc., Last accessed May 5, 2009.

EPA (2007), Guidance on the Use of Models and Other Analyses for Demonstrating Attainment of Air Quality Goals for Ozone, PM2.5, and Regional Haze, http://www.epa.gov/scram001/guidance/guide/final-03-pm-rh-guidance.pdf, EPA-454/B-07-002, 162, Last accessed March 26, 2009.

Grell, G., J. Dudhia, and D. Stauffer (1994), A description of the Fifth Generation Penn State/NCAR Mesoscale Model (MM5), Tech. Rep. NCAR/TN-398+STR, National Center of Atmospheric Research (NCAR) Tech Note.

Janjic, Z. I. (1994), The step-mountain Eta coordinate model: Further developments of the convection, viscous sublayer, and turbulence closure schemes, Mon. Wea. Rev., 122, 927–945.

Knoderer, C. A., S. A. Bratek, C. P. MacDonald (2008), Spatial and Temporal Characteristics of Winds and Mixing During TexAQS-II, Final Report to Texas A&M University for Texas Commission on Environmental Quality Proposal under Grant Activity 582-5-64593-FY08-20, Sonoma Technology Inc, Petaluma, CA, April 2008.

NCAR (2005a), Appendix C: How to Use Noah Land-Surface Model Option, PSU/NCAR Mesoscale Modeling System Tutorial Class Notes and User's Guide, http://www.mmm.ucar.edu/mm5/documents/MM5_tut_Web_notes/App-C/append-c.htm, Last accessed May 5, 2009.

NCAR (2005b), MM5 Online Tutorial Home Pages, http://www.mmm.ucar.edu/mm5/On-Line-Tutorial/teachyourself.html, Last accessed May 5, 2009.

NCEP, (2009), GCIP NCEP Eta model output, CISL RDA: ds609.2 Home Page, http://dss.ucar.edu/datasets/ds609.2/, Last accessed May 13, 2009.

Nielsen-Gammon (2007a), Preliminary Analysis of Ozone Meteorology during TexAQS-II Ozone Episodes, Interim Report to the Texas Commission on Environmental Quality under Proposal for Grant Activity 582-5-64593-FY07-21.

Nielsen-Gammon (2007b), Comprehensive meteorological analysis of TexAQS II episodes, Task 3 Deliverable for Texas Commission on Environmental Quality Proposal for Grant Activity 582-5-64593-FY07-21.

Stauffer, D. R., and N. L. Seaman (1990), Use of four-dimensional data assimilation in a limited area mesoscale model. Part I: Experiments with synoptic-scale data, Mon. Wea. Rev., 118, 1250–1277.

Stauffer, D. R., and N. L. Seaman (1994), Multiscale four-dimensional data assimilation, J. Appl. Meteor., 33, 416–434.

Stauffer, D. R., N. L. Seaman, and F. S. Binkowski (1991), Use of four-dimensional data assimilation in a limited area mesoscale model. Part II: Effects of data assimilation within the planetary boundary layer, Mon. Wea. Rev., 119, 734–754.

TCEQ (2005), 2005 Air Pollution Events, http://www.tceq.state.tx.us/compliance/monitoring/air/monops/sigevents05.html, Texas Commission on Environmental Quality (TCEQ), Last accessed May 21, 2009.

TCEQ (2006), 2006 Air Pollution Events, http://www.tceq.state.tx.us/compliance/monitoring/air/monops/sigevents06.html, Texas Commission on Environmental Quality (TCEQ), Last accessed May 21, 2009.

TCEQ (2009), Meteorological modeling performance evaluation products, Texas Commission on Environmental Quality (TCEQ) file transfer protocol (FTP) site, (ftp://ftp.tceq.state.tx.us/pub/OEPAA/TAD/Modeling/HGB8H2/mm5).

ATTACHMENT 1

Sea Surface Temperature (SST) Characteristics
Houston-Galveston-Brazoria Attainment Demonstration SIP Revision

2.12.1 Sea Surface Temperature (SST) Characteristics

2.12.1.1 Introduction

The temperature gradient between land and water bodies is a vital characteristic for a meteorological model to adequately simulate land and sea (lake) breezes. The land/sea breeze phenomenon has been shown to re-circulate pollutants in the Houston area, thus exacerbating its air quality issues (Banta et al., 2005; Darby, 2004). To improve the representation of the land/sea breeze in MM5, the inputs for land characteristics and sea surface temperatures (SST) were updated with LandSat and Geostationary Operational Environmental Satellite (GOES) based data. The development and use of the updated SST inputs will be discussed below while the satellite-based land use is detailed in Attachment 2: Land Use and Land Cover (LULC) Characterisrtics.

2.12.1.2 SST Development

SST is a constant field in MM5, meaning it is not updated or calculated by the model. It can be a single value per model grid square throughout the model run or it can be time-varied. Most analysis products used to initialize MM5, such as the National Center for Environmental Prediction's (NCEP) North American Mesoscale Model (NAM) output, do not contain actual sea surface temperatures. In those cases the MM5 preprocessor REGRID uses skin temperature as a substitute. The MM5 community has determined using skin temperatures can cause unrealistic temperature features at coastlines, an unwanted result for the Houston-Galveston area (NCAR, 2005).

To overcome the coastline misrepresentations, the model can be supplied with a separate source of real SST data. NCEP produces a daily, high-resolution (~10 km), global SST analysis that can be directly input into REGRID with a modified Vtable (NCAR, 2005). The NCEP SST product is based on Advanced Very High Resolution Radiometer (AVHRR) satellite, ship, and buoy data (NCEP, 2009). The AVHRR sensor is onboard the Polar Operational Environmental Satellites (POES), which orbit the Earth 14.1 times per day. The satellite ground tracks do not repeat every day so there can be gaps in coverage. The NCEP SST data was used in the initial development of the 2005 and 2006 meteorological modeling and was found to yield higher resolution temperature gradients and improved model performance (Figure 2.12.1.2-1: *Variation of NCEP SST product (degrees Kelvin) in MM5 along the coast of Texas and Louisiana over six hours on June 21, 2005*).

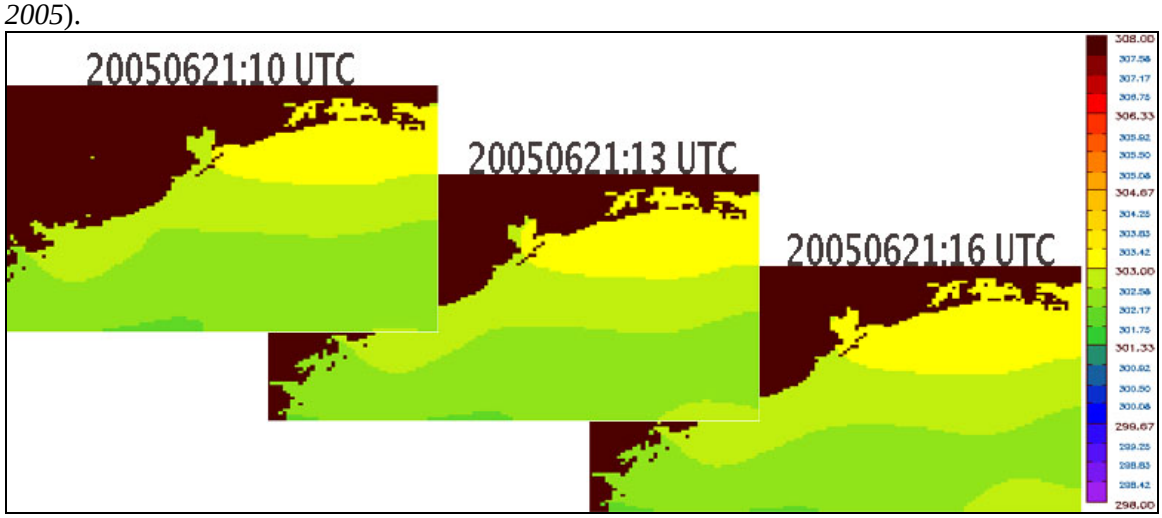

Figure 2.12.1.2-1: Variation of NCEP SST product (degrees Kelvin) in MM5 along the coast of Texas and Louisiana over six hours on June 21, 2005

The land/sea breeze coastal wind direction veers throughout the day from changing temperature and pressure gradients between the Gulf of Mexico and the land surface. Galveston Bay can also induce a bay breeze, affecting areas along its coast. Since the Bay is a shallow body of water, it can have stronger diurnal temperature variations than the Gulf of Mexico. A higher resolution

SST dataset was sought to better represent these dynamic processes where the NCEP product may have difficulty.

Geostationary orbiting satellites stay fixed over the equator (i.e. synchronized with the motion of the Earth), thus constantly providing sensor measurements and essentially eliminating orbital data gaps. The GOES retrievals provide hourly 6km resolution datasets that are able to capture the higher resolution SST processes. The GOES data does have limitations due to missing data from clouds, interference, sun glint, and satellite downtime. This data was used in the final meteorological modeling of the 2005 and 2006 episodes.

2.12.1.3 Satellite Data Adaptation Methodology

Because the GOES data is at a 6km resolution, the data had to be aggregated for the 12, 36, and 108 km domains. It had to be spatially interpolated to provide data for every 4 km grid square. Missing data had to be filled for all domains. Two methods were used to accommodate the GOES SST data to the MM5 modeling domains, one internally at TCEQ and one contracted to the University of Houston.

The processing of GOES data for MM5 input was first started by TCEQ's Data Analysis Team (Mercado and Harper, 2007). To aggregate the satellite data to the coarse grids, TCEQ used a python-ArcGIS tool combination. Missing data was imputed by temporally interpolating with a SAS® Loess routine (Cleveland et al., 1988) as shown by the magenta dots in Figure 2.12.1.3-1: *Example of TCEQ process for imputing missing GOES data by Loess interpolation and episodic medians for a single grid cell and day*. If missing data still remained, possibly due to continuous hours of cloudiness, the grid cell was filled with the cell's episode median value (blue stars) for that hour. The overall profile of the grid cell's SST follows the black line as a combination of actual, interpolated, and episodic median values.

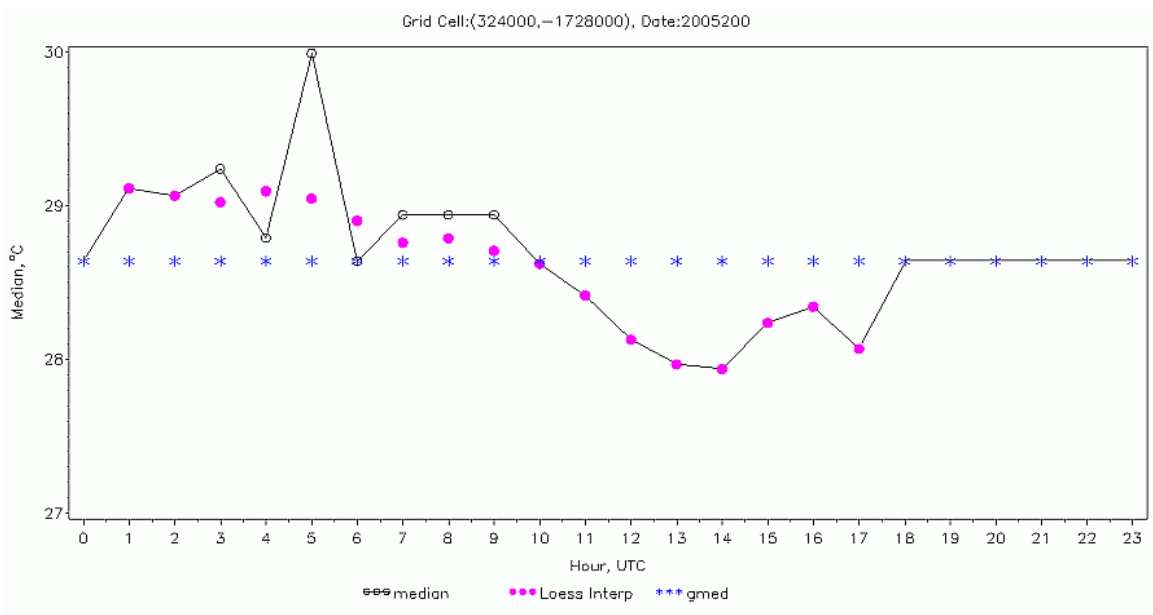

Figure 2.12.1.3-1: Example of TCEQ process for imputing missing GOES data by Loess interpolation and episodic medians for a single grid cell and day

To accommodate the 6 km GOES data to the MM5 4 km domain, the same temporal interpolation as the coarse grids was applied but missing data still existed due to the 6 km resolution of the original GOES data. To overcome the spatial gaps, TCEQ applied a kriging algorithm with a land mask to produce more reliable estimates near coastal areas. Figure 2.12.1.3-2: *Final TCEQ 4km SST Example for August 3, 2005 at 12 UTC for the northwest Gulf of Mexico. Warmer temperature are red, cooler are green, the land is brown* shows an example for one hour of the final TCEQ SST product in the northwestern Gulf of Mexico.

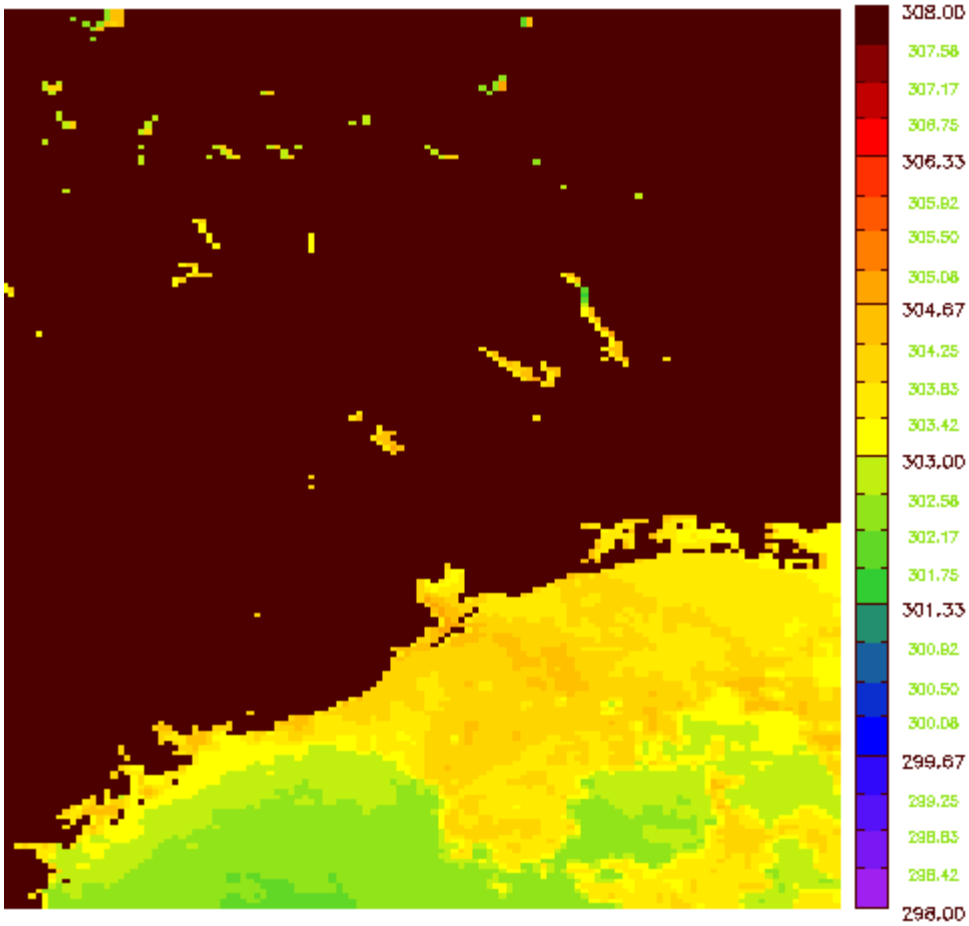

Figure 2.12.1.3-2: Final TCEQ 4km SST Example for August 3, 2005 at 12 UTC for the northwest Gulf of Mexico; Warmer temperature are red, cooler are green, the land is brown.

The University of Houston (UH) was contracted to create the tools necessary to translate the GOES SST data to a format that could be easily input to MM5. In the process of creating those tools, UH employed a different methodology to adapt the native GOES data to the MM5 domains (*Byun et al.*, 2007, *Byun et al.*, 2008). UH used the IDL® programming language for all processing of the GOES data, including data aggregation.

Based on the normal diurnal temperature variation of sea surface temperatures, UH fitted a sine curve to each grid cell's mean monthly SST. The SST was assumed to be a function of location (such as Galveston Bay or the middle of the Gulf of Mexico) and time (hourly and seasonal) as depicted in Figure 2.12.1.3-4: *UH SST Function (from Byun et al., 2007)*.

$$SST(x, y, t_s, t_d) = a \cdot \sin(\frac{2\pi}{24}(t_d - d)) + m$$

$$a = a_{monthly_mean}(x, y)$$

$$d = d_{monthly_mean}(x, y)$$

$$m = m_{monthly_mean}(x, y) + m_{daily}(t_s)$$

where a is the amplitude of SST variation, d is the phase shift, m is the mean SST, t_d is hour of a day, and t_s is day number.

Figure 2.12.1.3-4: UH SST Function (from Byun et al., 2007)

Missing hourly SST values were filled with the mean monthly SST for that hour from the sine curve estimate. Figure 2.12.1.3-5: *Missing SST values (white cells) in the left plot are filled with estimates from UH's SST function to create the right* ***plot*** shows the results of applying the UH SST Function to estimate missing SST data.

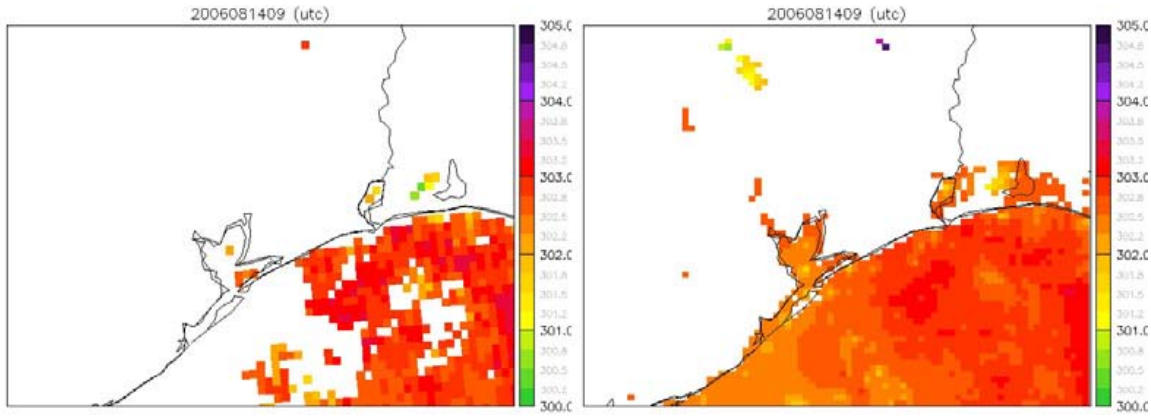

Figure 2.12.1.3-5: Missing SST values (white cells) in the left plot are filled with estimates from UH's SST function to create the right plot

When the TCEQ and UH processing of the GOES SST were complete, graphical comparisons were made to determine if gross differences appeared. The two products showed similar features, such as warmer coastline temperatures, and as Figure 2.12.1.3-6: *TCEQ SST (left plot) compared to the UH SST (right plot) for August 6, 2005 at 21 UTC exhibits the cross-hatch pattern of replaced missing data in the UH processing* shows, the UH product exhibited a cross-hatch pattern that was not evident in the TCEQ product.

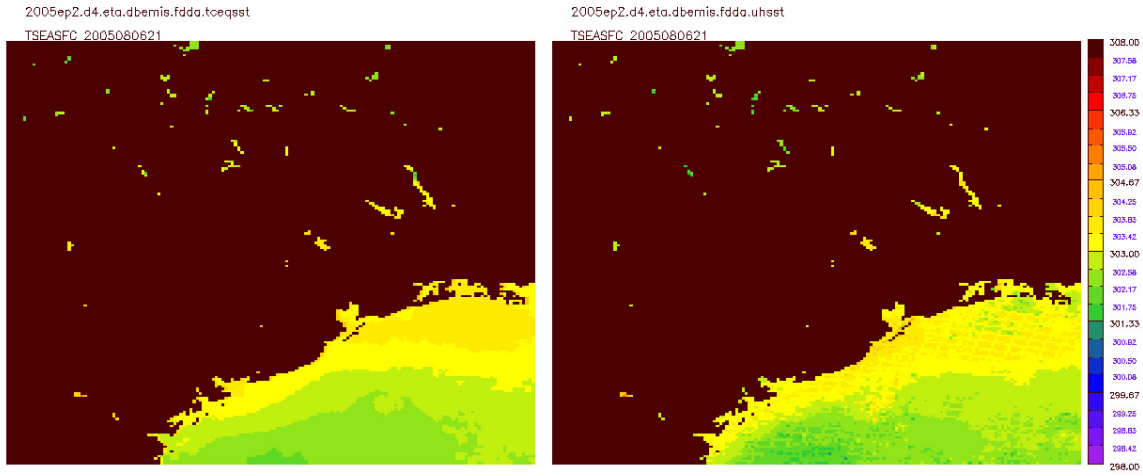

Figure 2.12.1.3-6: TCEQ SST (left plot) compared to the UH SST (right plot) for August 6, 2005 at 21 UTC exhibits the cross-hatch pattern of replaced missing data in the UH processing

Based on the cross-hatch pattern, UH reviewed their processing and found their methodology did not account for the missing data created when adapting the 6 km GOES data to the 4 km MM5 domain. Thus, the cross-hatch was a pattern of replaced missing data from the monthly mean estimate. To overcome this problem, UH doubled the resolution of the GOES dataset via horizontal interpolation for domains finer than 6 km (Byun et al., 2008) (Figure 2.12.1.3-7: *The final UH SST product does not have the cross-hatch issues (August 6, 2005 at 21 UTC is shown)*).

Any cells missing SST data after the interpolation were filled with the monthly mean diurnal value.

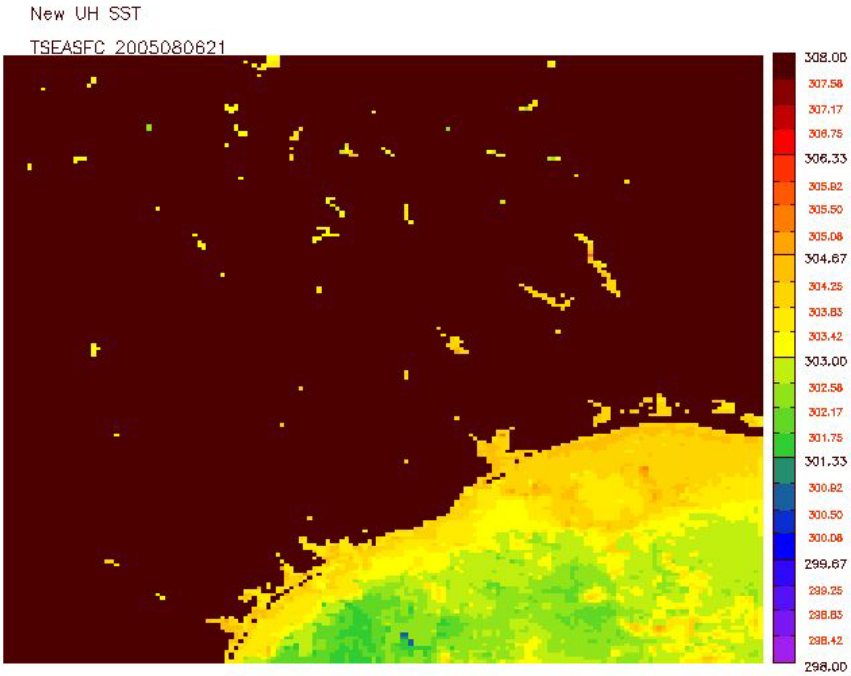

Figure 2.12.1.3-7: The final UH SST product does not have the cross-hatch issues (August 6, 2005 at 21 UTC is shown)

The processing methodologies were also reviewed to determine which would be more efficient. To create a modeling episode's hourly SST for each grid cell and MM5 domain, the TCEQ processing took approximately two working days. By contrast, the UH processing using IDL® created the final products within a few hours. Because the final products were similar in terms of SST representation, the UH methodology was chosen for its superior efficiency.

2.12.1.4 Inputting GOES SST into MM5

To compliment the IDL® processing of the raw GOES SST data, UH developed IDL® code to replace SST values in MM5 input datasets. During an MM5 run, the SST data (MM5 variable TSEASFC) are read from the LOWBDY input files. The SST data is also included in the MMINPUT input files. The UH IDL® code reads the time headers from the MM5 input files and replaces the TSEASFC values with the corresponding GOES SST data. All other variables are untouched and MM5 can be run as normal.

2.12.1.5 MM5 Performance

Comparisons of modeled surface wind and temperature performance were made during the evolution of the sea surface temperature products. If similar model performance was observed when using a higher resolution product, the higher resolution product was chosen. Table 2.12.15-1: *Table of error percentages from 4km runs for the 2005ep2 episode with different sea surface temperature products* details the percentage of date-time points where the 4km MM5 wind and temperature error was less than the defined metric. On average the performance between the different SST types was similar, thus the UH GOES SST product was chosen for the final model configuration.

Table 2.12.1.5-1 – Table of error percentages from 4km runs for the 2005ep2 episode with different sea surface temperature products

SST Type	Geographic Area/Zone	Wind Direction (°) Error ≤ 30 / 20 / 10	Wind Speed (m/s) Error ≤ 2 / 1 / 0.5	Temperature (°C) Error ≤ 2 / 1 / 0.5
NCEP NAM Skin Temp.	Region 12	Not Available	98 / 75 / 44	83 / 55 / 28
NCEP AVHRR SST	Region 12	68 / 58 / 37	99 / 74 / 41	85 / 55 / 32
TCEQ GOES SST	Region 12	66 / 57 / 35	98 / 75 / 43	87 / 54 / 33
UH GOES SST	Region 12	66 / 53 / 35	99 / 76 / 43	87 / 55 / 28

2.12.1.6 References

Banta, R. M., C. J. Senff, T. B. Ryerson, J. Nielsen-Gammon, L. S. Darby, R. J. Alvarez, S. P. Sandberg, and M. Trainer (2005), A bad air day in Houston, Bull. Am. Meteorol. Soc., 86, 657–669.

Byun, D. W., S. Kim, F. Cheng, H. Kim and F. Ngan (2007), Improved Modeling Inputs: Land Use and Sea-Surface Temperature, Final Report to the Texas Commission on Environmental Quality for Grant Activity No. 582-05-64594-FY07-03.

Byun, D. W., F. Ngan, F. Cheng, H. Kim and S. Kim (2008), Improvement of MM5 Surface Characteristics, Final Report to the Texas Commission on Environmental Quality for Grant Activity No. 582-05-64954-FY08-04.

Cleveland, W. S., S. Devlin, E. Grosse (1988), Regression by Local Fitting, Journal of Econometrics, 37, 87--114.

Darby, L.S., 2005: Cluster Analysis of Surface Winds in Houston, Texas, and the Impact of Wind Patterns on Ozone. *J. Appl. Meteor.*, **44**, 1788–1806.

ITT Visual Information Systems (2009), IDL – Data Visualization Solutions web site, http://www.ittvis.com/ProductServices/IDL.aspx, Last accessed March 25, 2009.

Mercado, F., C. Harper (2007), Description of GOES Data Processing Procedure, TCEQ Data Analysis Team Internal Draft Report.

NCAR (2005), Chapter 5: REGRID, PSU/NCAR Mesoscale Modeling System Tutorial Class Notes and User's Guide, http://www.mmm.ucar.edu/mm5/documents/MM5_tut_Web_notes/REGRID/regrid.htm, Last accessed March 11, 2009.

NCEP, (2009), National Center for Environmental Prediction RTG_SST_HR Experimental Analysis web site, http://polar.ncep.noaa.gov/sst/ophi/, Last accessed March 25, 2009.

ATTACHMENT 2

Land Use and Land Cover (LULC) Characteristics
Houston-Galveston-Brazoria Attainment Demonstration SIP Revision

2.12.2 Land Use and Land Cover (LULC) Characteristics

2.12.2.1 Introduction

All meteorological processes (wind flow, planetary boundary layer development, temperature inversions, cloud formation, latent and sensible heat fluxes, etc) are influenced by the planet's land-surface characteristics. The land use and land cover (LULC) attributes such as vegetation type, soil characteristic, and topographic features all play roles in the changing weather patterns. For the coastal environment, the land-water interaction is a dominating feature in the local meteorology and must be accurately simulated by the mesoscale model. For the 2005 and 2006 TexAQS II modeling episodes, MM5's LULC data was updated with satellite-based data in attempt to improve the exchange of heat, momentum, and moisture between the surface and atmosphere.

2.12.2.2 Model Representation

In MM5 most terrestrial features are represented via the TERRAIN_DOMAINx files, which are created by the pre-processor TERRAIN. Note that one of the key surface variables not included in the TERRAIN files is sea surface temperature, which is in the LOWBDY files (see Attachment 1: *Sea Surface Temperature (SST) Characteristics*). The TERRAIN program interpolates elevation, vegetation fraction, land use categories, soil types, and other LULC information to the domain resolution and sets up the land-surface model (LSM). TERRAIN also adds a land/water mask to determine if a grid cell is 50% or more water (e.g. lake, bay, river, ocean).

TERRAIN offers six resolutions of United States Geological Survey (USGS) Version 2 data for input: 1 degree; 30, 10, 5, 2 minute; 30 second [(USGS, 2008a). For MM5 Version 3.4 and later, the coarse USGS data was recreated using the high-resolution global 30-second data [(Wang, 2000). Prior version's coarse data originated from different sources and had errors. The USGS Version 2 dataset is based on 1992-1993 Advanced Very High Resolution Radiometer (AVHRR) satellite data.

2.12.2.3 Land Use Category Updates

From 1992 to 2005, significant changes in the land use can be expected as urban areas expand, vegetation grows (dies), and land types change. For the 2005 and 2006 TexAQS II episodes, the TERRAIN data was updated with Landsat satellite-based data from the 2001 National Land Cover Database (NLCD). The 2001 NLCD is a 30-meter resolution, multi-season collaboration of Landsat 5 and 7 satellite data, centered on 2001, and Digital Elevation Model data [(Homer et al., 2007; USGS, 2008b). The University of Texas Center for Space Research (UT-CSR) classified the 2001 NLCD with a focus on woody vegetation for biogenic modeling purposes [(Wells, 2006). This analysis focused on the coastal areas of Texas, Louisiana, and Mississippi as shown in Figure 2.12.2.3-1: *UT-CSR/NLCD map [(Byun et al., 2007) (30m resolution)*. Note that one of the key surface variables not included in the TERRAIN files is sea surface temperature, which is in the LOWBDY files (see Attachment 1 Sea Surface Temperature (SST) Characteristics).

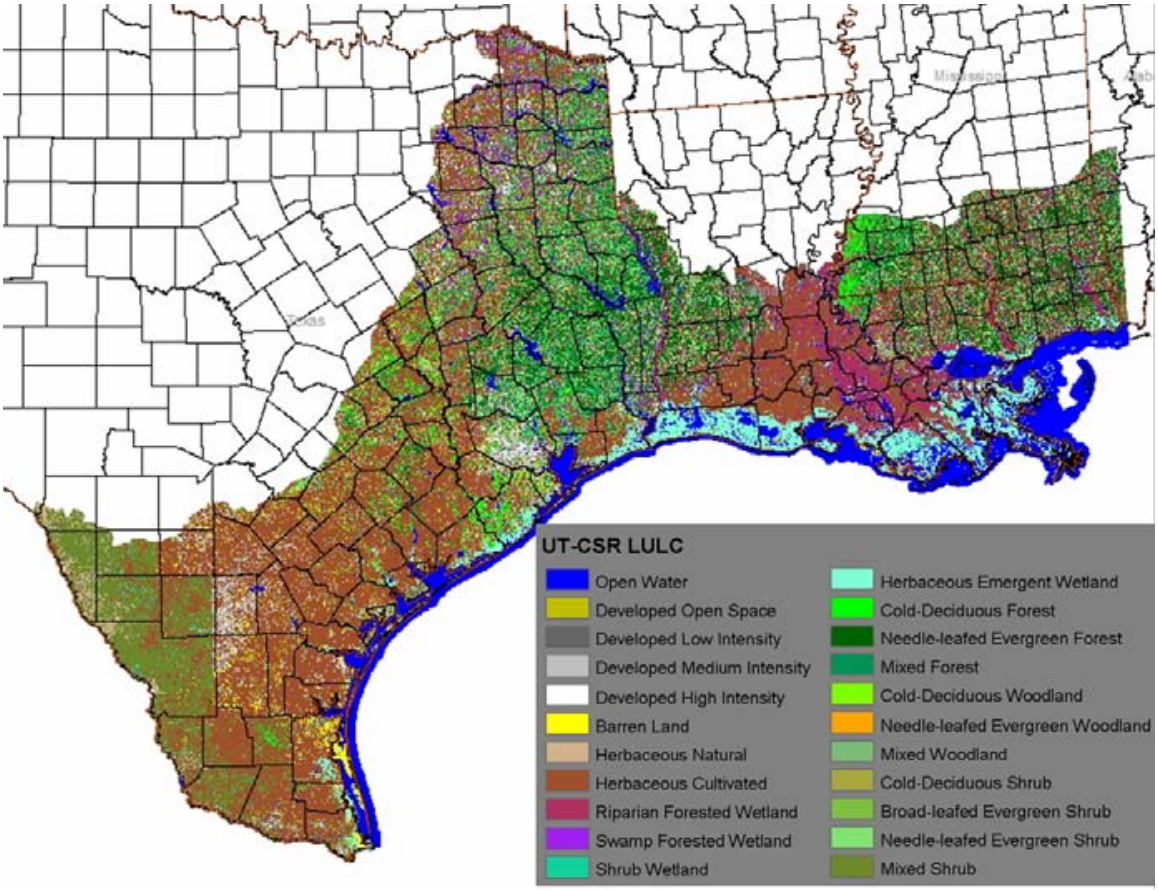

Figure 2.12.2.3-1 : UT-CSR/NLCD map [(Byun et al., 2007) (30m resolution)

On contract to TCEQ Byun et al. [(2007 and 2008) evaluated the UTCSR data for use in MM5, referred hereafter as the UTCSR data. Based on MM5 simulations with the UTCSR data and their previous experience with Texas land use data, Byun et al. [(2007) found the Houston urban area to be underrepresented in size with the UTCSR data. To improve the urban area classification, a Houston urban-focused Texas Forest Service (TFS) dataset was merged with the UTCSR data. The TFS data is based on similar Landsat 7 data from 1999-2001 and aerial photography [(GEM, 2003). After the urban area correction, the UTCSR 26 category data was classified based on the 24 category USGS data typically used in MM5. This allowed MM5 to be run without code and LANDUSE.TBL modification.

The final land use dataset for the 2005 and 2006 modeling episodes was a combination of original USGS version 2 data, TFS urban classifications, and UTCSR data (Figure 2.12.2.3-2: *Top: USGS 12km LULC; Bottom: UTCSR 12km LULC*). In the final dataset, 'mixed dry/irrigated cropland and pasture' replaced much of the 'dry cropland' in south and east Texas. Wetland areas were also more numerous along the Louisiana and Texas coastlines and river bottoms.

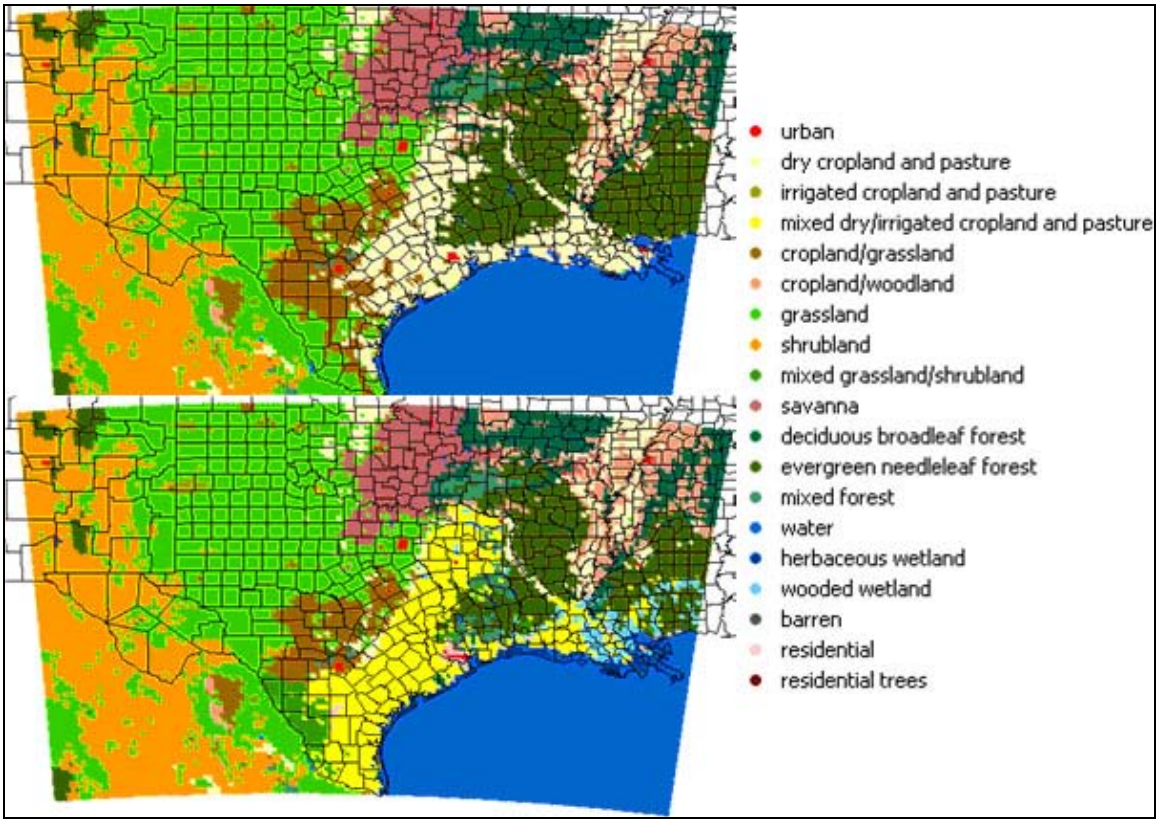

Figure 2.12.2.3-2: Top: USGS 12km LULC; Bottom: UTCSR 12km LULC; note the change from dry cropland (off-white) to mixed dry/irrigated cropland (yellow), the increase in wetlands along the southeast Texas and Louisiana coasts, and the increase in urban classifications around Houston from the TFS data (adapted from Byun et al., 2007)

2.12.2.4 Vegetation Fraction Updates

Vegetation fraction is a key terrestrial feature that MM5 uses to determine the exchange of heat and moisture between the surface and atmosphere, especially for evapotranspiration. The vegetation fraction data was reconstructed from the 30m UTCSR category data and shading factors (Byun et al. 2008). The standard MM5 vegetation fraction data was sourced from 5 years of monthly AVHRR satellite data, which provided seasonal variations. Since the UTCSR data was collected only in the summer periods, the improved vegetation fraction data should only be used during modeling of summer-time months.

The 2005 and 2006 modeling episodes are from late May – early October, thus the UTCSR vegetation fraction data should be representative. Figure 2.12.2.4-1: *Top: Original USGS Vegetation Fraction; Bottom: UTCSR Vegetation Fraction* exhibits the updated UTCSR vegetation fraction versus the standard MM5 dataset for the southeast area of Texas and Louisiana. One of the biggest improvements was the removal of an artificial zone of high vegetation fraction east of Galveston Bay that was reflected in MM5 surface temperature predictions.

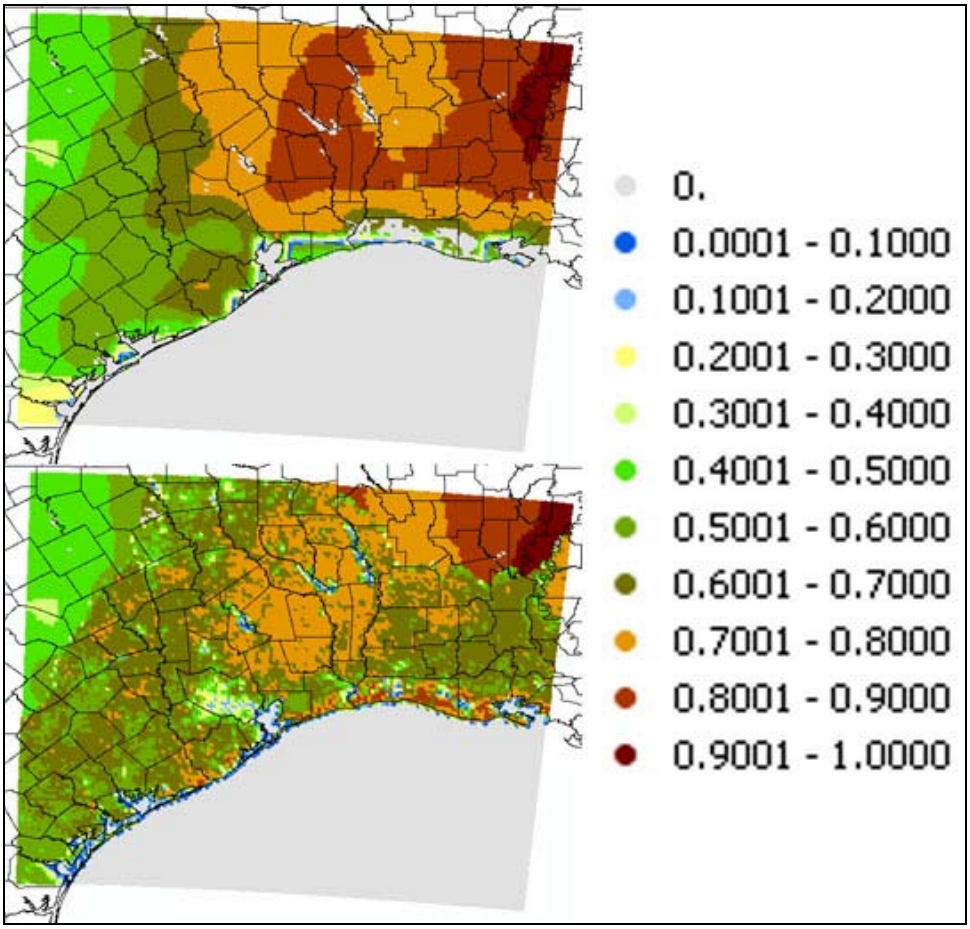

Figure 2.12.2.4-1: Top: Original USGS Vegetation Fraction; Bottom: UTCSR Vegetation Fraction; note the removal of the artificial zones of vegetation fraction along the coast (adapted from Byun et al., 2008)

2.12.2.5 Soil Type Updates

The gridded soil data used by the NOAH Land-Surface model is provided by NCEP's North American Model (NAM, formerly Eta). The NAM resolution is approximately 32 km, too coarse to accurately resolve river and lake basins. Byun et al. (2008) found that around these inland water bodies, MM5 was simulating surface temperatures with a high bias. This problem was exacerbated when the soil type near the water body was classified as dry clay, as it does not transfer heat and moisture efficiently. In that case, the river bottoms were effectively turning into 'brick rivers.' Other sources of soil data were researched but found to be similar to the NAM product.

Byun et al. (2008) introduced two new clay soil types to account for the moisture content of the soil near water bodies. "Clay 1" represents clay with water content between one and 50%. "Clay 2" represents clay with water content from 50 to 90%. To represent these new soil types, the soil parameter table (SOILPARM.TBL) was modified by replacing the lava and white sand types, which are not represented in the MM5 domains. Of the soil parameters, only the 'BB' value of "Clay 1" and "Clay 2" was changed compared to the "Clay" type. The 'BB' parameter is part of the equation that associates the soil's water content and the soil's water potential [(Chen and Dudhia, 2001). Figure 2.12.2.5-1: *Top: USGS Soil Types; Bottom: UTCSR Soil Types* details the changes from adding the additional clay types.

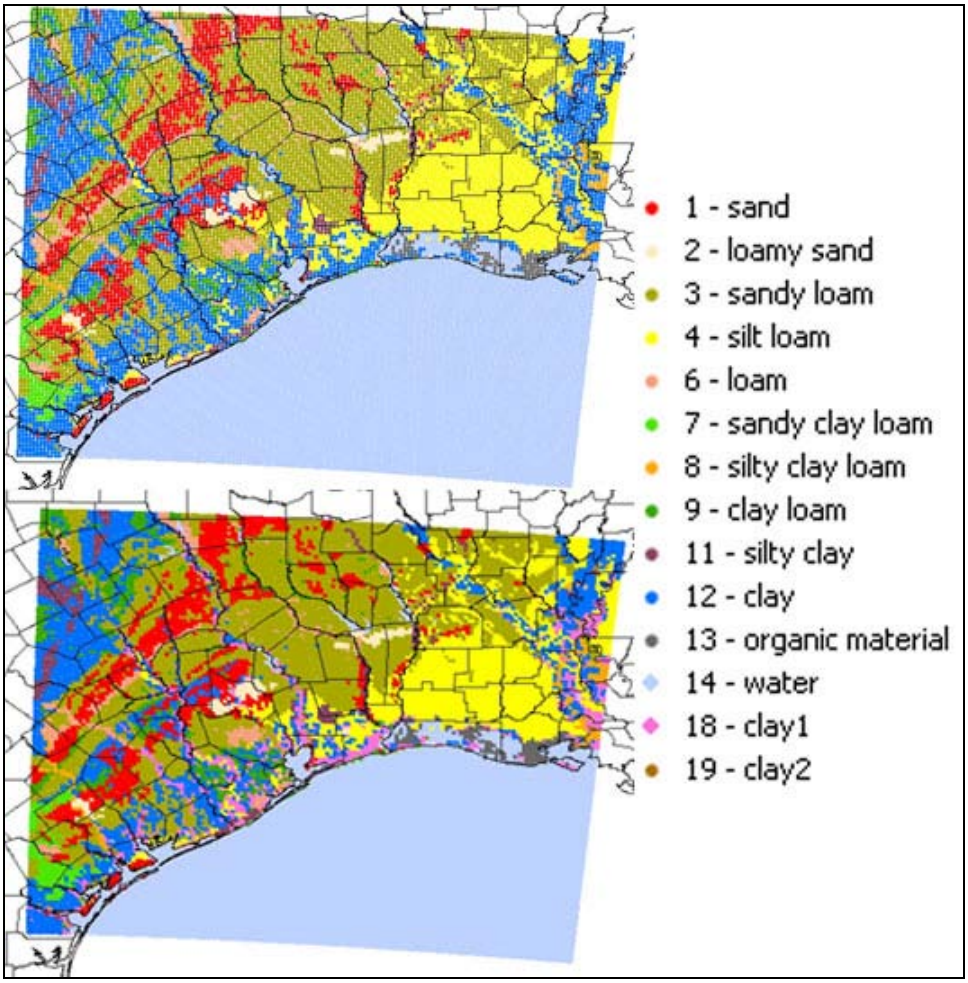

Figure 2.12.2.5-1: Top: USGS Soil Types; Bottom: UTCSR Soil Types; note the addition of clay1 and clay2 soil types along the rivers and coastal areas (adapted from Byun et al., 2008)

2.12.2.6 Land/Water Mask Update

A land/water mask is created by the TERRAIN preprocessor and passed to the MM5 input files. The land-surface model uses different surface-atmosphere exchange algorithms according to the land/water mask. In Houston area, many emission sources are located along the coastal interface and it is vital that those areas are represented as accurately as possible. When updating to the UTCSR data, Byun et al. (2008) discovered that some coastal grid cells were incongruent to the original USGS data in terms of being land or water. To overcome the land use discrepancy, the land/water mask was recreated using the UTCSR data (Figure 2.12.2.6-1: *Black points represent 4km cells where UTCSR land/water mask differed from original USGS land/water mask (adapted from Byun et al., 2008)*).

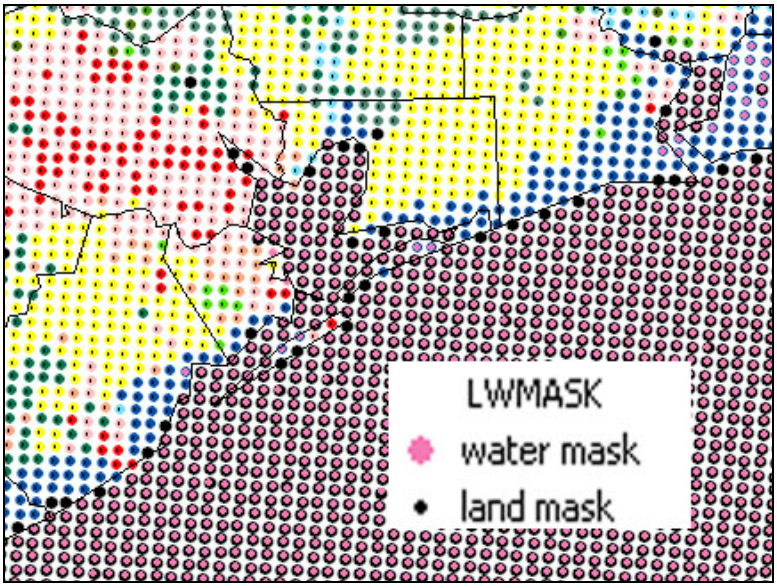

Figure 2.12.2.6-1: Black points represent 4km cells where UTCSR land/water mask differed from original USGS land/water mask (adapted from Byun et al., 2008)

2.12.2.7 Inputting UTCSR Data into MM5 TERRAIN Files

Byun et al. (2007, 2008) created Fortran programs for TCEQ to update the land use, soil, vegetation, and land/water mask information in MM5. The programs convert the UTCSR data to the MM5 domain projection and aggregate it to the domain resolution. Once the data is appropriately configured, a separate Fortran program replaces the USGS data in the MM5 TERRAIN file with the corresponding UTCSR data. All other variables are untouched and MM5 can be run as normal.

2.12.2.8 Model LULC Consistency

In previous TCEQ modeling efforts, the models used separate sources of LULC data. By replacing the USGS data with the UTCSR data in MM5, the underlying LULC data is consistent between the meteorology, biogenic and photochemical models. While the models categorize the LULC data uniquely, the year and source of data are not a basis of model discrepancy.

2.12.2.9 Model Performance

As the meteorological modeling of the TexAQS II episodes was developed, many MM5 simulations were completed to test model configurations. Because of the timing of contract deliverables and TCEQ state implementation plan (SIP) timelines, model runs without the updated LULC, but with all other final options, were not completed. Not all episodes were able to be run with the same configurations over the development of the SIP modeling. However, comparisons of the intermediate and final LULC model runs were made for all episodes by choosing model runs with the most similar options.

Table 2.12.2.9-1: *Percent accuracy statistics for intermediate and final UTCSR LULC MM5 runs for all meteorological modeling episodes***.** compares the average performance of MM5 with the intermediate UTCSR LULC and with the final UTCSR LULC category updates. This version of the UTCSR data contains the soil type additions, land/water mask update, and TFS urban area correction. The table lists the percentage of hours where the model was within the benchmarks for wind direction, wind speed, and temperature for the all of the TexAQS II meteorological episodes.

Table 2.12.2.9-1: Percent accuracy statistics for intermediate and final UTCSR LULC MM5 runs for all meteorological modeling episodes; Note that UTCSR Final runs may not correspond to final SIP configuration.

LULC Type	Episode	Zone	Wind Dir. (°) Error ≤ 30 / 20 / 10	Wind Speed (m/s) Error ≤ 2 / 1 / 0.5 m/s	Temp. (°C) Error ≤ 2 / 1 / 0.5
UTCSR Intermediate	2005ep0	Region 12	71 / 61 / 41	96 / 70 / 35	67 / 35 / 21
UTCSR Final	2005ep0	Region 12	76 / 67 / 49	98 / 73 / 40	78 / 49 / 30
UTCSR Intermediate	2005ep1	Region 12	82 / 69 / 45	100 / 90 / 60	68 / 42 / 18
UTCSR Final	2005ep1	Region 12	82 / 71 / 40	100 / 93 / 60	74 / 50 / 28
UTCSR Intermediate	2005ep2	Region 12	65 / 52 / 32	97 / 75 / 44	73 / 44 / 24
UTCSR Final	2005ep2	Region 12	67 / 54 / 33	98 / 75 / 40	78 / 57 / 32
UTCSR Intermediate	2006ep0	Region 12	75 / 62 / 41	97 / 73 / 40	78 / 47 / 23
UTCSR Final	2006ep0	Region 12	76 / 63 / 45	97 / 72 / 38	85 / 57 / 33
UTCSR Intermediate	2006ep1a	Region 12	76 / 65 / 43	100 / 86 / 45	76 / 54 / 31
UTCSR Final	2006ep1a	Region 12	80 / 67 / 43	100 / 83 / 43	83 / 61 / 39
UTCSR Intermediate	2006ep1b	Region 12	67 / 55 / 32	95 / 54 / 19	85 / 58 / 33
UTCSR Final	2006ep1b	Region 12	69 / 53 / 31	96 / 56 / 22	82 / 54 / 29
UTCSR Intermediate	2006ep1c	Region 12	87 / 76 / 53	98 / 59 / 31	61 / 32 / 15
UTCSR Final	2006ep1c	Region 12	84 / 76 / 57	96 / 57 / 29	69 / 33 / 16
UTCSR Intermediate	2006ep1d	Region 12	82 / 65 / 34	98 / 74 / 37	78 / 47 / 24
UTCSR Final	2006ep1d	Region 12	85 / 66 / 37	98 / 77 / 43	77 / 53 / 34

As the tabulated statistics show, the impact of the final UTCSR LULC data was not drastic for winds or temperature. In many cases the final UTCSR data provided small error benefits, especially for temperature. For all episodes the final UTCSR data was used in the SIP modeling configuration.

2.12.2.10 References

Byun, D. W., S. Kim, F. Cheng, H. Kim and F. Ngan (2007), Improved Modeling Inputs: Land Use and Sea-Surface Temperature, Final Report to the Texas Commission on Environmental Quality for Grant Activity No. 582-05-64594-FY07-03.

Byun, D. W., F. Ngan, F. Cheng, H. Kim and S. Kim (2008), Improvement of MM5 Surface Characteristics, Final Report to the Texas Commission on Environmental Quality for Grant Activity No. 582-05-64954-FY08-04.

Chen, F., and J. Dudhia (2001), Coupling an advanced land-surface hydrology model with the Penn State - NCAR MM5 modeling system. Part I: Model implementation and sensitivity, Mon. Wea. Rev., 129, 569–585.

GEM (2003), Satellite data processing for land use and cover type classification, Final report to the Texas Forest Service for Project TFS-3-027.

Homer, C., J. Dewitz, J. Fry, M. Coan, N. Hossain, C. Larson, N. Herold, A. McKerrow, J.N. VanDriel and J. Wickham. (2007). Completion of the 2001 National Land Cover Database for the Conterminous United States, Photogrammetric Engineering and Remote Sensing, Vol. 73, No. 4, pp 337-341.

USGS (2008), Global Land Cover Characteristics Data Base Version 2.0, http://edc2.usgs.gov/glcc/globdoc2_0.php, Last accessed March 23, 2009.

USGS (2008), National Land Cover Database 2001 (NLCD 2001), http://www.mrlc.gov/nlcd.php, Last accessed March 23, 2009.

Wang, W. (2000), Status Report on MM5 Pre- and Post-processing Programs in Version 3, http://www.mmm.ucar.edu/mm5/workshop/ws00/mesouser.pdf, Last accessed March 23, 2009.

Wells, G., (2006): The New Eastern Texas Land Use Land Cover Classification Project, HARC Project Contact number: H-46-T28-2004-T2, University of Texas-Austin Center for Space Research, Austin, Texas.

ATTACHMENT 3

Data Assimilation
Houston-Galveston-Brazoria Attainment Demonstration SIP Revision

2.12.3 Data Assimilation

2.12.3.1 Introduction

Data assimilation is a process by which observations are blended with modeled analyses to produce a result closer to reality. In MM5, observed parameters are assimilated during the model run through a process called Four-Dimensional Data Assimilation (FDDA), or nudging, by adding an additional term to the equations of motion (Stauffer and Seaman, 1990; Stauffer et al., 1991; Stauffer and Seaman, 1994). This process helps overcome errors in initialization data and limitations in the model's physics that can accumulate over time.

A MM5 model prediction can be analysis nudged to a gridded field for winds, temperature, and water vapor. MM5 can also be observationally nudged to high resolution meteorological data from sources such as surface stations, radar/sodar profilers, rawinsondes, aircraft measurements, etc. TCEQ has successfully used analysis and observational nudging in past SIP modeling efforts and others have demonstrated the benefit of nudging on model performance (ATMET, 2003; Byun et al., 2008; Jia and Morris, 2003; Nielsen-Gammon, 2002; Nielsen-Gammon et al., 2007; Otte, 2008a; Otte, 2008b). EPA recommends using FDDA to make sure the model does not significantly diverge from reality (EPA, 2007). Both types of data assimilation were performed for the meteorological modeling of the 2005 and 2006 episodes and are described herein.

2.12.3.2 Analysis Nudging

Analysis nudging is a process by which the model forecast is 'relaxed' towards a gridded field, which could be three-dimensional and/or surface data of winds, temperature, and water vapor. In MM5, analysis nudging is typically run by copying the model's input file MMINPUT_DOMAINx to MMINPUT2_DOMAINx for the coarse grids only. The operational National Center for Environmental Prediction (NCEP) North American Mesoscale Model (NAM) output was used for input and analysis nudging in MM5 for the 2005 and 2006 episodes. EPA recommends nudging winds throughout the vertical atmosphere, temperature and moisture above the boundary layer only. That setup has been adopted for this modeling application. MM5 default nudging strengths and radii of influence were used. Surface analysis nudging was not used.

2.12.3.3 Observational Nudging

Unlike analysis nudging that uses a gridded field of data, observational nudging incorporates individual measurements at specific locations (three-dimensional) and times into the model forecast. This type of nudging is usually conducted on the finest scale grid, which allows local measurements to influence the large-scale meteorological phenomena from the coarse domains. Examples of typically used sources for observational nudging include radar profilers, rawinsondes, surface stations, pilot balloons, satellite soundings, and aircraft. For this application, radar and sodar profiler wind data was chosen as the source of observational nudging. The 2005ep0 episode (May 18 – June 5, 2005) lacked sufficient profiler data as only data from Cleburne and La Porte were available. This episode was supplemented with surface observations from the hourly National Center for Atmospheric Research's ds472.0 dataset (CISL, 2009). Observational nudging was limited to wind speed and direction on the 4km domain only.

As part of the second Texas Air Quality Study (TexAQS II), a network of radar and sodar wind profilers was deployed (Figure 2.12.3.3-1: *TexAQS II Profiler Locations*). Sonoma Technology Inc. (STI) collected and quality assured the upper air wind data for use in data analysis and modeling projects by removing migrating birds and other artifacts. More information regarding STI's quality assurance techniques can be found in their report (Knoderer and MacDonald, 2007). The quality assurance of the ds472.0 surface data was limited to gross error analysis, such as wind speed greater than 100 m/s or less than 0 m/s.

Figure 2.12.3.3-1: TexAQS II Profiler Locations

The quality assured upper air wind data has a vertical resolution of 60-100 meters (m) from 40 m above ground level (agl) to over 10,000 m agl, depending on the type and siting of the profiler. MM5's observational nudging requires the data be listed according to sigma layer at a frequency up to a tenth of an hour (NCAR, 2005). The TexAQS II upper air wind data was averaged within the MM5 sigma layers according to the vertical distance from the middle of the sigma layer (1/r weighting). The frequency of the profiler observations was generally hourly but some recorded data on a fifteen or thirty minute interval. The observations were time-shifted ahead to account for the overall period of the measurement rather than the start time (Nielsen-Gammon, 2008) and then rounded to the tenth of the hour. The ds472.0 data was referenced to MM5 layer 43 (surface) and rounded to the nearest tenth of the hour.

The latitude/longitude coordinates of the profilers and ds472.0 stations were projected onto the Lambert Conformal MM5 4km grid, and the wind observations were rotated using a version of a Perl script posted to the MM5-Users listserv (Petre, 2007). TCEQ staff modified the script to calculate grid indices for any of the nested MM5 grids. Thus, observational nudging files were created for the 4 km grid and the 12 km grid for some tests. Finally, the Perl script formatted the Fortran binary file required for MM5 input.

Default nudging strengths and radii of influence were used for the observational nudging, though sensitivity tests were performed to test alternative configurations as detailed below. Nielsen-Gammon (2008b) reviewed the setup for observational nudging and found the configuration to perform better than alternatives.

2.12.3.4 Configuration Summary

FDDA in MM5 allows the user to adjust how strong the model will be nudged (relaxed) towards the observation or analysis field. The MM5 community has developed default nudging strength coefficients that appear in the mm5 run script (mm5.deck). EPA (2007) recommends Analysis Nudging coefficients not greater than 1.0×10^{-4} for winds and 1.0×10^{-5} for moisture and Observational Nudging coefficients that do not cause inconsistency over the modeling domain. The final configuration for the 2005 and 2006 episodes used the MM5 default nudging strengths,

with only the Analysis Nudging wind coefficient (GV=2.5 x 10^{-4}) deviating from EPA's recommended plan. The choice for the Analysis Nudging wind coefficient was based on the MM5 default value and previous TCEQ and contractor modeling experience. Nielsen-Gammon (2008b) reviewed the modeling setup for the TexAQS II episodes and determined the configuration to be superior to alternatives. Table 2.12.3.4-1: *MM5 Nudging Parameter Values* summarizes the parameter values used.

Table 2.12.3.4-1: MM5 Nudging Parameter Values

		Nudging Coefficients (s^{-1})			Radius of Influence		
Domain	Nudging Type	Winds	Temp.	Moisture	Horiz.	Vert.	Data Source
108 km	Analysis 3-D	2.5E-4	2.5E-4	1.0E-5	-	-	NCEP NAM
36 km	Analysis 3-D	1.0E-4	1.0E-4	1.0E-5	-	-	NCEP NAM
12 km	Analysis 3-D	1.0E-4	1.0E-4	1.0E-5	-	-	NCEP NAM
4 km	Observational	4.0E-4	-	-	240 km	0.001 sigma	TexAQS II Profiler

2.12.3.5 Sensitivities

Alternate nudging configurations were performed to determine if other setups would provide results more suited to the Houston coastal area. The following sections detail those sensitivities.

2.12.3.6 Observational Nudging on the 12km Domain

While the 4km MM5 domain is quite extensive in size (184 by 166 4km grid cells, (see Chapter 3: Photochemical Modeling), five TexAQS II profilers were not within its boundaries as shown in Figure 2.12.3.6.1: *TexAQS II profilers and MM5 12km (blue) & 4km (red) domains*. To determine if the course MM5 output could be improved in order to provide better 4km inputs, observational nudging was run on the 12km domain with all available quality assured TexAQS II profiler data.

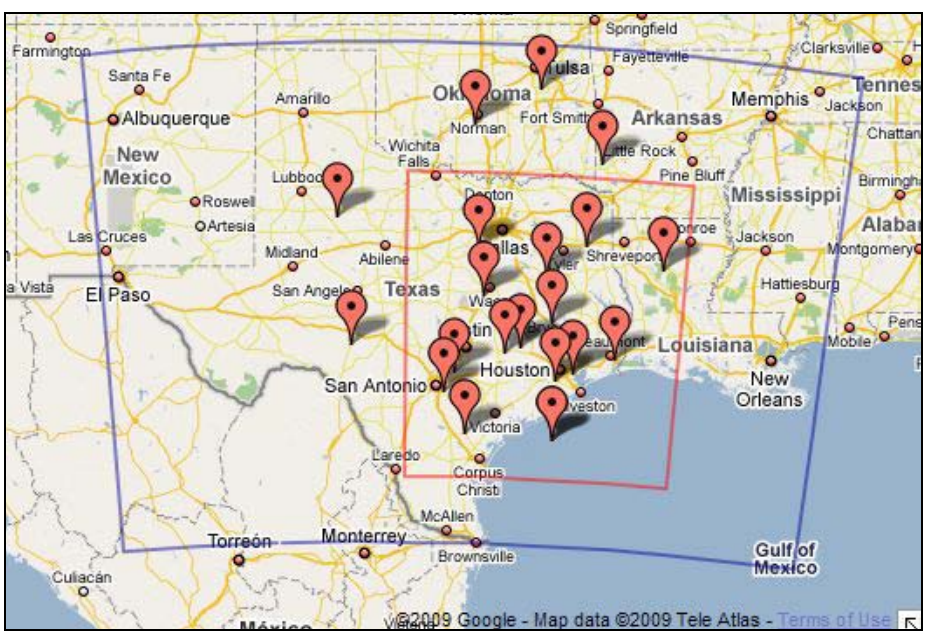

Figure 2.12.3.6-1: TexAQS II profilers and MM5 12km (blue) & 4km (red) domains

By adding observational nudging to the 12km domain, the 12km MM5 performance was not significantly changed. Figure 2.12.3.6-2 – *12km Scatter plots: Texas Average Wind Speed*

Comparison shows average 12km wind speed scatter plots of all Texas ds472.0 surface monitoring sites versus the corresponding MM5 grid cells for every hour of the 2005ep2 episode (July 25 – August 9, 2005). The box in the upper right of each plot details the percentage of date-time points where the MM5 error was less than two, one, and 0.5 meters/second. The values are almost identical indicating that the 12km observational nudging did not have much impact on average wind speed.

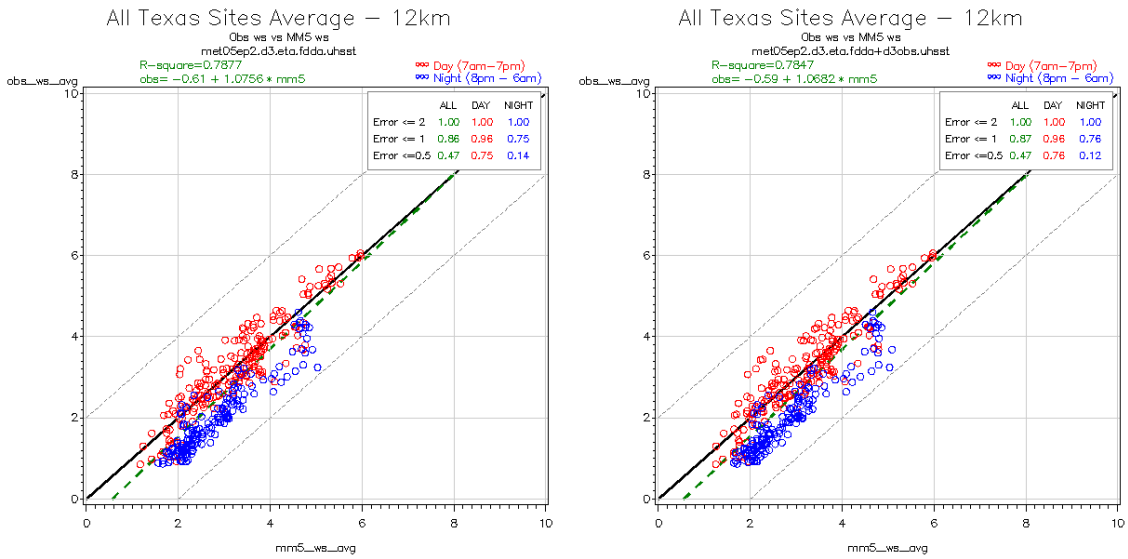

Figure 2.12.3.6-2: 12km Scatter plots – Texas Average Wind Speed Comparison (left plot shows standard 12km run, right plot shows 12km run w/ observational nudging)

Table 2.12.3.6-1: *Table of error percentages from 12km runs with and without observational nudging for 2005ep2 episode* shows the error percentages for wind direction, wind speed, and temperature for the MM5 runs with and without 12km observational nudging when compared to all Texas ds472.0 sites. Again, the results are similar indicating that the observational nudging did not have a significant impact on the 12km domain.

Table 2.12.3.6-1: Table of error percentages from 12km runs with and without observational nudging for 2005ep2 episode

Model Run	Wind Dir. Error ≤ 30 °	Wind Dir. Error ≤ 20 °	Wind Spd. Error ≤ 2 m/s	Wind Spd. Error ≤ 1 m/s	Temp. Error ≤ 2 °C	Temp. Error ≤ 1 °C
Standard Run	**80**	63	100	86	**99**	**80**
With 12km Nudging	80	**64**	100	**87**	98	79

While the 12km domain did not show a significant average response, winds and temperature in the 4km domain exhibited more change. 4km model runs were evaluated at all TCEQ Continuous Air Monitoring Stations (CAMS), Houston area CAMS (TCEQ Region 12), and subsets of monitors called zones (Figure 2.12.3.6-3: *All 4km TCEQ CAMS (left) and Region 12 CAMS (right)*).

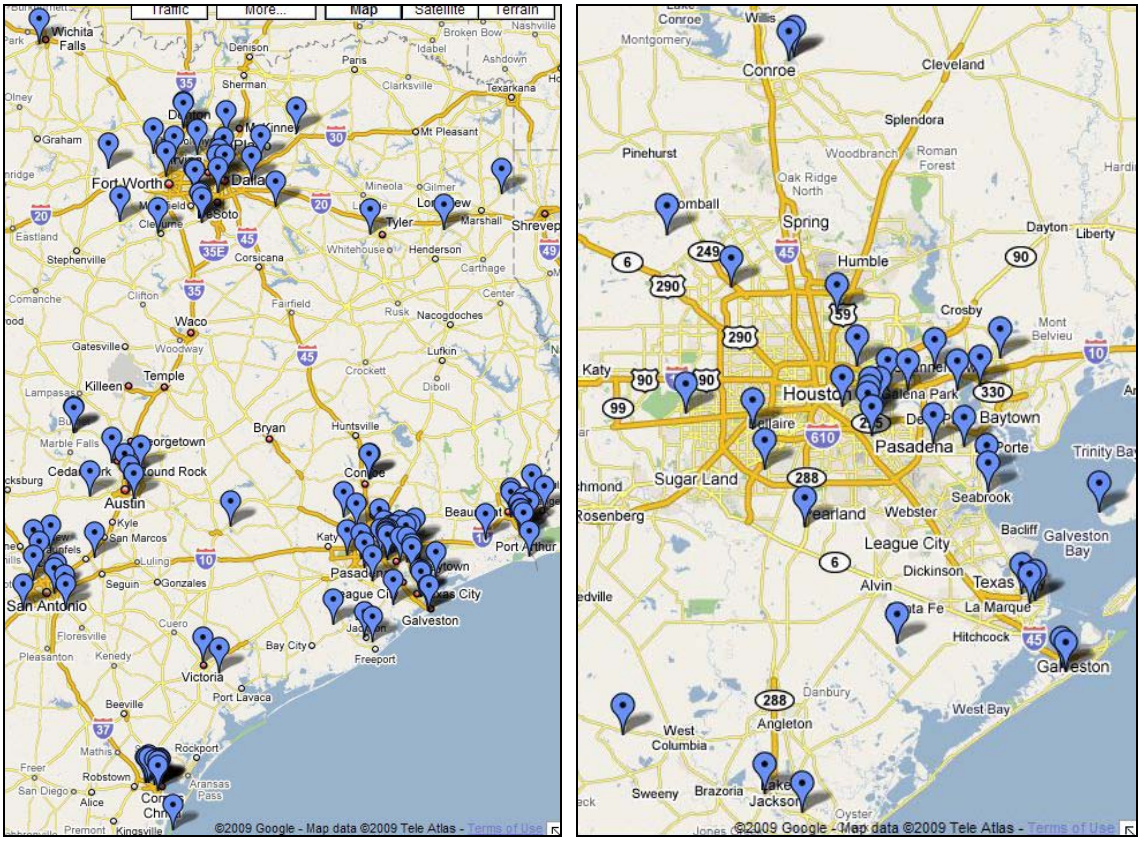

Figure 2.12.3.6-3: All 4km TCEQ CAMS (left) and Region 12 CAMS (right)

Figure 2.12.3.6-4: *4km wind speed scatter plots for Region 12 without (left) and with (right) 12km 4km observational nudging for 2005ep2 episode* shows the 4km performance of wind speed with and without observational nudging on the 12km domain for every hour of the 2005ep2 episode (July 25 – August 9, 2005). The two model runs perform similarly indicating that on average throughout the Houston area the 12km observational nudging did not have much of an impact.

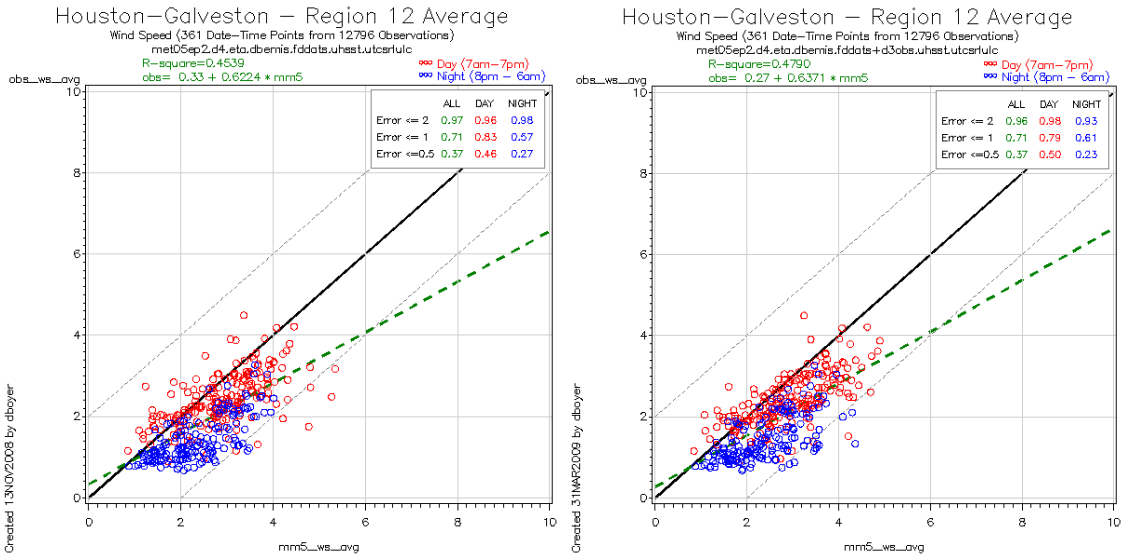

Figure 2.12.3.6-4: 4km wind speed scatter plots for Region 12 without (left) and with (right) 12km observational nudging for 2005ep2 episode

Because of the large number of CAMS monitors in the Houston region, an area wide average may smooth out smaller scale features. Zones of CAMS monitors were chosen to represent smaller geographic areas as shown in Figure 2.12.3.6-5: *CAMS in Model Performance Zones*. Evaluating model runs to the Houston Region and Zone averages instead of individual CAMS monitors proved to be efficient, allowing more sensitivities of the eight TexAQS II meteorological modeling episodes.

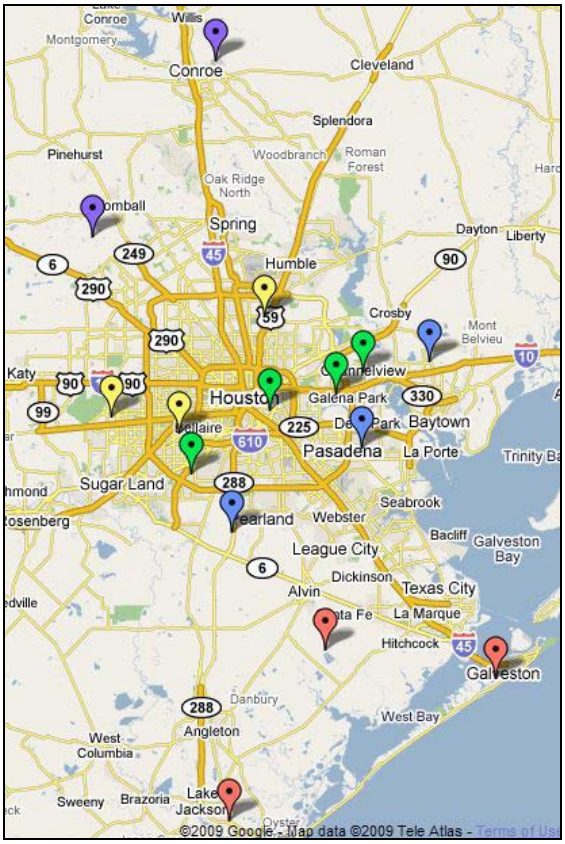

Downwind

Northwest Harris Co. C26
Conroe Relocated C78

Northwest Core

Westhollow C410
Bayland Park C53
Aldine C8

Southeast Core

Croquet C409
Regional Office C81
HRM-3 C603
Channelview C15

Ship Channel

Manvel Croix Park C84
Deer Park C35
Wallisville Road C617

Coastal Zone

Clute C11
Mustang Bayou C619
Galveston Airport C34

Figure 2.12.3.6-5: CAMS in Model Performance Zones

Compared to the Region 12 average, the wind and temperature response to 12km observational nudging was very similar in the Zones for the 4km domain. The change in wind speed and direction error was small and differed by Zone. Temperature appeared to improve slightly for all areas.

Table 2.12.3.6-2: *Table of error percentages from 4km runs with and without 12km observational nudging for 2005ep2 episode* details the response in winds and temperature on the 4km domain to the 12km observational nudging for the 2005ep2 episode.

Table 2.12.3.6-2: Table of error percentages from 4km runs with and without 12km observational nudging for 2005ep2 episode

12km Nudging?	Geographic Area/Zone	Wind Direction Error ≤ 30 °	Wind Speed Error ≤ 2 m/s	Temperature Error ≤ 2 °C
NO	Region 12	**69**	**97**	86
YES	Region 12	68	96	**88**
NO	Coastal Zone	59	96	80
YES	Coastal Zone	**61**	96	**83**
NO	Ship Channel	55	94	84
YES	Ship Channel	55	94	**86**
NO	Southeast Core	**59**	**96**	80
YES	Southeast Core	57	94	**84**
NO	Northwest Core	47	88	65
YES	Northwest Core	47	**91**	**66**
NO	Downwind	39	78	80
YES	Downwind	**40**	**80**	**83**

Because of the insignificant impact on the 12km and 4km domains, MM5 modeling with 12km observational nudging was not investigated further.

2.12.3.7 Radius of Influence Tests

The TexAQS II profilers were sited throughout the state of Texas and neighboring states to collect upper air wind data for many areas with air quality degradation and for pollutant transport studies. This is in contrast to the TexAQS 2000 air quality study where the profiler locations surrounded the Houston area (Figure 2.12.3.7-1: *TexAQS 2000 (blue) and TexAQS II (red) upper air sites*). Because of the more diffuse network of upper air sites, the horizontal radius of influence (ROI) for observational nudging was considered to be a parameter worth investigating.

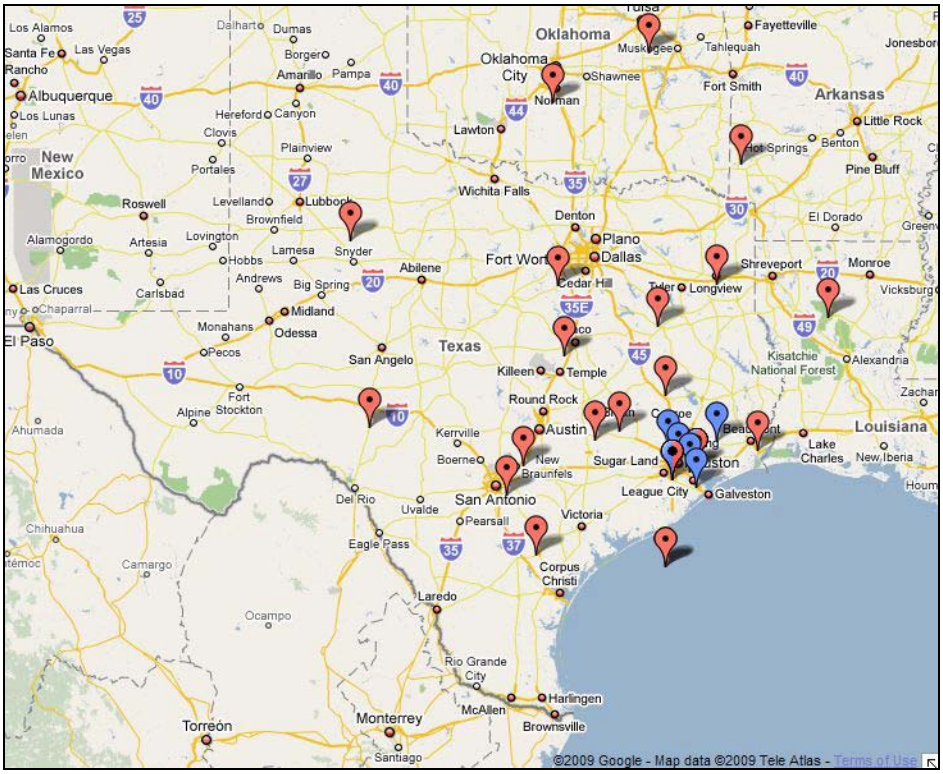

Figure 2.12.3.7-1: TexAQS 2000 (blue) and TexAQS II (red) upper air sites

The default horizontal ROI for observational nudging is 240 km and is controlled by the mm5.deck variable RINXY. The strength of the nudging is distanced-weighted according to a Cressman-type function. When a 240 km ROI circle is plotted on each profiler, as in Figure 2.12.3.7-2: *TexAQS II Profilers with 240 km Radii of Influence*, all profilers locations are impacted by other profilers. Modeling with the default ROI could produce smoothed wind fields, effectively losing finer details.

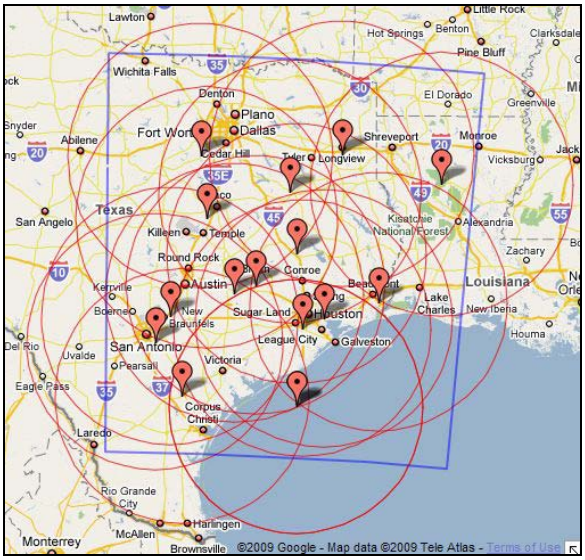

Figure 2.12.3.7-2: TexAQS II Profilers with 240 km Radii of Influence

To determine if the wind fields were being impacted, MM5 was run with ROIs of 120 and 80 km. Figure 2.12.3.7-3: *TexAQS II Profilers with 120 (left) and 80 km (right) Radii of Influence* shows

the profilers with the smaller ROIs. With the smaller ROI, less upper air sites interact with each other.

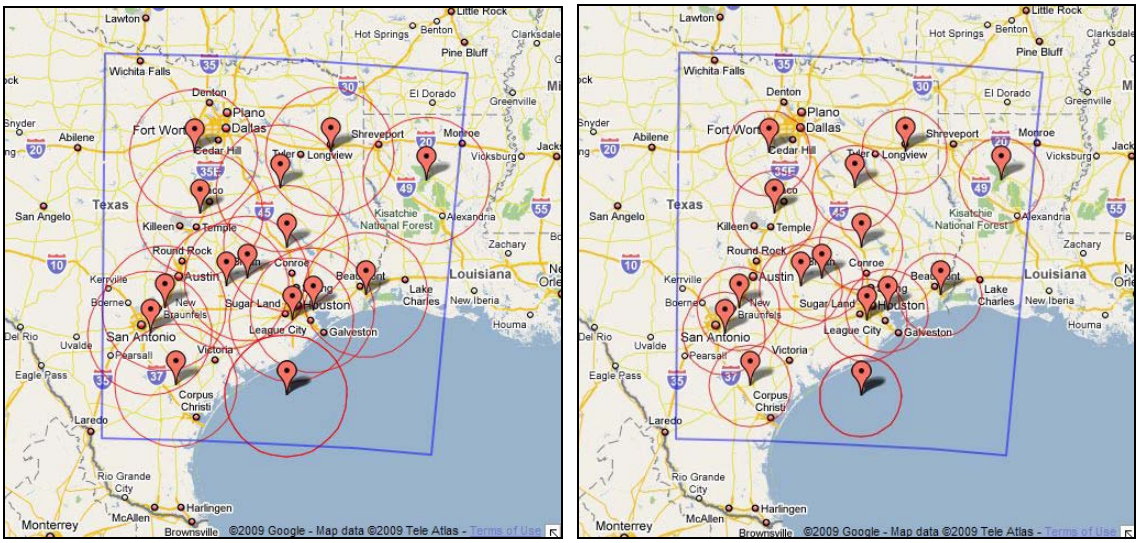

Figure 2.12.3.7-3: TexAQS II Profilers with 120 (left) and 80 km (right) Radii of Influence

On an average basis, the use of a smaller ROI did not have much impact on the average error in the Houston area (TCEQ Region 12). Table 2.12.3.7-1: *Average MM5 model performance using different observational nudging radii of influence* displays the percent of hours where MM5 had average error less than the parameter benchmark for all Region 12 CAMS monitors and Houston zones.

Table 2.12.3.7-1: Average MM5 model performance using different observational nudging radii of influence

Geographic Area/Zone	Radius of Influence (km)	Wind Direction Error ≤ 30 °	Wind Speed Error ≤ 2 m/s	Temperature Error ≤ 2 °C
Region 12	240 (default)	**65**	97	73
Region 12	120	63	**99**	73
Region 12	80	60	98	**74**
Coastal Zone	240 (default)	**55**	96	**73**
Coastal Zone	120	51	**97**	72
Coastal Zone	80	51	96	67
Ship Channel	240 (default)	**57**	**97**	66
Ship Channel	120	54	97	68
Ship Channel	80	52	96	**71**
Downwind	240 (default)	41	**85**	**72**
Downwind	120	**42**	83	72
Downwind	80	40	79	72

Results from the ROI sensitivities were also investigated in terms of forward trajectories produced from surface wind sites and the corresponding surface modeled data. This metric was used to determine if the wind flows were modified by the smaller ROIs.

Figure 2.12.3.7-4: *Forward trajectories comparing surface observations (red) to model runs with observational nudging ROIs of 120 (blue) and 240 km (green) for July 28, 2005 at 6 AM* exhibits a 12-hour forward trajectory starting from 19 points in the Houston area at 6:00 AM CST on July 28, 2005 and compares the model runs of 120 (blue points) and 240 km (green) with surface observations (red). Figure 2.12.3.7-5: *Forward trajectories comparing surface observations (red)*

to model runs with observational nudging ROIs of 120 (blue) and 80 km (green) for July 28, 2005 at 6 AM exhibits the same time period but compares the 120 km ROI run (blue) with the 80 km run (green).

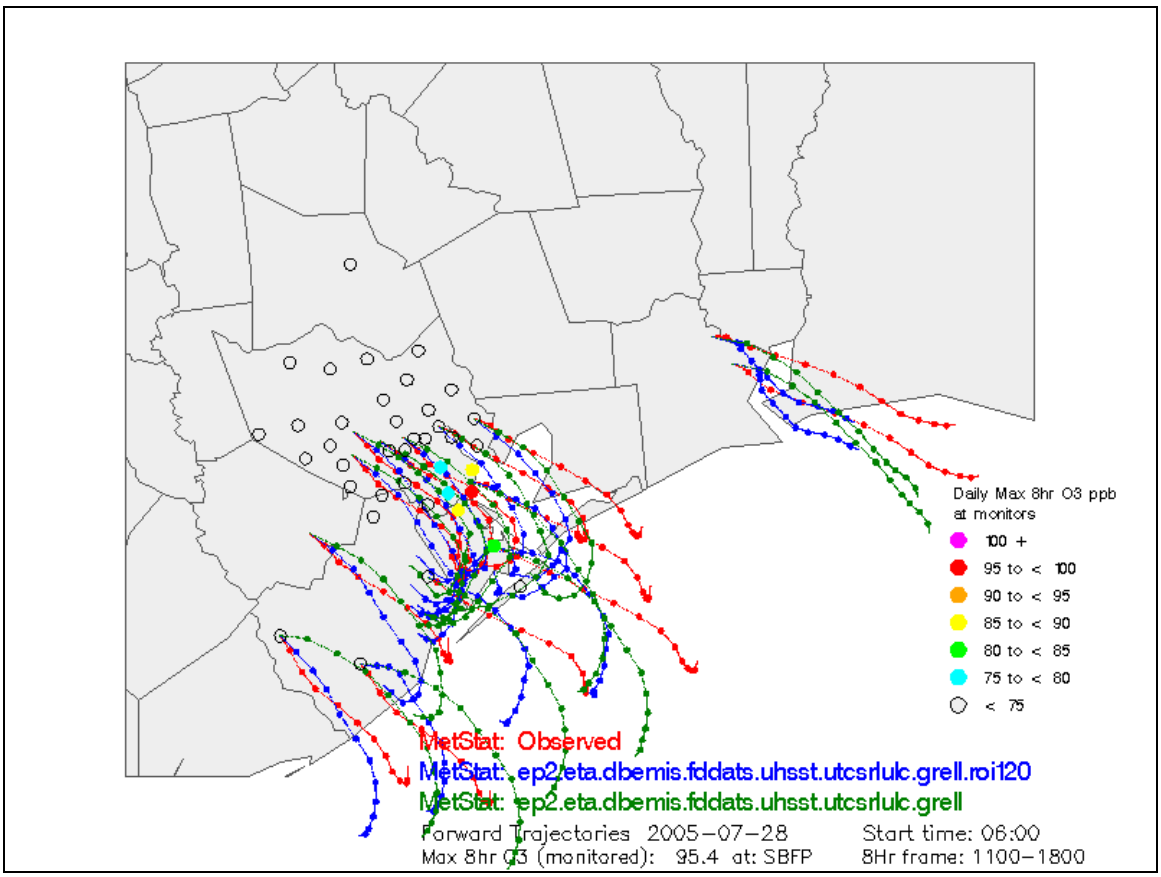

Figure 2.12.3.7-4: Forward trajectories comparing surface observations (red) to model runs with observational nudging ROIs of 120 (blue) and 240 km (green) for July 28, 2005 at 6 AM

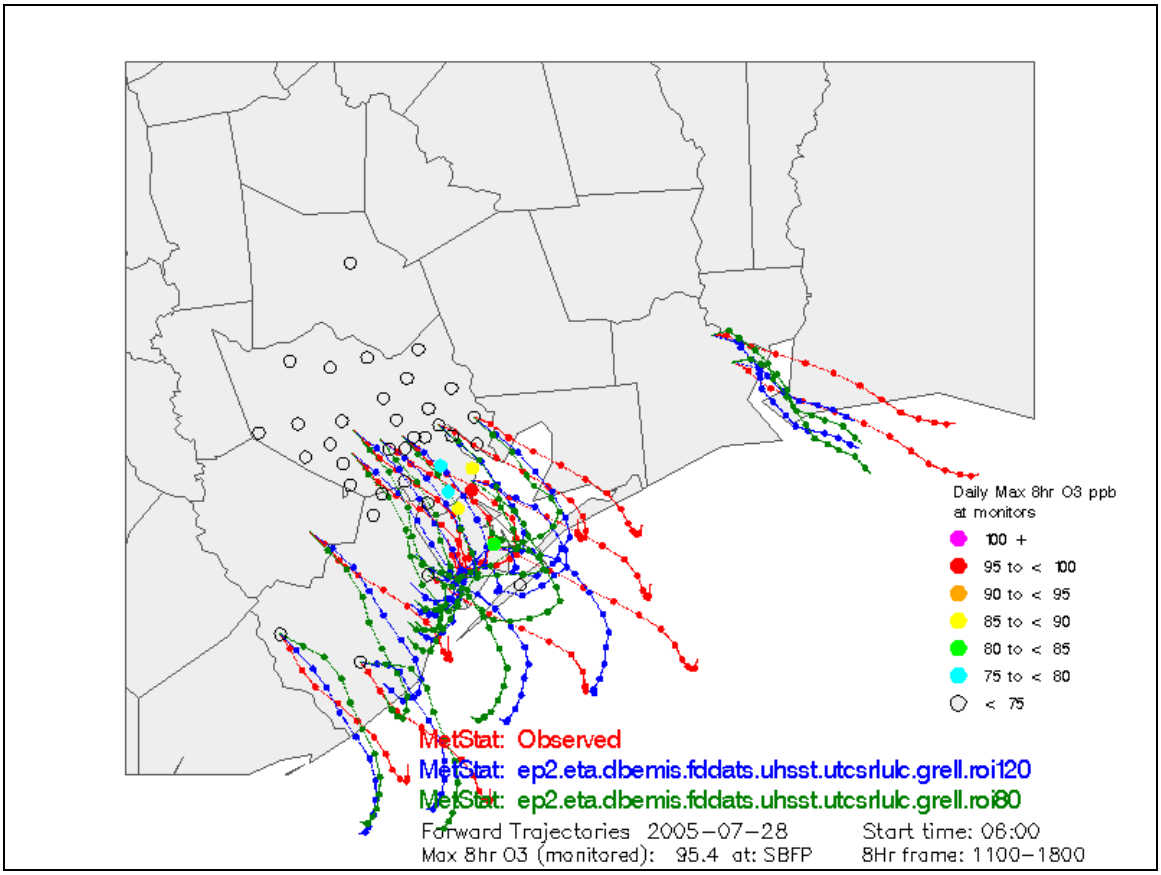

Figure 2.12.3.7-5: Forward trajectories comparing surface observations (red) to model runs with observational nudging ROIs of 120 (blue) and 80 km (green) for July 28, 2005 at 6 AM

By evaluating the MM5 runs with different ROIs, it was determined that the default 240 km performed equally or better than other choices. While small differences were noted in the trajectories and error statistics, significant changes did not appear to occur. These conclusions compliment those found by Nielsen-Gammon (2008b). Radius of Influence parameter tests were also conducted when model sensitivities were nudged with ds472.0 data and will be described in the surface nudging section.

2.12.3.8 Surface Observational Nudging

To summarize the MM5 performance when surface nudging was used and when surface nudging was not used for episode 2005ep0 (May 18 - June 4, 2005), 2005ep1 (June 15 - June 30, 2005), and 2005ep2 (July 25 - August 9, 2005), statistics for meteorological variables were calculated for the Houston-Galveston area (HGB). The model performance was determined by comparing the CAMS hourly surface wind speed, wind direction, and temperature to the corresponding hourly MM5 values. The performance was evaluated by calculating the percent of compliance of the surface wind speed within 1m/s, the wind direction within 30 degrees, and the temperature within 1 degree Celsius.

Figure 2.12.3.8-1: *Wind speed performance for episodes 2005ep0, 2005ep1, and 2005ep2* shows the Houston-Galveston area (HGB) daily performance of the wind speed for the three episodes with and without surface nudging. Wind direction and temperature are captured in Figure 2.12.3.8-2: *Wind direction performance for episodes 2005ep0, 2005ep1, and 2005ep2* and Figure 2.12.3.8-3: *Surface temperature performance for episodes 2005ep0, 2005ep1, and 2005ep2* respectively.

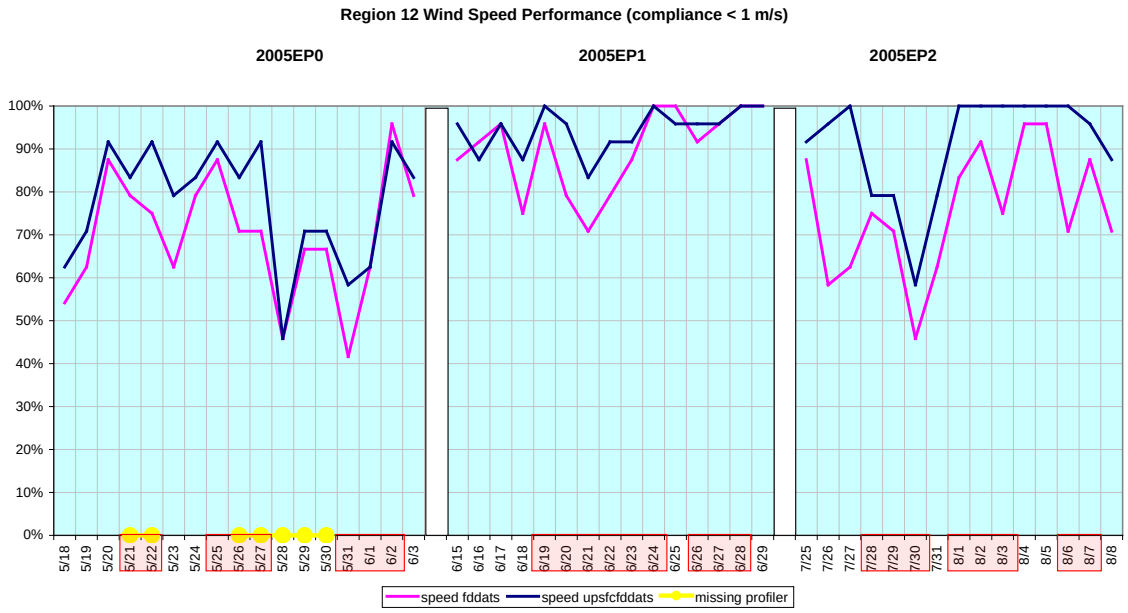

Figure 2.12.3.8-1: Wind speed performance for episodes 2005ep0, 2005ep1, and 2005ep2

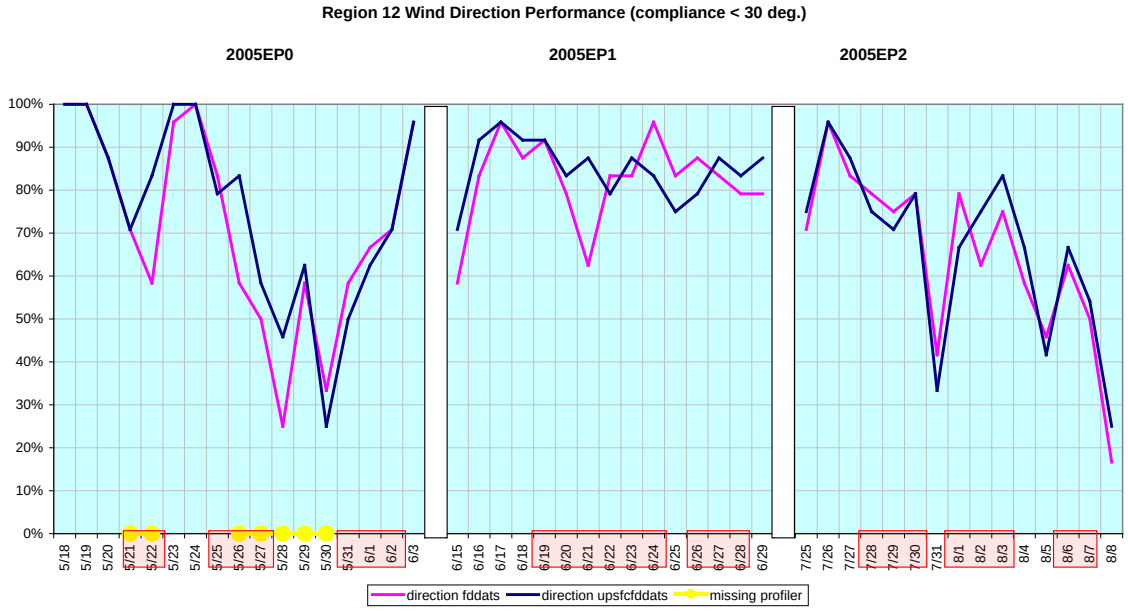

Figure 2.12.3.8-2: Wind direction performance for episodes 2005ep0, 2005ep1, and 2005ep2

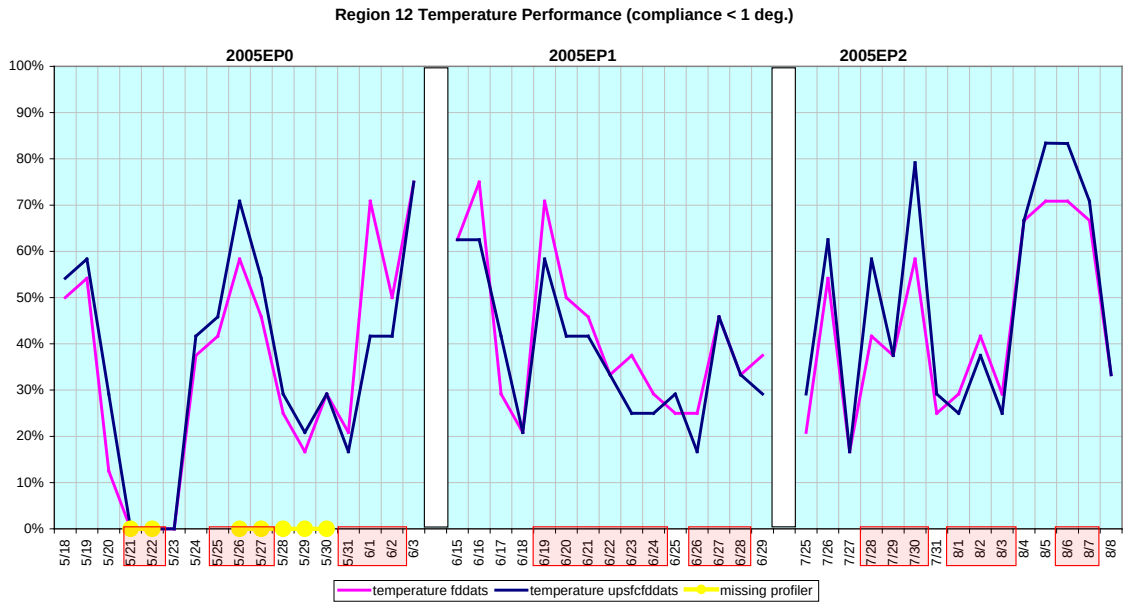

Figure 2.12.3.8-3. Surface temperature performance for episodes 2005ep0, 2005ep1, and 2005ep2

Table 2.12.3.8-1: *Summary of the MM5 model performance for the Houston-Galveston area (HGB) for wind speed, wind direction, and temperature for the high ozone days for episodes 2005ep0, 2005ep1, and 2005ep2* shows a summary of the performance results for the three episodes for the Houston-Galveston (RGB) region for the days with high ozone. The wind speed performance results show that the MM5 runs with surface nudging performed equally or better than without surface nudging on 100% of the days with high ozone. As for the wind direction and temperature, the MM5 runs with surface nudging performed equally or better than without surface nudging on 52% and 52%, respectively, of the days with high ozone.

Table 2.12.3.8-1: Summary of the MM5 model performance for the Houston-Galveston area (HGB) for wind speed, wind direction, and temperature for the high ozone days for episodes 2005ep0, 2005ep1, and 2005ep2

		2005ep0	2005ep1	2005ep2	Total	Percent
	Number of high ozone days	8	9	8	25	
Wind Speed	Days where sfc nudging is equal or better	8	9	8	25	100%
Wind Direction	Days where sfc nudging is equal or better	5	3	5	13	52%
Temperature	Days where sfc nudging is equal or better	5	3	5	13	52%

Detailed 2005ep0 episode average model performance in percent with and without surface nudging for different Zones, which include: Houston-Galveston Region (R12); Zone 1 (Coastal); Zone 2 (Ship Channel); Zone 3 (Southeast Core); Zone 4 (Northwest Core); Zone 5 (Downwind), are summarized in Table 2.12.3.8-2: *2005ep0 summary of the MM5 model performance in percent for the Houston-Galveston area (R12) and the five Zones for compliance of wind speed within 1m/s, wind direction within 30 deg., and temperature within 1 deg. for the episode average*. Of special note for this episode is that profiler data only became available on May 19

for Cleberne (near Fort Worth) and La Porte (in HGB) and other profiler data did not become available until June.

Table 2.12.3.8-2: 2005ep0 summary of the MM5 model performance in percent for the Houston-Galveston area (R12) and the five Zones for compliance of wind speed within 1m/s, wind direction within 30 deg., and temperature within 1 deg. for the episode average

2005ep0	Wind Speed	Wind Direction	Temperature
R12 with sfc nudging	77	75	36
upper air only (when available)	70	71	35
Zone 1 with sfc nudging	65	72	32
upper air only (when available)	63	62	33
Zone 2 with sfc nudging	65	68	34
upper air only (when available)	54	60	34
Zone 3 with sfc nudging	63	70	32
upper air only (when available)	55	65	33
Zone 4 with sfc nudging	66	64	25
upper air only (when available)	60	61	26
Zone 5 with sfc nudging	57	58	34
upper air only (when available)	54	56	33

Comparisons for the 2005ep1 and 2005ep2 episodes are captured respectively in Table 2.12.3.8-3: *2005ep1 summary of the MM5 model performance in percent for the Houston-Galveston area (R12) and the five Zones for compliance of wind speed within 1m/s, wind direction within 30 deg., and temperature within 1 deg. for the episode average* and Table 2.12.3.8-4.: *2005ep2 summary of the MM5 model performance in percent for the Houston-Galveston area (R12) and the five Zones for compliance of wind speed within 1 m/s, wind direction within 30 deg., and temperature within 1deg. for the episode average*.

The normal expectation is that by nudging to surface data, the statistics should improve. For 2005ep1, there is only a marginal improvement over using upper-air data only.

Table 2.12.3.8-3: 2005ep1 summary of the MM5 model performance in percent for the Houston-Galveston area (R12) and the five Zones for compliance of wind speed within 1m/s, wind direction within 30 deg., and temperature within 1 deg. for the episode average

2005ep1	Wind Speed	Wind Direction	Temperature
R12 with sfc nudging	94	85	38
upper air only	90	82	42
Zone 1 with sfc nudging	69	75	29
upper air only	65	68	32
Zone 2 with sfc nudging	85	69	35
upper air only	80	67	37
Zone 3 with sfc nudging	86	75	34
upper air only	83	72	36
Zone 4 with sfc nudging	85	61	25
upper air only	78	64	32
Zone 5 with sfc nudging	73	55	27
upper air only	67	59	33

.

Table 2.12.3.8-4: 2005ep2 summary of the MM5 model performance in percent for the Houston-Galveston area (R12) and the five Zones for compliance of wind speed within 1m/s, wind direction within 30 deg., and temperature within 1 deg. for the episode average

2005ep2	Wind Speed	Wind Direction	Temperature
R12 with sfc nudging	91	66	49
upper air only	75	65	44
Zone 1 with sfc nudging	78	59	38
upper air only	74	55	37
Zone 2 with sfc nudging	79	56	47
upper air only	63	53	45
Zone 3 with sfc nudging	81	55	48
upper air only	67	57	43
Zone 4 with sfc nudging	75	49	17
upper air only	58	48	16
Zone 5 with sfc nudging	55	44	48
upper air only	43	41	43

<u>Sensitivity of observational nudging in MM5 to the radius of influence</u>

The standard radius of influence used in the observational nudging is 240 km. This number is representative of an appropriate range for upper air data from rawinsonde or profiler data, which are typically widespread (i.e., low spatial resolution). Since only one radius of influence parameter is permitted in MM5 when reading an observational nudging file, the value selected for this parameter may be more appropriate for upper air data or surface data but likely will not represent both sets of data well. The surface data used for the nudging is the ds472.0 surface observations, which have a higher spatial resolution than the profiler data, and would ideally require a smaller radius of influence to fully utilize all the surface data. To test the sensitivity of the MM5 simulations to the radius of influence, a radius of influence of 60 km was used instead

of 240 km. Figure 2.12.3.8-4: *MM5 daily model performance for 2006ep1c with a radius of influence of 240 km* shows the 2006ep1c episode (September 16 - 29, 2006) daily model performance using the standard 240 km. Figure 2.12.3.8-5: *MM5 daily model performance for 2006ep1c with a radius of influence of 60 km* is the same format but with a radius of influence of 60 km. The high ozone day (September 20) showed that the wind direction performance didn't change when the radius of influence was decreased to 60 km. However, the wind speed performance slightly degraded. As for the high ozone day of September, 26, the wind speed improved and the wind direction degraded when the 60 km radius of influence was used. On September 27, both the wind speed and wind direction performance improved when 60km was used for the radius of influence.

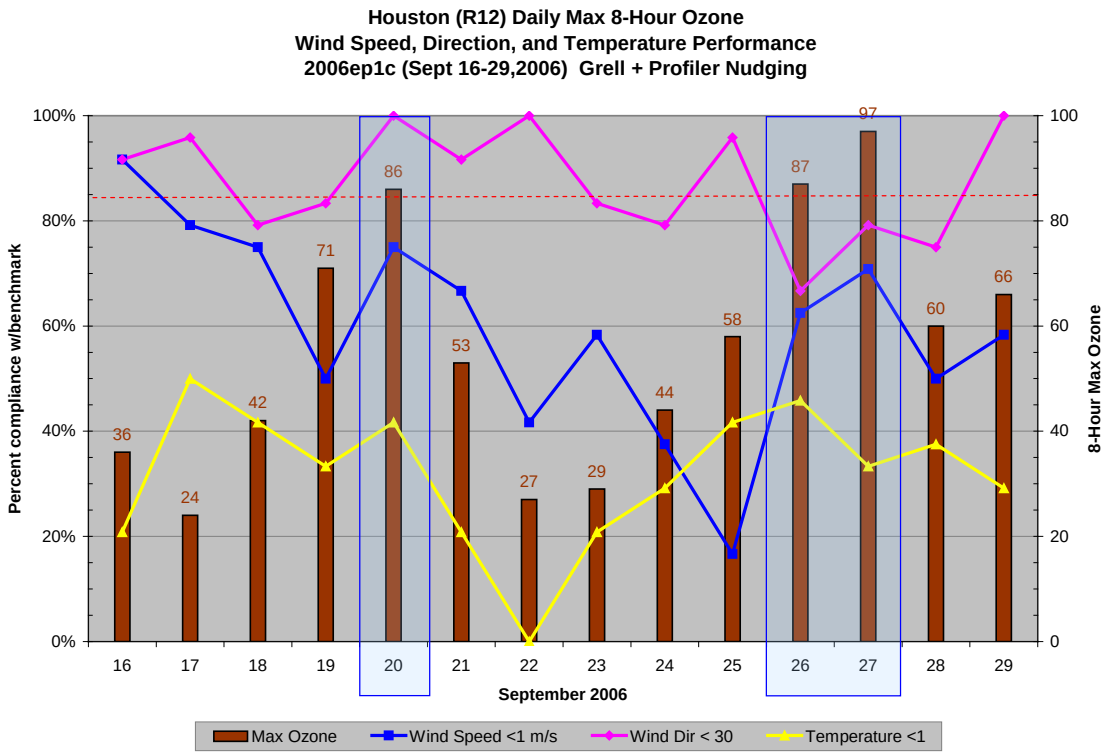

Figure 2.12.3.8-4: MM5 daily model performance for 2006ep1c with a radius of influence of 240 km

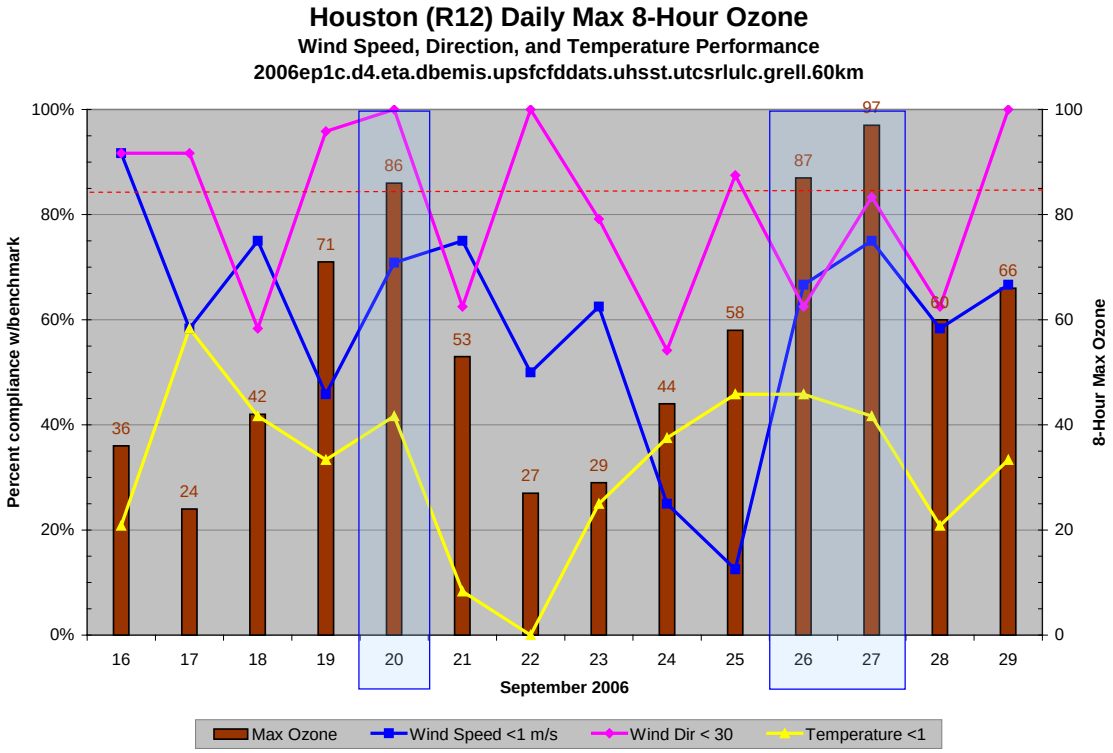

Figure 2.12.3.8-5: MM5 daily model performance for 2006ep1c with a radius of influence of 60 km

Two segmented runs (partial period) of 2006ep1c were simulated to test the 60 km radius of influence, as well as a 30 km value. The first segment is Sep. 18-20 for the high ozone day on September 20. September 18 is for the MM5 spin-up and September 19 is for the CAMx spin-up. The second segment is September 24-27, 2006, for the high ozone days on September 26 and 27. September, 24 is for the MM5 spin-up and September 25 is for the CAMx spin-up. The full 2006ep1c episode with the 60 km radius of influence and the overlay of the two segmented runs with the 60 and 30 km radius of influence are displayed in Figure 2.12.3.8-6: *MM5 daily model performance for 2006ep1c with a radius of influence of 60km, overlaid with segmented runs with 60 and 30 km radius of influence*

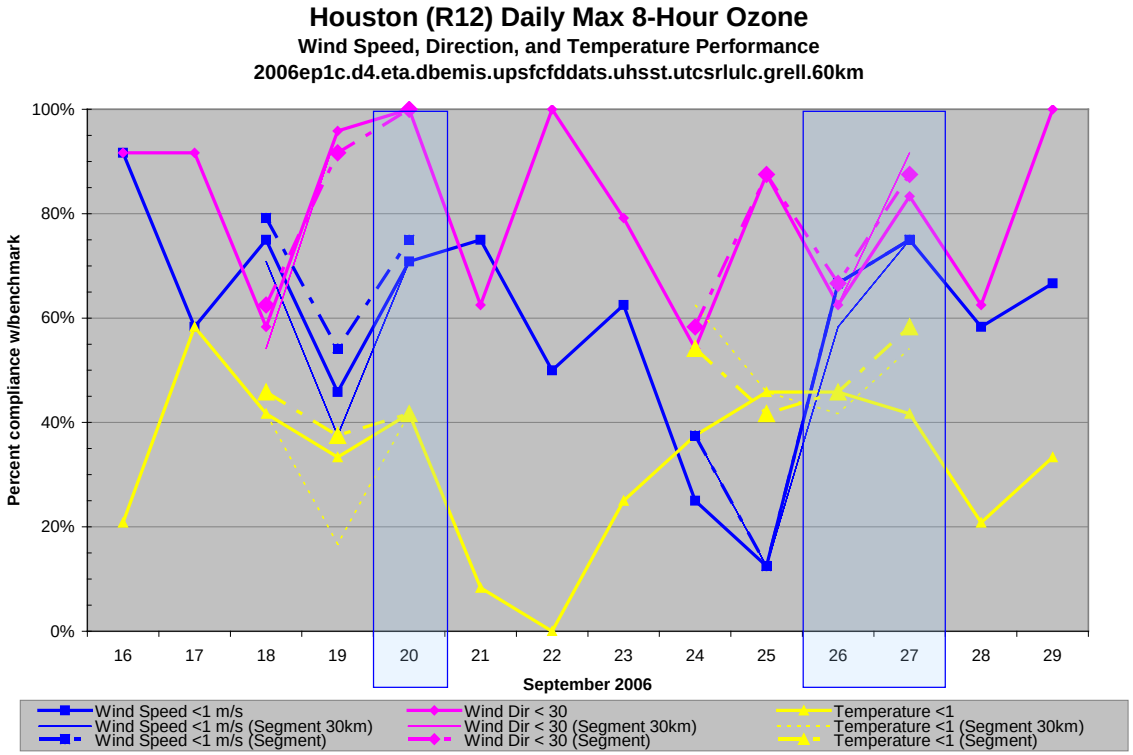

Figure 2.12.3.8-6: MM5 daily model performance for 2006ep1c with a radius of influence of 60 km, overlaid with segmented runs with 60 and 30 km radius of influence.

Table 2.12.3.8-5: *Performance summary of the segmented 60 km and 30 km runs* summarizes the performance of the segmented 60 km and 30 km runs. The upward arrows indicates improvement compared to the full run with 60 km, the downward arrow indicates degradation compared to the full run, and "same" indicates no change.

Table 2.12.3.8-5: Performance summary of the segmented 60km and 30km runs

		Sep. 19	**Sep. 20**	**Sep. 25**	**Sep. 26**	**Sep. 27**
60km	Wind Direction	↓	same	same	↑	↑
	Wind Speed	↑	↑	same	same	same
	Temperature	↑	same	↓	same	↑
30km	Wind Direction	same	same	same	same	↑
	Wind Speed	↓	same	same	↓	same
	Temperature	↓	same	↑	↓	↓

<u>Sensitivity of MM5 to observation-nudging coefficient (s^{-1}) for wind (GIV)</u>

The observational nudging in MM5 uses a nudging coefficient parameter for the wind (GIV) set to 0.0004. In order to test the sensitivity of MM5 to different values for GIV, two MM5 runs were performed that used the profiler and the surface data (ds472) for nudging with a radius of influence of 60 km, instead of the standard 240km value. Figure 2.12.3.8-7.a: *Performance plot for the wind speed using the default GIV (0.0004) and the 5 times the standard observation-nudging coefficient of (5x0.0004=0.002) for the Houston (R12)* shows the MM5 performance for Houston (R12) for episode 2006ep1c (September 16-29, 2006) with a 60 km radius of influence for the nudging of the wind with the standard observation-nudging coefficient of 0.0004. When the observation-nudging coefficient of 0.002 was used, the wind speed performance improved on most days including the high ozone days (September 20, 26, and 27). The entire 4 km domain is captured in Figure 2.12.3.8-7.b: *Performance plot for the wind speed using the default GIV*

(0.0004) and the 5 times the standard observation-nudging coefficient of (5x0.0004=0.002) for the entire 4 km domain.

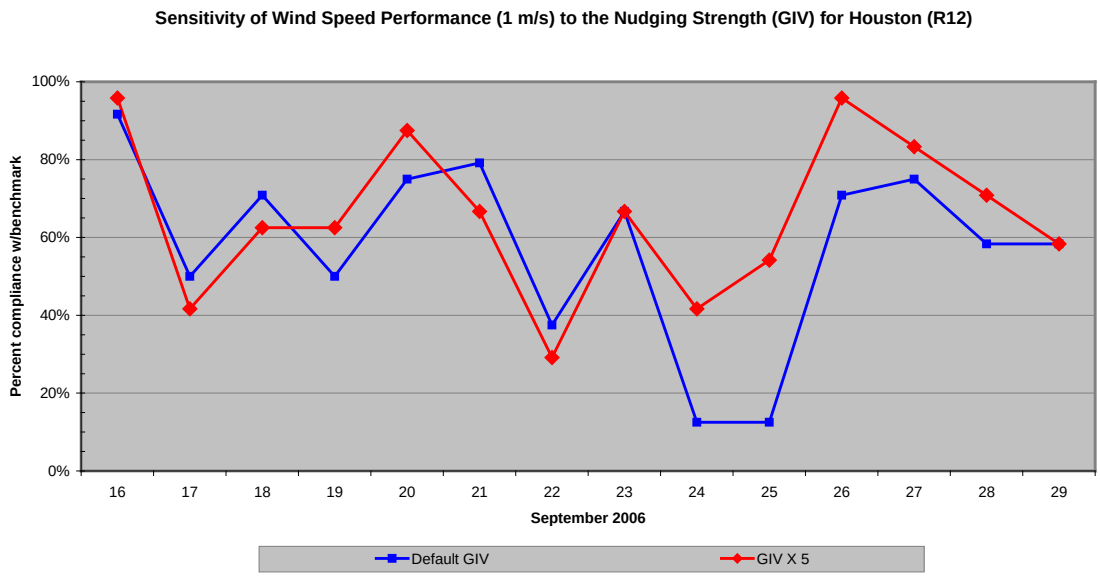

Figure 2.12.3.8-7.a: Performance plot for the wind speed using the default GIV (0.0004) and the 5 times the standard observation-nudging coefficient of (5x0.0004=0.002) for the Houston (R12)

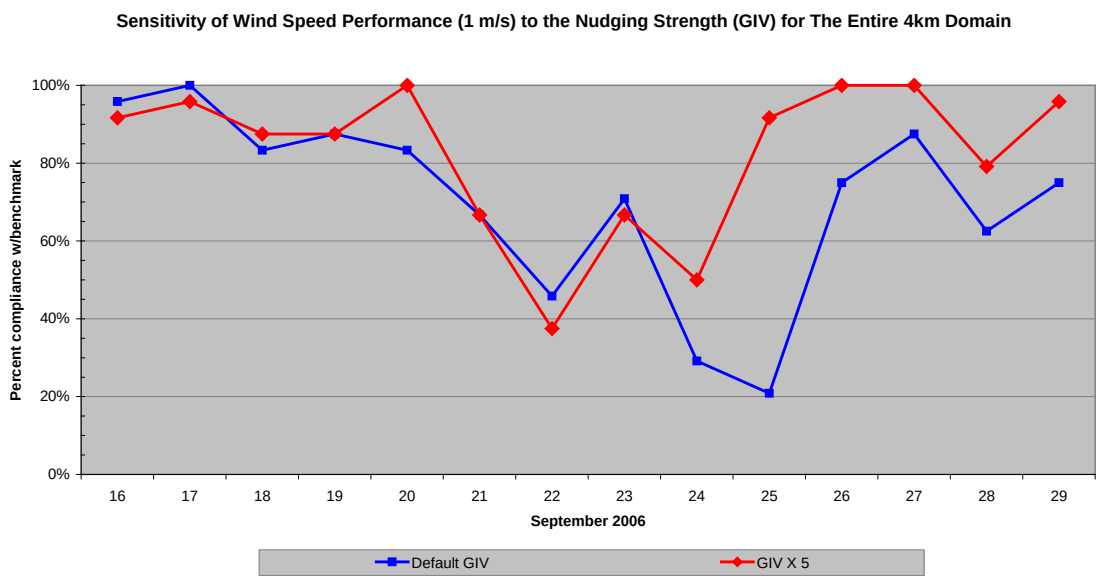

Figure 2.12.3.8-7.b: Performance plot for the wind speed using the default GIV (0.0004) and the 5 times the standard observation-nudging coefficient of (5x0.0004=0.002) for the entire 4 km domain

Figure 2.12.3.8-8.a: *Performance plot for the wind direction using the default GIV (0.0004) and the 5 times the standard observation-nudging coefficient of (5x0.0004=0.002) for the Houston (R12)* shows that the performance of the wind direction also improved or stayed the same on all days except September 27, which was a high ozone day, and Figure 2.12.3.8-8.b: *Performance plot for the wind direction using the default GIV (0.0004) and the 5 times the standard observation-nudging coefficient of (5x0.0004=0.002) for the entire 4 km domain* shows the performance of the wind speed and wind direction for the entire 4 km domain.

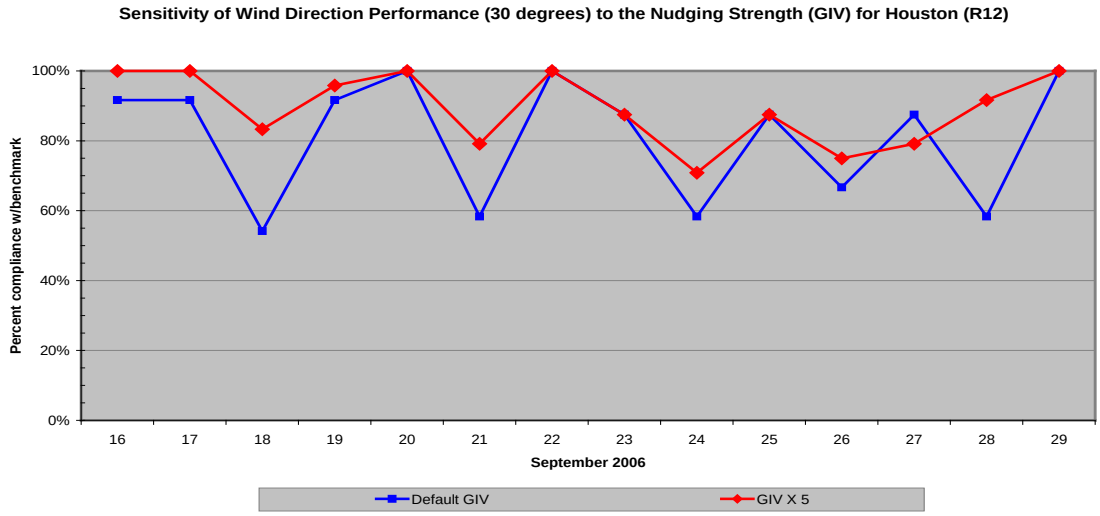

Figure 2.12.3.8-8.a: Performance plot for the wind direction using the default GIV (0.0004) and the 5 times the standard observation-nudging coefficient of (5x0.0004=0.002) for the Houston (R12)

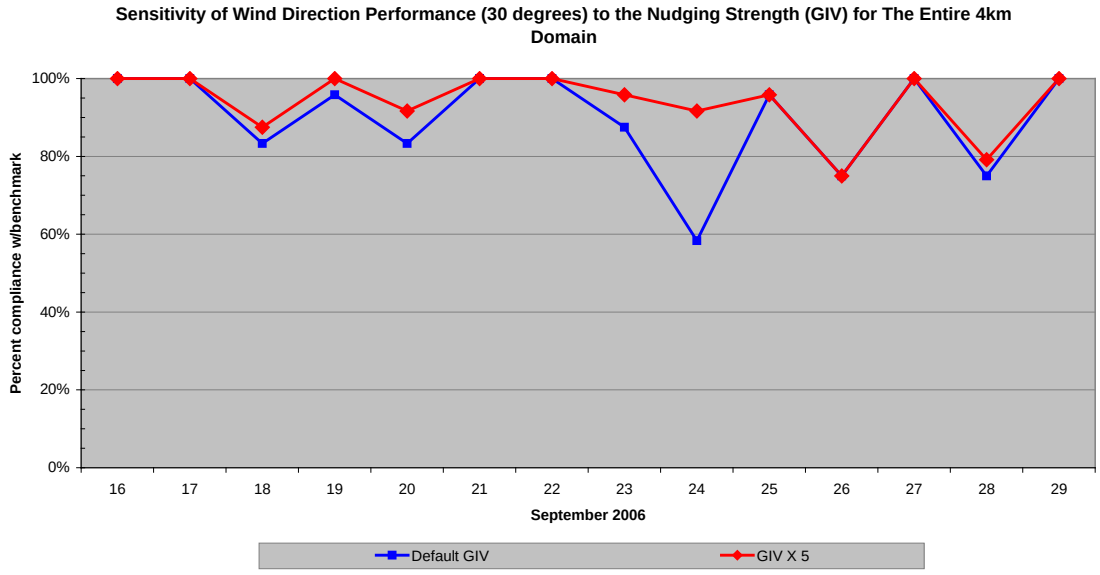

Figure 2.12.3.8-8.b: Performance plot for the wind direction using the default GIV (0.0004) and the 5 times the standard observation-nudging coefficient of (5x0.0004=0.002) for the entire 4 km domain

Forward Trajectories

The differences between the forward trajectories using the MM5 model runs with Grell and the model runs with Grell and surface nudging were evaluated. The standard trajectory plots show 12-hour-forward trajectories plotted for 19 sites using Grell (in blue) with the corresponding 19 trajectories from the cams surface observation in red. The corresponding 19 trajectories with

Grell and surface nudging can be overlaid in green. The 12-hour-forward trajectories can be displayed starting at any hour of the day.

The geographic coordinates for each trajectory at five minute intervals are available in files as either latitude and longitude, or as LCP (distance in km) in the north-south and east-west directions. For the trajectory analysis, three days with high ozone from 2005ep0, two days with high ozone from 2005ep1, and two days with high ozone from 2005ep2 were selected using the LCP data file. For each of the seven days selected, the 12-hour-forward trajectory starting at 6 am were used for both the MM5 Grell and the MM5 Grell with surface nudging. At each 5 minute interval an error was calculated, which is the distance from that point for a given station to the corresponding point for the same station in the trajectory generated using the observed data. The error divergence was determined as the averaged error for every 5 minutes for 19 stations for both the Grell and the Grell with surface nudging The following figures provide a summary of the results for the seven days selected:

For Figure 2.12.3.8-9*: 12 hour forward trajectories at 19 stations starting at 6 am on May 21, 2005. Error divergence (top) and trajectories (bottom).*the error divergence with Grell and surface nudging is less than with Grell only. Note that both modeled trajectories divergence significantly after four hours.

For Figure 2.12.3.8-10: *12 hour forward trajectories at 19 stations starting at 6 am on May 27, 2005. Error divergence (top) and trajectories (bottom)* the error divergence with Grell and surface nudging is less than with Grell only. Note that both model runs have comparable wind speeds (similar trajectory lengths), but there is more clockwise rotation with surface data added.

For Figure 2.12.3.8-11*: 12 hour forward trajectories at 19 stations starting at 6 am on June 2, 2005. Error divergence (top) and trajectories (bottom*) the error divergence for both model runs is virtually identical.

For Figure 2.12.3.8-12: *12 hour forward trajectories at 19 stations starting at 6 am on June 21, 2005. Error divergence (top) and trajectories (bottom),* Surface nudging does not have a significant improvement for either accumulated error or trajectories.

For Figure 2.12.3.8-13: *12 hour forward trajectories at 19 stations starting at 6 am on June 22, 2005. Error divergence (top) and trajectories (bottom).* Surface nudging does not have a significant improvement for either accumulated error or trajectories.

For Figure 2.12.3.8-14: *12 hour forward trajectories at 19 stations starting at 6 am on August 1, 2005. Error divergence (top) and trajectories (bottom).* the error divergence for both model runs is virtually identical.

For Figure 2.12.3.8-15: *12 hour forward trajectories at 19 stations starting at 6 am on August 2, 2005. Error divergence (top) and trajectories (bottom).* Surface nudging does not have a significant improvement for either accumulated error or trajectories.

Thus, for several of the high ozone days, use of surface nudging may produce trajectories which are “closer” to the trajectories based on observational data alone, but on several other days, there is not a significant difference is modeled trajectories.

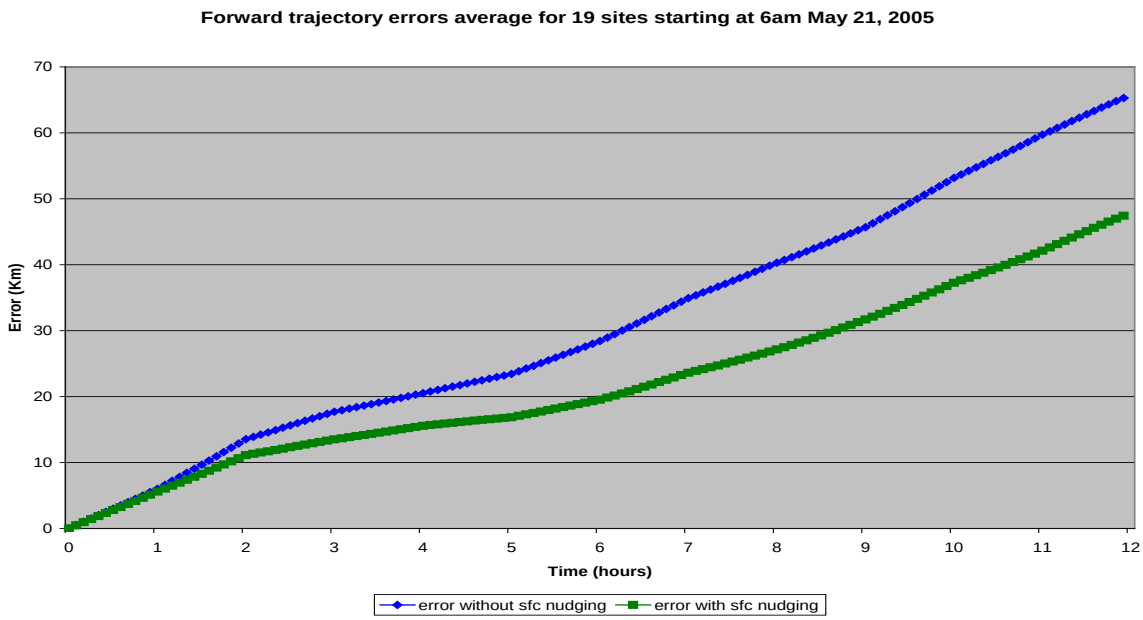

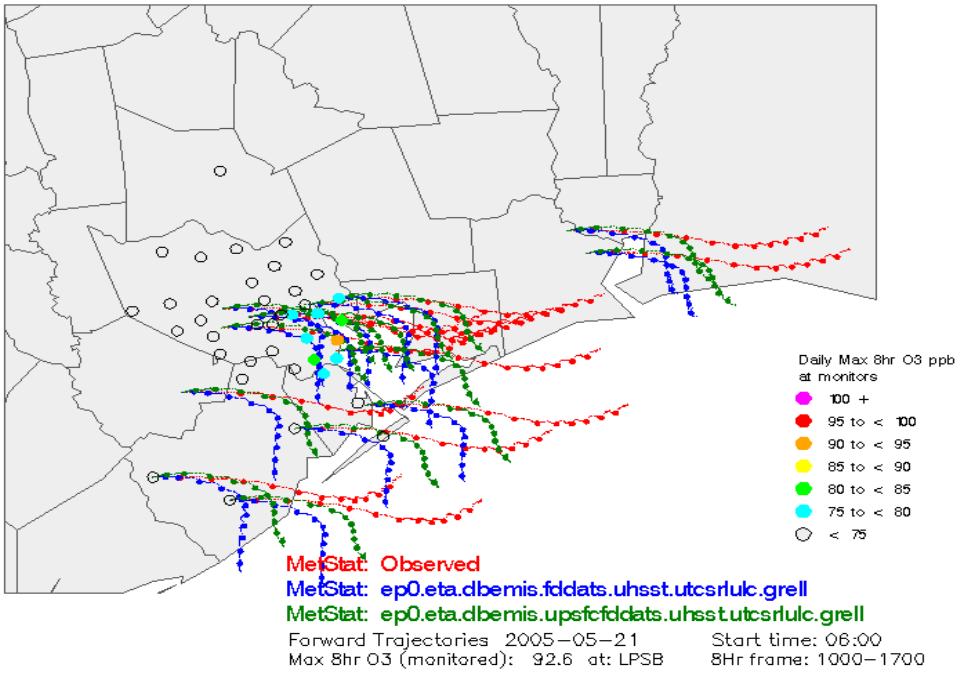

Figure 2.12.3.8-9: 12 hour forward trajectories at 19 stations starting at 6 am on May 21, 2005. Error divergence (top) and trajectories (bottom).

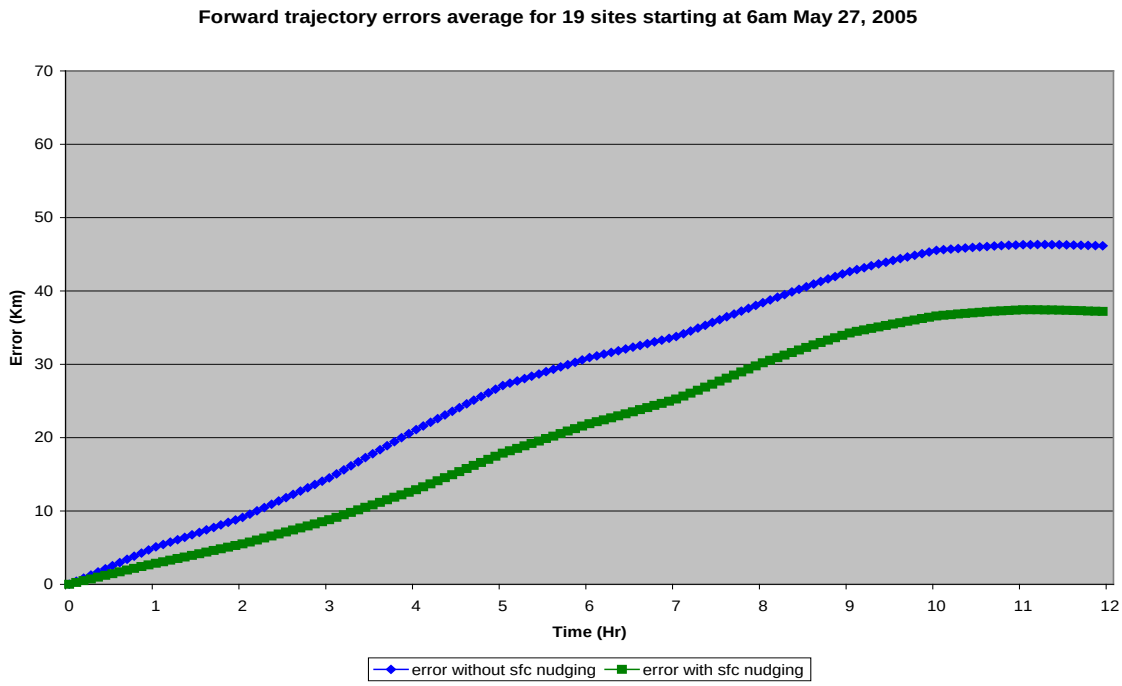

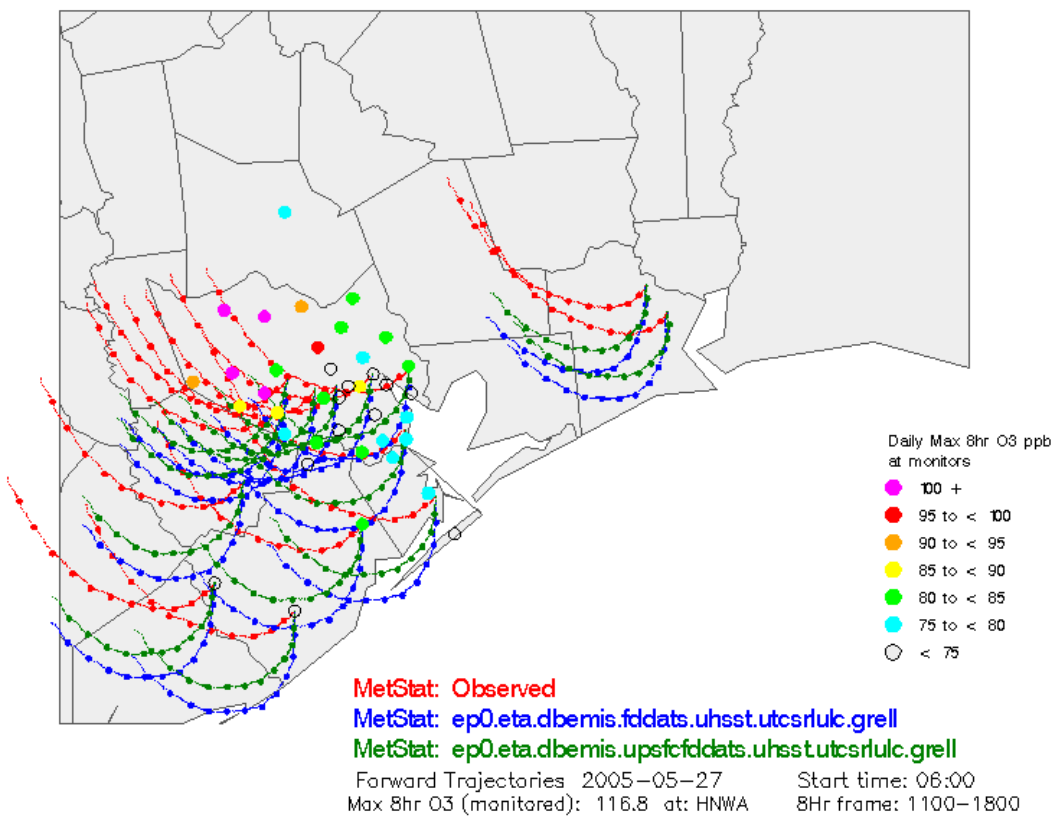

Figure 2.12.3.8-10: 12 hour forward trajectories at 19 stations starting at 6 am on May 27, 2005. Error divergence (top) and trajectories (bottom).

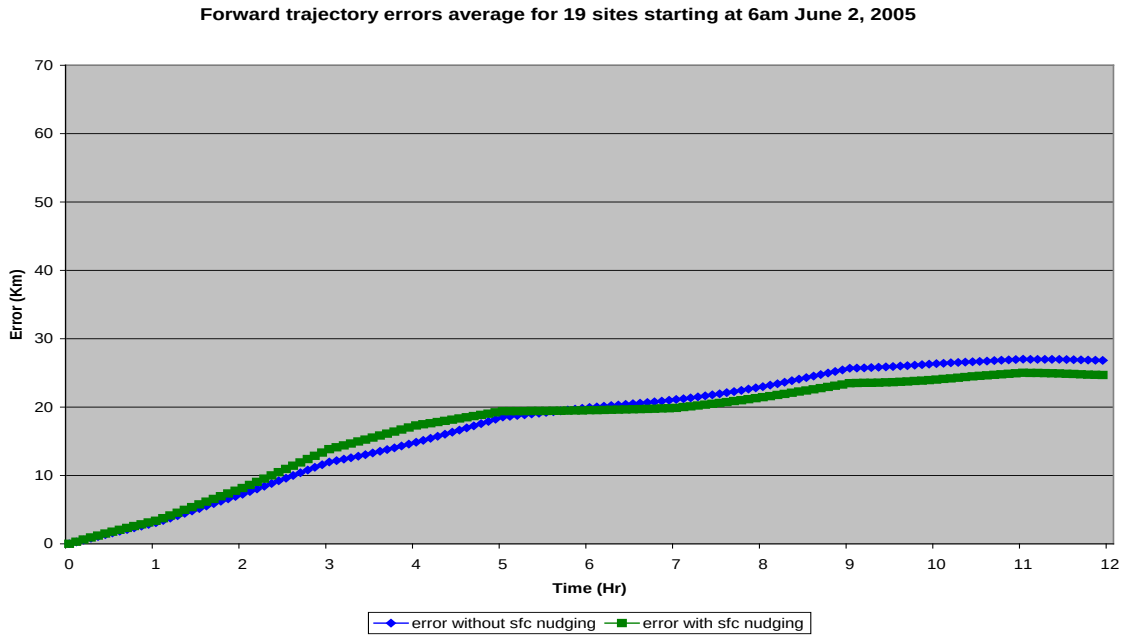

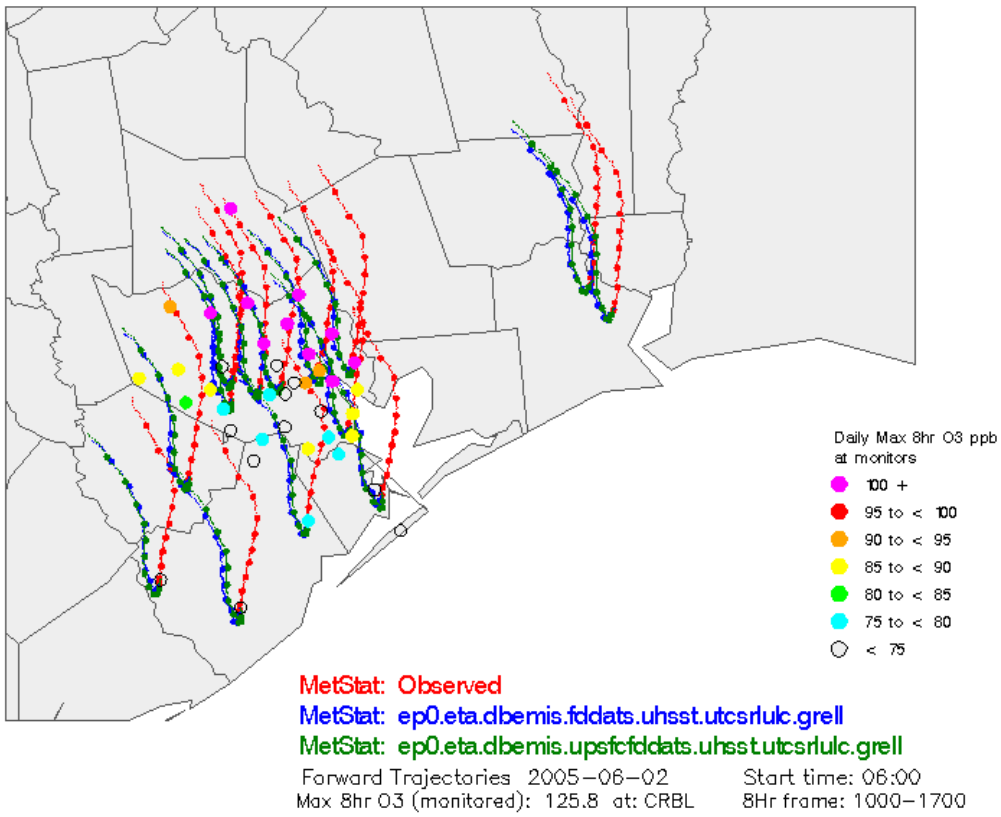

Figure 2.12.3.8-11: 12 hour forward trajectories at 19 stations starting at 6 am on June 2, 2005. Error divergence (top) and trajectories (bottom).

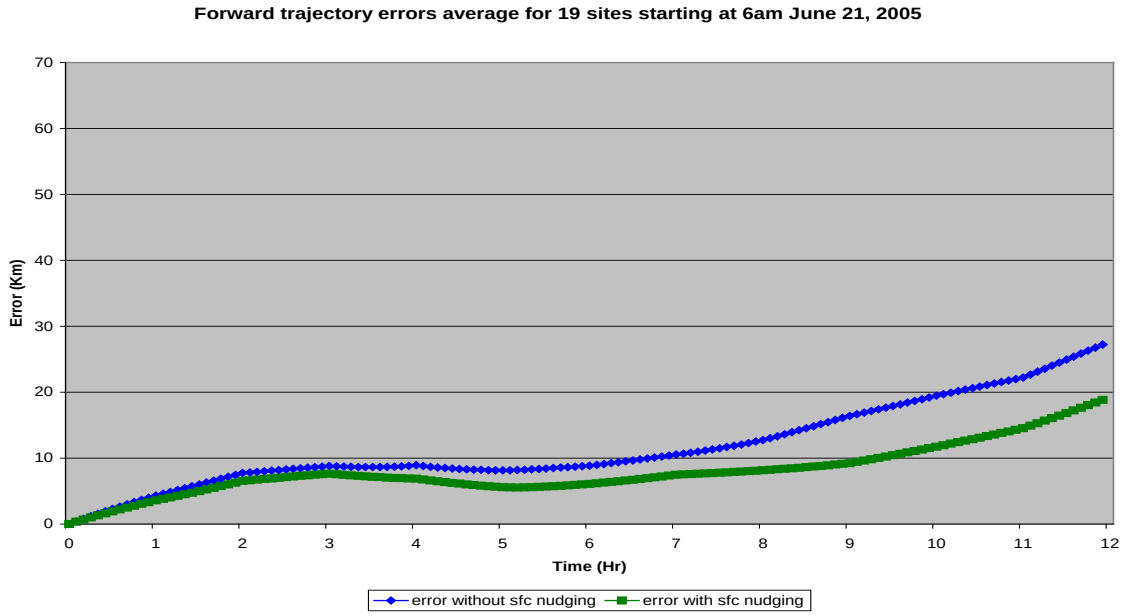

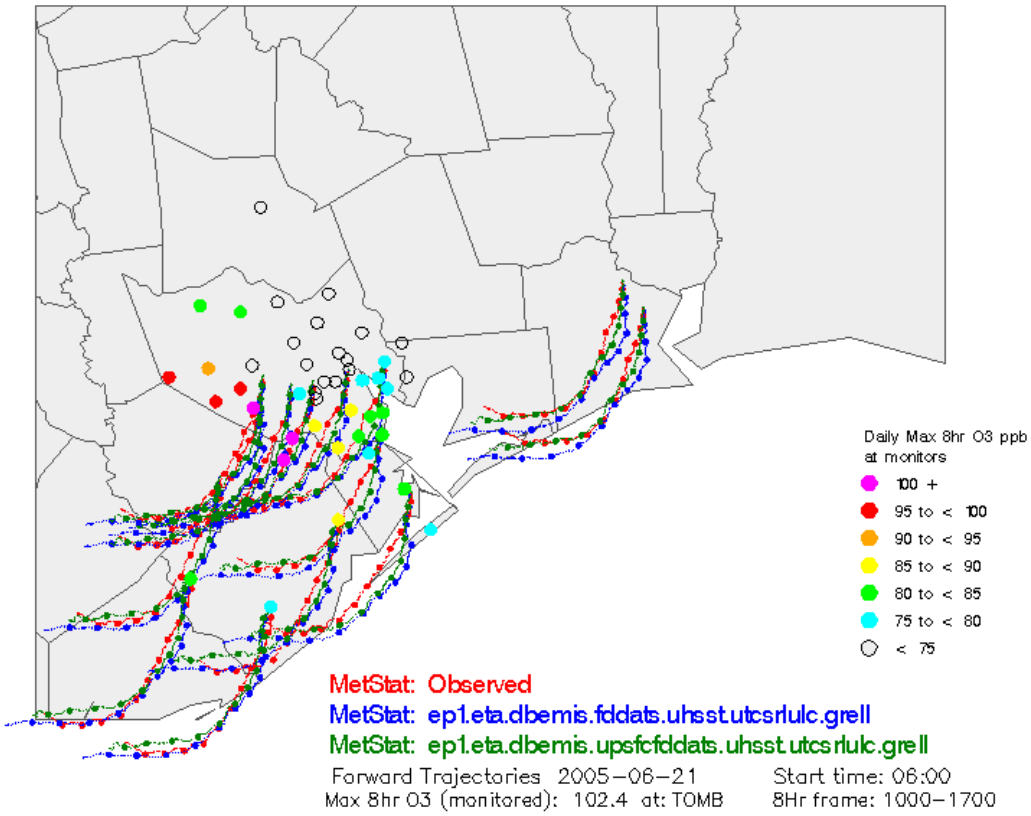

Figure 2.12.3.8-12: 12 hour forward trajectories at 19 stations starting at 6 am on June 21, 2005. Error divergence (top) and trajectories (bottom).

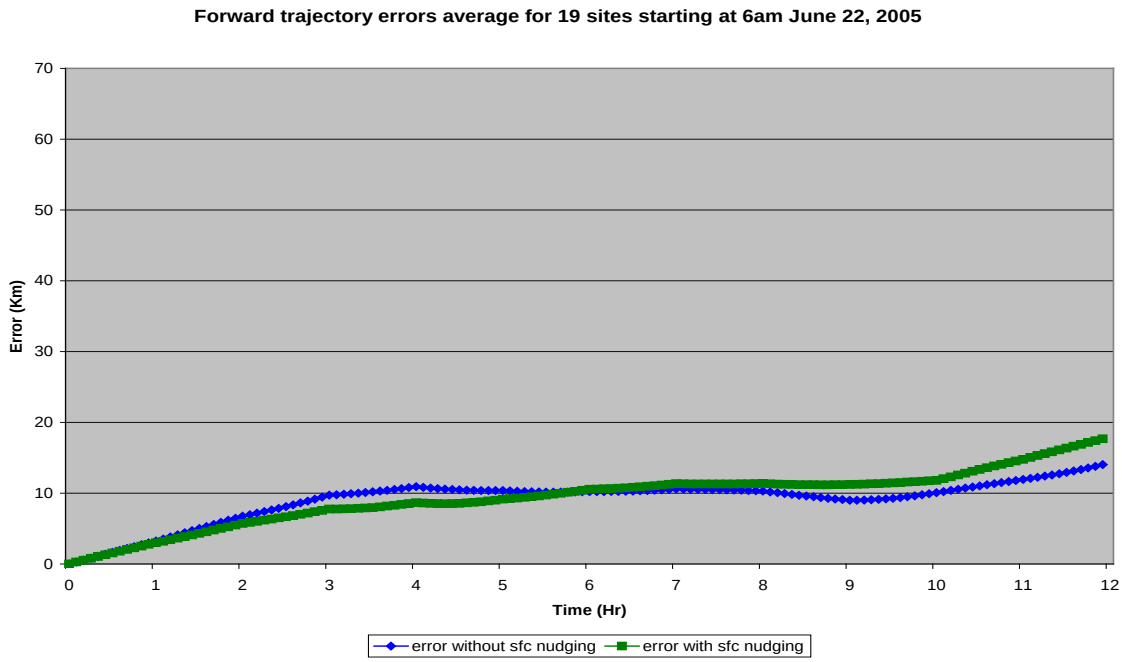

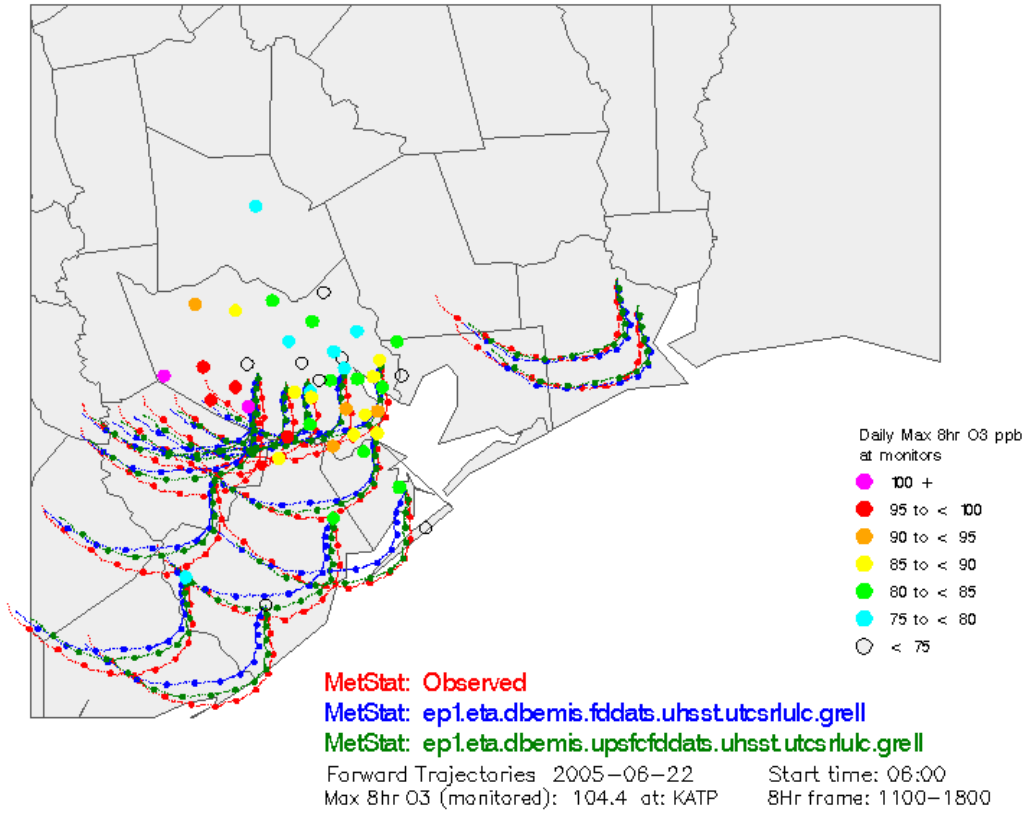

Figure 2.12.3.8-13: 12 hour forward trajectories at 19 stations starting at 6 am on June 22, 2005. Error divergence (top) and trajectories (bottom).

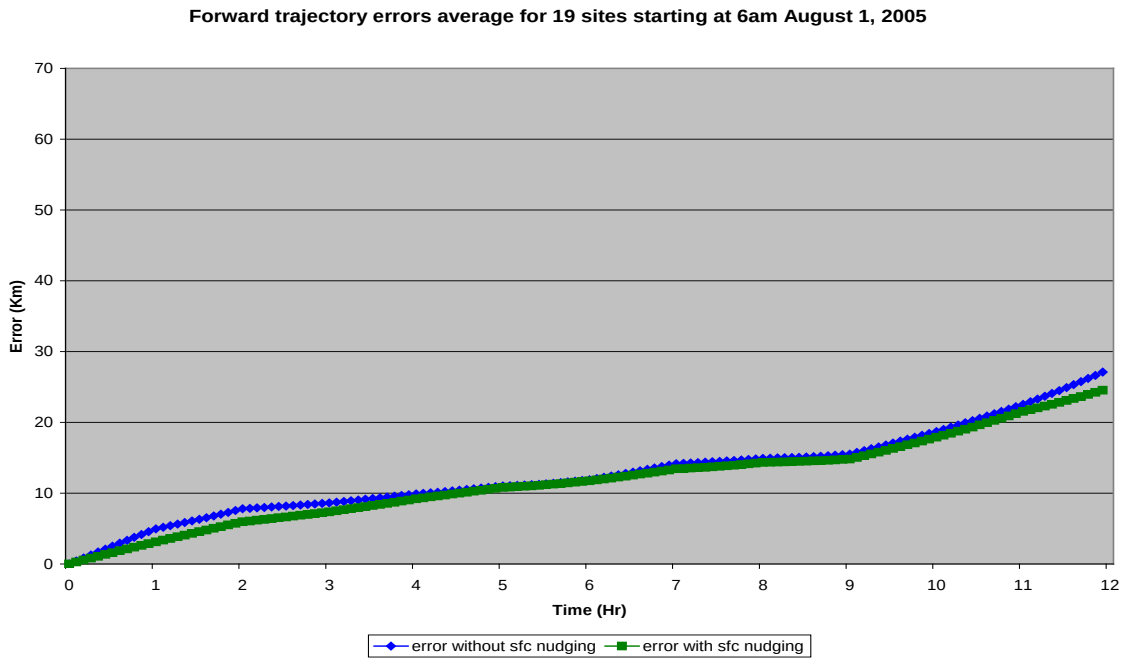

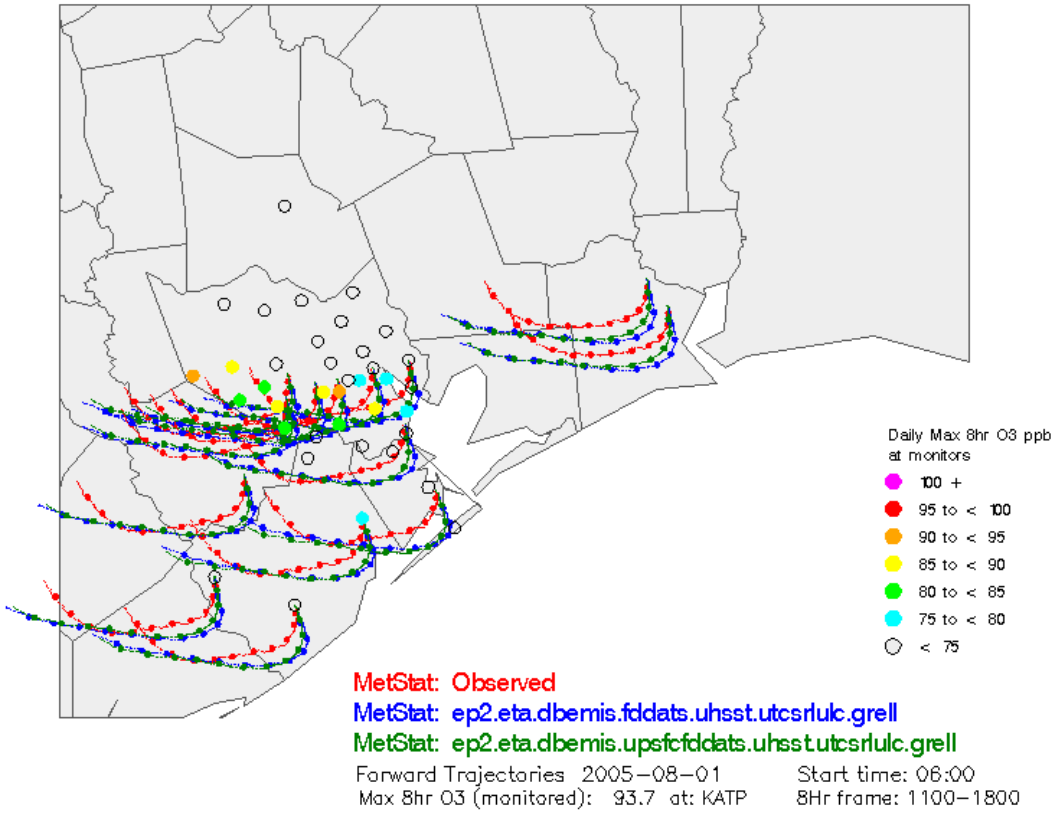

Figure 2.12.3.8-14: 12 hour forward trajectories at 19 stations starting at 6 am on August 1, 2005. Error divergence (top) and trajectories (bottom).

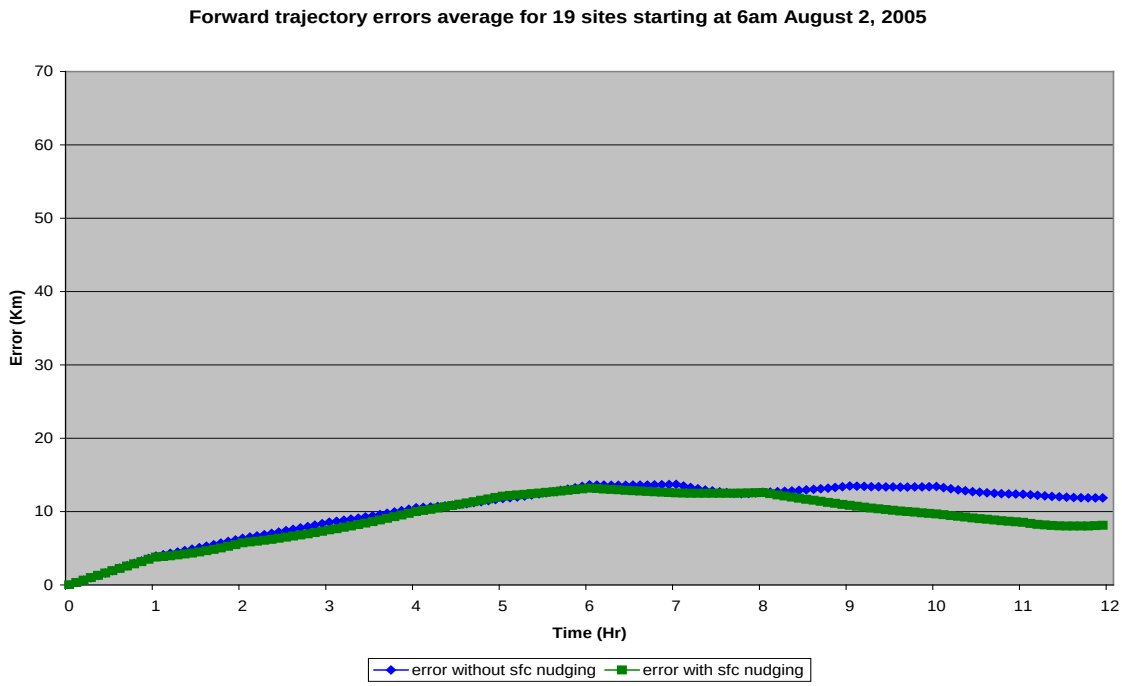

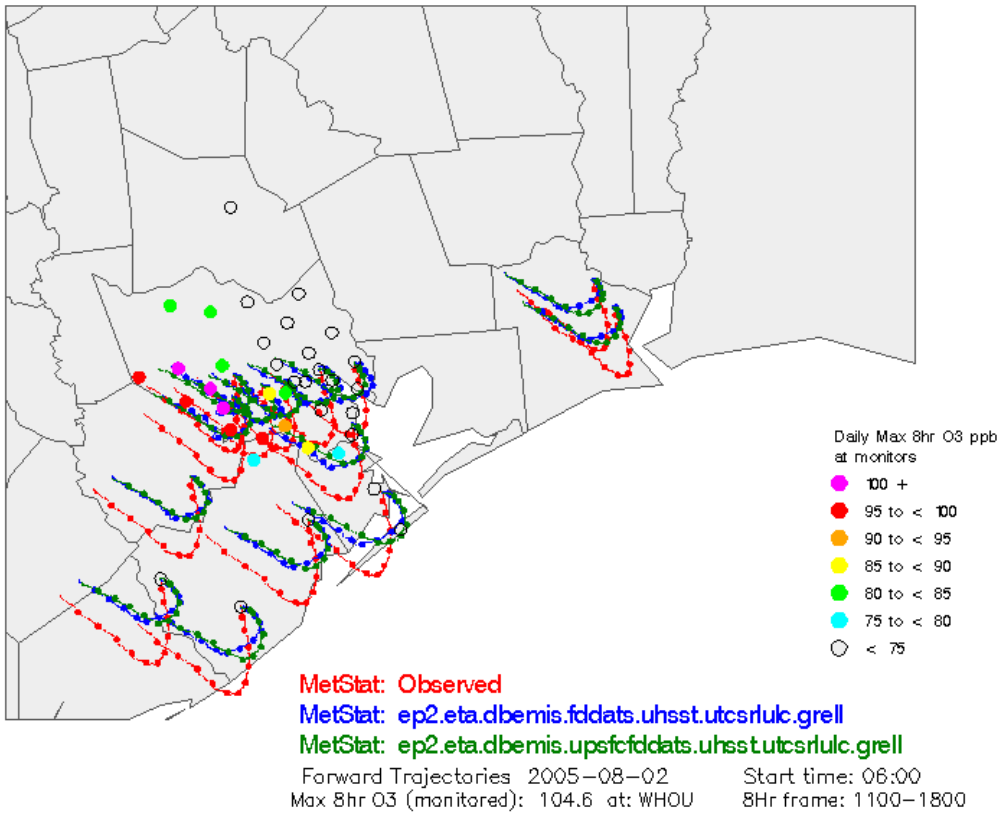

Figure 2.12.3.8-15: 12 hour forward trajectories at 19 stations starting at 6 am on August 2, 2005. Error divergence (top) and trajectories (bottom).

2.12.3.9 References

ATMET (2003), MM5 Simulations for TexAQS 2000 Episode, Final report to the Houston Advanced Research Center and the Texas Commission on Environmental Quality, 12 August 2003.

Byun, D., F. Ngan, X. Li, D. Lee, S. Kim, H. Kim (2008), Evaluation of Retrospective MM5 and CMAQ Simulations of TexAQS-II Period with CAMS Measurements, 2007 TexAQS-II Modeling Project: Final Report to the Texas Commission on Environmental Quality for Grant No. 582-5-64594-FY07-02, University of Houston.

CISL (2009), ds472.0 Home Page, Computational and Information Systems Laboratory Research Data Archive, http://dss.ucar.edu/datasets/ds472.0/, Last accessed March 26, 2009.

EPA (2007), Guidance on the Use of Models and Other Analyses for Demonstrating Attainment of Air Quality Goals for Ozone, PM2.5, and Regional Haze, http://www.epa.gov/scram001/guidance/guide/final-03-pm-rh-guidance.pdf, EPA -454/B-07-002, 162, Last accessed March 26, 2009.

Jia, Y., R. Morris (2003), Meteorological Modeling of the August 1999 Episode to Support the 8-Hour Ozone Early Action Compacts for Tulsa and Oklahoma City, Draft Final Report to the Oklahoma Department of Environmental Quality, ENVIRON International Corporation, Novato, CA.

Knoderer, C. A., C. P. MacDonald (2007), TexAQS II radar wind profiler, radio acoustic sounding system, sodar and lidar data quality control and mixing height derivation, final report by Sonoma Technology, Inc. to Texas A&M University for Texas Commission on Environmental Quality Grant Activity No. 582-5-64593-FY07-20.

NCAR (2005), Chapter 13: I/O FORMAT, PSU/NCAR Mesoscale Modeling System Tutorial Class Notes and User's Guide, http://www.mmm.ucar.edu/mm5/documents/MM5_tut_Web_notes/IO/io.htm, Last accessed March 26, 2009.

Nielsen-Gammon, J. W. (2002), Meteorological Modeling for the August 2000 Houston-Galveston Ozone Episode: PBL Characteristics, Nudging Procedure, and Performance Evaluation, Report to the Technical Analysis Division of the Texas Natural Resource Conservation Commission, Texas A&M University.

Nielsen-Gammon, J. W., R. T. McNider, W. M. Angevine, A. B. White, and K. Knupp (2007), Mesoscale model performance with assimilation of wind profiler data: Sensitivity to assimilation parameters and network configuration, J. Geophys. Res., 112, D09119, doi:10.1029/2006JD007633.

Nielsen-Gammon, J. (2008), Analysis of TexAQS II Meteorological Data, Final Report to the Texas Commission on Environmental Quality for Grant Activity No. 582-5-64593-FY07-20, Texas A&M University.

Nielsen-Gammon, J. (2008b), Model Configuration and Performance with Wind Profiler Nudging, A report to the Texas Commission on Environmental Quality for Grant Activity No. 582-5-64593-FY07-20.

Otte, T. L., 2008a: The impact of nudging in the meteorological model for retrospective air quality simulations. Part I: Evaluation against national observation networks. *Journal of Applied Meteorology and Climatology*, 47, 1853-1867.

Otte, T. L., 2008b: The impact of nudging in the meteorological model for retrospective air quality simulations. Part II: Evaluating collocated meteorological and air quality observations. *Journal of Applied Meteorology and Climatology*, 47, 1868-1887.

Petre, J. (2006), Post to MM5-Users listserv, http://mailman.ucar.edu/pipermail/mm5-users/2006/001040.html, Last accessed March 26, 2009.

Rogers, E., T. L. Black, D. G. Deaven, G. J. DiMego, Q. Zhao, M. Baldwin, N. W. Junker and Y. Lin (1996), Changes to the operational ``Early" Eta analysis/forecast system at the National Centers for Environmental Prediction. Wea. Forecasting, 11, 391-413.

Rogers, E., D. Deaven and G. J. DiMego (1995), The regional analysis system for the operational "early" Eta model: original 80-km configuration and recent changes. Wea. Forecasting, 10, 810-825.

Stauffer, D. R., and N. L. Seaman (1990), Use of four-dimensional data assimilation in a limited area mesoscale model. Part I: Experiments with synoptic-scale data, Mon. Wea. Rev., 118, 1250–1277.

Stauffer, D. R., and N. L. Seaman (1994), Multiscale four-dimensional data assimilation, J. Appl. Meteor., 33, 416–434.

Stauffer, D. R., N. L. Seaman, and F. S. Binkowski (1991), Use of four-dimensional data assimilation in a limited area mesoscale model. Part II: Effects of data assimilation within the planetary boundary layer, Mon. Wea. Rev., 119, 734–754.

ATTACHMENT 4

Application of Grell Cumulus Scheme
Houston-Galveston-Brazoria Attainment Demonstration SIP Revision

2.12.4 Application of Grell Cumulus Scheme

2.12.4.1 Introduction

Central to the development of precipitation forecasts is a correct determination of the effects of clouds. The first predictive meteorological models tracked fronts from which forecasters estimated possible precipitation. Concurrent with the development of mesoscale models (typically representing features from 10 to 100 km), modelers have attempted to account for the physical effects of clouds. In a real atmosphere, convection (clouds) results from physical instabilities which redistributes moisture and heat in such a way as to re-stabilize the atmosphere.

Quite a large set of meteorological literature is devoted to convective parameterizations. In this report, the term "parameterization" refers to a mathematical scheme or algorithm that accounts for a real physical process which cannot be properly resolved at a particular grid scale used for modeling. Since processes such as cloud formation are real, they must be accounted for or else the model will be inaccurate and possibly unstable. On the other hand, "resolution" is not well-defined since a given feature usually is "resolved" across several grid cells. For example, as large air masses move along fronts, widespread lifting can produce stratiform (wide, relatively flat) clouds. For a modeling domain with 20 km grid cells, this type of cloud may be resolved, but cumulus (puffy) clouds which can develop from strong vertical motion will not be resolved without a convective parameterization. However, a series of cumulus clouds might evolve a mesoscale structure. A frontal passage may trigger cumulus convection which leads to more cumulus clouds forming in the wake of the front. These so-called "mesoscale convective complex" (MCC) might be resolved.

Air quality simulations of tropospheric ozone depend in large part on mostly clear episodic days for photochemical reactions; however, even partial cloud cover can strongly impact radiative processes, surface heating and PBL development. More importantly, longer episodes require a better characterization of clouds because an incorrect amount of precipitation can bias soil moisture across several days.

Despite the recognition of cloud importance for air quality modeling, the meteorological literature has understandably focused on validation of convective parameterizations based upon four criteria related directly to precipitation events: first, does precipitation trigger at the right time? Secondly, does the meteorological model predict the correct peak precipitation? Thirdly, does the area extent of precipitation match observations? Finally, does the total precipitation agree with what is observed? Although clouds affect air quality in multiple and pervasive ways, validation is mostly qualitative in nature: do modeled clouds seem to be in approximately the same place as clouds observed in the visible portion of the spectrum by, say, Geostationary Operational Environmental Satellites (GOES).

The next section discusses the general configuration of MM5 at the TCEQ as implemented for the present round of SIP modeling for the Houston-Galveston-Brazoria (HGB) nonattainment area. The original motivation to use a cumulus parameterization on the 4 km grid will also be discussed as well as the current operational rationale. A series of results will follow in section 3 with a discussion of those features which seem relevant for air quality modeling. Section 4 will include a general discussion on why the decision to try a cumulus parameterization on the 4 km MM5 grid might seem reasonable from an air quality modeling perspective, even though TCEQ staff are aware that a convective scheme of any kind at a 4 km grid scale is generally not recommended. The final concluding section will include expected impacts on the subsequent air quality modeling.

2.12.4.2. MM5 Model Configuration for HGB and Motivation for the Grell Cumulus Parameterizaton on the 4 Km Grid.

The preliminary MM5 configuration adopted for all of the TexAQS II episodes is described in Section 2.1 of Appendix A: *Meteorological Modeling for the HGB Attainment Demonstration SIP Revision for the 1997 Eight-Hour Ozone Standard*. In addition to noting that the Grell cumulus scheme was used on the three coarse grids (108 km/36 km/12 km) on all runs described here, it is also important to note that 2-way nesting was used on the three coarse grids. The 4 km MM5 grid is run as a one-way nest; i.e., the output from the 12 km grid was run through the NESTDOWN program to extract the initial and boundary conditions for the 4 km MM5 run.

The motivation for applying the Grell cumulus parameterization on the MM5 4 km grid came as the result of a suggestion by the State Climatologist, Dr. John Nielsen-Gammon, to test whether the areal extent and timing of predicted cloud cover might be improved on particular episode days. The episode days of concern were those for which the photochemical model (CAMx) did not adequately replicate the observed ozone and for which the cloud coverage was poorly predicted.

Figure 2.12.4.2-1: *Lower left graphic is MM5CAMx output for cloud optical depth at 12 pm CST on August 2, 2005 using Grell cumulus parameterization on the 4 km domain* shows an example of the type of graphical analysis used by TCEQ staff to examine predicted cloud coverage. The graphic of modeled cloud optical depth (left side) overlays a GOES image of the visible spectrum showing *cloud fraction*. The red outline in the GOES image corresponds to the MM5CAMx graphic.

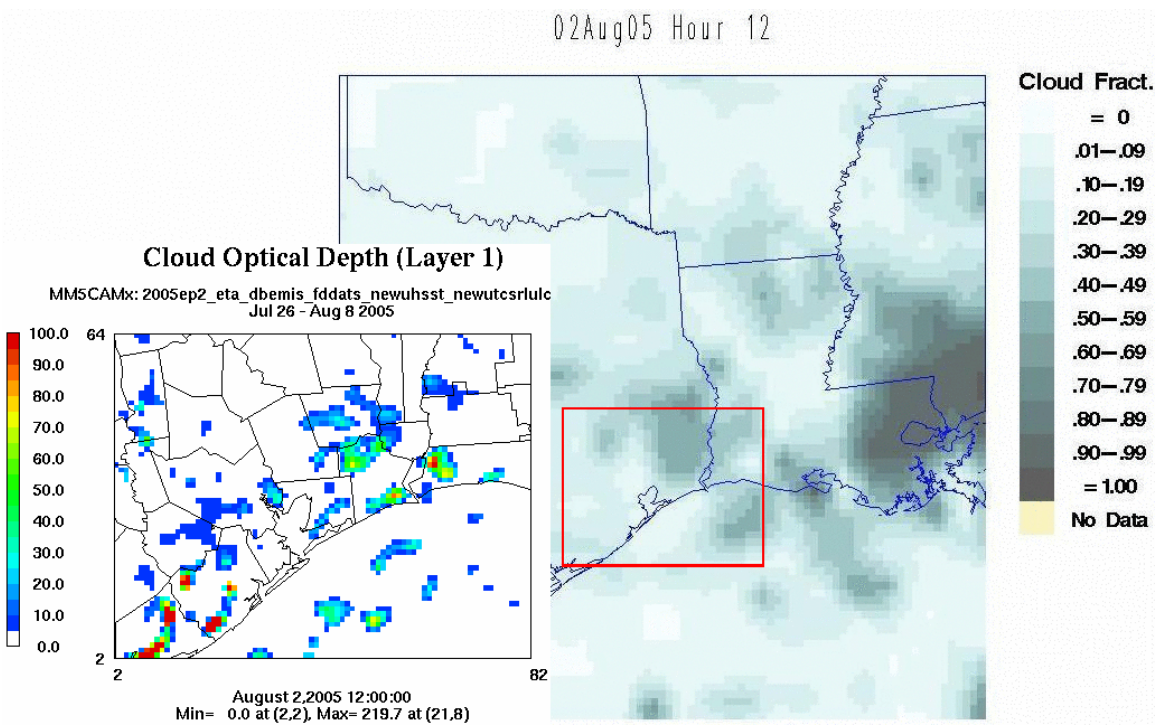

Figure 2.12.4.2-1: Lower left graphic is MM5CAMx output for *cloud optical depth* at 12 pm CST on August 2, 2005 using Grell cumulus parameterization on the 4 km domain; (Cloud optical depth calculated from MM5 output using Grell)

Figure 2.12.4.2-2: *Lower left graphic is MM5CAMx output for cloud optical depth at 12 pm CST on August 2, 2005 without using Grell cumulus parameterization applied in the 4 km domain* shows the same input MM5 configuration except without Grell cumulus on the 4 km grid. Troubling comparisons between modeled cloud optical depth and GOES cloud fraction, as depicted in this figure, were the motivation, as indicated above, for investigating the addition of a convective parameterization on the 4 km grid. Clearly, the application of the Grell cumulus has an impact on the CAMx input field, and furthermore, the CAMx input field shown in Figure 2.12.4.2-1 seems to compare more favorably with the GOES cloud fraction. (Note: August 2, 2005 is presented as an example because it is a peak ozone day during the July-August 2005 episode.) What is perhaps counter-intuitive is that the addition of Grell on the 4 km grid seems to have reduced the role of clouds. However, the application of the Grell parameterization affects the simulation other meteorological variables, which can play a role in whether or not clouds are simulated. An additional discussion about our understanding of how the Grell parameterization affects other variable is presented in the next section.

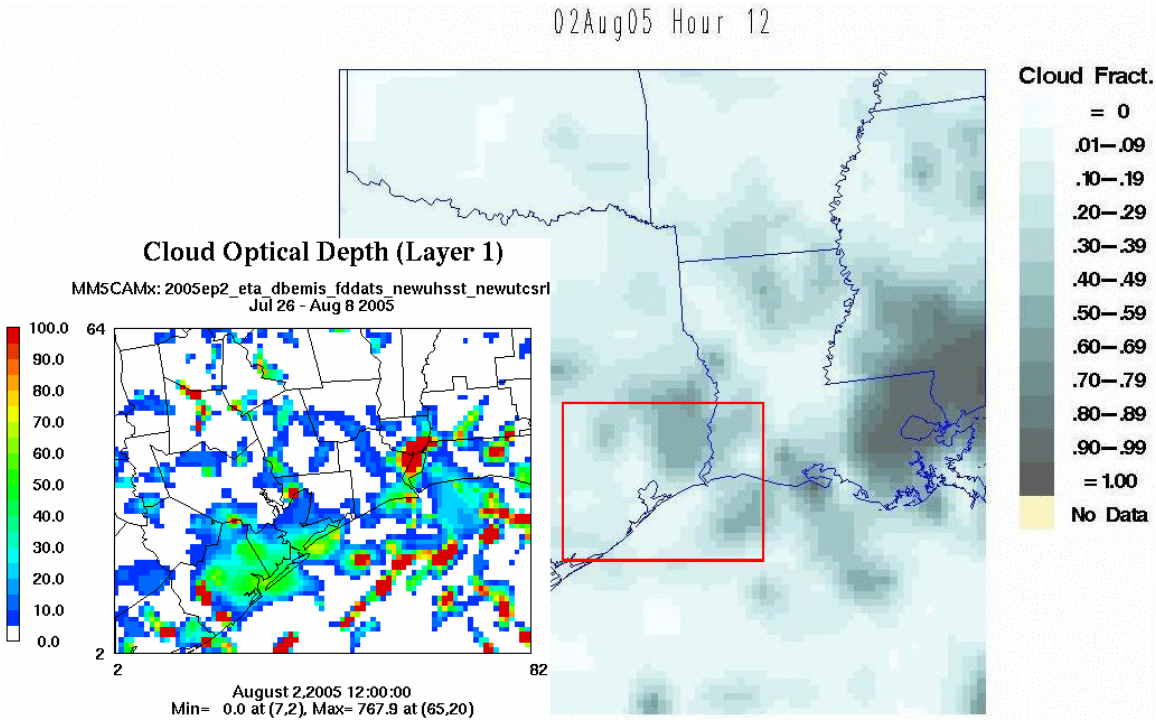

Figure 2.12.4-2: Lower left graphic is MM5CAMx output for *cloud optical depth* at 12 pm CST on August 2, 2005 without using Grell cumulus parameterization applied in the 4 km domain

An examination of many such graphics comparing modeled and observed cloud coverage for days modeled during the May-June 2005 episode, the June 2005 episode, and the reminder of the July-August 2005 episode led TCEQ staff to conclude that using the Grell cumulus parameterization on the 4 km grid does not compromise the meteorological modeling performance in simulating clouds.

2.12.4.3. Operational Rationale for Using Grell Cumulus Parameterization on the 4 km Grid

As indicated, the application of a cumulus parameterization impacts the simulation of other meteorological variables. Therefore it is not only the clouds that are affected. One noticeable feature of adding Grell on the 4 km grid was the smoothing of surface divergences in the wind field. An example of this is shown in Figure 2.12.4.3-1: *Surface Wind Map for June 23, 2005, 2 PM (CST) without Grell* and Figure 2.12.4.3-2: *Surface Wind Map for June 23, 2005, 2 PM (CST) with Grell.* In the first figure the surface winds in the northern half of the domain exhibit divergent features, while the second figure shows these patterns to have been smoothed by the addition of Grell. Since these divergent features are essentially localized and temporary, meteorological modeling performance measures, such as statistics of accuracy in wind speed and direction averaged across all monitors, or graphics of the time series of modeled versus monitored winds over all the days of an episode, do not typically show obvious differences between MM5 modeling with Grell and MM5 modeling without Grell on the 4 km grid, even in an area with a high density of monitors, such as HGB. Therefore, although these features have been noticed by many MM5 modelers, generally they are not considered a source of concern. However, by establishing particular regions of interest, and by focusing on particular episode days, differences in model configuration (i.e., with and without Grell) can be discerned, and differences in performance measures can be distinguished, especially if surface divergent winds coincide with a surface monitor.

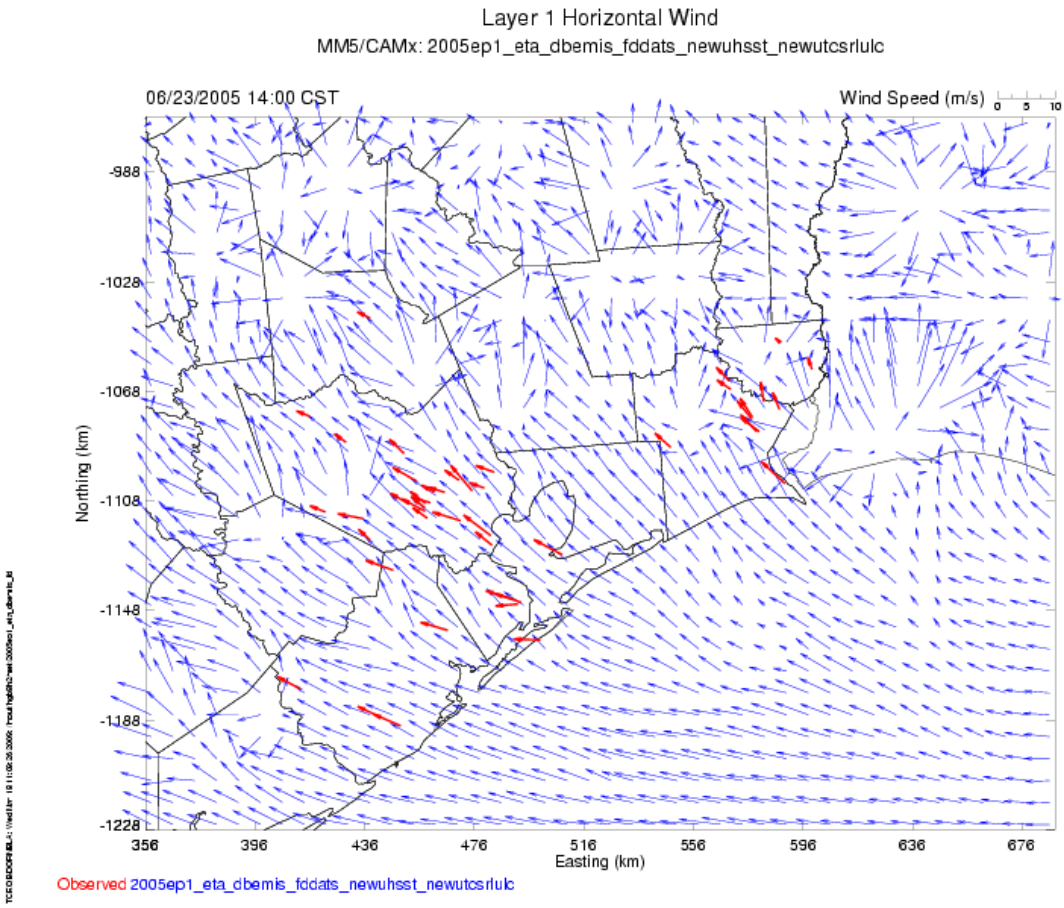

Figure 2.12.4.3-1: Surface Wind Map for June 23, 2005, 2 PM (CST) without Grell (Observations are the red vectors)

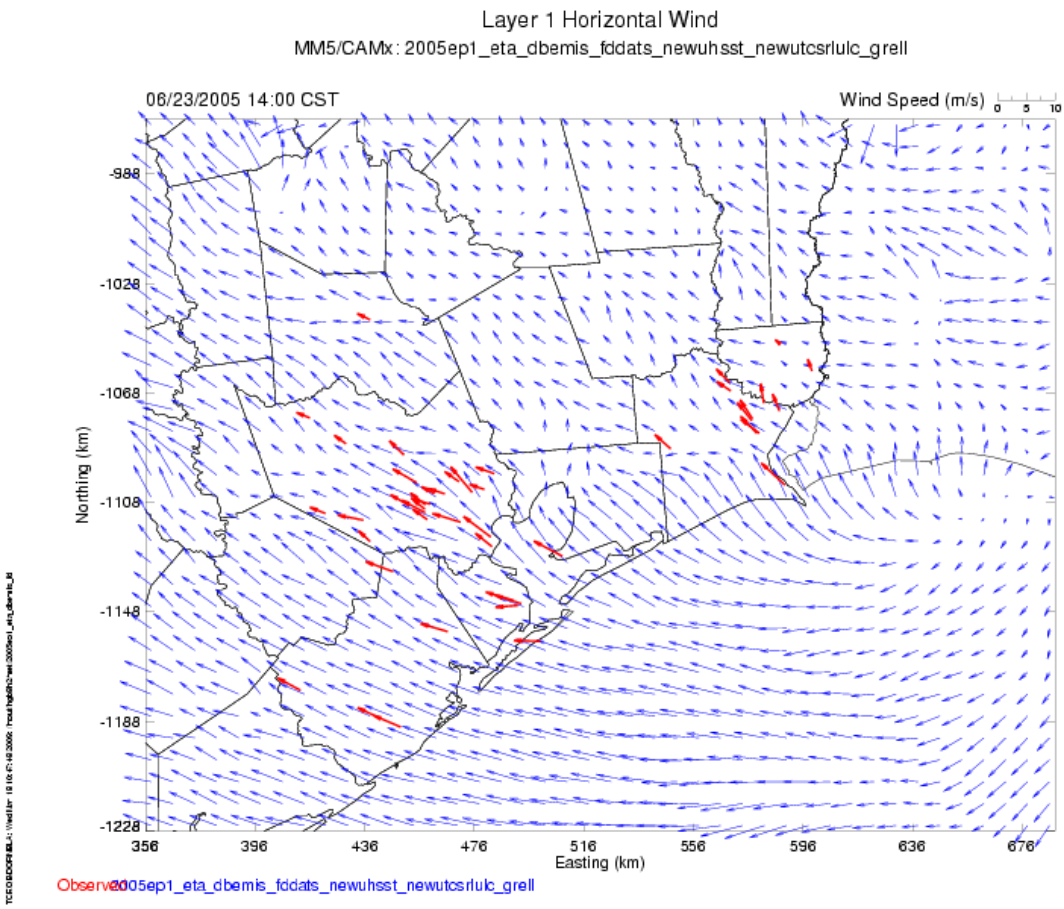

Figure 2.12.4.3-2: Surface Wind Map for June 23, 2005, 2 PM (CST) with Grell (Observations are the red vectors)

Figure 2.12.4.3-3: *Portion of HGB domain with monitors grouped by zones* shows a portion of the HGB domain with monitors grouped by distance from the Gulf of Mexico coastline. Monitors within these groupings (i.e., zones) were grouped and analyzed separately. Zone 1 is closest to the coast and Zone 5 is furthest inland. Table 2.12.4.3-1: *Monitor Site Codes used by the TCEQ* lists the site codes for the monitors in this figure.

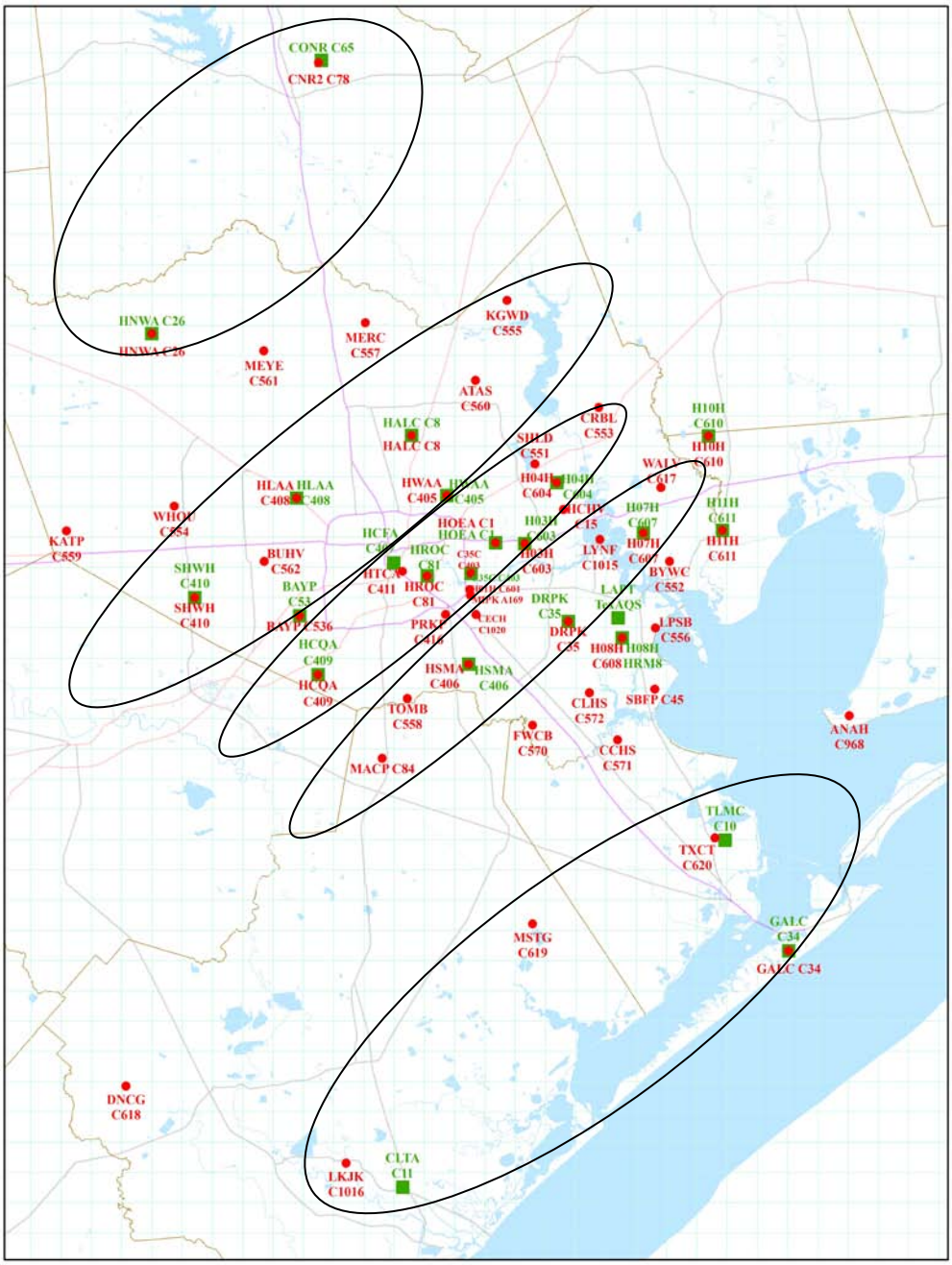

Figure 2.12.4.3-3: Portion of HGB domain with monitors grouped by zones

Table 2.12.4.3-1: Monitor Site Codes used by the TCEQ

Site Code	Selected Site Name
BAYP	Bayland Park, Harris Co., TX
C35C	Clinton, Harris Co., TX
CNR2	Conroe Relocated, Montgomery Co., TX
DRPK	Deer Park, Harris Co., TX
GALC	Galveston, Galveston Co., TX
H03H	HRM-3, Haden Road, Harris Co., TX
H08H	HRM Site 8, La Porte, Harris Co., TX
H10H	HRM-10, Mt Belvieu, Chambers Co., TX
H11H	HRM-11, , Chambers Co., TX
HALC	Aldine, Houston, Harris Co., TX
HCHV	Channelview, Houston, Harris Co., TX
HCQA	Croquet, Houston, Harris Co., TX
HNWA	NW Harris, Tomball, Harris Co., TX
HOEA	Houston East, Houston, Harris Co., TX
HROC	Houston Regional Office, Harris Co., TX
HSMA	Swiss and Monroe,, Harris Co., TX
HTCA	Texas Avenue, Houston, Harris Co., TX
HWAA	North Wayside, Houston, Harris Co., TX
LYNF	Lynchburg Ferry, Harris Co., TX
MACP	Manvel Croix Park, Brazoria Co., TX
MSTG	Mustang Bayou, Brazoria Co., TX
SBFP	Seabrook Friendship Park, Harris Co., TX
SHWH	Westhollow, Houston, Harris Co., TX
TXCT	Texas City, Galveston Co., TX
WALV	Wallisville Road, Harris Co., TX
CLTA	Clute C11

Zone 1 (Coastal) is represented by the following sites: Clute C11 (CLTA), Mustang Bayou C619 (MSTG) and Galveston Airport C34 (GALC);
Zone 2 (Ship Channel) is represented by the following sites: Manvel Croix Park C84 (MACP), Houston Deer Park C35 (DRPK) and Wallisville Road C617 (WALV);
Zone 3 (Southeast Core) is represented by the following sites: Croquet C409 (HCQA), the Houston Regional Office C81 (HROC), HRM3 Haden Road (H03H) and Channelview C15 (HCHV);
Zone 4 (Northwest Core) is represented by the following sites: Houston Westhollow C410 (SHWH), Houston Aldine C8 HALC), and Houston Bayland Park C53 (BAYP); and
Zone 5 (Downwind) is represented by the following sites: Northwest Harris County C26 (HNWA) and the relocated Conroe monitor C78 (CNR2).

For the various episodes, performance measure differences between the model configurations focused on those days with high and wide-spread maximum daily eight-hour ozone concentrations. The performance measure used was a metric related to the accuracy of the modeled surface winds. In particular, MM5 modeled wind speed and direction were compared to

surface observations from the monitors in the above zones for the selected episode days. Figure 2.12.4.3-4: *Percent of averaged hourly wind speeds < 1 m/s by zone on June 2. 2005*, Figure 2.12.4.3-6: *Percent of averaged hourly wind speeds < 1 m/s by zone on June 21, 2005*, Figure 2.12.4.3-8: *Percent of averaged hourly wind speeds < 1 m/s by zone on August 2, 2005*, and Figure 2.12.4.3-10: *Percent of averaged hourly wind speeds < 1 m/s by zone on June 8, 2006* show bar charts by zone of the fraction of averaged hourly modeled versus observed wind speed differences less than 1.0 m/s. MM5 modelers have typically used a wind speed metric with a threshold of 2.0 m/s. However, since the overall MM5 modeling was fairly good, a tighter threshold was warranted for this evaluation. Figure 2.12.4.3-5: *Percent of averaged hourly wind directions < 30 degrees by zone on June 2, 2005*, Figure 2.12.4.3-7: *Percent of averaged hourly wind directions < 30 degrees by zone on June 21, 2005*, Figure 2.12.4.3-9: *Percent of averaged hourly wind directions < 30 degrees by zone on August 2, 2005*, and Figure 2.12.4.3-11: *Percent of averaged hourly wind directions < 30 degrees by zone on June 8, 2006*, show bar charts by zone of the fraction of hourly averaged modeled versus observed wind directions with differences less than 30 degrees. The bars in these figures are paired and color coded so that MM5 configured without Grell (colored blue) are set to the left and the corresponding MM5 configured with Grell (colored maroon) are plotted to the right.

The differences in the accuracy, as determined by these metrics, of the modeled wind speed and direction between the configurations (i.e., with and without Grell) varies by episode day and by zone. For the majority of episode days and monitoring zones considered, the Grell configuration improved wind speed accuracy although the wind direction accuracy was degraded. Of the selected episode days in these four sets of figures, June 2 has poorest over all wind speed and direction accuracy with the Grell configuration and August 2 has the best over all wind speed and direction accuracy.

With the consideration that these modeled surface winds are input to an air quality model, the wind speed has more of an influence (e.g., transport and dispersion) than the wind direction. In addition, wind direction measurements often have large error especially at low wind speeds. This led the TCEQ staff to conclude that using the Grell configuration does not compromise the meteorological modeling performance.

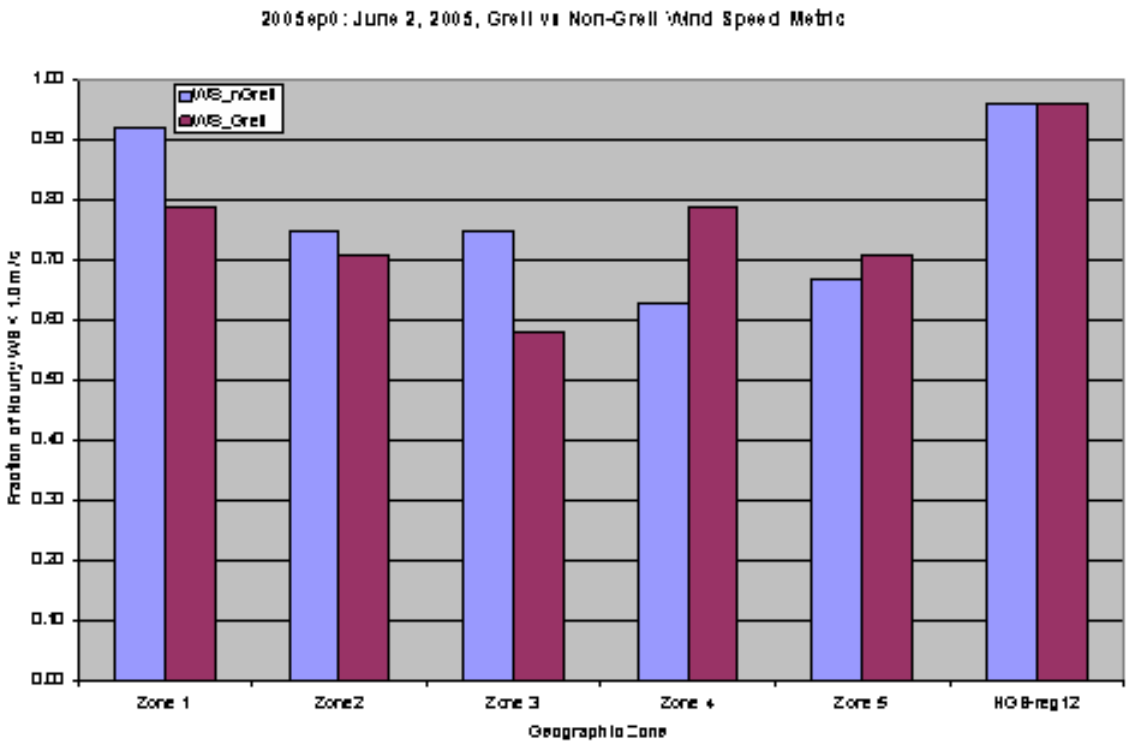

Figure 2.12.4.3-4: Percent of averaged hourly wind speeds < 1 m/s by zone on June 2. 2005

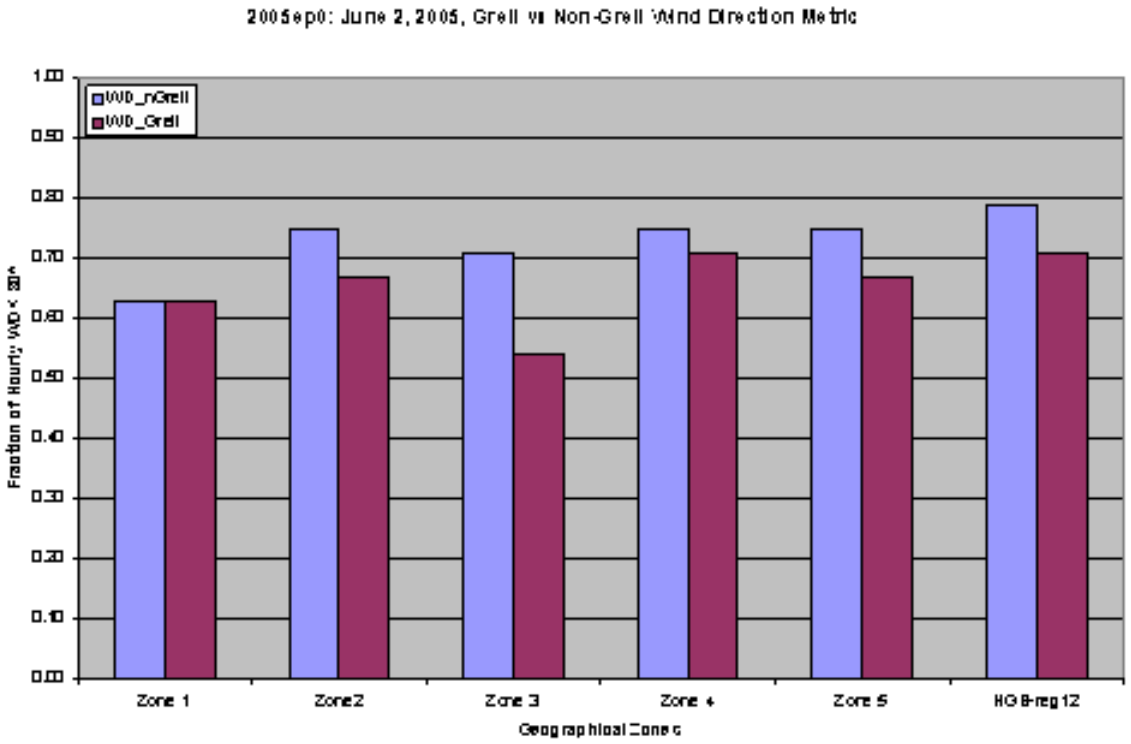

Figure 2.12.4.3-5: Percent of averaged hourly wind directions < 30 degrees by zone on June 2, 2005

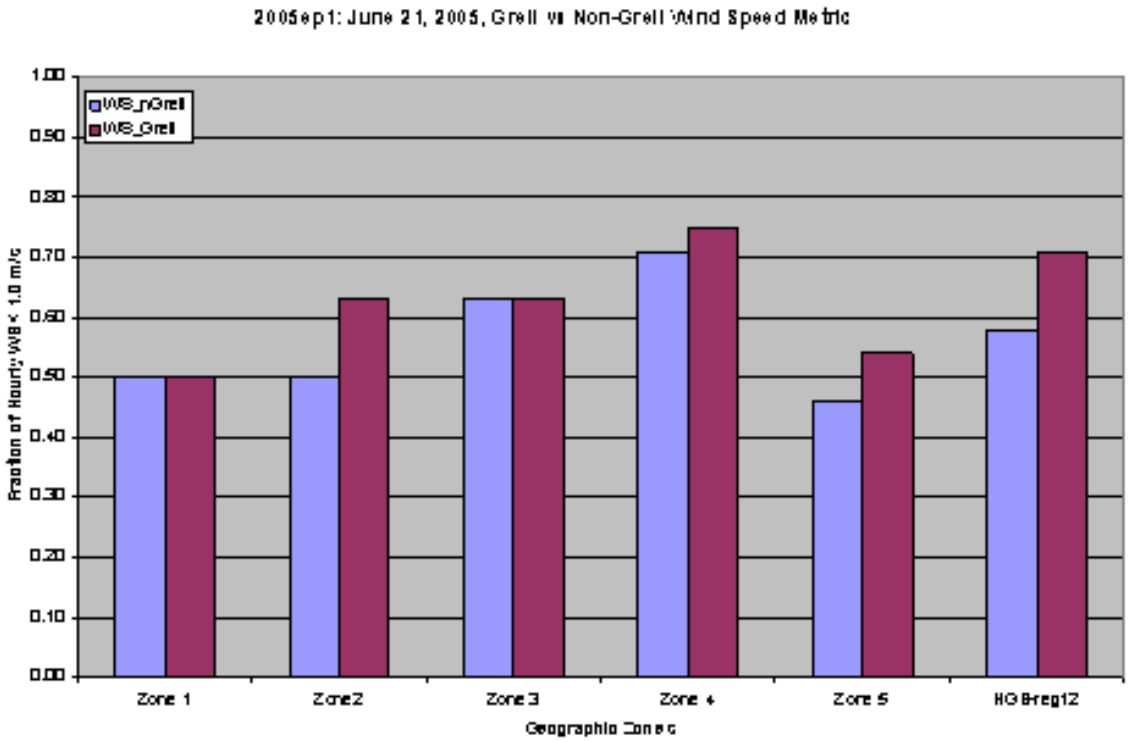

Figure 2.12.4.3-6: Percent of averaged hourly wind speeds < 1 m/s by zone on June 21, 2005

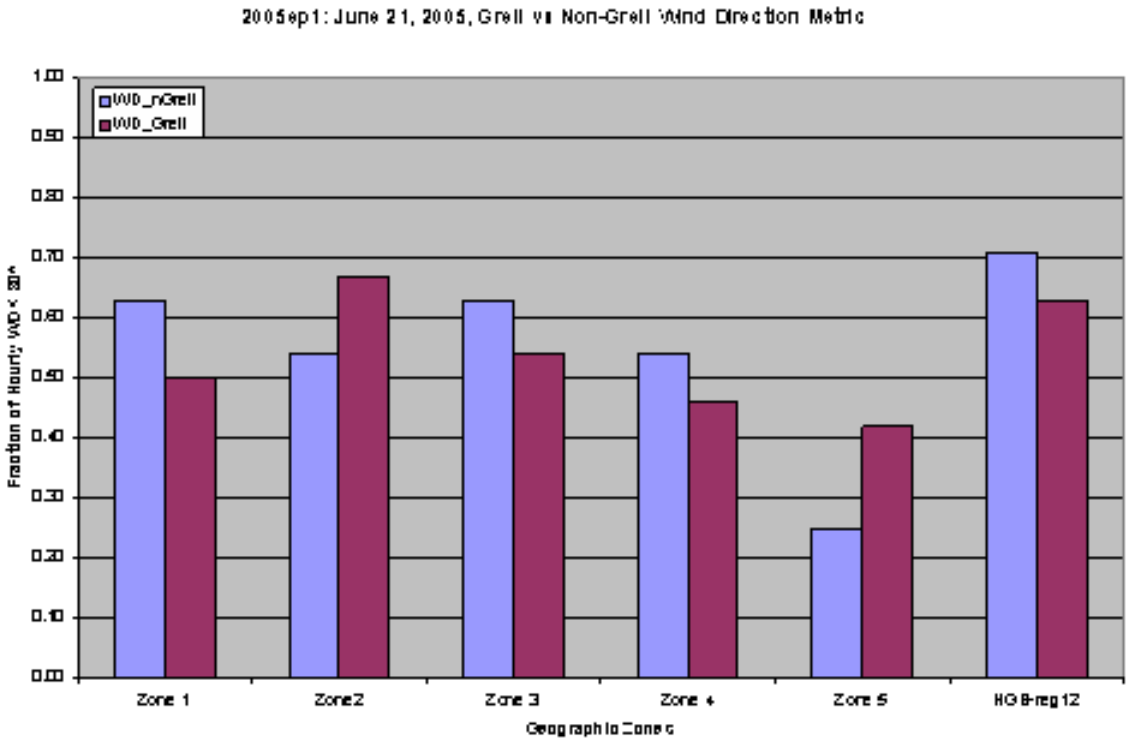

Figure 2.12.4.3-7: Percent of averaged hourly wind directions < 30 degrees by zone on June 21, 2005

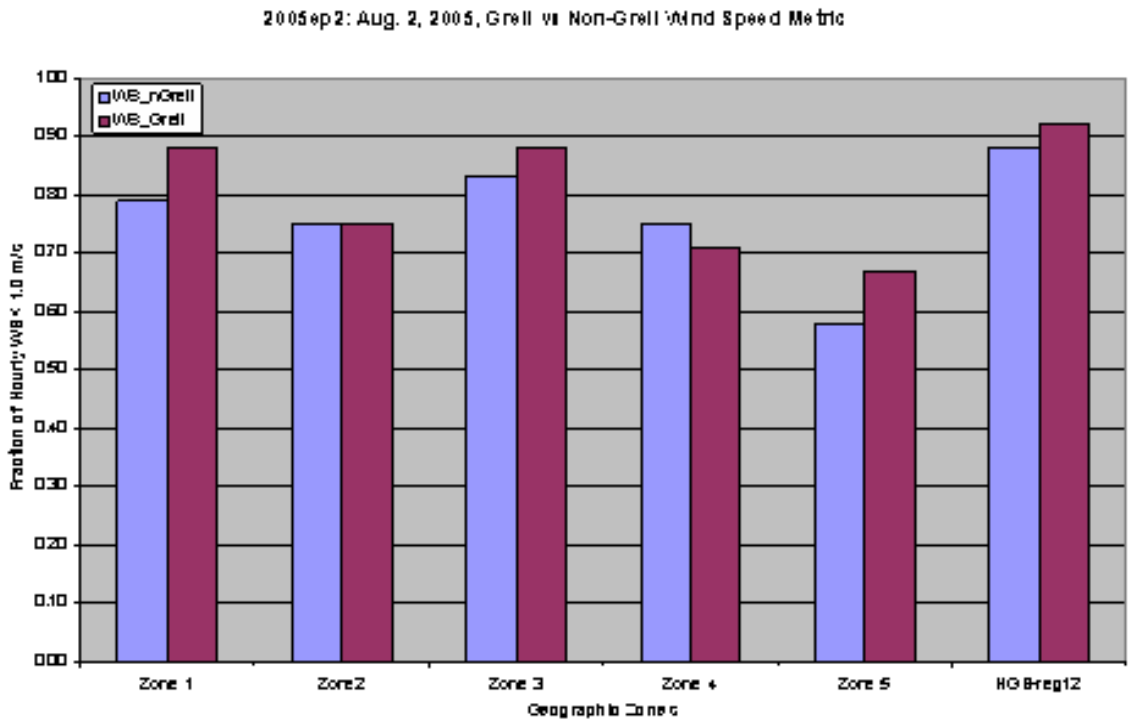

Figure 2.12.4.3-8: Percent of averaged hourly wind speeds < 1 m/s by zone on August 2, 2005

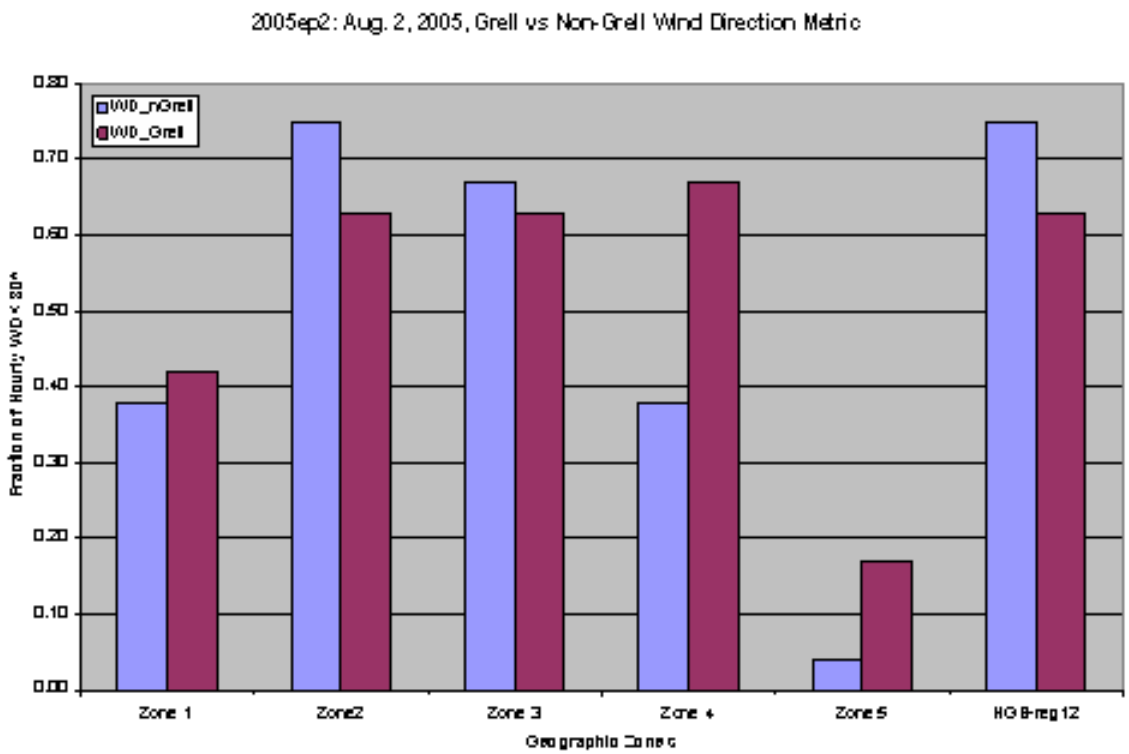

Figure 2.12.4.3-9: Percent of averaged hourly wind directions < 30 degrees by zone on August 2, 2005

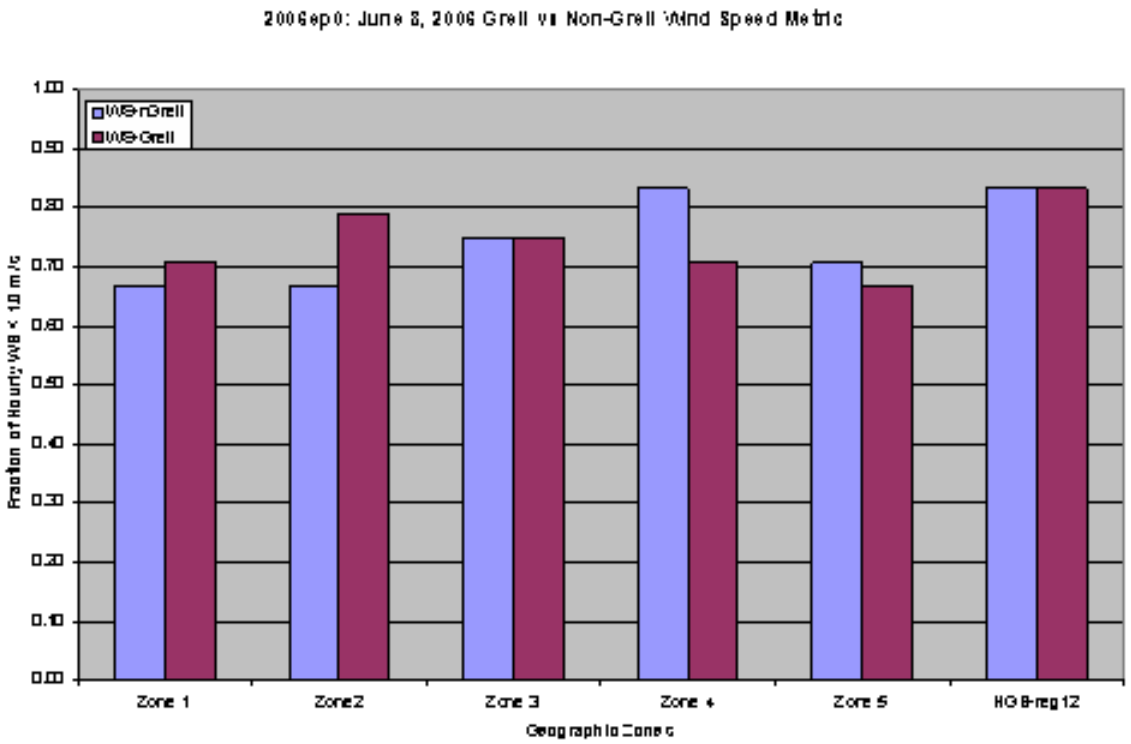

Figure 2.12.4.3-10: Percent of averaged hourly wind speeds < 1 m/s by zone on June 8, 2006

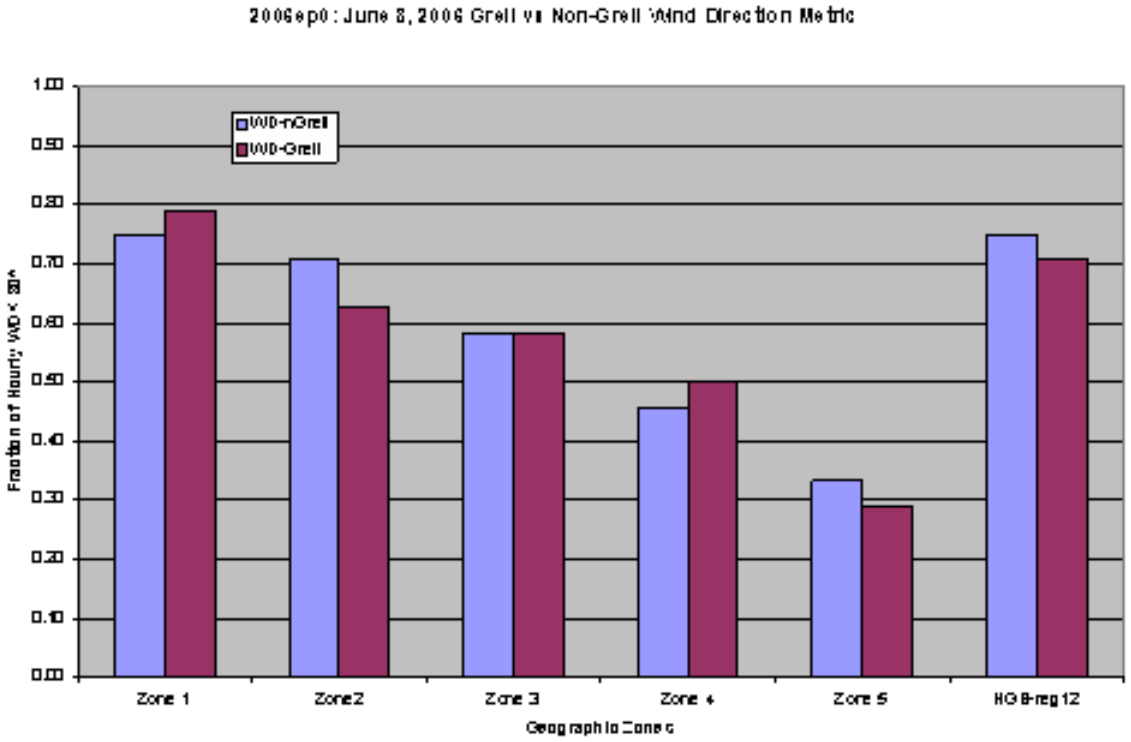

Figure 2.12.4.3-11: Percent of averaged hourly wind directions < 30 degrees by zone on June 8, 2006

The close proximity of the Houston Ship Channel (HSC), an area with a high density of industrial sources, to Galveston Bay and the Gulf of Mexico with the associated land sea breeze phenomena creates complicated wind flow patterns of ozone precursor emissions. Therefore the TCEQ staff felt the wind speed and direction metrics used to evaluate the difference in the MM5 configurations (i.e., with or without Grell on the 4 km grid) needed to be supplemented with a performance measure that considers the dynamic features of the winds. Therefore an additional performance measure was considered which compares the forward trajectory paths of modeled and observed air parcels advected by the winds. This performance measure is better characterized as a graphical evaluation rather than a metric since there are no recommended criteria for determining the correct path of an air parcel. This graphical evaluation was conducted for the same selected episode days.

The density of trajectories needs to be high enough to represent the multitude of emission source locations in the HGB area that can contribute to high ozone concentrations down wind, without obscuring the plots. Although even with a relatively high density of trajectories, there is no assurance that any of the air parcels from the selected emanating locations will be advected over a particular monitor due to the complexity and numerous sources in the HGB area. In addition the density of trajectories needs to be high enough to reflect whether or not the wind pattern associated with the land-sea breeze phenomena has been adequately replicated.

Although the starting point and time are arbitrary, the TCEQ staff has focused on emission source locations such Houston Ship Channel (HSC) and roadway intersections, as well as starting the trajectories at 6 AM and 9 AM (CST). Air parcels emanating from emission source locations between 6 AM and 9 AM are typically those that are predominately associated with maximum ozone concentrations occurring later in the day although, the industrialized HSC can give rise to notable emissions of highly reactive pollutants at anytime. The observed forward trajectories are plotted based upon surface winds measured at CAMS sites from standard 10 meter towers. Although the data have been quality assured, CAMS winds are tabulated as hourly averages from shorter averages of 5 minute measurement periods. The lowest model layer simulates winds at 17 meters, which is notably higher than the observations, so the modeled hourly averaged wind speeds are adjusted to reflect a 10 meter level. These caveats need to be taken into consideration when comparing observed and modeled forward trajectories, since they can contribute to accumulated differences in wind speed and direction.

In Figure 2.12.4.3-12: *12 Hour Forward Trajectories of Air Parcels From Multiple Source Locations for 6 AM (CST) June 22, 2005* and Figure 2.12.4.3-13. *12 Hour Forward Trajectories of Air Parcels From Multiple Source Locations for 9 AM (CST) June 22, 2005*, 12 hour forward trajectories are shown for June 22, 2005, starting at 6 AM and 9 AM (CST), respectively. These trajectories show the transport paths of air parcels emanating from various emission locations (e.g., stacks, intersection). Monitoring sites are color coded by the magnitude of the maximum daily eight-hour ozone concentration recorded at that site. Comparing the trajectories in these two plots shows how the ensemble of trajectories migrates for different starting times (i.e., different air parcel emanating times).

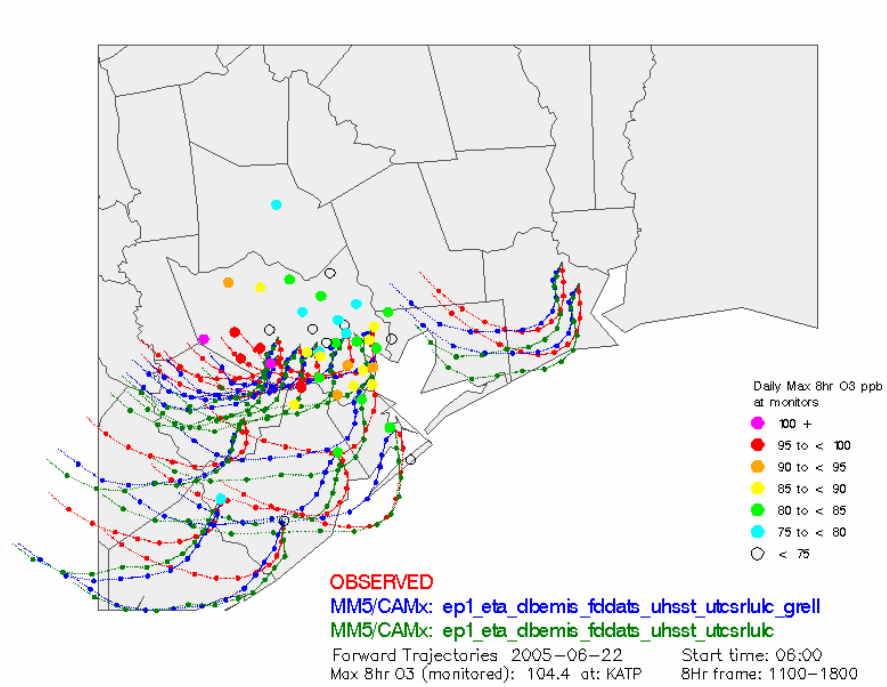

Figure 2.12.4.3-12: 12 Hour Forward Trajectories of Air Parcels From Multiple Source Locations for 6 AM (CST) June 22, 2005

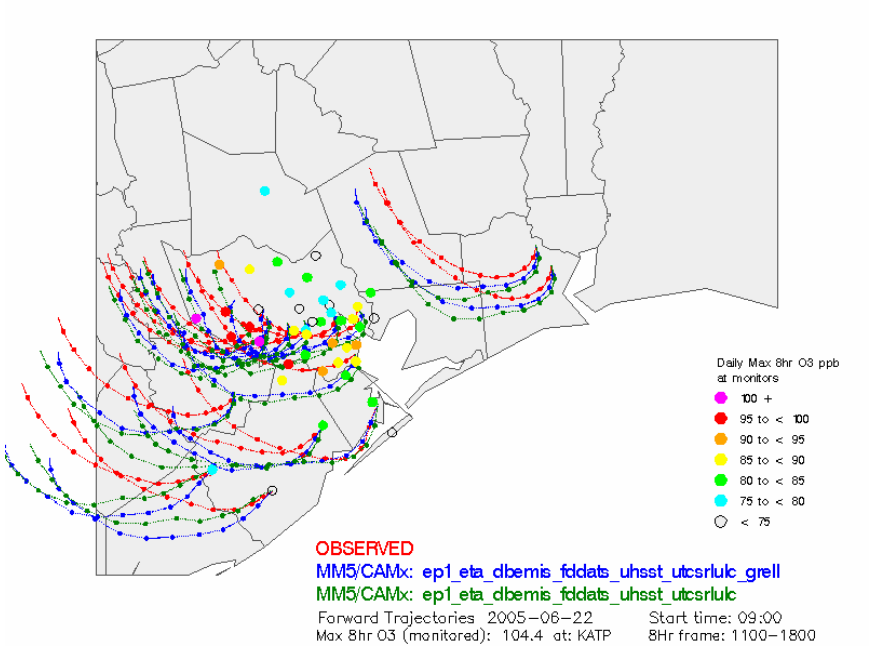

Figure 2.12.4.3-13: 12 Hour Forward Trajectories of Air Parcels From Multiple Source Locations for 9 AM (CST) June 22, 2005

The ensemble of trajectories for the air parcels emanating at 9 AM shows that they are not carried as far south as the air parcels emanating at 6 AM. Therefore, between 6 and 9 AM on June 22, 2005, the ensembles of trajectories migrated northward.

Also notable from both figures are the stronger winds simulated by MM5 for both the configuration with and without Grell, on June 22, 2005. The differences between the MM5 simulated and CAMS observed winds, which accumulate most strongly in the first few hours, are especially noticeable in the Beaumont Port Arthur area and south of Houston nearer the coast. The accumulation of the stronger modeled winds occurring early in the trajectory carry the air parcels further to the southwest before the land sea breeze phenomena induced the clockwise rotation in wind direction. Focusing on the trajectories of the 6 AM and 9 AM air parcels emanating from the HSC, the trajectories derived from the MM5 simulated winds with the Grell configuration appear to compare slightly more favorably with the trajectories derived from the CAMS observed winds.

The comparability of the trajectories derived from the winds for the two modeled configurations (i.e. with and without Grell) and the observed winds varied by episode day. For most of the days the trajectories for the two modeled configurations were somewhat similar, although they both generally compared less favorably with the trajectories derived from observed winds. However, for the episode days considered, the configuration with Grell appears to provide a slight improvement in the 6 AM and/or 9 AM trajectories. This led the TCEQ staff to conclude that using the Grell configuration does not compromise the meteorological modeling performance in the HGB area.

2.12.4.4. Discussion

The previous sections have presented an operational rationale for investigating the use of the Grell cumulus parameterization on a 4 km grid. The "conventional wisdom", however, is that convective parameterizations are reasonable for domains with grid spacing of 10-12 km or greater, and that convection can be explicitly modeled at smaller scales. General modeling guidance support this type of model configuration (Grell, 1993, Grell, Dudhia and Stauffer, 1994). On the other hand, grid-resolved "explicit" convection also depends upon a different set of parameterizations – the explicit moisture physics schemes which account for the influence on precipitation due to nucleation, coagulation, fall speed, supercooling of water, and various icing processes.

Since TCEQ staff have chosen to investigate a non-standard configuration, this section will include a short series of points arguing why this is not completely unreasonable. Those points will recognize that 1) the traditional mix of explicit and parameterized convection is implemented to avoid "double counting" and thus we may expect to avoid harm by trying something new, 2) scale-separation between explicit and parameterized convection has been conjectured as necessary, but may not reflect all met regimes, 3) Grell is being used to stabilize an already generally fair-weather environment, and 4) the default of an explicit-only treatment is also prone to limitations as scale *increases*.

Molinari and Dudek (1990) provide an important review of the "partitioning" between grid-resolved convection and the sub-grid convective parameterization. Although these authors argue for a hybrid scheme in which water content from a cumulus parameterization is provided directly to an explicit moisture scheme, they note,

"Calculation techniques are such that modelers do not allow 'double counting'; energy and moisture are conserved in such situations because grid-scale condensation is computed at the end of the time step after all other processes have acted (e.g., Kanamitsu 1975)". Experiments by TCEQ staff support other anecdotal reports that partitioning between the cumulus parameterization and explicit moisture physics vary across episode, and will be dependent on grid resolution. As pointed out below, however, the partitioning by the Grell cumulus

parameterization might be responsible for less condensable water than other cumulus schemes and thus allow the explicit moisture parameterization to do most of the work.

Molinari and Dudek cite earlier work by Arakawa and Chen (1987) who favored the idea of "scale separation" yet noted that nature does not create a clear example of a spectral gap between cloud scales and mesoscale. They note, importantly, that the lack of a spectral gap is generally unavoidable in the temporal development convection as well as continuous range of spatial scales seen in cloud systems. The discussion section of their paper makes the following assessment: "For models with grid spacing less than 2-3 km, the fully explicit approach is clearly superior to parameterized approaches, even though a 1-km grid spacing can fully simulate only the largest convective clouds (Lilly 1990)… For grid spacing from about 3 to 20-25 km, it remains uncertain whether a general solution exists." (Molinari and Dudek, pg. 339)

The concern by model developers at the intermediate range of scales mentioned above is that parameterized convection can grow quickly to grid scale – on a large grid this could produce far too much precipitation. Furthermore, the likelihood of parameterized convection growing to grid scale increases with increased resolution. In such a situation, it would be preferable to see parameterized clouds become quickly secondary to grid-scale convective clouds. Although TCEQ staff have observed episodic variability in this regard, the Grell scheme seems most likely to transition from cumulus precipitation to grid-scale explicit moisture precipitation.

Wang and Seaman (1995) investigate a comparison of convective parameterizations in MM5. This paper investigates the various metrics described earlier in this report which are of primary concern for traditional precipitation forecast validation. They note the desirability of finding a reasonable partition between parameterized and grid-scale rainfall, in part for stability reasons. In particular, the note that, "This is because the sub-grid-scale convective parameterization represents a more rapid upward transport of heat and moisture, and hence can stabilize a column faster." Although many model developers are interested in the correct evolution and intensity of a mesoscale convective system, we conjecture that this parameterization can stabilize a fair weather atmosphere. More importantly for our case study, Wang and Seaman note in their experiments that compared to other convective schemes available within the MM5 model, "… the Grell scheme quickly switches from convective to resolved-scale dominance before the MCS matures…" Again, this observation is only part of a larger and traditional case study of warm and cold weather experiments; however, this is suggestive of the type of behavior which one would like to see in a cumulus parameterization if it is applied on an 4 km grid.

The question of the applicability of applying a cumulus parameterization on a 4 km grid can be recast by asking whether an explicit moisture parameterization is alone sufficient to stabilize the atmosphere and capture appropriate precipitation. Weisman, Skamarock, and Klemp (1995) studied the resolution dependence of explicitly modeled convective systems. Citing earlier work such as Molinari and Dudek among others, these authors agreed that convective parameterizations were necessary for resolutions between 20 and 50 km. They summarized the development work of the previous decade and concluded, "nonhydrostatic cloud model simulations employing grid resolutions of 2 km or less have shown much success in replicating the observed structure and evolution of convection, including the upscale growth from individual convective cells to full mesoscale convective systems." Thus, at sufficient resolution, an explicit moisture scheme alone should be sufficient for capturing convective behavior. With sufficient forcing, the explicit moisture physics on a four kilometer grid may be adequate since these authors offer, "that 4 km resolution is sufficient to reproduce most system-scale aspects of squall-line behavior over a 6-h period, with resolutions of 8 km or larger resulting in significantly slower system evolution and stronger system-scale circulation."

2.12.4.5 Conclusion

Air quality episodes are typically fair weather periods, and at one time clouds were ignored entirely by choice of short pollution events. Longer episodes may be punctuated by periods of precipitation, but the question of how to best characterized cloud development in a way which does not compromise the frequent light winds and mesoscale land-sea breeze has been an open question. The effects described here have been subtle, but arguably the most important objective of not unfairly distorting the behavior of the meteorological evolution of these episodes has been accomplished while improving the over-all characterization of fields that need to be input into the photochemical model.

2.12.4.6 References

Arakawa, A., and J.-M. Chen, 1987: Closure assumption in the cumulus parameterization problem. *Short and Medium Range Numerical Weather Prediction*. T. Matsuno, Ed., Meteor. Soc. Japan, Universal Academic Press, 107-131.

Grell, G. A., 1993: Prognostic evaluation of assumption used by cumulus parameterizations, *Mon. Wea. Rev*., **121**, 764-787.

Grell, G. A., J. Dudhia, and D. R. Stauffer, 1994: A description of the fifth generation Penn State/NCAR mesoscale model (MM5), NCAR Tech. Note NCAR/TN-398-STR, 138 pp.

Lilly, D. K., 1990: Numerical prediction of thunderstorms—has its time come? *Quart. J. Roy. Meteor. Soc.*, **116**, 779-798.

Molinari, J. and M. Dudek, 1992: Parameterization of convective precipitation in mesoscale numerical models: A critical review. *Mon. Wea. Rev.*, **120**, 326-344.

Wang, W., and N. L. Seaman, 1997: A comparison study of convective parameterization schemes in a mesoscale model, *Mon. Wea. Rev*., **125**, 252-278.

Weisman, M. L., W. C. Skamarock, and J. B. Klemp, 1997: The resolution dependence of explicitly modeled convective systems, *Mon.Wea. Rev*., **125**, 527-548.